ARS JOURNAL
RUSSIAN SUPPLEMENT

Igor Jurkevich, Editor

What an Astronaut Will See and Encounter When Flying at a Speed Approaching That of Light . . . . . S. M. Rytov 678

Qualitative Investigation of the Trajectories of Difference Equations Near a Fixed Point . . . . . A. M. Panov 682

Fall of a Spherical Drop in the Presence of Evaporation or Condensation of Vapors at Its Surface . . . . . V. S. Novoselov 686

Relation of Frequency of Ultra Short Wave Field Amplitude Decay, Drift Speed of Inhomogeneities in the Troposphere, and Carrier Frequency . . . . . A. A. Semenov and G. A. Karpeyev 688

Ignition in a Flow by Hot Bodies . . . . . S. A. Gol'denberg 691

Melting Diagram for the Titanium-Vanadium-Molybdenum Ternary System . . . . . I. I. Kornilov and R. S. Poliakova 694

Variation of the Albedo of the First Artificial Earth Satellite as a Result of the Influence of External Factors . . . . . I. M. Yatzunsky and O. V. Gurko 698

An Artificial Comet as a Method for Optical Observation of a Cosmic Rocket . . . . . I. S. Shklovskii 699

Upper Atmosphere Density Determination, Based on Flight Observations of the Third Soviet Artificial Earth Satellite . . . . . P. E. El'iasberg and V. D. Yastrebov 706

Results of Investigation of the Meteoric Matter by Means of Instruments Installed on Cosmic Rockets . . . . . T. N. Nazarova 713

Measurement of Cosmic Rays by Means of Geophysical Rockets . . . . . Yu. Shafer and A. V. Yarygin 715

DIGEST OF TRANSLATED RUSSIAN LITERATURE 720

Published Under National Science Foundation Grant-in-Aid

What an Astronaut Will See and Encounter When Flying at a Speed Approaching That of Light

S. M. RYTOV

In our time, when the most daring dreams about reaching cosmic space are coming true, when artificial satellites and cosmic rockets developed by man's hands are penetrating the boundless distances of the solar system, human thought seeks for new, untested ways to conquer the cosmos. People not only dream, but begin to compute mathematically the possibilities of flying to other stars of our galaxy. How can we conquer the enormous distance separating us from even the nearest stars? The future astronaut will be able to bridge it during his lifetime only if his ship will move with a speed approaching that of light. The observer moving with a speed approaching that of light ("relativistic speed"), exists now on the pages of fantastic novels only. Although one writes about photon rockets[1] there is yet no real basis for developing them. Will it ever be possible for a flight with relativistic speed to become a reality? The history of science and of technology convincingly proves that the most categorical "no" cannot be applied to the future. What seems impossible today can become completely feasible tomorrow. But, even in our time and with the contemporary level of knowledge, one can foresee a part at least of the difficulties and obstacles which will be met and will have to be overcome by the future relativistic navigator to the stars. The motion involving relativistic speed hides several surprises which are discussed in this article.

WE DO not intend to touch upon the question of how to accomplish the motion of a macroscopic body with relativistic speed. Let us assume that this problem has been somehow solved and a relativistic interstellar ship has been developed. And although we know that there are no macroscopic bodies whose speed could even approximately approach that of light, it seems to us curious and instructive to look at the surrounding world through the eyes of the passenger of a relativistic spaceship.

The picture before his eyes would be rather unusual. We have not read its description yet and this is quite natural: We deal with the strongly expressed relativistic effects only in the physics of elementary particles. How changed will the star-filled sky look to our astronaut and how different will be the picture of the firmament for him? What will a star look like from a relativistic spaceship passing nearby? What will be the effect of the interstellar medium, the micrometeorites, interstellar dust and gas on the spaceship and its crew?

View of the Celestial Sphere

In order to answer these questions, one should recall certain theses ensuing from the special theory of relativity.

Let us imagine two systems. One of them is at rest, that is, it is motionless with relation to the "fixed stars" or, as is the case with the sun and the Earth, it moves with ordinary astronomical speeds of tens and hundreds of kilometers per second. The other is connected with the starship and moves relatively to the first with a speed comparable to the speed of light. There are definite correlations between the coordinates and the time in both systems.[2] From these correlations it follows that for a moving observer the light of a distant star arrives at a different angle than for a motionless one. This phenomenon is called aberration. Besides, the frequency of the observed light vibrations also changes, creating the so-called Doppler effect. As a result of these effects, the view of the starry sky will be considerably changed.

Let us imagine that for a motionless observer the sky is uniformly filled with stars as shown on Fig. 1, left, where stars are situated at angles of 0, 15, 30, . . ., 165 and 180°. Because of the aberration, we shall have a new arrangement of the same stars for an observer in motion (Fig. 1, right), namely, the stars accumulate in front of the starship and spread out behind it. If we assume that the speed of the starship is 0.866 of the speed of light[3] (c = 300,000 km/sec), then the whole front hemisphere of the motionless observer will be seen by the astronaut in a cone with the vertex angle of 30° (see Fig. 1, right). If the speed of the starship is 0.95 of the speed of light, this cone will have its vertex angle equal to only 18°.

The change in the position of stars does not exhaust the peculiarities of the sky picture as observed visually from the system in motion, since the spectral composition of the radiation is also changed. There is only one specific direction

---

Translated from *Priroda* (*Nature*), no. 4, 1960. Translated by A. E. Godlewsky, New York.

[1] See Sänger, E., *About the Mechanics of Photon Rockets*, IL, 1958.

[2] We are discussing the Lorenz transformation on connecting the coordinates and time (x, y, z, t) in a motionless system K with the corresponding values (x', y', z', t') in a system K' moving with the relative velocity v. With the relative motion along a common axis x these transformations look as follows

$$x = \frac{x' + \beta ct'}{\sqrt{1 - \beta^2}} \qquad y = y' \qquad z = z'$$

$$t = \frac{t' + (\beta/c)x'}{\sqrt{1 - \beta^2}} \qquad \left(\beta = \frac{v}{c}\right)$$

[3] This value is taken only because it simplifies the computation.

in which those changes will not be observed. If the speed of the starship is 0.866 of the speed of light, then, in the motionless system, the angle between this direction and the direction of motion of the starship will be 54°50′, and in the system moving with the fore-mentioned speed the angle will be 125°10′. For all the stars situated at an angle smaller than 54°50′ there will be a decrease in frequencies, so that all frequencies emitted by a star, when viewed by a moving observer, will be displaced to the long wave length part of the spectrum (red shift). For stars situated at an angle greater than 54°50′ frequencies are displaced toward the short wave length part of the spectrum (violet shift).

The stars whose light arrives at the 54°50′ angle have for the observer in motion the same spectrum as for the motionless observer.[4]

Fig. 2 shows what color stars will appear to have for an observer moving with the above-mentioned speed (0.866c) provided they are not in the direction of the zero Doppler effect. Let us assume that in a rest system a star radiates light on one of the three waves of the visible spectrum, namely 4000 and 8000 Å (the limit of the visible part) and 5000 Å (the green line). Then, if this star is outside of the cone shown with dotted lines in Fig. 2, the light visible to the motionless observer will become invisible to the astronavigator, since it will be displaced either to the ultraviolet or to the infrared regions of the spectrum. If the star is situated in the direction of the zero Doppler effect, its color will not change. With deviation from this direction but within the bounds of the cone shown by dotted lines, wave lengths will alter as shown in Fig. 2 by dash-lined circles.

Naturally, the inverse phenomenon will also occur: The radiation invisible for the motionless observer will appear in the visible part of the spectrum for the astronavigator. Traveling with the same speed, the astronavigator will see behind himself the sources sending ultraviolet waves with wave lengths from 1070 to 2140 Å and in front of himself the sources sending infrared waves with wave lengths from 14,950 to 29,900 Å.

Distortion of Form of a Passing Star

It is a well-known fact that the Lorenz transformation leads to the longitudinal contraction in lengths, so that a sphere passing the observer with the relativistic speed appears noticeably flattened in the direction of the motion; in other words it becomes an ellipsoid.[5] Such a configuration is indeed a true one. Such is the simultaneous position of points of a moving sphere at a given time according to the watch of an observer at rest. We are now interested in another question—not in the simultaneous real position of the points of a body in motion, but in their simultaneous apparent position. This is quite different, because at any moment we shall see positions of the points of a body in motion at different times. This occurs because the light entering the eyes of an observer at the same moment of time takes different times to reach the eyes from different points of a body in motion. We are discussing here again essentially the phenomenon of aberration, but we are interested now not in the infinitely distant sources but in the

[4] For the stars in the motionless system K from which the radiation comes at the angle $\alpha = 90°$, the Doppler effect produces in the system K' a wave shortened $\sqrt{1-\beta^2}$ times. For the stars whose radiation arrives at an angle α such that $\cos\alpha = \beta$ in the system K' the radiation will come at the angle $\alpha' = 90°$, and one obtains the so-called purely transverse Doppler effect—the lengthening of the wave $\sqrt{1-\beta^2}$ times. (This effect is called transverse because the observer K' sees the star in the direction perpendicular to the direction of motion. It is a purely relativistic effect.) Finally, the waves arriving from the sources situated exactly astern the starship, will become longer $\sqrt{(1+\beta)/(1-\beta)}$ times, and waves from those directly in front of the starship will become as many times shorter.

[5] The longitudinal contraction in length occurs by the ratio $\sqrt{1-\beta^2}:1$ so that the ellipsoid will have just this ratio of axes.

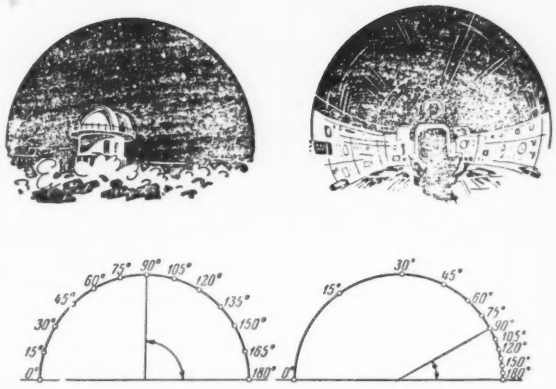

Fig. 1 View of the celestial sphere. Above left: Ordinary view of sky as seen by inhabitants of Earth moving together with Earth with usual astronomical velocities (tens and hundreds of km per sec). Below left: "Normal" protractor with uniformly situated degrees. The firmament is spangled with stars also "uniformly." Above right: For a relativistic astronavigator moving with the speed of 260,000 km/sec, approaching the speed of light, all the stars "accumulate" around point to which rocket moves. Below right: "Relativistic" protractor; scale of degrees became such that in direction of rocket's motion the former 90° angle now occupies on the celestial sphere only 30° of a "normal" protractor

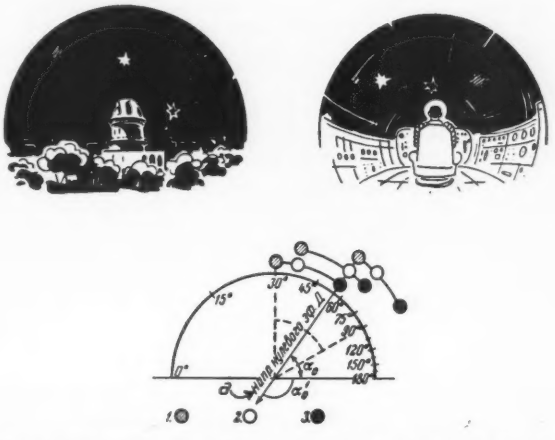

Fig. 2 Top left the stars: Red, 1; green, 2; violet, 3; the fourth shown with dotted lines is invisible (infrared). On the right, the astronaut also sees the three stars but they have all moved in the direction of the rocket motion and changed their colors: The violet became invisible, the green became violet, the red became green and the invisible star became red. Below: If the astronavigator moves to the right and looks along the line of zero Doppler effect, the stars seen in this direction keep their ordinary "Earthly" color. If he looks at the stars situated a little nearer to the course of the ship, he will see them with the previously described changes. When observing them in the directions still nearer to the course of the ship, all visible colors will become invisible (ultraviolet) and will be replaced by the "formerly" infrared colors. [a] Direction of zero Doppler effect

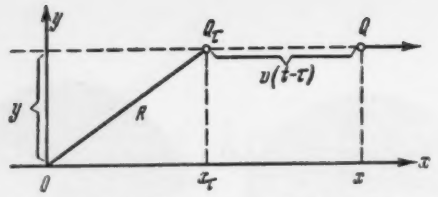

Fig. 3 Diagram explaining difference between the real and apparent positions of a point source

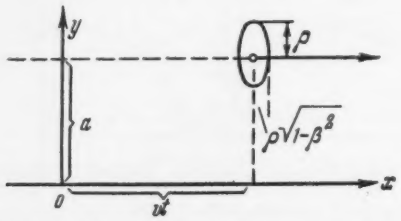

Fig. 4 Diagram explaining relation between axes of a real ellipse

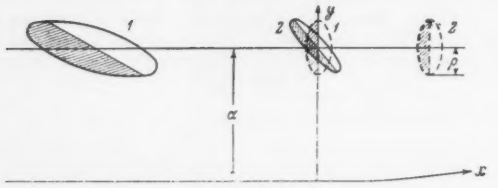

Fig. 5 Two true positions of a sphere in motion (dotted line) and their corresponding apparent positions and configurations (solid curves)

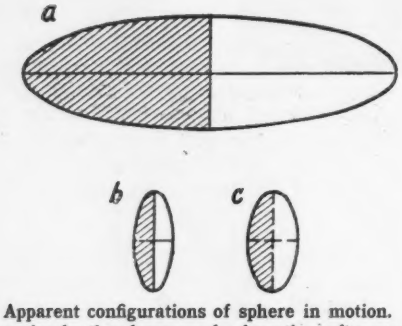

Fig. 6 Apparent configurations of sphere in motion. a—long before passing by the observer; b—long time after meeting him; c—picture of real ellipse

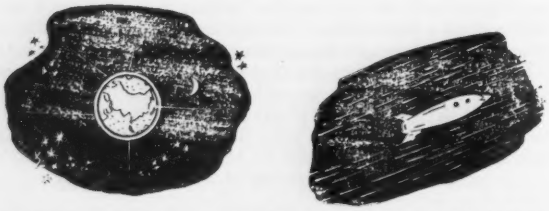

Fig. 7 Stream of primary cosmic particles falling on Earth (left) is 10^{10} weaker than the stream which will be met by a cosmic spaceship (right)

sources situated at finite distances. It is not difficult to find out the connection between the real and the apparent positions of such a point source.

Let us assume now (it does not change anything physically and it simplifies the discussion) that the observer is at rest at the point O of the system K and a point source passes by him with the speed v parallel to the axis x at a certain "target distance" y (Fig. 3). At the given time t according to the watch K, when the source is at point Q, the observer sees it at its previous position Q_τ which it occupied at the time $\tau < t$ while $t - \tau$ is the time of propagation of light from Q_τ to O $[t - \tau = (R/c)]$. Thus, the real abscissa x and the apparent abscissa x_τ differ by the segment $v(t - \tau)$. This permits computation of the apparent position of each point of the body, the real position of which is known at the given time t.

At any given time t according to the clock of the observer K, the real configuration of the sphere passing by him is (as it follows from the Lorenz transformation) an ellipsoid (this means in plane section x, y an ellipse with its center at the point $x = vt$, $y = a$ and with semi-axes $\rho\sqrt{1 - \beta^2}$ and ρ). See Fig. 4.

The apparent configuration proves to be essentially different from the real one and varies with time.

In Fig. 5 are shown two real positions of a moving "sphere" (the dotted curves 1 and 2) and their corresponding apparent positions and configurations (the solid curves 1 and 2). In construction it is assumed that the distance between the observer and the trajectory of the center of the sphere (the "target distance") is five times larger than the radius of the sphere and that the speed is equal to 0.866 of the speed of light. Curves 1 correspond to the time when the center of the sphere is in front of the observer, and curves 2 to the moment of time when the center of the figure is seen opposite the point O.

Whereas the real configuration is (in the plane of the drawing) a uniformly moving ellipse with the ratio of axes 1:2, the apparent configuration is an oval which, while moving, turns around and considerably changes its form as well as its forward velocity. In addition to Fig. 5, Fig. 6 shows the apparent forms of a star a long time before and a considerable time after passing the observer.

As long as the approaching sphere is far away, it has the form of an ellipsoid elongated in the direction of motion.[6] While approaching, it loses the exact form of the ellipse and turns over with the sharp end toward the observer, as shown by curves 1 and 2 on Fig. 5. At the same time, the distance between the apparent position and the real one as well as the apparent speed decrease. A sufficient time after the encounter, the sphere again becomes an ellipsoid which is now more flattened in the direction of motion than the real ellipsoid[7] (c on Fig. 6). For the speed equal to 0.866 of the speed of light, the distance from the center of the ellipsoid to the observer is at any given time approximately two times smaller than in reality, and it moves away with an apparent speed also approximately two times slower than the real speed.[8]

Naturally, if the real relative speed is known, a recomputation for the rest system can always be made and the real picture restored. This pertains to the configuration of the oncoming star as well as the view of the starry sky as a whole, as discussed previously.

[6] In the plane section of the drawing one gets an ellipse. Its semi-axes are equal to $\rho\sqrt{(1 + \beta)/(1 - \beta)}$ and ρ. (In our example it is 3.78 ρ and ρ, a on Fig. 6.) The center of this ellipse is removed on axis x a distance which seems increased $1/(1 - \beta)$ times in comparison with the real distance $s = v(t)$ and, correspondingly, approaches the observer with the apparent speed $v/(1 - \beta)$ (in our example 7.47 v).

[7] The semi-axes of the ellipsoid are equal to $\rho\sqrt{(1 - \beta)/(1 + \beta)}$ and ρ (in our example it is 0.27 ρ and ρ, b on Fig. 6).

[8] The center of the ellipse from the observer is not $s = vt$, but $s/(1 + \beta)$ and it moves away with the speed $v/(1 + \beta)$.

The odd changes in the form of the passing star shown above cannot, however, be seen directly without measuring the distances to various points of its surface. The projection of complex figures previously mentioned on the celestial sphere always remains in the form of a round disk. Thus, the relativistic contraction of the sphere in the direction of its motion will not be discovered by simple visual observation.[9]

The spectrum of radiation of the passing star is, of course, also changed. While approaching, such a star is seen because of its infrared radiation; at a certain moment during the encounter, the wave lengths go through their "rest" values and then the ultraviolet radiation of the star falls in the visible part of the spectrum. All this does not occur very fast—recall that light needs approximately 17 min to cross the orbit of the Earth. With the speed of 0.866*c*, the crossing of this distance will require about 20 min and about 10 min according to the astronaut's clock.

Relativistic Dust and Wind

The starship moving in cosmic space is in the oncoming stream of micro- and macroparticles (the interstellar gas, micrometeoritic bodies, etc.). If we disregard their speed, they strike against the starship with the speed of its motion. One can compute the amount of energy resulting from the collision of the starship and the particles moving in interstellar space. It appears, that at the speed of 0.866*c*, a particle with a mass of 1 mg will have 21 billion calories of kinetic energy. This amount of energy would be sufficient to vaporize 30 tons of ice or 10 tons of iron. The impulse of such a particle will be equal to 520 kg-m-sec^{-1}; that is, it will be approximately the same as that of a cyclist riding with the speed of 30 km/hr.

What results can be expected when a micrometeorite strikes against the massive hull of a starship? Let us find out what is the kinetic energy of one of the nucleons of the meteorite in comparison with the binding energy of the same nucleon in the nucleus of the atom.

While moving with the speed of 0.866*c*, one nucleon possesses 1 billion ev of energy, whereas the binding energy in nuclei (of elements with atomic weights of more than 20) is only about 8 million ev. Thus, one can fully disregard not only the binding energy of the atoms in the crystalline lattice, but also the binding energy of nucleons in the nuclei of atoms—in the material of the meteorite as well as in the material of the starship. This means that atoms of micrometeorites bury themselves in the envelope of the starship as a group of heavy cosmic particles each of which will spend its energy practically independently of all the others.

The energy of several billion ev per nucleon corresponds to the "soft" cosmic rays; that is the mean free path of the nuclei of iron, silicon, etc., plunging with such speeds into the material of the same density, is measured by several centimeters or by a few tens of centimeters. Afterwards, their energy will be spent in formation of still "softer" particles and, at the end, will be absorbed by the hull of the starship because of great ionization losses. Thus, a collision between a micrometeorite with the mass of 1 mg and a sufficiently large mass of metal will cause a catastrophic thermoexplosion of the whole starship.

The effect caused by smaller dust particles will be, naturally, proportionally weaker, but they occur, on the other hand, much oftener. Apparently, the average mass of particles of the interstellar dust substance lies between 10^{-9} and 10^{-11} gm and the average density of this substance in the galaxy is of the order of 10^{-25} gm/cm^3. At the speed of 0.866*c*, the flow of dust to the hull of the starship will be about 2.6×10^{-15} gm/cm^2 · sec. This corresponds to the flow of energy of 3.4 cal/cm^2 · min and is almost two times larger than the solar constant.[10] If we assume that the overall surface of the starship is 20 times larger than its cross-sectional area, and that its emissivity is an order of magnitude lower than that of an ideal black body, then the thermodynamic equilibrium will occur when the temperature of the ship's envelope is near 100 C. Dust concentrations 10 times larger than the average will heat[11] the ship to 400 C.

Beside the dust and meteorites, the starship will encounter a stream of interstellar gas, mostly hydrogen, whose average density in the galaxy is by one order higher than the density of the dust: Approximately one hydrogen atom per 1 cm^3 (about 10^{-24} gm/cm^3).

One could ask at what speed it would be expedient to use a straight flow photon engine[12] in which the "combustion" of the interstellar gas will provide enough energy to permit compensating for the resistance of the gas to the motion of the starship. Let us assume even that we have succeeded in doing this. However, the difficulty lies in another direction.

For the relativistic ship, the interstellar hydrogen becomes a stream of protons with energies exceeding one billion ev; in other words a stream of cosmic rays whose intensity is of the order of 10^{10} of particles per 1 cm^2 per 1 sec. Let us remember that for a nonrelativistic observer the intensity of primary cosmic rays is equal only to two particles per 1 cm^2 per 1 sec. Consequently, even assuming that the processes of destroying or overheating of the starship are somehow averted, we still face this enormous (exceeding by 10^{10} times the usual dose) amount of cosmic irradiation capable of killing instantaneously any living being.

It follows from the foregoing, that the problem of a sufficiently efficient engine is not the only essential problem standing in the way of relativistic astronavigation. It is no less important to find the means of "clearing" the cosmic space in front of the starship, in other words, to eliminate from its way all kind of micro- and macroparticles or to find some other means of protection from them. This problem seems to us no less difficult than the development of a photon engine.

[9] See Terrell, T., "Invisibility of the Lorenz Contraction," *Phys. Rev. Letters*, vol. 3, no. 10, 1959, p. 501.

[10] By the solar constant we mean the amount of calories received by one square centimeter of a surface perpendicular to sun's rays and situated at the boundary of the Earth's atmosphere. On the average it equals 1.94 cal/cm^2 · min.

[11] However, the question about the degree of heating of the hull of a rocket is rather complicated, as a considerable loss of energy is possible because of the x-ray radiation.

[12] See Pierce, J. R., "Relativity and Space Travel," Proc. IRE, vol. 47, no. 6, 1959, p. 1053.

Qualitative Investigation of the Trajectories of Difference Equations Near a Fixed Point

A. M. PANOV

Sverdlovsk State Pedagogical Institute

THE SOLUTION of the problem of the stability of intermittent control systems plays an important role in modern technology (1).[1] The works of Tsypkin (2), Perron (3), Bellman (4), Skalkina (5) and Koval' (6) have been devoted to an investigation of the stability of the solutions of finite difference equations, one of the basic mathematical devices used to compute intermittent control systems. The qualitative investigation of systems described by nonlinear difference equations is a problem that is interesting, but which has been only slightly developed.

Let us examine a system of difference equations

$$\begin{aligned} y_{n+1} &= A_m y_n^m + A_{m-1} y_n^{m-1} x_n + \ldots + A_0 x_n^m + \eta_1(x_n y_n) \\ x_{n+1} &= B_l y_n^l + B_{l-1} y_n^{l-1} x_n + \ldots + B_0 x_n^l + \eta_2(x_n y_n) \end{aligned} \quad \ldots\ldots [1]$$

where the functions $\eta_1(xy)$, $\eta_2(xy)$ satisfy the conditions[2]

$$\left.\begin{aligned} \eta_i(xy) &= o(r^m, r^l) \\ \eta_i(0,0) &= 0 \\ r &= \sqrt{x^2 + y^2} \\ m \geqslant 2 \qquad & l \geqslant 2 \end{aligned}\right\} \quad [B]$$

The system of equations

$$\begin{aligned} y_{n+1} &= P_m(x_n y_n) = \sum_{k=0}^{m} A_k y_n^k x_n^{m-k} \\ x_{n+1} &= Q_l(x_n y_n) = \sum_{k=0}^{l} B_k y_n^k x_n^{l-k} \end{aligned} \quad \ldots\ldots [2]$$

will be called a "simplified" system, corresponding to system of Eqs. 1. If we first limit ourselves to the case $m = l$, system 2, after conversion to polar coordinates, becomes the system

$$\begin{aligned} r_{n+1} &= [P_m^2(1,k_n) + Q_m^2(1,k_n)]\cos^{2m}\varphi_n \cdot r_n^{2m} \\ k_{n+1} &= P_m(1,k_n)/Q_n(1,k_n) \end{aligned} \quad \ldots\ldots [3]$$

where

$$k_n = \tan \varphi_n = y_n/x_n$$

The approach of the trajectories of system 2 to the coordinate origin in any direction indicates that the limit $\lim k_n = k$ exists.

The equation for determining such directions

$$k = P_m(1,k)/Q_m(1,k)$$

is called the *characteristic* equation; its roots are characteristic rays.

The first of Eqs. 3 can be written as

$$r_{n+1}^2 = \left[\frac{P_m^2(1,k_n) + Q_m^2(1,k_n)}{(1 + k_n^2)^m}\, r_n^{2(m-1)}\right] r_n^2$$

In order that the trajectory approach the coordinate origin, the requirement that

$$\frac{P_m^2(1,k) + Q_m^2(1,k)}{(1 + k^2)^m}\, r_0^{2(m-1)} < 1$$

suffices. Since the expression

$$[P_m^2(1,k) + Q_m^2(1,k)]/(1 + k^2)^m$$

is bounded for all k's, in what follows the neighborhood of the coordinate origin U is assumed such that the trajectory which begins at any point in this vicinity cannot leave it. For this it suffices to select

$$r_0 < \inf_k \left[\frac{(1 + k^2)^m}{P_m^2(1,k) + Q_m^2(1,k)}\right]^{1/2(m-1)}$$

System 2 can be examined as setting the vector field for the plane; the vector

$$\bar{\rho}_0 = \{P_m(x_0 y_0) - x_0, Q_m(x_0 y_0) - y_0\}$$

is determined at each point $(x_0 y_0)$. Obviously, this field will be continuous in this neighborhood U. If k_0 is not a characteristic ray, then for any trajectory $\{(x_n y_n)\}$ beginning at ray $k = k_0$ and tending toward zero, we can always find an n_0 such that for $n > n_0$ this trajectory determines the field $\{\bar{\rho}_{n+1} - \bar{\rho}_n\}$, whose vector can intersect the radius vector $k = k_0$ only in the direction of one sign. Therefore, analogous to (8) p. 101, we have the following theorem:

Theorem 1 *Let $k_1^0 < k < k_2^0$ be an angle which does not include the characteristic ray. Then one can find such a small r_0 that on any trajectory starting in the sector $k_1^0 < k < k_2^0$, the variable k_n varies monotonically with n and the trajectory leaves the sector.*

Proof: Let us assume the contrary; whatever ρ_0 be, a trajectory can be found which is included in the sector $k_1^0 < k < k_2^0$ and such that along it k_n changes non-monotonically. Let us now examine the numerical sequence $\rho_1 \rho_2 \ldots \rho_m \to 0$ and let $L_1 L_2 \ldots L_m \ldots$ be the sequence of trajectories in-

---

Translated from *Izvestiia Vysshikh Uchebnikh Zavedenii, Matematika (Bulletin of the Institutes of Higher Learning, Mathematics)*, 1960, no. 1, pp. 166–174. Translated by Primary Sources, New York.

[1] Numbers in parentheses indicate References at end of paper.

[2] The case $m = 1$, $l = 1$ is examined in (7).

cluded in the sectors

$$T_1: 0 \leqslant \rho < \rho_1 \qquad k_1^0 < k < k_2^0$$

$$T_2: 0 \leqslant \rho < \rho_2 \qquad k_1^0 < k < k_2^0$$

$$\cdots\cdots\cdots\cdots\cdots\cdots\cdots$$

$$T_m: 0 \leqslant \rho < \rho_m \qquad k_1^0 < k < k_2^0$$

$$\cdots\cdots\cdots\cdots\cdots\cdots\cdots$$

respectively. Since, by assumption, the function k_n changes non-monotonically on L_m $(m = 1, 2, \ldots)$, on the strength of field continuity there exists a point $(\bar{\rho}_m k_m)$, included in T_m, in which the field direction coincides with the direction of the radius vector $k = k_m$, or is the exact opposite of it. The numbers $\{k_m\}$ form a bounded sequence, and therefore a convergent subsequence can be selected from it. With no loss of generality, it can be assumed that the initial sequence is convergent. Let the limit of this sequence be $\bar{k}$. Obviously, $k_1^0 < \bar{k} < k_2^0$. Then, from the definition of characteristic number, the direction $k = \bar{k}$ is characteristic, and we arrive at the contradiction of the condition of the theorem; the theorem is proved.

Let us examine some sufficiently small sector of radius R with its center at a particular point. The radii which bound the sector will be called the sides of the sector and the circumferential arc its boundary. This sector is called a *normal region* if:

1 It includes only one characteristic direction and its sides L_1 and L_2 are not characteristic.

2 Within the sector and at its edges the field direction is non-orthogonal to the direction of the radius vector drawn at a given point.

Let us examine any point Q on the side of the sector. Since the sector is a normal region, at any point of U which at the same time is a point in the sector, the field vector is directed toward the particular point. Therefore there are always three possibilities for the location of field vectors at the sides of the normal regions:

a The field vectors at all points L_1 and L_2 are directed out of the sector; such a normal region is called a *type-I region.*

b The field vectors on the sides are directed into the sector; such a normal region is called a *type-II region.*

c The field vectors for L_1 are directed into the sector, and for L_2 out of the sector; this is a *type-III region.*

In what follows we shall examine that part of the normal region which is located entirely within U. Let the normal region contain ray $k = \bar{k}$. Let us assume that $\bar{k}$ is not a root of the equation $Q_m(1,k) = 0$.

Then for system 3 in the normal region we have

$$k_{n+1} - k_n = \frac{P_m(1,k_n) - k_n Q_m(1,k_n)}{Q_m(1,k_n)} = \frac{C(k_n - \bar{k})^s + o(|k_n - \bar{k}|^s)}{G_0 + o(|k_n - \bar{k}|)} \qquad [4]$$

Here the following possibilities can obtain:

1 $\bar{k}$ is a root of odd order and $CG_0 > 0$.
2 $\bar{k}$ is a root of odd order and $CG_0 < 0$.
3 $\bar{k}$ is a root of even order.

Let us examine each case individually. In the first case, from expression 4 we get

$$\operatorname{sign}(k_{n+1} - k_n) = \operatorname{sign} CG_0(k_n - \bar{k})^s \qquad [5]$$

On side $L_1 (k_n > \bar{k})$ we get $k_{n+1} > k_n$, and on side $L_2 (k_n < \bar{k})$ we have $k_{n+1} < k_n$. In this case the normal region is a type-I region.

In case 2, on side L_1 we have $k_{n+1} < k_n$, and, analogously, for L_2 we get $k_{n+1} > k_n$; the second case gives a normal type-II region. In this case, in light of Eq. 4, for k_n's sufficiently close to $\bar{k}$ we have

$$k_{n+1} - k_n \approx (C/G_0)(k_n - \bar{k})^s$$

Let us examine

$$k_{n+1} - \bar{k} \approx (C/G_0)(k_n - \bar{k})^s + k_n - \bar{k} = [(C/G_0)(k_n - \bar{k})^{s-1} + 1](k_n - \bar{k})$$

If $s > 1$, we will have

$$\operatorname{sign}(k_{n+1} - \bar{k}) = \operatorname{sign}(k_n - \bar{k})$$

i.e., rays $k = k_n$ and $k = k_{n+1}$ are located on one side of the characteristic ray. The trajectory approaches the coordinate origin along ray $k = \bar{k}$, always remaining on one side of it.

If $s = 1$

$$k_{n+1} - \bar{k} \approx [C/G_0 + 1](k_n - \bar{k})$$

When $C/G_0 > -1$, the entire trajectory is again located on one side of the characteristic ray $k = \bar{k}$. When $C/G_0 < -1$ we have

$$\operatorname{sign}(k_{n+1} - \bar{k}) = -\operatorname{sign}(k_n - \bar{k})$$

If

$$|C/G_0 + 1| < 1$$

then

$$|k_n - \bar{k}| \to 0$$

and each trajectory in the normal region tends toward the coordinate origin, bordering on the characteristic ray $k = \bar{k}$; whereas in the case $C/G_0 < -1$ the even half of the trajectory is located on one side of the characteristic ray and the uneven half of the trajectory is on the other side.

If $|C/G_0 + 1| > 1$, $|k_n - \bar{k}|$ increases with an increase in n, and the trajectory emerges from the region through the side, although the sector is a type-II region.

The case $|C/G_0 + 1| = 1$ is critical. The behavior of the trajectory will depend on higher order terms in the expansion of the expressions

$$P_m(1,k) - kQ_m(1,k) \qquad Q_m(1,k)$$

This means that in case 2 the trajectories approach the coordinate origin along the characteristic ray $k = \bar{k}$, remaining inside a sufficiently small sector, except for the case $s = 1$, $|C/G_0 + 1| > 1$, when the trajectory leaves this sector.

Let us examine the third case: $\bar{k}$ is an even root. With no loss of generality, we can consider that $CG_0 > 0$; from Eq. 5 we then get

$$\operatorname{sign}(k_{n+1} - k_n) = +1$$

On both sides of the characteristic ray we have $k_{n+1} > k_n$; i.e., we get a normal type-III region. In light of the equality

$$\operatorname{sign}(k_{n+1} - k) = \operatorname{sign}\{[(C/G_0)(k_n - \bar{k})^{s-1} + 1](k_n - \bar{k})\}$$

we get, for k_n's close to $\bar{k}$

$$\operatorname{sign}(k_{n+1} - \bar{k}) = \operatorname{sign}(k_n - \bar{k})$$

i.e., the rays $k = k_n$ and $k = k_{n+1}$ are located on one side of the characteristic ray $k = \bar{k}$. On one side of the characteristic ray all trajectories emerge at the coordinate origin, approaching the ray $k = \bar{k}$; on the other side the trajectories move away from the characteristic ray and leave the normal region. The characteristic ray divides this region into two parts, one of which is the region of attraction, the other the region of repulsion.

Let us now examine the remaining case, when $k = \bar{k}$ is simultaneously the root of the equation $Q_m(1,k) = 0$, i.e., the equalities

$$\bar{k} = P_m(1,\bar{k})/Q_m(1,\bar{k}) \qquad Q_m(1,\bar{k}) = 0 \qquad [6]$$

are fulfilled. If $P_m(1,\bar{k}) \neq 0$, it follows that $\bar{k} = \infty$, i.e., $\lim k_n = \infty$, and the entire trajectory approaches the coordinate origin along the Oy axis, about which a normal type-II region can be constructed.

If $P_m(1,\bar{k}) = 0$, considering Eq. 6, system 1 can be written in the form

$$y_{n+1} = (y_n - \bar{k}x_n)Y_1(x_n y_n) = x_n^m(k_n - \bar{k})^{s_1}Y_2(1,k_n)$$
$$x_{n+1} = (y_n - \bar{k}x_n)X_1(x_n y_n) = x_n^m(k_n - \bar{k})^{s_2}X_2(1,k_n)$$

where

$$Y_2(1,\bar{k}) \neq 0$$
$$X_2(1,k) \neq 0$$

If $s_1 < s_2$

$$k_{n+1} = [Y_2(1,k_n)]/[(k_n - \bar{k})^{s_2-s_1}X_2(1,k_n)]$$

and if k_n has a limit, it is $\lim k_n = \infty$.

In this case the trajectories can approach the coordinate origin only along the Oy axis. Analogously, in the case $s_1 > s_2$, the trajectories will approach only along the Ox axis.

In the case $s_1 = s_2$ we have the characteristic equation

$$\bar{k} = \frac{P_m(1,\bar{k})}{Q_m(1,\bar{k})} = \frac{Y_2(1,\bar{k})}{X_2(1,\bar{k})}$$

where $X_2(1,\bar{k}) \neq 0$; i.e., we again arrive at the previously examined cases.

Now we can eliminate one of the limitations imposed on system 1, namely, the case $l \neq m$, not examined previously, using the rotation of a plane

$$\xi = \alpha x - \beta y \qquad \alpha^2 + \beta^2 = 1$$
$$\eta = \beta x + \alpha y$$

which reduces to the case $l = m$, already examined. Using such rotation, system 1 becomes

$$\xi_{n+1} = \alpha\tilde{Q}_l(\xi_n\eta_n) - \beta\tilde{P}_m(\xi_n\eta_n) + \omega_1(\xi_n\eta_n)$$
$$\eta_{n+1} = \beta\tilde{Q}_l(\xi_n\eta_n) + \alpha\tilde{P}_m(\xi_n\eta_n) + \omega_2(\xi_n\eta_n) \quad [7]$$

where

$$\omega_1 = \alpha\eta_2 - \beta\eta_1$$
$$\omega_2 = \beta\eta_2 + \alpha\eta_1$$

With no loss of generality, we can assume that $l > m$, and system 7 then takes the form

$$\xi_{n+1} = -\beta\tilde{P}_m(\xi_n\eta_n) + \gamma_1(\xi_n\eta_n)$$
$$\eta_{n+1} = \alpha\tilde{P}_m(\xi_n\eta_n) + \gamma_2(\xi_n\eta_n) \quad [8]$$

where γ_1 and γ_2 unite the highest order terms. From this

$$k_{n+1} = \frac{\eta_{n+1}}{\xi_{n+1}} = \frac{\alpha\tilde{P}_m(\xi_n\eta_n) + \gamma_2(\xi_n\eta_n)}{-\beta\tilde{P}_m(\xi_n\eta_n) + \gamma_1(\xi_n\eta_n)}$$

and when $\xi_n \to 0$, $\eta_n \to 0$, we have $\lim k_{n+1} = -\alpha/\beta$. System 8 has one characteristic ray $\bar{k} = -\alpha/\beta$. Further examination of system 8 is completely analogous to the examination of system 3 given previously.

This method makes it possible to get an idea of the behavior of trajectories near all characteristic rays.

In the remaining part of region U, however, the behavior of the trajectories is described by Theorem 1. Thus, for system 2 a full picture of the location of trajectories in the vicinity of a singular point can be obtained.

Let us now turn to an examination of "complete" system 1 and determine the role and influence of the supplementary functions $\eta_i(xy)$ on the behavior of trajectories near a characteristic ray.

To find the characteristic rays, the limits

$$\lim k_{n+1} = \lim \frac{P_m(1,k_n) + \eta_2(x_n y_n)/x_n^m}{Q_m(1,k_n) + \eta_1(x_n y_n)/x_n^m}$$

must be computed, and for $x_n \neq 0$ we get the characteristic equation

$$\bar{k} = P_m(1,\bar{k})/Q_m(1,\bar{k})$$

which coincides with the characteristic equation for "simplified" system 2. The exceptional case $x_n = 0$ corresponds to the approach of the trajectories to the coordinate origin along the Oy axis, i.e., to the direction $k = \infty$. Except for this direction, the characteristic rays of systems 1 and 2 are identical. The behavior of trajectories near the Oy axis can be studied by introducing a new angular coefficient

$$\chi_{n+1} = \frac{x_{n+1}}{y_{n+1}} = \frac{Q_m(\chi_n,1) + \eta_1(x_n y_n)/y_n^m}{P_m(\chi_n,1) + \eta_2(x_n y_n)/y_n^m}$$

The latter equation must be investigated near the straight line $\chi = 0$, where, obviously, $y \neq 0$. If the characteristic direction $\chi = 0$ actually exists, the equality

$$0 = Q_m(0,1)/P_m(0,1)$$

should be fulfilled for it, but this latter is equivalent to the fact that the characteristic equation for system 2 has the root $k = \infty$. Thus the characteristic rays are invariant relative to any functions $\eta_1(xy), \eta_2(xy)$ which satisfy conditions B; i.e., the characteristic rays of system of Eqs. 1 satisfy the equation $k = P_m(1,k)/Q_m(1,k)$.

From system 1 we have

$$k_{n+1} = \frac{P_m(1,k_n) + \eta_2(x_n y_n)/x_n^m}{Q_m(1,k_n) + \eta_1(x_n y_n)/x_n^m} \quad [9]$$

In the light of the foregoing, we can consider that the approach to the coordinate origin occurs in a direction other than along the Oy axis; i.e., k is a finite value, and, starting with some n, x_n does not equal zero. From this and also from conditions B, we have

$$\lim_{r\to 0} \frac{\eta_i(xy)}{x^m} = \lim_{r\to 0} \frac{\eta_i(xy)}{r^m \cos^m\varphi} = 0$$

Therefore Eq. 9 can be written another way

$$k_{n+1} = [P_m(1,k_n) + \epsilon_2(x_n y_n)]/\,[Q_m(1,k_n) + \epsilon_1(x_n y_n)] \quad [10]$$

where $\epsilon_i(xy) = o(x^m)$ for sufficiently small y's.

Theorem 2 *If functions $\eta_i(xy)$ satisfy conditions B, there is a vicinity U of a particular point such that any trajectory of system 1, beginning at any point in U, tends asymptotically toward the coordinate origin.*

Proof: We have

$$r_{n+1}^2 = x_{n+1}^2 + y_{n+1}^2 = P_m^2(x_n y_n) + Q_m^2(x_n y_n) + R(x_n y_n)$$

where

$$R(xy) = 2P_m(xy)\eta_1(xy) + 2Q_m(xy)\eta_2(xy) + \eta_1^2(xy) + \eta_2^2(xy)$$

Since the functions $\eta_i(xy)$ satisfy conditions B, while functions P_m, Q_m are limited in U, from this we have

$$r_{n+1}^2 = \left\{[P_m^2(1,k_n) + Q_m^2(1,k_n)]\cos^{2m}\varphi_n \cdot r_n^{2m-2} + \frac{R(x_n y_n)}{r_n^2}\right\} r_n^2$$

Finally we have

$$r_{n+1}^2 = \left\{\frac{P_m^2(1,k_n) + Q_m^2(1,k_n)}{(1+k_n^2)^m} \cdot r^{2m-2} + \frac{R(x_n y_n)}{r_n^2}\right\} r_n^2 \quad [11]$$

Since $R(xy) = o(r^m)$, for r's less than some r'

$$\frac{|R(xy)|}{r^2} < \frac{1}{2}$$

holds. Further, the inequality

$$\frac{P_m^2(1,k) + Q_m^2(1,k)}{(1 + k^2)^m} r^{2m-2} < \frac{1}{2}$$

is fulfilled for r's less than r'', where

$$r'' = \inf_k \left\{ \frac{(1 + k^2)^m}{2[P_m^2(1,k) + Q_m^2(1,k)]} \right\}^{1/(2m-2)}$$

From this and from the foregoing, we find for $r < \min \{r', r''\}$ from Eq. 11 we have $r_{n+1}^2 < r_n^2$, whence the proof of the theorem immediately follows.

Now we should investigate cases of the invariant nature of the normal regions relative to functions $\eta_1(xy)$, $\eta_2(xy)$.

Let us select some characteristic direction $k = \bar{k}$ and construct about it a normal region, completely within U. From Eq. 10 we get

$$\Delta k_n = k_{n+1} - k_n = \frac{P_m(1,k_n) - k_n Q_m(1,k_n) + \epsilon_2 - k_n \epsilon_1}{Q_m(1,k_n) + \epsilon_1} \qquad [12]$$

The case when $k = \bar{k}$ is a root of equation $Q_m(1,k_n) = 0$ was examined previously, so that we will consider $Q_m(1,\bar{k}) \neq 0$. Let the sides of the normal region be determined by the rays $k = \bar{k} + k^0$, $k = \bar{k} - k^0$. We can select k^0 so small that in a sufficiently small normal region the denominator of expression 12 does not revert to zero and has a sign identical with that of $Q_m(1,\bar{k}) = G_0$. Therefore Eq. 12 takes the form

$$\Delta k_n = \frac{C(k_n - \bar{k})^s + o(|k_n - \bar{k}|^s) + f(x_n y_n)}{G_0 + o(|k_n - \bar{k}|) + \epsilon_1(x_n y_n)} \qquad [13]$$

where

$$f(xy) = \epsilon_2(xy) - (y/x)\epsilon_1(xy) = o(x^m)$$

On the ray $k = \bar{k} + k^0$, for points sufficiently close to the coordinate origin, we have, from Eq. 13

$$\text{sign } \Delta k_n = \text{sign } CG_0(k_n - \bar{k})^s = \text{sign } CG_0 \text{ sign } (k_n - \bar{k})^s \qquad [14]$$

This same equality will also be obtained for the ray $k = \bar{k} - k^0$ for points located sufficiently close to the coordinate origin. The type of normal region for the "simplified" system 2 is determined by relationship 14. This, then, is proof of the following theorem.

Theorem 3 *The type of normal region of system* 1 *is invariant relative to any functions* $\eta_1(xy)$ *and* $\eta_2(xy)$ *which satisfy conditions B.*

All the foregoing examinations were made on the assumption that the characteristic direction

$$k = P_m(1,k)/Q_m(1,k) \qquad [15]$$

is actually an equation, and is not satisfied identically. But it can be shown that Eq. 15 is an identity and all k's will be characteristic. On this basis we can consider k finite and $Q_m(1, k)$ not equal to zero. Then Eq. 13 takes the form

$$\Delta k_n = k_{n+1} - k_n = \frac{\epsilon_2(x_n y_n) - k_n \epsilon_1(x_n y_n)}{Q_m(1,k_n) + \epsilon_1(x_n y_n)} \qquad [16]$$

Since $Q_m(1, \bar{k}) \neq 0$, we can select k_n so close to $\bar{k}$ that sign $Q_m(1, k_n) = \text{sign } G_0$. Then we get

$$\text{sign } \Delta k_n = \text{sign } \{G_0[\epsilon_2(x_n y_n) - k_n \epsilon_1(x_n y_n)]\} \qquad [17]$$

The function $f(xy) = \epsilon_2(xy) - (x/y)\epsilon_1(xy)$ has a limit of zero at the coordinate origin if the tendency occurs along a direction different from the Oy axis. For further investigation of the nature of ray $k = \bar{k}$ we must place limits on the function $f(xy)$.

References

1 Trans. IInd All-Union Conference on the Theory of Automatic Control, *AN SSSR, M (Acad. Sci. USSR, Moscow)*, 1954.

2 Tsypkin, Ya. Z., "The Theory of Intermittent Control," *Avtomatika i Telemekhanika, (Automation and Telemetry)*, vol. X, no. 3, 1949.

3 Perron, O., "The Stability and Asymptotic Behavior of the Solution of a System of Finite Difference Equations," *J. für die Reine und Angewandte Mathem. (J. Pure and Appl. Math.)*, vol. 161, no. 1, 1929.

4 Bellman, R., "On the Boundedness of Solutions of Nonlinear Differential and Difference Equations," American Mathematical Society, Trans., vol. 62, no. 3, 1947.

5 Skalkina, M. A., "The Connection Between the Stability of the Solutions of Differential and Finite-Difference Equations," *Prikladnaia Matematika i Mekhanika (J. Appl. Math. and Mech.)*, vol. 19, no. 3, 1955.

6 Koval', P. I., "The Stability of the Solutions of Systems of Linear Difference Equations," *Ukrainskii Matematicheskii Zhurnal (Ukrainian Mathematical J.)*, vol. 9, no. 2, 1957.

7 Panov, A. M., "Behavior of the Trajectories of a System of Finite-Difference Equations in the Vicinity of a Particular Point," *Ural'skii Gosudartsvennyi Universitet, Uch. Zap. (Ural State University, Scientific Notes)*, no. 19, 1956, pp. 88–99.

8 Nemytskii, V. V. and Stepanov, V. V., "A Qualitative Theory of Differential Equations," GITTL, M-L (State Publishing House of Technical and Theoretical Literature, Moscow-Leningrad), 1949, p. 101.

—Submitted June 12, 1958

Reviewer's Comment

The results of this paper are directly applicable to the study of the stability of nonlinear sampled-data control systems with two variables. Systems of the kind defined in the paper can be synthesized by the incorporation of computer elements in the feedback loop. These techniques are also applicable to continuous systems which are approximated by discretized systems. The use of such approximate methods for linear systems is given in *Control System Synthesis* by J. C. Truxal.

The paper is indicative not only of the Russian interest in nonlinear system analysis, but also of the fact that Russian mathematicians and engineers often find common grounds of interest.

—Charles Saltzer
Department of Mathematics
University of Cincinnati

Fall of a Spherical Drop in the Presence of Evaporation or Condensation of Vapors at Its Surface

V. S. NOVOSELOV

1. In his study of the fall of a spherical drop of water in a stationary atmosphere, saturated with water vapor, Sommerfeld (1)[1] proceeds from the assumption that as a result of condensation the mass of the drop increases in proportion to its surface area. This law, however, holds true only for evaporation in a vacuum.

In the case of slow fall in a gaseous medium both the rate of condensation and the rate of evaporation obey Maxwell's law

$$dm/dt = ekr \qquad [1]$$

In Eq. 1, m is the mass of the drop; e is equal to ± 1 (plus sign for condensation, minus sign for evaporation); the positive constant k depends on the diffusion coefficient and the difference in vapor concentration at the surface of the drop and at a distance from it; r is the radius of the drop.

If the fall is not slow (Re from 100 to 1000), then, as the experiments of Froessling (3) and other investigators (2) have shown, the rates of condensation and evaporation are given by

$$dm/dt = epr\sqrt{rv} \qquad [2]$$

where p = constant > 0 and v is the velocity of the drop. Eq. 2 is also confirmed by boundary layer theory (2).

Two problems are discussed here, namely, the slow and rapid fall of a drop in a stationary gaseous medium in the presence of condensation or evaporation of vapors at its surface. Since before condensation and after evaporation the vapor particles have zero velocity, the reaction (4), owing to the change in mass, will be equal to, $(dm/dt)\bar{v}$.

2. For slow fall the resistance of the medium is taken as $-\alpha\pi r^2\bar{v}$, where α = constant > 0. Projecting onto the vertical x-axis, directed downwards, we get

$$m\ddot{x} = mg - (\alpha\pi r^2 + ekr)\dot{x} \qquad [3]$$

We have

$$m = \gamma\tfrac{4}{3}\pi r^3 \qquad [4]$$

where γ is the density. Differentiating Eq. 4 with respect to time and equating the result to Eq. 1, we find

$$r = \sqrt{r_0^2 + vt} \qquad v = ek/2\pi\gamma \qquad [5]$$

By virtue of Eqs. 4 and 5, Eq. 3 can be transformed into

$$\ddot{x} = \frac{3}{2}\left[\frac{\alpha}{2\gamma\sqrt{r_0^2 + vt}} + \frac{v}{r_0^2 + vt}\right]\dot{x} = g \qquad [6]$$

If we may neglect the resistance of the medium ($\alpha = 0$), then, integrating Eq. 6 and bearing in mind Eq. 5, we find

$$\dot{x} = \frac{1}{r^3}\left[\dot{x}_0 r_0^3 - \frac{2}{5}\frac{g}{v}(r_0^5 - r^5)\right] \qquad [7]$$

Integrating linear Eq. 6 for $\alpha = 0$, we get

$$\dot{x} = \frac{c_1}{(r_0^2 + vt)^{3/2}\, e^{a\sqrt{r_0^2 + vt}}} + \frac{4g\gamma}{3\alpha}\left[\sqrt{r_0^2 + vt} - \frac{4}{a} + \frac{12}{a^2\sqrt{r_0^2 + vt}} - \frac{24}{a^3(r_0^2 + vt)} + \frac{24}{a^4(r_0^2 + vt)^{3/2}}\right] \qquad [8]$$

Here we have introduced the notation $a = 3\alpha/2v\gamma$. The constant in solution 8 is equal to

$$c_1 = \left[\dot{x}_0 - \frac{4g\gamma}{3\alpha}\left(r_0 - \frac{4}{a} + \frac{12}{a^2 r_0} - \frac{24}{a^3 r_0^2} + \frac{24}{a^4 r_0^3}\right)\right] r_0^3 e^{ar_0} \qquad [9]$$

Let us consider the case of small condensation or small evaporation, and limit ourselves in Eq. 8 to terms containing the first power of the parameter v. From Eq. 9 we get

$$\dot{x} = \frac{4g\gamma r_0}{3\alpha} - \left(\frac{4g\gamma r_0}{3\alpha} - \dot{x}_0\right) e^{-3\alpha t/4\gamma r_0} + v\left\{\frac{4g\gamma}{3\alpha}\left(\frac{t}{2r_0} - \frac{8\gamma}{3\alpha}\right) + \left[-\frac{3}{16r_0^2}\left(\frac{4g\gamma r_0}{3\alpha} - \dot{x}_0\right)\left(\frac{\alpha t^2}{\gamma r_0} - 8t\right) + \frac{32g\gamma^2}{9\alpha^2}\right] e^{-3\alpha t/4\gamma r_0}\right\} \qquad [10]$$

In the case in question, Eq. 5 assumes the form

$$r = r_0 + \frac{1}{2}\frac{vt}{r_0}$$

Therefore, neglecting exponential terms, we find

$$\dot{x} = \frac{4g\gamma r}{3\alpha} - \frac{32v g\gamma^2}{9\alpha^2} \qquad [11]$$

Eq. 11 gives the limiting velocity of the drop, attained in the course of a lengthy period of time. This formula shows that in the presence of condensation the limiting velocity is reduced by an amount $16kg\gamma/9\pi\alpha^2$, and in the presence of evaporation increases by the same amount.

Integrating Eq. 7, we find

$$x = x_0 + \frac{2\dot{x}_0 r_0^2}{v}\left(1 - \frac{r_0}{r}\right) - \frac{g r_0^4}{v^2}\left[1 - \frac{4}{5}\frac{r_0}{r} - \frac{1}{5}\left(\frac{r}{r_0}\right)^4\right] \qquad [12]$$

Eq. 12 expresses the law governing the fall of a drop, when the resistance is negligibly small.

When $\alpha = 0$, integrating Eq. 8, we get

$$x = c_2 - \frac{2c_1}{v} e^{-ar}\left[\frac{1}{r} - aE_i(-ar)\right] + \frac{8g\gamma}{3v\alpha}\left(\frac{r^3}{3} - \frac{4vt}{a} + \frac{12r}{a^2} - \frac{24\ln r}{a^3} - \frac{24}{a^4 r}\right) \qquad [13]$$

Translated from *Vestnik Leningradskogo Universiteta* (*Bulletin of Leningrad University*), 1960, no. 7, pp. 116–119. Translated by Research Information Service, New York.

[1] Numbers in parentheses indicate References at end of paper.

where the constant c_2 is equal to

$$c_2 = x_0 + \frac{2c_1}{\nu} e^{-ar_0}\left[\frac{1}{r_0} - aE_1(-ar_0)\right] - \frac{8g\gamma}{3\nu\alpha}\left(\frac{r_0^3}{3} + \frac{12r_0}{a^2} - \frac{24\ln r_0}{a^3} - \frac{24}{a^4 r_0}\right) \quad [14]$$

In Eq. 13 the radius of the drop r is determined from Eq. 5. In Eqs. 13 and 14, $E_i(x)$ denotes an integral exponential function, equal to $\int_{-\infty}^{x} \frac{e^y}{y}\,dy$.

In the case of small condensation or small evaporation, integrating Eq. 10, we have

$$x = x_0 + \frac{4gr_0}{3\alpha}\left(\frac{4g\gamma r_0}{3\alpha} - \dot{x}_0\right)(1 - e^{-3\alpha t/4\gamma r_0}) + \frac{4g\gamma r_0 t}{3\alpha} + \nu\left[\frac{4g\gamma}{3\alpha}\left(\frac{t^2}{4r_0} - \frac{8\gamma t}{3\alpha}\right) - \frac{1}{4}\left(\frac{4g\gamma r_0}{3\alpha} - \dot{x}_0\right)\left(\frac{16\gamma r_0 t}{3\alpha} - t^2\right)e^{-3\alpha t/4\gamma r_0} + \frac{128g\gamma^3 r_0}{27\alpha^3}(1 - e^{-3\alpha t/4\gamma r_0})\right] \quad [15]$$

For large intervals of time, for which the exponential terms in Eq. 15 may be neglected, we get

$$x = x_0 + \frac{4gr_0}{3\alpha}\left(\frac{4g\gamma r_0}{3\alpha} - \dot{x}_0\right) + \frac{4g\gamma r_0 t}{3\alpha} + \nu\left[\frac{4g\gamma}{3\alpha}\left(\frac{t^2}{4r_0} - \frac{8\gamma t}{3\alpha}\right) + \frac{128g\gamma^3 r_0}{27\alpha^3}\right] \quad [16]$$

Note particularly that the derivative of Eq. 16 coincides with Eq. 11.

3. When the fall of the drop is rapid, the resistance of the medium is taken as $\beta\pi r^2 v^2$. Applying Eq. 2, in projection onto the vertical x-axis, we get

$$\ddot{x} = g - \frac{3}{4}\frac{\beta\dot{x}^2}{\gamma r} - \frac{3}{4}\frac{ep}{\pi\gamma r^{3/2}}x^{3/2} \quad [17]$$

Differentiating Eq. 4 and equating the result to the left member of Eq. 2 we have

$$\dot{r} = \frac{ep}{4\pi\gamma}\sqrt{\frac{\dot{x}}{r}} \quad [18]$$

We shall consider the case when p is small. The solution of Eqs. 17 and 18 may be sought in the form of a series of powers of $\mu = ep/4\pi\gamma$. For the sake of simplicity we shall limit ourselves to terms containing the first power of μ. Accordingly, we shall seek a solution of the form $r = \rho + \mu\xi$, $\dot{x} = v + \mu\eta$. In order to determine zero terms we obtain the equations

$$\dot{v} = g - \frac{3}{4}\frac{\beta}{\rho\gamma}v^2 \qquad \dot{\rho} = 0$$

Hence we have

$$\rho = r_0$$

$$v = v_1\frac{v_0 + v_1\tan\mathrm{h}\,(gt/v_1)}{v_1 + v_0\tan\mathrm{h}\,(gt/v_1)}$$

$$v_1 = 2\sqrt{gr_0\gamma/3\beta} \quad \ldots\ldots [19]$$

The variables ξ and η are determined by solving, with zero initial conditions, the equations

$$\dot{\eta} = -\frac{3}{2}\frac{\beta v}{\gamma r_0}\eta + \frac{3\beta}{4\gamma}\left(\frac{v}{r_0}\right)^2\xi - 3\left(\frac{v}{r_0}\right)^{3/2}$$

$$\dot{\xi} = \sqrt{v/r_0} \quad \ldots\ldots [20]$$

Eqs. 20 make it possible to determine ξ and η by quadratures.

As Eqs. 19 show, if the movement continues for a sufficient length of time, the quantity v approaches v_1. Since, when a body falls in a resisting medium, the limiting velocity is attained fairly rapidly, we shall assume that starting from a certain moment of time v becomes equal to v_1. Taking the moment of time referred to as the initial moment, we get

$$\dot{\eta} + \frac{3\beta v_1}{2\gamma r_0}\eta = \frac{3\beta}{4\gamma}\left(\frac{v_1}{r_0}\right)^2\xi - 3\left(\frac{v_1}{r_0}\right)^{3/2} \qquad \xi = \sqrt{\frac{v_1}{r_0}}\,t \quad [21]$$

On integrating Eqs. 21, we have

$$\eta = \sqrt{\frac{v_1}{r_0}}\left[\frac{t}{2}\frac{v_1}{r_0} - \frac{7\gamma}{3\beta}\left(1 - e^{-\frac{3\beta v_1}{2r_0}t}\right)\right] \quad [22]$$

By virtue of Eq. 22 we obtain

$$\dot{x} = 2\sqrt{\frac{gr\gamma}{3\beta}} - \frac{7ep}{12\gamma\beta}\sqrt{\frac{v_1}{r_0}}\left(1 - e^{-\frac{3\beta v_1}{2r_0}t}\right) \quad [23]$$

The first term in Eq. 23 represents the limiting velocity for a drop of radius r. The second term shows that the limiting velocity decreases for condensation and increases for evaporation. If we neglect the exponential term, then the change in the limiting velocity will be $(7p/6\pi\beta)(\sqrt{g\gamma/3\beta})$.

References

1 Sommerfeld, A., *Mekhanika (Mechanics)*, Moscow, GIIL, 1947.
2 Fuks, N. A., "Evaporation and Growth of Drops in a Gaseous Medium," Moscow, Izvestiia Akademii Nauk, USSR, 1958.
3 Froessling, N., *Gerlands Beitr. Geophys.*, vol. 52, 1938, p. 170.
4 Meshcherskiy, I. V., *Studies in the Mechanics of Bodies of Variable Mass*, Moscow-Leningrad, GITTL, 1949.

—Submitted April 10, 1959

Reviewer's Comment

This detailed analysis constitutes an excellent contribution to the scientific study of the ballistics of droplets, and represents a noteworthy extension of the previous papers by Ingebo (1) and Miesse (2,3), under slightly different assumptions. Whereas the latter investigators assumed an inverse variation of the drag coefficient (α) with the Reynolds number (confirmed by experimental data), the present analysis was based on a constant drag coefficient, which is a reasonable assumption for the large values of the Reynolds number characteristic of terminal velocity conditions. A further difference in the analysis results from Novoselov's inclusion of the (ekr) term in Eq. 3. Although this term can be derived directly by considering the first derivative of the momentum of the evaporating (or growing) drop, the following consideration of the basic definition for the momentum derivative ap-

plied to the total mass indicates that the additional term is of second order.

Consider the diagram

At time t, the droplet with mass M is traveling at velocity V. At time $(t + dt)$, an incremental mass dM has vaporized and accelerated to velocity $V + dV_2$ whereas the remaining liquid mass $(M - dM)$ has accelerated to velocity $V + dV_1$.

Since force is equal to the time derivative of momentum

$$F = \frac{d(MV)}{dt} = \frac{(M - dM)(V + dV_1) + dM(V+dV_2) - MV}{dt}$$

$$= M\frac{dV_1}{dt} + \text{terms of second order}$$

On the basis of the physical assumptions, the subsequent derivations are straightforward in nature and can be checked readily.

—CHARLES MIESSE
Armour Research Foundation
Illinois Institute of Technology

1 Ingebo, R. D., "Vaporization Rates and Drag Coefficients for Isooctane Sprays in Turbulent Air Streams," NACA TN 3265, 1954.
2 Miesse, C. C., "Ballistics of an Evaporating Droplet," JET PROPULSION, vol. 24, 1954, p. 237.
3 Miesse, C. C., "The Effect of a Variable Evaporation Rate on the Ballistics of Droplets," *J. Franklin Institute*, vol. 264, 1957, p. 391.

Relation of Frequency of Ultra Short Wave Field Amplitude Decay, Drift Speed of Inhomogeneities in the Troposphere, and Carrier Frequency

A. A. SEMENOV and G. A. KARPEYEV

Department of Radiowave Propagation Moscow University

1. Theoretical Introduction

IN MANY respects the rate (or quasi frequency) of fading of a field determines the limits and possibilities of increasing the amount of information transmitted by a signal in unit time. In connection with tropospheric dynamics, on the other hand, investigating the rate of fading of a radio signal may enable us to determine some of the dynamic parameters of the troposphere from the fluctuation characteristics.

In order to make a theoretical evaluation of the effect of regular drift of the medium and random motion of inhomogeneities, we shall consider, basing ourselves on the classical model of tropospheric scattering, an expression for the space-time correlation function $F(\mathbf{r}_0, \tau)$ of the complex amplitude of the field at the points P_1 and P_2 (1)[1] (see Fig. 1)

$$F(\mathbf{r}_0, \tau) = \int_v\int_v \frac{\rho(\mathbf{r}'', \tau)}{\Pi R i} \times \exp\{i\varphi + i[(\mathbf{r}''\nabla\mathbf{k})]\mathbf{r}'' + i\mathbf{k}\mathbf{r}'' - i\mathbf{k}_2'\mathbf{r}_0\}\, d\mathbf{r}d\mathbf{r}'' \quad [1]$$

where

$$\mathbf{k} = (2\pi/\lambda)(\mathbf{n}_1 + \mathbf{n}_2)$$
$$\mathbf{k}_2' = (2\pi/\lambda)\mathbf{n}_2'$$
$$\varphi = (\mathbf{k}_1 - \mathbf{k}_1')\mathbf{R}_0 + (\mathbf{k}_2 - \mathbf{k}_2')R_{01}$$

When $\mathbf{r}_0 = 0$, we get the special case of signal reception at a

Translated from *Vestnik Moskovskogo Universitela* (*Bulletin of Moscow University*), no. 6, 1959, pp. 131–136. Translated by Research Information Service, New York.

[1] Numbers in parentheses indicate References at end of paper.

single point (2). However, for theoretical investigations and comparison with experiment, even this case reveals the extreme limitation of a simplified treatment of the dependence of the rate of fading on the drift speed of the inhomogeneities in particular attempts to represent the correlation function of fluctuations in ϵ in the form of the product of two functions with separate dependence on the space and time displacements (3).

Actually, we shall introduce the moving system of coordinates

$$\mathbf{r}(\xi, \eta, \xi, t) = \mathbf{r}(x, y, z) - \mathbf{v}_0 t \qquad [2]$$

The correlation coefficient of the complex amplitude of the field in the moving system of coordinates then assumes the form (for an averaging time $T \to \infty$)

$$\rho_1(\tau) = \frac{\int_v \rho_1(\mathbf{r}_1'', \tau) f(\mathbf{r}_1'', \mathbf{v}_0, \tau) \exp(i\mathbf{k}_0\mathbf{r}_1'') d\mathbf{r}_1''}{\int_v \rho_1(\mathbf{r}_1'') f(\mathbf{r}_1'') \exp(i\mathbf{k}_0\mathbf{r}_1'') d\mathbf{r}_1''} \exp(i\mathbf{k}_0\mathbf{v}_0\tau) \qquad [3]$$

where

$\rho_1(\mathbf{r}_1'', \tau)$ = space-time correlation coefficient of the dielectric constant

$f(\mathbf{r}_1'', \mathbf{v}_0, \tau)$ = a function obtained from Eq. 1 as a result of corresponding substitution of coordinates of moving system

As is known (3), for a certain average value $\mathbf{k}_0$ of the vector $\mathbf{k}$ we may write

$$\frac{2\pi}{\lambda} \sin\frac{\alpha_0}{2} \leq |\mathbf{k}_0| \leq \frac{2\pi}{\lambda} \sin\frac{\alpha_0 - \alpha_1 + \alpha_2}{2}$$

where α_0 is the angle between the axes of the directional diagrams of the transmitting and receiving antennas and α_1 and α_2 are their half widths. Hence it follows that the character of the fluctuations in the field is determined not only by the properties of the process of fluctuation in the dielectric constant and the drift speed of inhomogeneities but also by the characteristics of the transmitter-receiver systems.

A single valued dependence of $\rho_0(\tau)$ on $\rho_1(\mathbf{r}_1'', \tau)$ is possible only on condition that $f(\mathbf{r}_1'', \mathbf{v}_0, \tau)$ and $f(\mathbf{r}_1'')$ are constant.

Then

$$\rho_0(\tau) = \text{const} \frac{\int \rho_1(\mathbf{r}_1'', \tau) \exp(i\mathbf{k}_0\mathbf{r}_1'') d\mathbf{r}_1''}{\int \rho_1(\mathbf{r}'') \exp(i\mathbf{k}_0\mathbf{r}_1'') d\mathbf{r}_1''} \exp(i\mathbf{k}_0\mathbf{v}_0\tau) \qquad [4]$$

or

$$\rho_0(\tau) = \text{const} \frac{\Phi_0(\mathbf{k}_0, \tau)}{\Phi_0(\mathbf{k}_0, 0)} \exp(i\mathbf{k}_0\mathbf{v}_0\tau) \qquad [5]$$

where $\Phi(\mathbf{k}_0, \tau)$ is the spatial Fourier transform of the correlation coefficient of ϵ. In particular, when $\prod_i Ri$ = constant and $\mathbf{k} = \mathbf{k}_0$ = constant these conditions are fulfilled, and, moreover, from formula 5, constant = 1, which gives

$$\rho_0(\tau) = \frac{\Phi_0(\mathbf{k}_0, \tau)}{\Phi_0(\mathbf{k}_0, 0)} \exp(i\mathbf{k}_0\mathbf{v}_0\tau) \qquad [6]$$

which is the result previously obtained (3). If, $\rho_1(\mathbf{r}_1'', \tau)$ is put in the form of a product as in (3)

$$\rho_1(\mathbf{r}_1'', \tau) = \rho'(\mathbf{r}_1'')\rho''(\tau) \qquad [7]$$

then from Eq. 1 (to obtain ρ from F it is necessary to divide expression 1 by the integral not depending on time)

$$\rho_0(\tau) \equiv \rho''(\tau) \qquad [8]$$

that is, the frequency spectrum of the amplitude fluctuations of the field does not depend on the drift speed. This contradicts known experimental data (4).

Turning back to the fundamental expression, Eq. 1, with the spacing of the receiving antennas taken into account, for a moving system of coordinates we get (1)

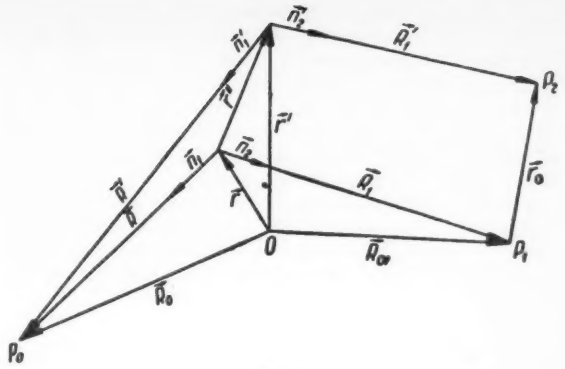

Fig. 1

$$F(\mathbf{r}_0'', \tau) = \int_v\int_v \frac{\rho_1(\mathbf{r}_1'', \tau)}{\prod_i Ri} \times \exp[i\varphi_1 + \mathbf{K}\mathbf{r}_1'']d\mathbf{r}_1 d\mathbf{r}_1'' \exp[i\mathbf{K}_0\mathbf{v}_0\tau - i\mathbf{K}\mathbf{r}_0] \qquad [9]$$

where φ_1, $\mathbf{K}$ are functions of the space-time displacement and frequency.

The dependence of the character of the field fluctuations on the frequency, geometrical conditions of propagation and drift speed proves to be rather complex; however the existence of this dependence is well known. Furthermore, Eq. 9 points to the existence of spatial anisotropy of the correlation function of the field, even when the correlation function of the dielectric constant of the medium is isotropic. The fluctuation frequency N is defined as the number of zeros of the centered amplitude of the field E'

$$E' = E(t) - E_0$$

in unit time. The quantity N is determined from the correlation function $\psi(\tau)$ of the envelope of the random process (7)

$$N = \frac{1}{\pi}\left[-\frac{\psi''(0)}{\psi(0)}\right]^{1/2}$$

The function $\psi(\tau)$ may be expressed in terms of the function $F(\mathbf{r}_0, \tau)$

$$\psi(\tau) = \frac{\pi}{4 - \pi}\left[\frac{1}{4}F_0^2(\tau) + \frac{1}{64}F_0^4(\tau) + \ldots\right]$$

where $F_0(\tau) = F(0, \tau)/F(0, 0)$.

2. Comparison With Experiment

The experimental data are far from sufficient to establish any strict dependence of the fluctuation frequency on the drift speed and the carrier frequency. It is known that for any given value of the wind speed a considerable spread in the values of the fading frequency may be observed, but the average values of this quantity have an almost linear dependence on the drift speed (1).

It may be of interest to make a statistical quantitative evaluation of this dependence. Let us take, for example, the results of a day's variation in fluctuations on the frequencies f_1 = 9390 mc per sec and f_2 = 3000 mc per sec (for Oct. 22–23, 1957) (5). Fig. 2 shows the variation in the speed of these fluctuations at the frequencies mentioned and the wind speed along the measuring range. The correlation coefficient between wind speed and fluctuation frequency is 0.86 for f_1

and 0.72 for f_2. Other measurements have given analogous results. Thus for October 28–29, these quantities were equal to 0.82 and 0.65, respectively. They bear witness to a constant deviation from a linear dependence of fluctuation frequency on wind speed. Accordingly models based on an attempt to link the rate of fading and the drift speed by means of ordinary Doppler relationships are far removed from the actual nature of ultra shortwave fading.

This may be confirmed by comparing the autocorrelation radius and the wind speed. Fig. 3 gives data obtained from measurements of the autocorrelation radius of the amplitude of the field of a signal, reflected from a standard reflector at a frequency f_1 = 9390 mc per sec over a 36-km measuring range, and the trace of the wind speed. The graph indicates the considerable effect of an increase in the wind speed in reducing the correlation radius, but the dependence is nevertheless far from linear.

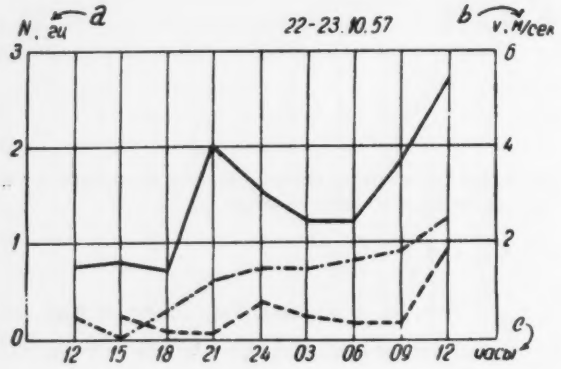

Fig. 2 [a]cps; [b]m per sec; [c]hr

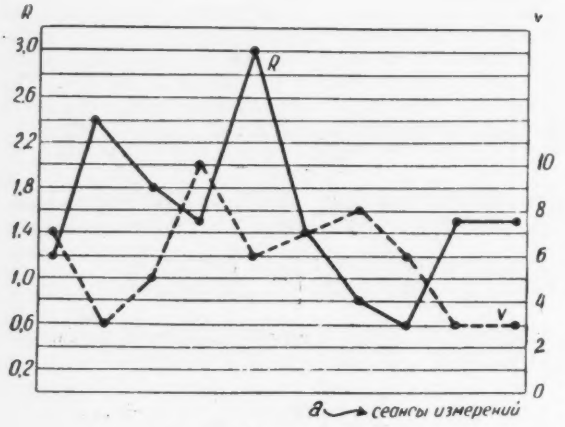

Fig. 3 [a]Measuring session

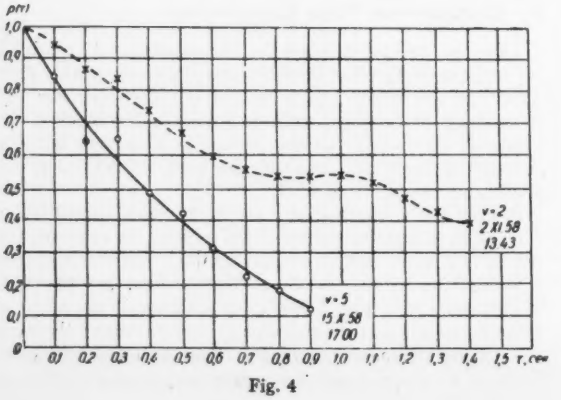

Fig. 4

Fig. 4 shows the results of measuring the correlation coefficient of the reflected field (f_2 = 3000 mc per sec) for the two wind speeds 5 and 2 m per sec. The graph demonstrates the same tendency, and at the same time points to the rather complex character of the dependence of the correlation dimensions on drift speed.

We have very little experimental information on the dependence of fading on carrier frequency. The results we present are taken from the literature (1,6). For the simplest model we have the simplified relationship (3)

$$N = \varphi(\mathbf{v}_0)[(f/f_0)^{4/3} + (f/f_0)^2]^{1/2} \qquad [10]$$

where

f = carrier frequency
f_0 = some parameter characterizing the propagation conditions

Here the first term is linked with the random motion of the inhomogeneities and the second with regular drift.

The dependence of the rate of fading on the carrier frequency varies from linear when the effect of the average drift speed is dominating, to exponential with the exponent $\frac{2}{3}$ when the main part in fading is played by turbulent motion.

Fig. 5 shows the dependence of the rate of fading on the carrier frequency for three frequencies (O, from data in (6); ×, experimental results). The graph clearly shows an increase in fading with increased carrier frequency, but, in contrast to the conclusions reached in (6), it is impossible to confirm the existence of a linear dependence. As we saw, theoretical calculations throw light on this problem and do not permit us to count on getting a linear dependence.

Note, in conclusion, that the averaging interval, used in processing the experimental results, has an important influence on the determination of the quantity characterizing the rate of fading. Statistical calculations and experimental results have shown that a stationary value is reached in the course of an averaging time of 6–8 min.

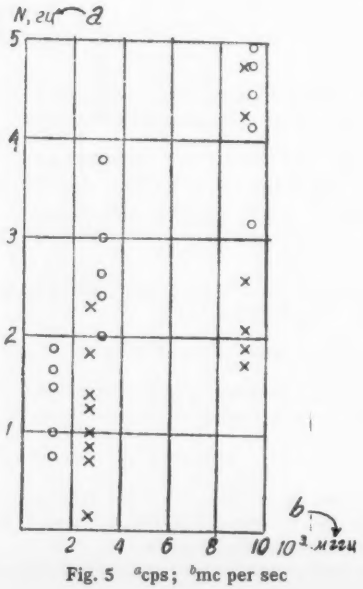

Fig. 5 [a]cps; [b]mc per sec

References

1 Semenov, A. A. and Karpeyev, G. A., *Izv. Vysshikh Uchebnykh Zavedenii (Proc. Inst. Higher Education), Radiotekhnika (Radio Technology)*, 1958, no. 6.
2 Semenov, A. A. and Karpeyev, G. A., *Izv. Vysshikh Uchebnykh Zavedenii Fizika (Physics)*, 1958, no. 6.
3 Silverman, R. A., J. Appl. Phys., vol. 28, no. 4, April 1957.
4 Semenov, A. A. and Karpeyev, G. A., *Vestn. MGU (Bull. Moscow Univ.), Mathematical, Mech., Phys., Chem. Series*, 1957, no. 6.
5 Semenov, A. A. and Karpeyev, G. A., *NDShV, Physico-Mathematical Sciences*, 1958, no. 4.
6 Trolese, L. G., Proc. IRE, vol. 43, no. 10, Oct. 1955.
7 Paue, C., *Teoriya Peredachi Elektricheskikh Signalov Pri Nalichii Pomekh (Theory of Transmission of Electric Signals in the Presence of Noise)*, IL, Moscow, 1953

—Submitted April 11, 1959

Reviewer's Comment

Results similar to those presented in this paper, and relating the speed of fading to the carrier frequency, have appeared in recent American and European work. In this respect one might note the recent review of Staras and Wheelon (1). Considerable confusion appears to exist with respect to this aspect of scatter propagation, which may be associated with the scaling of the antennas. Thus, ratios of fading rates in excess of that of the frequencies have been found by Bell Laboratories (2) and Lincoln Laboratory (3) workers, who used scaled antennas. Others, not using such antennas, found nearer to an F dependence. Doherty (4) also finds the fading rate a function of antenna aperture.

The relation between fading rate and upper wind on the path is also uncertain. Thus, both positive correlation (5) and no correlation (4) have been experienced.

The statistical reliability of data is associated with both the stationarity of the propagation medium and the sampling time. The former aspect has been investigated recently by Finney (6), who finds a typical stationary period of 1–5 min (the Soviet authors determine reliable sampling periods to be 6–8 min).

One gets the impression that there is some disagreement in experimental data on almost every aspect of long distance scatter propagation (3). In addition to those mentioned which apply to the paper being reviewed, there are:

1 The distance dependence of the fading rate (5,7).
2 The envelope distribution (5–7).
3 More basic, the mechanism itself (5–8).

—Albert W. Adey
Defence Research Telecommunications Establishment
Ottawa, Canada

1 Staras, H. and Wheelon, A. D., "Theoretical Research on Tropospheric Scatter Propagation in the U.S., 1954–57," IRE Trans., AP-7, Jan. 1959, p. 80.
2 Hogg, D. C. and Lowry, L. R., "Short Term Fading at 460 and 4110 Mc/s," IRE Trans., AP-7, Jan. 1959, p. 107.
3 "Long Range Tropospheric Transmission," Proc. IRE, vol. 48, Jan. 1960, p. 30.
4 Doherty, L. H. and Neal, G., "A 215 mile, 2720 Mc/s Radio Link," IRE Trans., AP-7, April 1959, p. 117.
5 "Proceedings of the International Conference on Radio Wave Propagation," Liege, Belgium, Oct. 1958. reported in Proc. IRE, vol. 47, June 1959, p. 1147. Published as "EM Wave Propagation," M. Desirant and J. L. Michiels, Eds., Academic Press, Inc., N. Y., 1960.
6 Finney, R. G., "Short Time Statistics of Tropospheric Radio Wave Propagation," Proc. IRE, vol. 47, Jan. 1959, p. 84.
7 Josephson, B. and Carlson, G., "Fading Characteristics of 3000 Mc/s Transhorizon Signals," IRE Trans., AP-6, April 1958, p. 173.
8 Ames, L. A. et al., "Some Characteristics of Persistent VHF Radio Wave Field Strengths far Beyond the Radio Horizon," Proc. IRE, vol. 47, May 1959, p. 769.

Ignition in a Flow by Hot Bodies

S. A. GOL'DENBERG

Power Institute
Academy of Sciences, USSR

THE QUESTION of ignition by hot bodies in a flow has been treated by Khitrin (1)[1] on the basis of classical methods of solving problems concerned with the cooling of bodies in an ideal liquid.

Translated from *Izvestiia Akademii Nauk SSSR, Energetika i Avtomatika (Bulletin of the Academy of Sciences, USSR, Power and Automation)* 1960, no. 2, pp. 195–197. Translated by Research Information Service, New York.

[1] Numbers in parentheses indicate References at end of paper.

In this paper the problem of ignition by hot bodies in a flow is solved by the methods of boundary layer theory with particular reference to a laminar boundary layer. The most rigorous formulation of the problem involves the simultaneous solution of the following nonlinear differential equations for a two-dimensional flow

$$U\frac{\partial U}{\partial X} + V\frac{\partial U}{\partial Y} = \nu\frac{\partial^2 U}{\partial Y^2} \qquad [1]$$

$$\frac{\partial U}{\partial X} + \frac{\partial V}{\partial Y} = 0 \qquad [2]$$

$$U\frac{\partial T}{\partial X} + V\frac{\partial T}{\partial Y} = \frac{\lambda}{c_p\rho}\frac{\partial^2 T}{\partial Y^2} + qF(C, T) \qquad [3]$$

$$U\frac{\partial C}{\partial X} + V\frac{\partial C}{\partial Y} = D\frac{\partial^2 C}{\partial Y^2} - F(C, T) \qquad [4]$$

where

$F(C, T) = K_0 f(C) \exp(-E/RT)$ is an expression for the reaction velocity
q = thermal effect of the reaction
U, V = velocity components
T = temperature
E = activation energy
$f(C)$ = some function of the concentration of one of the reactants, of which there is an insufficiency

If, however, we assume that in the initial stage of the process, say in flow around a heated plate, the velocity boundary layer and the temperature boundary layer vary little up to the moment of ignition of the mixture, and that the basic reaction leading to spontaneous ignition proceeds in a narrow zone within the boundary layer, then with the process represented in this way the problem can be reduced to a solution of Eqs. 1–4 but without a source. Numerical integration of the complete system of Eqs. 1–4 has established (2) that in the initial stage of heat exchange the chemical reaction has a slight effect on the velocity boundary layer and the temperature boundary layer; there is a sharp variation in the temperature profile in a narrow zone along the plate.

In this case the boundary conditions may be written thus

$$U = V = 0 \text{ when } Y = 0 \qquad U = U_0 \text{ when } Y = \infty$$

$$T = T_s \quad \text{when } Y = 0 \qquad T = T_0 \text{ when } Y = \infty$$

(T_s is the temperature at the surface of the body.) Because of the similarity between the temperature and concentration fields Eq. 4 is not taken into account. In a particular case

$$\frac{T_s - T}{T_s - T_0} = \frac{U}{U_0}$$

when $Pr = 1$.

It is known that in order to solve the equations of hydrodynamics, we can introduce the new variables (3)

$$\eta = Y\sqrt{U/\nu X} \qquad \psi = \sqrt{\nu X U} f(\eta)$$

thus making it possible to reduce the problem to ordinary differential equations (X, distance along the plate; ψ, stream function). In particular, for longitudinal flow around the plate the solution of Eqs. 1–4 without a source will be

$$q_1(X) \simeq 0.322\lambda\sqrt{U_0/\nu X}\,(T_s - T_0) \qquad [5]$$

or

$$\alpha_x \simeq 0.332\lambda\sqrt{U_0/\nu X} \qquad [6]$$

where α_x is the heat transfer coefficient.

In accordance with the conclusions of the thermal theory of ignition (4,5), the critical condition of ignition is $q_1 = q_2$. Here q_2 is the heat liberated by the reaction around an incandescent body in a narrow zone of the boundary layer ($\xi < \delta$, where δ is the thickness of the boundary layer); q_1 is the heat removed from the body as a result of thermal emission. In the general case (4,5)

$$q_1 = \alpha(T_s - T_0) \quad \text{or} \quad q_1 = Nu_x(\lambda/X)(T_s - T_0)$$

$$q_2 = \lambda\left[\frac{2q}{\lambda}\int_{T_\xi}^{T_s} F(C,T)dT\right]^{1/2}$$

Thus, with these critical conditions we can write

$$Nu_x\frac{\lambda}{X}(T_s - T_0) = \left[2q\lambda\int_{T_\xi}^{T_s} F(C, T)dT\right]^{1/2} \qquad [7]$$

In accordance with (4 and 5) we have approximately

$$\left(\frac{Nu_x}{X}\right)^2 \simeq K\left(\frac{T_s}{T_s - T_0}\right)^2 \exp\left(-\frac{E}{RT_s}\right) \qquad [8]$$

or

$$\left(\frac{Nu_x}{X}\right)^2\left(\frac{T_s - T_0}{T_s}\right)^2 \simeq K\exp\left(-\frac{E}{RT_s}\right) \qquad [9]$$

When $T_s = T_f \simeq T_K$ (T_f is the flame temperature and T_K is the final temperature of the products of combustion), from Eq. 7 we can get the following dependence for concentration ignition boundaries

$$\frac{Nu_x}{X} \simeq \beta\frac{S}{\lambda/c_p\rho} \qquad [10]$$

The latter relationship arises from the following considerations

$$q_2 = \lambda\left[\frac{2q}{\lambda}\int_{T_\xi}^{T_K} F(C, T)dT\right]^{1/2}$$

but since we know from the theory of flame propagation (6) that

$$S = \frac{1}{c_p\rho(T_K - T_0)}\left[2q\lambda\int_{T_\xi}^{T_K} F(C, T)dT\right]^{1/2}$$

(S is the normal velocity of the flame), formula 10 is easy to obtain from Eq. 7.

When Nu_x varies in accordance with the law of Eq. 6, instead of Eqs. 8 and 10, we can write

$$\frac{X}{U_0} = K_1\left(\frac{T_s - T_0}{T_0}\right)^2 \exp\left(\frac{E}{RT_s}\right) \qquad [11]$$

$$\left(\frac{U_0 X}{\nu}\right) = \beta_1\left(\frac{SX}{a}\right)^2 \qquad [12]$$

where $a = \lambda/C_p\rho$.

It follows from Eq. 11 that for a given composition of the mixture and temperature of the body T_s, the ratio $X/U_0 \simeq$ constant for variation in the velocity of flow. This may be explained by the fact that with increase in U_0 the inflammation of the mixture will occur at a distance X along the incandescent plate, at which the condition $X/U_0 \simeq$ constant is observed (it is known that with an increase in X, α_x decreases, since in a laminar boundary layer $\alpha \sim 1/\sqrt{X}$). In other words, as U_0 increases, the flame will shift along the incandescent body, to where the critical conditions of ignition are observed. The limiting condition, corresponding to collapse of the flame, is realized when $X = L$ and $U_0 = U_K$ (L is the length of the incandescent plate).

Formula 11 yields another important conclusion: For a given constant velocity of flow U_0 and variation in T_s, the ratio X/U_0 must vary approximately in accordance with the law

$$\frac{X}{U_0} \simeq B\exp\left(\frac{E}{RT_s}\right) \qquad [13]$$

This conclusion may also be derived from the theory of similarity, if we take into account Eq. 3, and from the solutions of Boussinesq and King (1).

The ratio X/U_0 has the dimension of time, which may be called characteristic, $X/U_0 = \tau$. However, we should bear in mind that in a given case τ is not the induction period of generally accepted terminology and, as shown, is linked with the heat exchange conditions.

The basic conclusions, obtained by means of boundary layer theory, may also be extended to the case of plane parallel flow around curved surfaces with the condition that $\delta \ll r_0$, where r_0 is the radius of curvature.

Calculations for the ignition process are somewhat more complicated for axially symmetrical bodies. However in this case, too, the boundary layer equation can be reduced to the calculation of a plane laminar boundary layer with the condition that $\delta \ll r_0$ (7). Proof of this is afforded by experimental data on mass and heat exchange in longitudinal flow around a cylinder, in accordance with which $Nu_x \simeq A\sqrt{Re_x}$ (8,9).

These are the basic conclusions which it is possible to draw from a simplified model of the process of ignition by a hot body, which, however, permits us to establish the principal parameters governing ignition in a flow by a hot body and its physical pattern.

In certain cases it is possible to solve the problem of ignition in a flow sufficiently rigorously without resorting to a highly simplified model of the process or to numerical integration of the entire system of Eqs. 1–4. Particularly interesting from a methodological point of view is the solution of the problem of ignition at a critical point in flow around a hot body, published in (10).

The author expresses his gratitude to L. N. Khitrin for useful discussion of and interest in the work.

References

1 Khitrin, L. N., "On Some Consequences of the Thermal Theory of Ignition in a Fast Flow," in *Seventh Symposium on Combustion*, London, 1958.

2 Tau Ji-Toong, "Ignition and Combustion in a Laminar Boundary Layer Over a Hot Surface," in *Sixth Symposium on Combustion*, 1957, p. 532.

3 Schlichting, G., *Boundary Layer Theory*, McGraw-Hill, N. Y., 1960; *also Teoriya pogranichnogo sloya*, IL, 1956.

4 Khitrin, L. N. and Gol'denberg, S. A., "Ignition of Gaseous Mixtures in a Flow by a Hot Body," *Doklady Akad. Nauk (Reports of the Acad. Sci., USSR)*, 1955, vol. 103, no. 2; "Concentration Boundaries of Ignition of Gaseous Mixtures in a Flow," *ibid.*, vol. 103, no. 3; "The Condition of Stabilization of the Combustion Front and the Rate of Flame Propagation at Boundaries," *ibid.*, vol. 103, no. 5.

5 Gol'denberg, S. A. and Khitrin, L. N., "Thermal Theory of Ignition of Gaseous Mixtures and Limit Phenomena," *Izvestiia Akad. Nauk, Otdel. Tekh. Nauk (Trans. Acad. Sci. USSR, Div. Tech. Sci.)*, no. 3, 1957.

6 Semenov, N. N., "Thermal Theory of Combustion and Explosions," *Uspekhi fizicheskikh nauk (Progress in Physical Sciences)*, 1940, vol. 24, no. 4.

7 Loytsyanskiy, L. G., *Mekhanika zhidkosti i gaza (Mechanics of Liquids and Gases)*, GITL, 1957.

8 Drayk, R. and Keyn, K., "Problem of Heat Emission in the Flow of a Rarified Gas at High Velocity," *Voprosy raketnoy tekhniki (Questions of Rocket Technology)*, 1954, no. 1 (19).

9 Pclonskaya, F. M. and Mel'nikova, I. V., "Investigation of Heat Exchange between a Gas and Solid Bodies," *Inzh.-fizichesk. zhurnal (Engng. Physics J.)*, 1958, no. 2.

10 Chambré, P., "On the Ignition of a Moving Combustible Gas Stream," *J. Chem. Phys.*, 1956, vol. 25, no. 3.

—Submitted December 8, 1959

Reviewer's Comment

This paper is devoted to a particular application of the general procedure described by Khitrin in (1). Knowledge of the approach to ignition problems as outlined in Khitrin's paper appears to be essential to understand Gol'denberg's paper. This reference can quite adequately substitute for (4 and 5) which are more difficult to obtain.

The present application describes in some detail the ignition of a flow aligned parallel to a hot, flat plate. Some comments are made on its extension to curved surfaces and axisymmetric bodies. The model is simplified with respect to the following points: Up to the point of ignition on the plate both the velocity and temperature boundary layers are assumed to develop as if there were no chemical reaction. Then the solution for the heat transfer from the plate to the stream is identical with the classical Blasius solution when $Pr = 1$ and the Reynolds analogy is employed. The effect of chemical reaction is introduced through Khitrin's general result for the chemical energy evolved in a thin region near a hot body.

For ignition, the heat evolved by the chemical reaction adjacent to the plate (Khitrin's result) must be just equal to the heat transferred away from the vicinity of the plate (Gol'denberg's application of the Blasius solution, in this case). Flame will occur when the chemical heat release is greater than the heat removed from the neighborhood of the surface.

The basic scheme of the phenomenon is rather pretty in its simplicity and directness. As such it gives the satisfying impression of cutting through the details to the heart of the problem. The ignition point on the plate is shown to depend in a simple way on the global activation energy and the free stream velocity. This result, given by Eq. 11, may also be compared with that of Cheng and Kovitz (*Sixth Combustion Symposium*, Reinhold, 1957, p. 424, Eq. 29) for ignition in the laminar wake of a flat plate. The results are very similar in essential content, although arrived at by totally different means. Additional related work is cited in the references.

The methodology of this paper exhibits a desire to avoid all lengthy computation until the last moment, if at all. General results, with reasonable justification, are obtained and interpreted. Although this extension of Khitrin's work (1) is not very great, it is worth while to see another example of how one can extract general information from a complicated problem by application of useful, illuminating simplifications. This is characteristic of the recent Russian work on combustion known to this reviewer.

—A. A. Kovitz
Gas Dynamics Laboratory
Northwestern University

Melting Diagram for the Titanium-Vanadium-Molybdenum Ternary System[1]

I. I. KORNILOV and
R. S. POLIAKOVA

IN AN investigation of the interaction of titanium with other elements, the refractory metals which tend to form solid solutions with titanium are of particular interest. Many elements of the transitional groups in the periodic system belong to these metals, including molybdenum and vanadium.

From the atomic-crystalline structure of Mo and V, it could be supposed that they tend to form solid solutions with β-modified titanium. The possibility of formation of continuous solid solutions in Mo and V binary systems with β-Ti was indicated by (1),[2] and it was confirmed by subsequent research (2–4). Binary systems that are part of the ternary system have been studied in considerable detail.

The Ti-V system has been the subject of many studies (2, 5–7). A structural diagram of this system was constructed in (2) (by employing ionic titanium), utilizing microstructural and electrical resistance measurement methods. It was found that the solidus curve reaches its minimum flat slope in the neighborhood of 30% V by weight (28.7 atm) at 1620 C.

The Mo-V system has been studied in (3, 6, 8 and 9). In (8), the effect of different elements upon the hardness of molybdenum, under different temperatures, was studied by using alloys obtained by the electric arc method. The results of this research showed that 6–8% vanadium alloying significantly increases the hardness of molybdenum at room temperature and at 760–871 C, whereas at 1649 C the hardness of the alloy is almost unchanged. In (6), studies were made of binary system alloys with up to 75% Mo. The authors discovered insignificant amounts of a new phase. However, the existence of this phase was not confirmed. By studying the lattice constants of Mo-V system alloys it was shown that molybdenum and vanadium are infinitely mutually soluble (3).

Metallographic research (9) showed that a constant series of solid solutions is formed in the Mo-V system. The authors plotted a melting diagram, however, since the vanadium which was used in this work contained a great amount of impurities, including aluminum; the melting point of vanadium was considerably below that given by other researchers.

Detailed studies of the Ti-Mo system (4, 10–12) established that the solubility of the Mo in α-Ti is about 1.86%, whereas β-Ti and Mo are infinitely mutually soluble. A complete structural diagram of the Ti-Mo system was constructed in (4) by methods of thermal analysis, microstructural and x-ray analysis. The solidus curve changes smoothly, depending on the composition of the alloy, rising from titanium to molybdenum. Such a change in the curve indicates the formation of solid solutions of molybdenum and titanium.

Translated from *Izvestiia Akademii Nauk SSSR, Otdel. Tekh. Nauk, Metallurgiia i Toplivo* (*Bulletin of the Academy of Sciences, USSR, Department of Technical Sciences, Metallurgy and Fuel Series*), 1960, no. 1, pp. 85–89. Translated by Primary Sources, New York.

[1] I. I. Davidov took part in this experiment.

[2] Numbers in parentheses indicate References at end of paper.

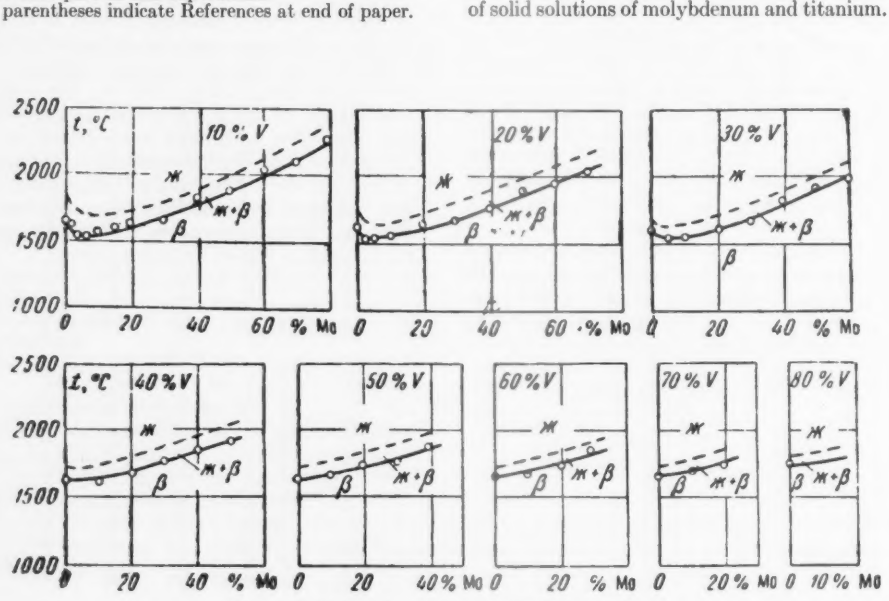

Fig. 1 Polythermic profiles of the Ti-V-Mo system

Table 1

Composition, weight %				Composition, weight %			
Ti	V	Mo	t, C	Ti	V	Mo	t, C
88	10	2	1630	65	30	5	1580
85	10	5	1550	60	30	10	1610
83	10	7	1550	50	30	20	1680
80	10	10	1580	40	30	30	1730
75	10	15	1610	30	30	40	1890
70	10	20	1640	20	30	50	1980
60	10	30	1670	10	30	60	2070
50	10	40	1840	50	40	10	1640
40	10	50	1910	40	40	20	1680
30	10	60	2050	30	40	30	1780
20	10	70	2130	20	40	40	1860
10	10	80	2300	10	40	50	1940
78	20	2	1580	40	50	10	1690
75	20	5	1580	30	50	20	1750
70	20	10	1610	20	50	30	1780
60	20	20	1680	10	50	40	1890
50	20	30	1720	30	60	10	1700
40	20	40	1820	20	60	20	1750
30	20	50	1950	10	60	30	1860
20	20	60	2000	20	70	10	1720
10	20	70	2120	10	70	20	1780
				10	80	10	1780

At the present time, alloys of the Ti-V-Mo system have been studied by authors of two research works. It was determined, by studying the lattice structure parameters of ternary alloys above the transformation temperature of vanadium (13), that at 900 C the components are infinitely mutually soluble. Titanium-rich alloys withstand transformation and have martensite-like structures.

In (14), changes were studied in the microstructure of alloys during the aging process. The research was conducted using metastable titanium-rich alloys. The hypothesis was that the introduction of two elements, which broaden the range of β-solid solutions, would assure the obtainment of a stable β-phase with a smaller overall content of alloy compounds. It was determined that in order to stabilize the β-phase at a temperature of 550 C, it was necessary to add more than 20% Mo or more than 30% V to titanium in binary systems. In ternary systems, for each of the proportions 1:3, 1:1 and 3:1, a total of more than 20% Mo-V had to be added.

It was the purpose of this study to examine and construct a complete melting diagram for the ternary Ti-V-Mo system.

The starting materials for the preparation of alloys were metals in powdered form: 99.6% pure magnesium-thermic titanium, 99.2% pure vanadium and 99.9% pure molybdenum.

In order to determine the melting point of the alloys, the metallo-ceramic method was used to prepare samples in 60 × 5 × 5-mm squares. The composition of the tested alloys was set up in parallel cross section (Table 1), with a constant vanadium content of 10, 20, 30, 40, 50, 60, 70 and 80%.

All alloys were baked at temperatures of 1500 C in a TVV-2 type furnace for a period of 50 hr. This baking period proved to be sufficient for titanium-rich alloys. Other alloys with a greater molybdenum and vanadium content were subjected to an additional baking period of 50 hr, at 1800 C.

In order to study the polymorphous transformation of ternary alloys in a solid state, specimens of 10-gm each were prepared by melting in an arc furnace. Homogeneity of composition was achieved by triple remelting. Waste during this process amounted to 1–2% of each batch.

The alloys thus obtained were sealed in quartz test tubes and subjected to heat treatments according to the following procedure: Heating to and maintaining the temperature at 1100 C for 100 hr; gradual reduction of the temperature to 800 C and maintaining it there for 50 hr; reducing the temperature again to 500 C, maintaining it for 300 hr, then cooling as the furnace cooled.

In view of the high melting point of these alloys, it was impossible to apply the usual method of thermal analysis and to determine the cooling curves by using the Kurnakov pyrometer. In determining the melting points of the alloys, we used the methods described in (15).

The initial melting point for each alloy was determined and verified on three specimens.

Table 1 provides the compositions for alloys and their initial melting points. Polythermic profiles of the Ti-V-Mo system (Fig. 1) were constructed from the obtained data. The solid lines represent the solidus curves according to the experimental data; the dotted lines show the approximate liquidus curves. In the diagram with a constant 10% V content, the solidus curve reaches its minimum slope with about 5–10% Mo; this is most probably accounted for by the location of the minimum on the solidus curve in the binary system.

The solidus curve minimum in the ternary system also appears in the study of alloys composed of 20–30% V. With other compositions in this system the solidus curve changes smoothly, depending on the alloy composition, rising from Ti-V to V-Mo. The concentration triangle (Fig. 2) shows the isotherms of solidus curves at 100 C intervals. These curves show the nature of the changes in the initial melting points of ternary alloys of the Ti-V-Mo system. The presence of the minimum slope of the melting point curve for the binary Ti-V system is reflected in the ternary system. The concentration triangle shows a slight depression in the area of 10–30% V, this minimum extending to 10% Mo. The melting point of ternary alloys shows a significant increase with the increase of their molybdenum content.

In order to confirm that the mutual solubility of the components is greater in a polymorphous transformation of titanium (namely β), Figs. 3, 4 and 5 show the microstructure of hardened alloys at a temperature of 1100 C.

In order to study the polymorphous transformation of ternary alloys in a solid state, a thermal differential analysis was conducted with the aid of Kurnakov pyrometer and a platinum-platino-rhodium thermocouple. Preliminary annealed, titanium-rich alloys were studied in this case. The temperature change curves of polymorphic transformation for ternary alloys, in relation to their compositions of a constant 10, 20 and 30% V (Table 2, Fig. 6), show that with an increase of the molybdenum and vanadium content of alloys there is a marked reduction in the polymorphic transformation temperature of titanium.

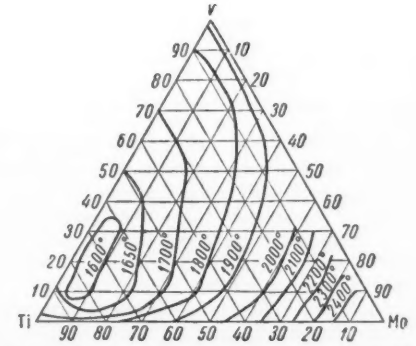

Fig. 2 Diagram of the solidus plane of the Ti-V-Mo system

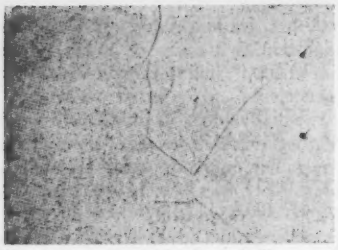

Fig. 3 Microstructure of a hardened alloy, containing 65 weight % Ti, 10 weight % V and 25 weight % Mo

Fig. 4 Microstructure of a hardened alloy, containing 40 weight % Ti, 40 weight % V and 20 weight % Mo

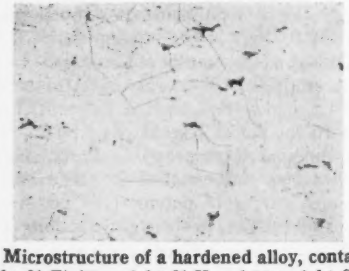

Fig. 5 Microstructure of a hardened alloy, containing 20 weight % Ti, 70 weight % V and 10 weight % Mo

Table 2

Composition, weight %				Composition, weight %			
Ti	V	Mo	t, C	Ti	V	Mo	t, C
88	10	2	675	73	20	2	615
85	10	5	670	70	20	10	585
80	10	10	660	65	20	15	540
70	10	20	550	65	30	5	555
60	10	30	410	60	30	10	450

The somewhat broadened range of existence of the two phases $\alpha + \beta$ may be attributed to the higher content of impurities in the titanium used in this experiment.

As a result of these studies, the approximate limitations of the α-, $\alpha + \beta$- and β-regions of the Ti-V-Mo ternary system may be determined. A three-dimensional diagram of the Ti-V-Mo system may be plotted (Fig. 7), by employing the data provided by the solidus curves of the alloys according to the selected profiles and differential thermal analyses of separate alloys, adjacent to the titanium end of the diagram.

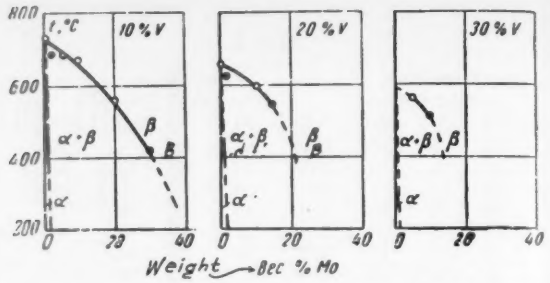

Fig. 6 Transformation temperature for the Ti-V-Mo system alloys

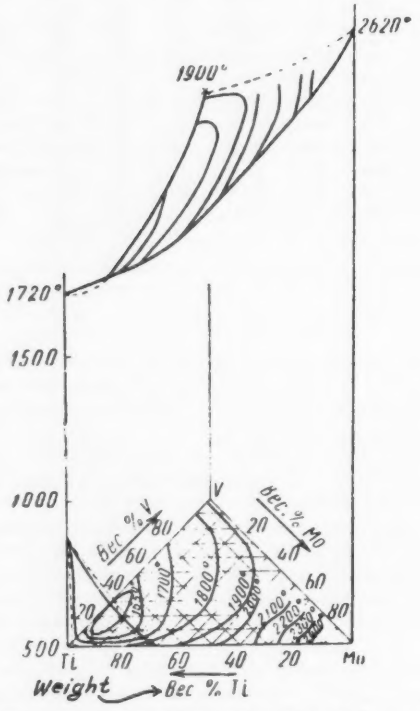

Fig. 7 Three-dimensional view of the structural diagram for the Ti-V-Mo system

Conclusions

1 The first investigation was conducted of the fusibility of the Ti-V-Mo system.

2 The smooth rate of change in the initial melting point curves of alloys, in relation to the compositions of these alloys, indicates that alloys of the ternary system crystallize as continuous hard solutions.

3 The minimum crystallization slope of these alloys is reflected by corresponding changes in the solidus plane for the Ti-V-Mo ternary system.

4 Microstructural analysis of hardened alloys confirmed the infinite mutual solubility of the elements studied at temperatures above that of polymorphic transformation of titanium.

5 The polymorphic transformation temperature of ternary alloys is reduced by increasing the molybdenum and vanadium content of the alloys.

6 Data obtained from the fusibility diagram is valid for the selection of practically usable compositions of ternary alloys with a given initial melting point.

References

1 Kornilov, I. I., "Solubility of Chemical Elements in Titanium," *Izvestiia Akad. Nauk, SSSR, OKhn* (*Bull. Acad. Sci., USSR, Div. of Chem. Sci.*), 1954, no. 3.

2 Aldenstedt, H. K., Requignot, Y. R. and Raymer, J. M., "The Titanium-Vanadium System," Trans. Amer. Soc. Metals, 1952, vol. 44, p. 990.

3 Pipitz, E. and Kieffer, R., "The Influence of Alloyed Additives on Firmness Properties and Recrystallization of Molybdenum in a Vacuum, *Z. Metallkunde* (*Metallurgy Periodical*), 1955, vol. 46, pp. 187–194.

4 Hansen, M., Kamen, E. Z., Kessler, H. D. and McPherson, "Systems of Titanium-Molybdenum and Titanium-Columbium," *J. Metals*, 1951, vol. 3, no. 10, p. 88.

5 Pietrokowsky and Duwez, P., "Partial Titanium-Vanadium Phase Diagram," Trans. AIME, 1952, vol. 194, p. 627.

6 Rostoker, W. and Tamamoto, A., "A Survey of Vanadium Binary Systems," Trans. Amer. Soc. Metals, 1954, vol. 46, p. 1136.

7 Powers, R. M. and Wilhelm, H. A., Atomic Energy Commission Publication, 1952.

8 Ham, J. L., "An Introduction to Arc-Cast Molybdenum and Its Alloys," Trans. Amer. Soc. Mech. Engrs., 1951, vol. 73, p. 723.

9 Baron, V. V., Gerasimov, Y. V. and Savitskii, Ye. M., "The Structure and Properties of the Vanadium-Molybdenum System," *Izvestiia Akad. Nauk, SSSR* (*Bull. Acad. Sci., USSR, Div. of Tech. Sci.*), 1958, no. 4.

10 Kroll, W., "Alterable Titanium Alloys," *Z. Metallkunde* (*Metallurgy Periodical*), 1937, vol. 29, p. 139.

11 Conser, B., "Titanium Alloys." *Ind. Engng. Chem.*, 1950, vol. 42, p. 222.

12 Craighead, C. M., Simmons, O. W. and Eastwood, Z. M., "Titanium Binary Alloys," *J. Metals*, 1950, vol. 188, no. 3, p. 485.

13 Taylor, I. Z., "Beta-Phase Parameters in the Ti-V-Mo System," *J. Metals*, 1956, vol. 8, no. 8, Sec. 2, pp. 959–961.

14 Carrew, W. F., Crossley, F. A. and Kessler, H. D., "Evaluation of the Structural Stability of Ti-Mo-V Alloys," *J. Metals*, 1956, vol. 8, no. 5, Sec. 2, pp. 491–496.

15 Kornilov, I. I. and Poliakova, R. S., "Investigation of the Nb-Mo System," Trans. In-ta Metallurgii im. A. A. Baikova AN SSR (Trans. A. A. Baykov Inst. Metallurgy, Acad. Sci., USSR), 1957, 2nd ed.

—*Submitted June 24, 1959*

Reviewer's Comment

The authors have confirmed what all the references have partially or completely shown, namely, that there is one phase (body-centered cubic or β) across the entire Ti-V-Mo diagram above the α to β transition temperature of titanium. The work is a contribution in that the authors have determined nearly the entire ternary solidus isotherms with the exception of the V-Mo binary line and have approximated the liquidus surface. Further, the ternary boundary separating the two-phase $\alpha + \beta$ field from the one-phase β field has been shown. The diagram was surveyed in large compositional jumps, i.e., 10 weight %, so determination of the extent of the ternary solid solution of V and Mo in α titanium was not made.

It is curious, with so much of the paper given to summing references, that (1–4) below were overlooked, and that the authors' research work was not compared with the references given. Characteristically, most American articles on phase diagrams have a preliminary statement as to why the system under investigation is of interest. In this country, x-ray diffraction data are usually used in addition to metallography and thermal analysis for determining solid-state phase boundaries. The Russians did not use this most helpful tool.

Much of the earlier phase diagram work on titanium alloys has been redone using higher purity alloying elements. The McQuillans (5) in their excellent book on titanium fully discuss the discrepancies among various investigators in the $\alpha/\alpha + \beta$ phase boundary in several titanium binary diagrams including Ti-V and Ti-Mo. The authors say nothing about the interstitial element impurity levels in the alloying elements used. Considering the very few alloys made on the titanium-rich end of the ternary system and the possibility of fairly high oxygen and nitrogen content, the boundaries would probably be changed by more careful work.

Fig. 7 which is the graphical summary of the results of the investigation is confused by the incorporation of Fig. 2 which obscures the ternary solid-state boundaries between β and $\alpha + \beta$ fields.

—Jack L. Taylor
Jet Propulsion Laboratory
California Institute of Technology

1 Duwez, P., "Effect of Cooling on the Alpha-Beta Transformation Temperature in Titanium and Titanium-Molybdenum Alloys." Trans. AIME, 1951, vol. 191, p. 765.

2 DeLazaro, D. J. and Rostoker, W., "The Influence of Oxygen Contents on Transformations in a Titanium Alloy Containing 11 Per Cent Molybdenum, "*Acta Metallurgica*, 1953, vol. 1, p. 674.

3 DeLazaro, D. J., Hansen, M., Riley, R. E. and Rostoker, W., "Time-Temperature-Transformation Characteristics of Titanium-Molybdenum Alloys," Trans. AIME, 1952, vol. 194, p. 285; also *J. Metals*, March 1952.

4 DeLazaro, D. J. and Rostoker, W., "Correlation Between Heat Treatment Microstructure, and Mechanical Properties of Titanium-Molybdenum Alloys," Trans. ASM, 1954, vol. 46, p. 292.

5 McQuillan, A. D. and McQuillan, M. K., *Metallurgy of the Rarer Metals—4 Titanium*, Academic Press, Inc., N. Y., 1956.

Variation of the Albedo of the First Artificial Earth Satellite as a Result of the Influence of External Factors

I. M. YATZUNSKY
and O. V. GURKO

THE VARIATION of the albedo and of the character of the surface reflection of a satellite as the result of the influence of the atmosphere, meteoric matter and other physical factors, plays a considerable role in the observation of a satellite, and may also be of independent scientific interest. In connection with this, an attempt was made to establish the fact of the variation in the surface reflectivity according to data from the observation of the first artificial satellite which had a mirror surface and, consequently, at the initial period of its existence had a specular reflection. This circumstance makes it easier to analyze available observations. The method used to determine the variation of the albedo of the first satellite in flight is based on the following facts:

1 The known differences between the specular and diffuse reflection of a sphere.

2 The possible decrease in the amount of the reflected light if the surface condition were altered by the influence of external factors.

In Fig. 1 is shown the dependence of the difference of stellar magnitudes ($\Delta m = m_s - m_d$) of a sphere on the phase θ for a specular and a diffused reflection of light (θ is the angle between the directions "satellite-sun" and "satellite-observer").

Evidently, with the increase of the angle θ, the difference Δm increases, and for $\theta > 135$–140 deg attains 2.5–3.0 magnitudes. Consequently, it is impossible to observe the diffuse reflection of a sphere in the direction almost "opposite" the sun, whereas the brilliance of a specular reflection of a sphere does not depend on the phase.

During the period from Oct. 4, 1957 to Dec. 6, 1957 more than 200 optical observations of the first Earth satellite were made with astronomical tubes of the AT-1 type. For all these observations the phase angles θ and the distance of the sun below the horizon Δ have been computed. Next, the data containing θ, Δ, the time of observation, the elevation β, the azimuths A, distances to the satellite $-S$, stellar magnitudes m (the average observed magnitude of the first satellite reduced to the distance of 500 km was approximately equal to 5–5.5) and differences Δm have been separated into two groups corresponding to the two periods of time considerably different from each other because of the conditions of observations. During the first period (from Oct. 9–Oct. 31, 1957) 159 observations were made with 106 passes of the satellite in 23 days (4.6 passes every 24 hr); during the second period (from Nov. 1–Dec. 7, 1957) 63 observations were made with 42 passes in 37 days (1.1 passes every 24 hr). At the same time, the number of ephemerides sent to stations during the first period was 904, i.e., 39 every 24 hr, and 1131 during the second period (30 every 24 hr). The insignificant relative decrease in the number of ephemerides does not explain the sharp drop in the number of observations in November. The main reason for the decrease in the number of observations was a large number of cloudy days during this period.

On the basis of the processed data of the 200 observations one can arrive at the following conclusions:

1 During the first period, numerous observations were made at small elevations (20 deg and less), that is, at large distances to the satellite. There are also observations with large phase angles ($\theta > 130$).

2 During the second period, there were no observations with great distances and large phase angles.

Table 1 shows the data concerning the number of observations with different β and θ during the two periods in question.

Table 2 shows the data for β_{at}, θ_{at}, S_{at} and the altitude of the satellite's flight above the observation points on ascending and descending parts of the orbit in the two described periods. By ascending (direct) loop, we define that part of the orbit which corresponds to the motion of the satellite from southern latitudes to the northern ones, by the descending (retrograde) loop we mean the motion from the northern latitudes to the southern ones.

From the data it is evident that in October the satellite did not yet lose its specular reflecting properties, since there were observations with phase angles θ up to 140 deg. If the surface deteriorates, i.e., if a sharp decrease of the specular reflection coefficient occurs, the brilliance of the satellite with $\theta = 140$ deg must be two and a half magnitudes smaller than with the

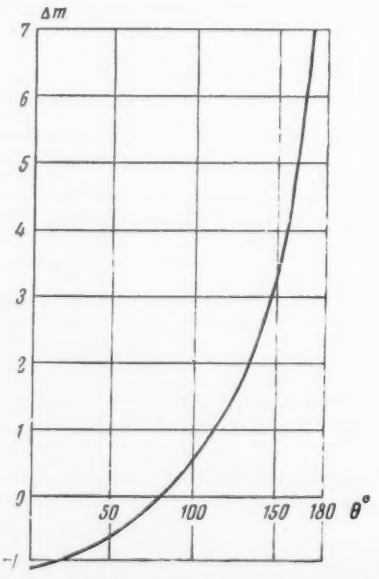

Fig. 1 The dependence of the difference $\Delta m = m_s - m_d$ on phase θ

Translated from *Artificial Earth Satellites*, 1960, no. 5. Translated by A. E. Godlewsky, New York.

Table 1

Number of observations during the period	Elevation β not more than 10°	15°	20°	25°	30°	Phase angle θ not less than 120°	130°	140°
10/9 to 10/31	4	6	14	21	35	20	7	1
6/1 to 12/7	0	1	1	2	3	0	0	0
Δm						1.3	1.8	2.5

Table 2

Period of observation	Average elevation β_{av}, deg	Average distance to satellite S_{av}, km	Average phase angle θ_{av}, deg	Average flight altitude in the regions of observation points, km: Ascending loops	Descending loops
10/9 to 10/31	48	503	92	225	400
11/1 to 12/7	56	425	78	220	410

specular reflection, and will, on the average, be equal to eight magnitudes. Under these conditions, observations of the satellite using tubes of the AT-1 type become almost impossible. In November, as shown in Table 1, there were no observations with large phase angles ($\theta > 120$ deg), although a relative number of cases of large and small phases (as well as elevations) corresponding to computed ephemerides for both periods is practically identical.

Hence, one can deduce not only the decrease of the satellite's albedo, but also the change in the character of reflection (diffuse instead of specular). A relative increase in the number of "non-observations" of the satellite in a clear sky during the second period (20% of non-observations in November compared with 10% in October) is a definite confirmation of our deduction.

Thus, the data reduction of the visual observations of the first artificial Earth satellite during its two months flight shows the alteration of the reflecting properties of the polished aluminum skin of the satellite under the influence of external factors.

An Artificial Comet as a Method for Optical Observation of a Cosmic Rocket

I. S. SHKLOVSKII

TO DETERMINE the orbit of a cosmic rocket its coordinates must be known. These can be obtained from radio-physical as well as from optical observations. There are, however, serious difficulties involved in carrying out the optical observations. Because of the great distance, the flux of solar radiation reflected by the cosmic rocket must be very small. Simple computations show that if a cosmic rocket is 100,000 km away from Earth, its apparent stellar magnitude (taking the phase into consideration) will be less than $+14^m$. At a distance of 400,000 km, its stellar magnitude will already be less than $+17^m$. Considering that such observations might be carried out for small angular distances from the moon, where the brightness of the night sky is rather great, it is apparent that the difficulties encountered here are of a serious nature. Moreover, telescopes with a moderate aperture and a large focal length (required to eliminate the disturbing bright background of the sky) give a small field of vision. Since the preliminary ephemerides of a cosmic rocket are rather approximate, in practice such telescopes cannot be aimed at the object. It may be concluded that astronomical observation of cosmic rockets, even at "lunar" distances can be achieved—if at all possible—by using several unique telescopes (of the type with 100- and 200-in. reflectors). However, one cannot base such observations on the one or two observatories where telescopes suitable for this purpose are available, since the probability of a failure resulting from adverse meteorological conditions may be very high.

Under such circumstances a question naturally arises.

Translated from *Artificial Earth Satellites*, 1960, no. 4, pp. 195–204. Translated by Research Information Service, New York.

Can the brightness of a cosmic rocket be increased artificially? The simplest method (1)[1] was proposed in the United States for application to artificial Earth satellites. The essence of this method consists of ejection from the rocket of a balloon, the surface of which must be made from a very thin, light and sufficiently strong synthetic material. Such a balloon would be carried aboard the rocket in a folded condition and after ejection it would be "inflated" by the means of a certain pneumatic mechanism. In this way a sphere having a diameter of 30 m or even 50 m can be formed. If covered by a suitable material, it will reflect the sunlight well.

Obviously, in this approach enhancement of the brightness of a cosmic rocket is achieved by increasing its surface. Practical accomplishment of this project, however, involves considerable technical difficulty. For example, with a diameter of only 70 cm the weight of the entire balloon system would be about 300 gm (1). From this it can be concluded that a balloon with a diameter of 30 m will weigh at least 100 kg. The stellar magnitude of such a balloon (with a 30-m diameter) at a distance of 100,000 km would be fainter than 11^m. As before, it would be difficult to observe such a faint object in integrated light against a rather bright celestial background. Summarizing, it can be said that this project is obviously not a complete solution to the problem of optical observation of a cosmic rocket. Another question suggests itself: Can a substantial increase in brightness of a cosmic rocket be obtained at least for a very short period? In other words, can a bright light flare be arranged on a rocket? The possibility of such a flare using known means of lighting should be discarded immediately, since, in view of the vast power it would require (of the order of 10,000 kw), the weight of the apparatus would become inadmissibly large.

Nevertheless, a flare of this sort can be achieved. Nature itself points to such a possibility—the phenomena of comets.

It is well known that the radiation of a comet is basically explained in terms of resonant scattering of solar light by different molecules (for example C_2, OH, CN, etc.) as well as by Na atoms. The luminescence of the gaseous tails is also explained by the resonant scattering of solar radiation by CO^+ and N_2^+ molecules [see for example the review by Swings (2)]. It is not difficult to estimate the total number of molecules responsible for the luminescence of the head and tail of the comet. The first such basic estimate for the comet of 1911 was made by Wurm (3) in 1943. The results of Wurm's computation are as follows.

The concentration of CO^+ molecules in the tail of the comet of 1911 at a distance of 0°.5 from its head (assuming that the thickness of the tail is 3.10^{10} cm) is approximately 1 cm^{-3}. The oscillator strength for the resonance band of this molecule was assumed to be equal to unity for this purpose.

Wurm obtained the total number of molecules $N_{c_2} = 1.5 \cdot 10^{32}$ for the head of the indicated comet, taking its reduced apparent stellar magnitude when passing its perigee ($r_p = 0.59$ a.u.) as equal to 3.6^m, and the oscillator strength for a C_2 molecule (basically responsible for the emission of the visible part of the spectrum) $f_{c_2} = 2.10^{-2}$.

If the oscillator strength of the emitting molecule or atom is close to unity, the number of molecules contained in the head of the comet is reduced to 3.10^{30}. Assuming the mass of such a hypothetical molecule to be 3.10^{-23} gm, we find that the total mass of the gas contained in the head of the comet which would produce the same optical effect as the comet of 1911 is of the order of 10^8 gm or 100 tons. This is a very small value (on a cosmic scale, naturally). The distance to this comet was approximately 1 a.u. If this distance had been 100,000 km, an approximately equal optical effect could have been obtained by a cloud of a suitable gas with a mass of about 300 gm. Here we have taken into consideration that during its perigee the comet of 1911 was considerably closer to the sun than to Earth.

[1] Numbers in parentheses indicate References at end of paper.

This naturally suggests the idea of ejecting a cloud of suitable gas from an interplanetary rocket in order to produce resonant fluorescence of the solar radiation. The solar photons thus dispersed by the cloud could be observed on Earth. Such a cloud could be called an "artificial comet."

On the basis of these considerations, we suggested the creation of an artificial comet as a method for optical observation of a rocket in interplanetary space.

Let us carry out the design for the artificial comet by a method different from the one used for the "real" comet (3). We will assume that sodium is the substance to be vaporized. As will be seen in the following, sodium is not an ideal material with which to build an artificial comet. It should be noted, however, that at the time we began our project, the United States had had experience in vaporizing sodium in the upper atmosphere, which made the basic technical steps necessary for the solution of this problem completely obvious. If one assumed the dispersion to be isotropic (such a limitation is unimportant), the number of quanta dispersed in a unit volume of the cloud in a unit time interval in a unit space angle will be equal to

$$\epsilon = (1/4\pi) n_1 B_{12} u_{12} \qquad [1]$$

where

u_{12} = spectral density of the solar radiation in the vicinity of Earth (in a frequency scale)
B_{12} = Einstein coefficient

The u_{12} value can be determined from the direct observations of the intensity distribution of sun radiation in the spectrum.

In accordance with the observations by Abbott and Wilsing, the intensity of radiation, averaged across the solar disk and computed per unit length of the spectrum in the vicinity of the D-lines, is equal to (4)

$$F_\lambda = 33 \cdot 10^{13} \text{ erg} \cdot \text{cm}^{-3} \cdot \text{sec}^{-1}$$

The residual intensity in the center of the lines is $r = 0.055$ (5). The spectral density of the solar radiation near Earth, using the frequency scale, is

$$u_{12} = \frac{\lambda^2}{c^2} \pi F_\lambda \left(\frac{r_\odot}{R}\right)^2 r \qquad [2]$$

where

$r_\odot$ = $6.99 \cdot 10^{10}$ cm, radius of the sun
R = $1.495 \cdot 10^{13}$ cm, distance between Earth and the sun

Utilizing known relationships between the Einstein coefficients, we obtained from Eqs. 1 and 2 the following expression for the surface brightness of the sodium cloud

$$I = \epsilon l = \frac{l}{4\pi} n_1 \frac{g_2}{g_1} \frac{A_{21} \cdot c^3}{8\pi h \nu^3} u_{12} = \frac{4l}{\pi} \frac{A_{21} g_2}{g_1} \frac{n_1 \lambda^5}{8hc^2} F_\lambda \left(\frac{r_\odot}{R}\right)^2 r \qquad [3]$$

Let us assume that I is the total brightness of both components of the yellow sodium doublet. For the D_1 line the oscillator strength is $f = \frac{2}{3}$, $A_{21} = 5 \cdot 10^7$ sec, $g_2/g_1 = 2p$; for line D_2, $f = \frac{1}{3}$, $A_{21} = 2.5 \cdot 10^7$ sec, $g_2/g_1 = 1$.

Completing the computation, we obtain

$$I = 5.6 \cdot 10^{-2} \, n_1 \, l \text{ photons cm}^{-2} \cdot \text{sec}^{-1} \cdot \text{ster}^{-1} \qquad [4]$$

From Eq. 4 it follows that each Na atom located in the field of solar radiation at a distance of 1 a.u. from the sun scatters about 0.7 of a quantum in the D resonance lines each second in all directions.

Let us assume now that at a distance $R_1 = 100{,}000$ km, q gm of sodium have been ejected in a gaseous state. Expanding in the vacuum after a certain time t, the sodium cloud will have a radius g. The velocity of expansion V_T of the cloud

will be of the order of the thermal velocities of the sodium atoms. Thus, $\rho = V_T t$.

If q exceeds a certain (quite small) value, the optical thickness of the cloud t in the resonance lines will be considerably larger than unity in the period of its initial expansion. First let us consider the radiation of an optically thin cloud, which will always occur when $\tau \ll 1$. The number of atoms in the cloud is

$$N_{Na} = q/m_{Na} = 2.6 \cdot 10^{22} \cdot q \qquad [5]$$

The radiation flux from the cloud

$$F_{cloud} = \frac{5.6 \cdot 10^{-2}}{R_1^2} \cdot N_{Na} \approx 15 \cdot q \text{ photons} \cdot \text{cm}^{-2} \cdot \text{sec}^{-1}$$

The radiation flux of the sun is $F_\odot = 1.32 \cdot 10^6 \text{ erg} \cdot \text{cm}^{-2} \times \text{sec}^{-1}$, and its bolometric apparent stellar magnitude $m_b = -26.95$. From this it follows that the bolometric stellar magnitude of an optically thin sodium cloud, having a weight of 1 gm when located 100,000 km from Earth, will be 14^m. Considering that the visible region of the spectrum accounts for about 15% of the energy, that the visible magnitude of the sun is $m_v = -26.86$, and that in the region of the D-lines the sensitivity curve of the eye reaches 0.7 of its maximum value, we find that the visual stellar magnitude of our cloud will be 12.5^m. If the mass of the optically thin cloud is 1 kg, then with the same R_1 its visual magnitude would be 5^m.

Let us consider the case in which the optical thickness of the cloud at the resonance lines is $\tau > 1$. In such a case, as a first approximation, the cloud can be compared to a surface reflecting the sunlight in a narrow spectral band $\Delta\lambda_1$, with an albedo equal to the residual intensity of the D-line in the spectrum of the sun, e.g., approximately 0.055. It should be noted that the albedo of the moon is about the same (0.07).

It τ is not very large, $\Delta\lambda_1 \approx \Delta\lambda_D$, where $\Delta\lambda_D$ is the Doppler width of the spectral line being dispersed by the cloud. If $\tau \gg 1$, then $\Delta\lambda_1 = k\Delta\lambda_D$, where $k = 2$–3.

On the basis of our analogy, let us estimate the surface brightness of a cloud the optical thickness of which is not very large, though larger than unity.

Assuming the sodium temperature in the cloud to be $T = 1500$ deg, we will find that

$$\Delta\lambda_D = (\lambda/c)\sqrt{2kT/m_{Na}} = 2 \cdot 10^{-2} \text{ Å} \qquad [6]$$

On the other hand, assuming the visual length of the spectrum as about 1000 Å, we will find that in the visual region the surface brightness of the cloud is about 75,000 times less than that of the moon.[2] Assuming for the latter the value of -14^m per deg^2, we find that the surface brightness of the cloud is -1.5^m per deg^2, e.g., several hundred times the brightness of the nocturnal sky.

If $\tau \gg 1$, then $\Delta\lambda_1$ can be approximately equated to $(2$–$3)\Delta\lambda_D$. It should also be considered that there are two sodium lines (D_1 and D_2), which increases the width of the spectral region where the albedo is sufficiently large. Thus, for a very dense sodium cloud the surface brightness can reach -3.5^m per deg^2.

As the cloud expands, its optical thickness will decrease rapidly (in proportion to ρ^{-2}), and the surface brightness will decrease first gradually (as long as $\tau > 1$) and then quickly in proportion to ρ^{-2}. During the very last stages of expansion into the vacuum when $\tau \ll 1$, the cloud will resemble a ring nebula with rather attenuated rims.

During a moonlit night if the sun has not sufficiently set beyond the horizon, the surface brightness of the sky can exceed the surface brightness of the sodium cloud.[3] With the use of light filters, however, the contrast of the cloud in relation to the celestial background can be considerably increased, since the radiation of the cloud is monochromatic. For example, if an interference filter with a transmission bandwidth of 30 Å is used, the contrast of the cloud in relation to the background is increased approximately 50 times, i.e., by more than four stellar magnitudes.

Let us now estimate the maximum linear dimensions of an optically thick cloud.

We will denote the radius of the cloud with an optical thickness of 2 by ρ_2. Obviously we will obtain the condition

$$\frac{S_\nu \cdot N_{Na}}{(4/3)\pi\rho_2^3} \cdot 2\rho_2 = \frac{S_\nu \cdot 2.6 \cdot 10^{22} q}{2\rho_2^2} = 2 \qquad [7]$$

where

$$S_\nu = \frac{\sqrt{\pi}e^2}{mc} \cdot \frac{1}{\Delta\nu_D} \cdot e^{-\left(\frac{\nu-\nu_0}{\Delta\nu_D}\right)^2}$$

is the absorption coefficient.

With $T = 1500$ deg, $\nu = \nu_0$ ($S_\nu \approx 10^{-11}$ cm^2) and $q = 1000$, obtain $\rho_2 \approx 10^7$ cm. Generally $\rho \sim q^{1/2}$, e.g., it depends comparatively little upon the mass of the cloud. At a distance of 100,000 km the maximum angular dimensions of an optically thick cloud with $q = 100$ are $6'.7$, and at distances of 400,000 km, e.g., near the moon, such a cloud would have angular dimensions of $1'.7$. Even with a camera having a short focal length such a cloud would be observed as an areal object.

A basic parameter is the duration during which the cloud will remain optically thick. With $V_T \sim 10^5$ m per sec (which corresponds to thermal velocities of sodium at $T = 1000$ C), the cloud will stay optically thick for about 100 sec, after which its surface brightness will start diminishing sharply in accordance with the further spreading of the cloud. The velocity of expansion of the cloud in space and the advancing speed of the cloud, which is equal to the rocket speed, are factors limiting the exposure. Obviously, it is required that during the exposure time the cloud should not move more than, say, half of its dimension in the field of vision. Obviously, longer exposures with $\tau > 1$ will not contribute to increased blackening. If, for example, the transverse component of the speed in regard to Earth is small, but the speed of spreading of the cloud is about 1.5 km per sec, the optimum exposure should not exceed 25 to 30 sec. This condition obviously determines the speed of the camera, that should be used to photograph the artificial comet. The requirement that the "comet" be photographed as an areal object determines the lower value of the focal ratio of the camera.

The aforementioned considerations permitted determination of the camera parameters with which the comet can be photographed. On this basis, we have worked out the technical requirements for the apparatus to be used for observation of the artificial comet.

The spreading of the cloud is limited by the ionization of the sodium atoms, produced by the ultraviolet radiation of the sun. The ionization potential of the sodium is equal to 5.12 ev. The flux of solar photons, the energy of which is less than 5.12 ev ($\lambda < 2400$ Å), capable of ionizing sodium in accordance with straight lines determined by $F(\lambda < 2400)$ is approximately $10^{14} \text{ cm}^{-2} \cdot \text{sec}^{-1}$.

According to Bates' calculations (6), the effective cross section of photo-ionization is very small for sodium, $\sigma_{Na} \approx 3.7 \cdot 10^{-19}$ cm^2 (at the absorption limit). The life of neutral sodium atoms in the interplanetary medium would be equal to

$$t_{Na} \approx 1/\sigma_{Na} F(\lambda < 2400) \qquad [8]$$

From this it follows, that $t_{Na} \approx 2.7 \cdot 10^4$ sec or 7.5 hr. This means that the effect of photo-ionization as a factor limiting the possibility of observation of an artificial sodium comet is completely without significance. Long before this its brightness decreases to the point where it becomes unobservable, as a result of expansion.

[2] We have taken into consideration the spectral sensitivity curve of the eye in the region of the D-line.

[3] *Editor's Note*: Dr. F. D. Miller of the University of Michigan Observatory has pointed out that this sentence is without meaning. It is difficult to see what the point is, since, if the sun is not sufficiently far below the horizon, the sky will be too bright, whatever the phase of the moon.

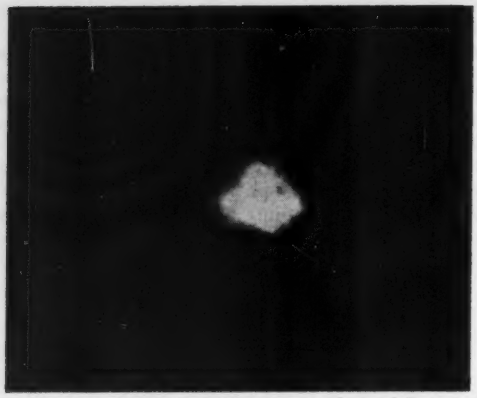

Fig. 1 Photograph of the artificial comet formed Jan. 3, 1959 during the flight of the first cosmic rocket

The idea of vaporizing sodium atoms in the upper atmosphere for exploration of its physical and chemical properties was first advanced by Bates (7) in 1950. In 1955, using a rocket, Edwards, Bedinger, Manring and Cooper performed an experiment, vaporizing 3 kg of sodium in Earth's atmosphere at altitudes of 52 to 113 km under dusk conditions (8). A rather intense luminescence was observed. A sharp change in the intensity of luminescence outside the boundary of Earth's shadow was not observed.

In 1956 a similar experiment was conducted by Bedinger and Manring under night conditions (9). Two kg of sodium vapor were introduced into the atmosphere at altitudes of 60 to 140 km. The intensity of the sodium luminescence varied considerably depending on the altitude, and at times was very considerable. These observations showed that sodium reacts quickly with the atoms and molecules of Earth's atmosphere. The life of sodium atoms at these elevations amounts to several minutes. It follows from this that to obtain a sodium flare under pure dusk conditions, the rocket should reach a rather considerable altitude. To carry out the described experiments, a special apparatus was developed for vaporizing sodium [see (8)] by burning chemically pure thermit. In accordance with (8), all of the sodium was converted into an atomic state in the process of vaporization.

Vaporization of 1 kg of sodium required to 3.2 kg of thermit. The Na_2 molecules, as indicated in (8), must be very few, since the dissociation energy of this molecule is very small. On the other hand, ionization of sodium did not also take place, since the vaporization temperature was comparatively low (T = 1000 C). We should note, however, that in the process of vaporization a considerable portion of the sodium can be used for creation of small, solid and liquid particles. This effect was not considered in (8).

During realization of the artificial comet project in the USSR, an apparatus was developed for the vaporization of sodium into an atomic state. To test the operation efficiency of the evaporator, an experiment was carried out on Sept. 19, 1958 in which a sodium vapor cloud illuminated by the sun was formed at a height of 440 km. A geophysical altitude rocket was used for this purpose. The absolute photometric measurements of the sodium cloud formed permitted determination of the quantity of the evaporated sodium atoms. From this the evaporation coefficient was found, and it proved to be rather high. At the same time, from observations of the diffusion of the formed cloud, the density of Earth's atmosphere at the height of 440 km was determined with great accuracy (10).

The artificial comet was first used during the flight of the first Soviet cosmic rocket on Jan. 3, 1959. At a preprogramed time, $3^h56^m20^s$ (Moscow time), 1 kg of sodium was evaporated from aboard this rocket. For observations of the artificial comet a network of stations had been prepared beforehand; they had been supplied with especially developed powerful miniature cameras (f = 250 mm, d/f = 1:2.5 and f = 500 mm, d/f = 1:5). Parameters of the cameras were determined by the conditions expected to prevail during observations of the aforementioned artificial comet. All cameras were equipped with multilayer interference filters with a transmission band of about 30 Å. The transparency of the filters was in the range of 30–50%. A special procedure was developed beforehand which made it possible to obtain coordinates for the artificial comet by tying it in with the stars.

Unfortunately, the weather was overcast at most of the observation stations. A confirmed photograph of the artificial comet was obtained at the Kislovodsk mountain station of the Central Astronomical Observatory (see Fig. 1).

The artificial comet was created the instant the cosmic rocket attained a distance of 119,500 km from Earth.

Preliminary evaluations gave the stellar magnitude of the comet as 7.5^m. This means that approximately 10% of the sodium was evaporated at about 100 gm. Consequently, the "life" of the artificial comet was only 30 sec. Regardless of the comparatively low efficiency of the evaporator, the first artificial comet performed its task. It allowed determination of the angular coordinates of the cosmic rocket with an accuracy considerably exceeding the radio tracking.

Topocentric coordinates for Kislovodsk (for the aforementioned instant) were

$$\alpha = 14^h08.4^m \qquad \delta = -5°04'$$

There is sufficient reason to believe that in the future the methods of creating and observing of artificial comets will be greatly improved.

During the flight of the second Soviet cosmic rocket on Sept. 12, 1959 at $12^h49^m30^s$, Moscow standard time, an ar-

Fig. 2 Photograph of the artificial comet formed at $21^h49^m30^s$ on Sept. 12, 1959 during the flight of the second cosmic rocket. a $21^h50^m03^s$

tificial sodium comet was formed. Successful observations of this comet were made simultaneously by Soviet and foreign observatories. Several dozen photographs of the different development stages of the comet were obtained. These photographs permitted determination of the rocket coordinates with good accuracy. The topocentric coordinates for Al'ma-Ata are

$$\alpha = 20^h36^m00.24^s \qquad \delta = 9°7'12.2''$$

The geocentric distance of the artificial comet was equal to 156,000 km. Its apparent photovisual magnitude was about 4.5^m. The angular diameter of the sodium cloud at the limit of possible observation reached 30′. The measured spreading speed of the artificial comet was 1.7 km per sec. The artificial comet could be observed on the cameras used for the observations during a 6-min period. On the photographs shown (Figs. 2a–2m), obtained with an electronic telescopic camera by V. F. Yesipov in Stalinabad, various stages of development of the artificial comet can be seen.

We will now consider a possible variation of the artificial comet method, having in our opinion bright future prospects.

Although sodium has several substantial advantages which permit its use in the creation of an artificial comet, it still has one essential drawback. The solar radiation dispersed is greatly weakened owing to the presence of strong Fraunhofer lines D_1 and D_2 in the sun's spectrum. Lithium does not have this drawback. As is known, there is practically no lithium in the sun, and therefore there is no resonance Fraunhofer

b $21^h50^m11^s$

c $21^h50^m20^s$

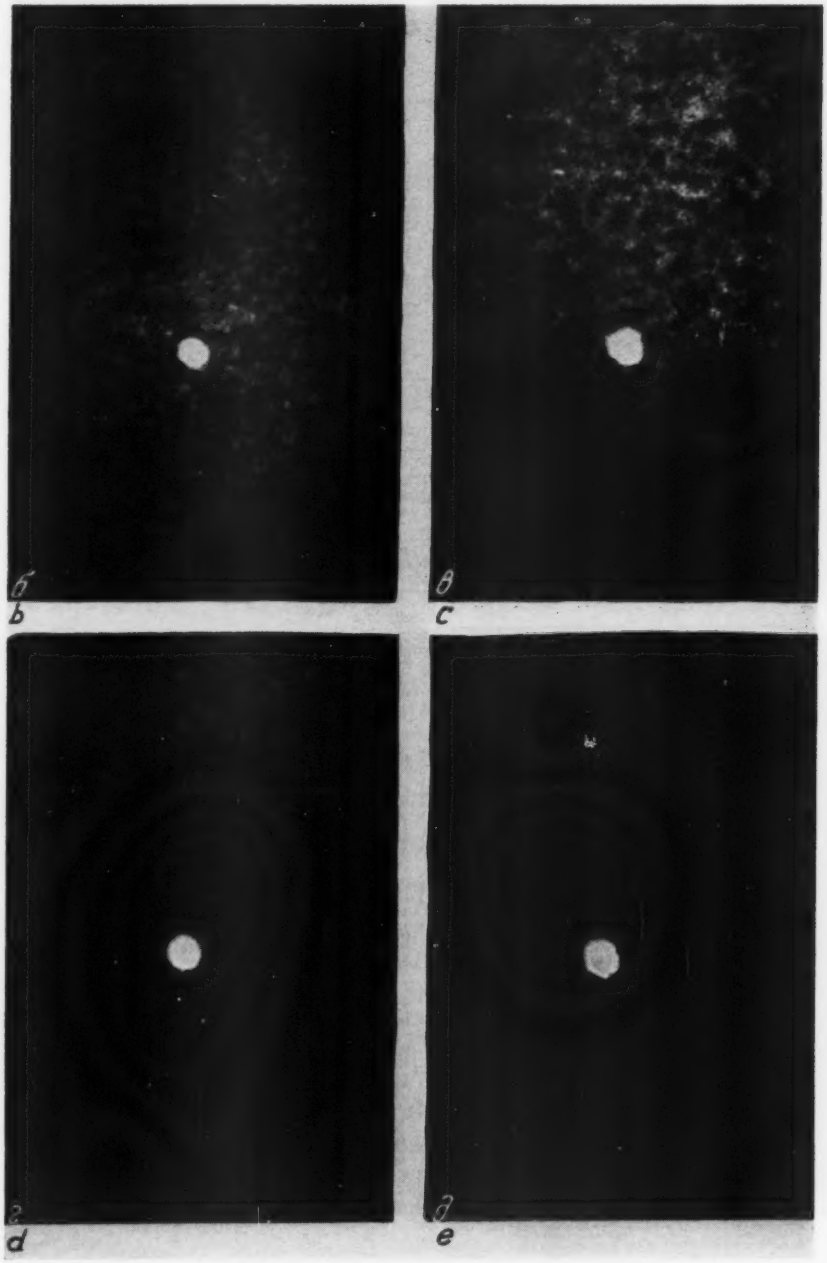

d $21^h50^m32^s$

e $21^h50^m43^s$

Fig. 2 continued

line λ6708. For this reason alone, we obtain a nearly 20-fold gain in radiation intensity. Furthermore, lithium is almost three times as light as sodium. It should be noted that the Einstein coefficient A_{21} for the line λ6708 is 1.6 times smaller than that of the sodium *D*-line.

The result of this is that for an equal quantity of dispersed photons an optically thin lithium cloud would contain approximately 40 times less mass than an optically thin sodium cloud (the thermit mass is not considered; we do not exclude the possibility of developing new evaporation methods). The surface brightness of the optically thick lithium cloud will be approximately -5^m (bolometric) per deg^2.

It is important to note, however, that the sensitivity of the human eye in the spectrum range 6708 Å is very small, especially under dusk conditions. That is why, for visual observation, artificial lithium comets are hardly useful at all.

However, the electronic optical converters with a corresponding photocathode can be quite efficient for observation of artificial lithium comets.

The ionization potential of lithium is 5.38 ev. According to (5), the effective photo-ionization cross section for Li at the absorption limit equals $3.2 \cdot 10^{-18}$ cm^2. Taking into account a higher lithium ionization potential, we will find that the life of the neutral lithium atoms in the interplanetary medium will be approximately five times shorter than that of sodium.

A practical solution of the problem of an artificial lithium

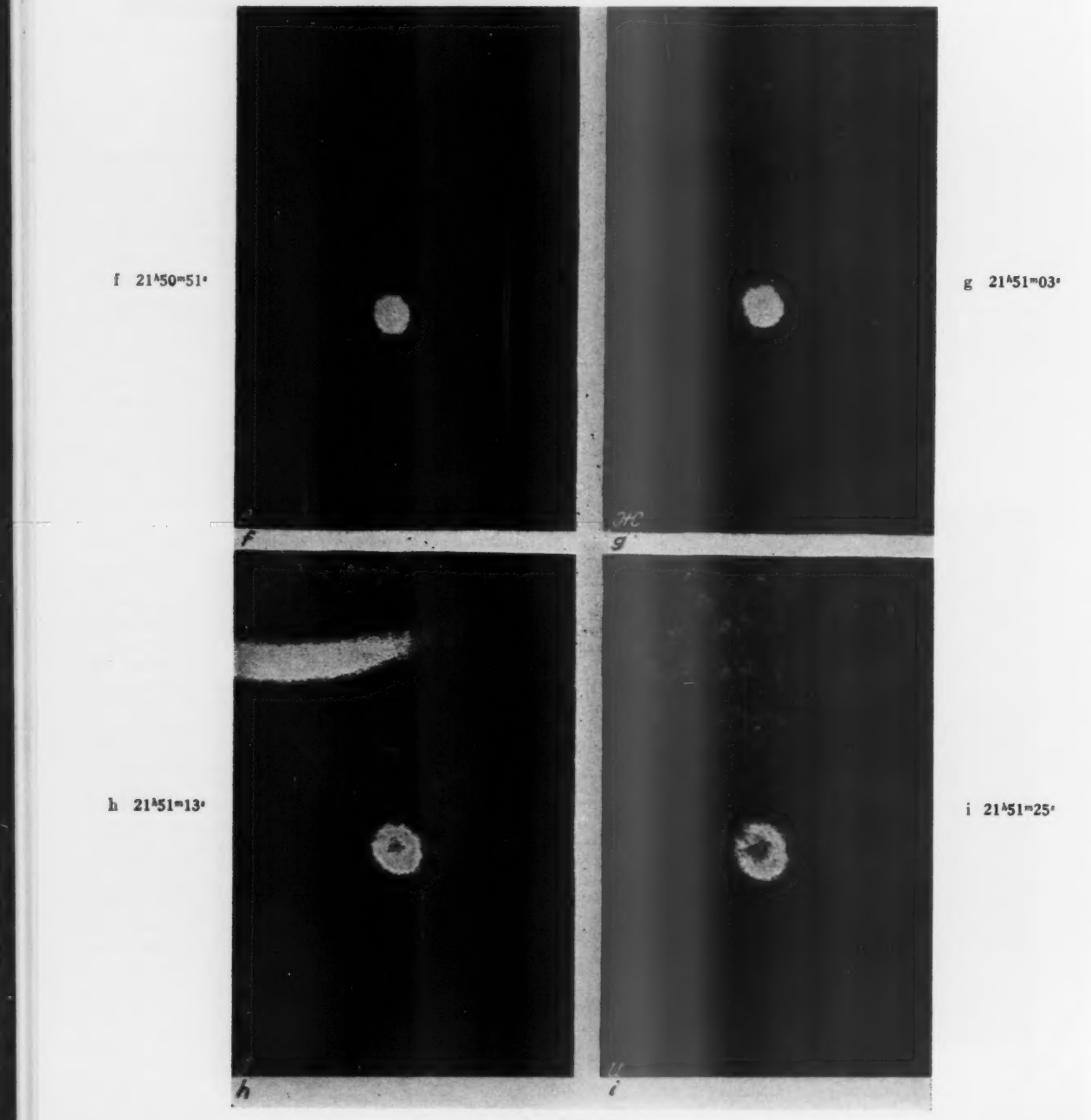

Fig. 2 continued

comet will also solve the problem of creating an interplanetary "tracer" rocket, at least in the vicinity of Earth, at distances of several thousand kilometers. The duration of flight in this region of interplanetary space is of the order of several tens of hours. If every 1–2 sec, 1 gm of lithium is evaporated, then the "comet," as can be easily computed, will be observed as a star of an approximate bolometric magnitude of 10.

During this, total consumption of lithium will amount to several tens of kilograms (under ideal conditions, of course, not considering thermit and other "parasitic" weights). Interplanetary tracer rockets could have various applications. In particular, they would solve completely the problem of observing "lunar" rockets in the interplanetary medium.

Lithium comets pave the way for optical observations of cosmic rockets at a distance of several millions and even tens of millions of kilometers.

It must again be emphasized, however, that a prerequisite for the development of lithium comets is the creation of a method of efficient evaporation of lithium. Corresponding apparatus and fuel must have the least possible weights. It is not impossible that the application of atomic energy in the future will permit solution of the fascinating task of creating an artificial lithium comet.

In conclusion let us consider one more question.

A variation of the artificial comet project is the dust comet project. Dust, as is generally known, scatters the sunlight in

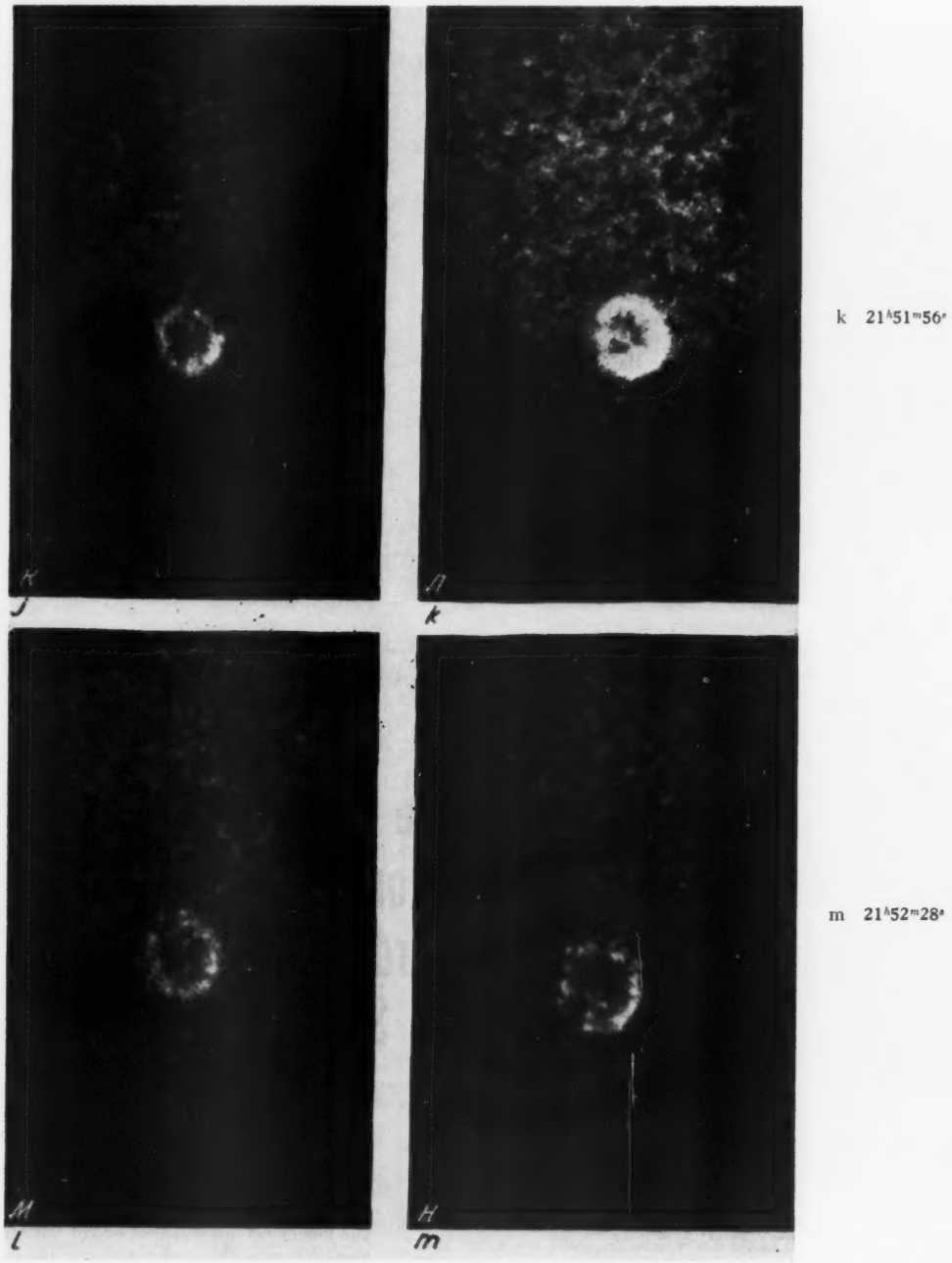

Fig. 2 continued

the realm of the solar system. This phenomenon is observed in a whole group of cases. For instance, dust tails are observed in some comets. Dust particles concentrated in the ecliptic plane create the optical effects of zodiacal light and the so-called Fraunhofer component of the solar corona. That is why it is interesting to compare the efficiency of artificial dust and gas comets.

Let us assume we have 1 kg of suitable material which, with the help of an appropriate mechanism, can be completely atomized into spherical particles of radius a. We will not discuss here the technical side of the problem or the practical possibility of the process of complete atomization.

The number of particles forming the dust cloud would be

$$N = \frac{1000}{4/3\pi a^3 \delta} \qquad [9]$$

where δ is the specific weight of the atomized substance.

Each dust particle would scatter the solar light in the direction of Earth with an effective cross section

$$\sum = K(\theta)\chi\pi a^2 \qquad [10]$$

where $k(\theta)$ is the scattering index, and the value χ depends on the nature and dimensions of the scattered particles.

To obtain numerical results let us assume that $a = 0.3\ \mu$ (smaller dust particles could hardly be obtained; even particles with $a = 0.3\ \mu$ are difficult to prepare).

Then, the value χ determined by diffraction effects will be, in accordance with (11), equal to 2 (for dielectric materials). Let us assume that the index is spherical, that is, $K(\theta) = 1$. Then the total surface of all dust particles will be equal to $N\Sigma = 1.6 \cdot 10^7 \text{cm}^2$, which is equal to the surface of a sphere with a diameter of 44 m.

On the other hand 1 kg of sodium vapor contains $2.6 \cdot 10^{25}$ atoms. Assuming that the effective cross section of resonance fluorescence is 10^{-11} cm², taking into consideration that the residual intensity in the sodium lines is $r = 0.055$, and that the equivalent width of the scattering coefficient is 0.02 Å (which constitutes $1/75{,}000$ of the effective extent of the visual part of the spectrum), let us find the "equivalent surface" of the sodium cloud, "smeared" over the entire visual part of the spectrum: $1.9 \cdot 10^5$ cm², e.g., 12 times larger than for a dust cloud of the same mass. Taking the index of scattering into consideration, one can considerably decrease the flux of the solar radiation scattered by the dust because the indexes of such particles are as a rule considerably elongated in the direction of scattering.

Summarizing, we can say that the efficiency of the dust comet is considerably lower than that of the sodium one (not to mention the lithium comet). An invaluable advantage of gaseous comets in comparison with dust comets is the monochromatic nature of their radiation, which makes it possible with the help of appropriate light filters to conduct observations during an increased background brightness.

The only advantage of the artificial dust comet is the length of its existence, because the dust particles fly apart rather slowly (the velocity is of the order 10^4 cm per sec).

On the basis of its efficiency, the artificial dust comet generally occupies an intermediate position between the gas comet and the balloon.

The question of utilizing as artificial comets certain molecules having resonance bands situated in the visual part of the spectrum (for instance CN) deserves special consideration. However, we will not discuss the "molecular" comets in this article.

References

1 Science News Letters, vol. 72, no. 16, 1957, p. 244.
2 Swings, P., *Vistas in Astronomy*, vol. II, London, 1956, p. 358.
3 Wurm, K., *Mitt. Hamburger Sternwarte*, vol. 8, 1943, p. 51.
4 Unsöld, A., *Physics of Stellar Atmospheres*, M., 1947.
5 Allen, C. W., *Astrophysical Quantities*, London, 1955, p. 137.
6 Bates, D., *Monthly Notices Royal Astron. Soc.*, vol. 106, 1946, p. 432.
7 Bates, D., *J. Geophysics Res.*, vol. 55, 1950, p. 347.
8 Edwards, Bedinger, Manring and Cooper, *The Airglow and the Aurorae*, London, 1957, p. 123.
9 Bedinger, Ghosh and Manring, *J. Geophysics Res.*, vol. 62, 1957, p. 170.
10 Shklovskii, I. S. and Kurt, V. G., *Artificial Earth Satellites*, no. 3, 1959, p. 66.
11 Shifrin, *Dispersion of Light in Turbid Media*, M., 1950.

Upper Atmosphere Density Determination, Based on Flight Observations of the Third Soviet Artificial Earth Satellite

P. E. EL'IASBERG
and
V. D. YASTREBOV

AS HAS been shown in a series of recently published papers (1,2),[1] the application of the observational results of the flight of artificial Earth satellites for determination of the density of the upper atmosphere, is one of the most accurate methods of solving the given problem. Nevertheless, observation of each individual satellite gives very limited data on the condition of the upper atmosphere, corresponding to the rather narrow range of height variation and other conditions (illumination, solar activity, etc.) determining the air density at high altitudes. Consequently, the accumulation

Translated from *Artificial Earth Satellites*, 1960, no. 4, pp. 18–30. Translated by Research Information Service, New York.

[1] Numbers in parentheses indicate References at end of paper.

of data obtained as a result of measurement of the orbital elements of various artificial Earth satellites for the purpose of obtaining original data for construction of a more complete dynamic model of the atmosphere (e.g., a model which will take into account the dependence of the atmospheric elements not only from the height but also from other factors) assumes great importance.

This paper is devoted to evaluation of the density determination results for the upper atmosphere, based on data gathered by the most accurate measurement of the orbital elements of the third Soviet artificial Earth satellite during the initial period of its existence.

When determining the satellite orbit, the following basic assumptions were made in regard to the nature of its motion:

a) The satellite was regarded as a physical point moving under action of the gravitational pull of Earth and the drag of the atmosphere.

b) The gravitational acceleration potential was determined from the expression

$$W = \alpha_{00}(R/r) + \alpha_{20}(R/r)^3 P_{20} \qquad [1]$$

where

R = average radius of Earth
r = distance to its center
P_{20} = $1/2(3 \sin^2 \phi - 1)$, a Legendre polynomial of the second order
ϕ = geocentric latitude

In the expression for the gravitational pull potential of the ellipsoid, the term $5\alpha_{40}(R/r)^5 P_{40}$ is not taken into account, because it is smaller than the members which appear when anomalies of the gravitational pull are considered. Coefficients α_{00} and α_{20} are constants, the values of which are determined by geometric dimensions and gravitational characteristics of the Earth ellipsoid accepted as the Earth model.

c) The acceleration due to drag was calculated using the equation

$$a_{Rx} = S\rho v^2 \qquad [2]$$

where

v = vector modulus of the satellite velocity in relation to a coordinate system, rigidly connected to Earth
ρ = air density at a given altitude
S = ballistic coefficient, the value of which is determined geometrically, by weight and by the aerodynamic properties of the satellite

Air density ρ as a function of the flight altitude of the satellite was determined by Eq. 3 which can be used conveniently by an electronic computer

$$\rho = A_i e^{k_{1i}(h-h_i)^2 - k_{2i}(h-h_i)} \qquad [3]$$

where h is the flight altitude of the satellite; A_i, k_{1i}, k_{2i} are constant coefficients used in the computations within the altitude intervals

$$h_i \leqslant h \leqslant h_{i+1} \qquad [4]$$

Coefficients A_i, k_{1i}, k_{2i} were first calculated on the basis of the accepted model of the atmosphere, whereby the number of intervals in Eq. 4 was selected to insure an acceptable approximation accuracy for the density as a function of altitude by Eq. 3.

d) The flight altitude h was computed using the equation

$$h = r - \bar{a}(1 - \alpha \sin^2 \psi) \qquad [5]$$

where a and α are, respectively, the long half axis and the flattening of the Earth ellipsoid. The error in altitude when computed in accordance with Eq. 5, connected with the deviation of the true vertical from the radius vector and the noncoincidence of the spheroid surfaces with the ellipsoid, does not exceed 30 m, and can be disregarded.

The motion of the satellite was observed in an orthogonal coordinate system $Oxyz$, rigidly connected to Earth. The point of origin of this coordinate system coincides with Earth's center, axis Oz passes through the north pole, axis Ox through the Greenwich meridian, axis Oy points to the east.

The following basic notations will be used subsequently

$q_j(t_i)$ = orbit elements in the coordinate system $Oxyz$ ($j = 1, 2, \ldots, 6$; t_i = time of carrying out of the ith measurement)
q_{j0} = initial conditions of motion, referred to a certain instant t_0
r_i = parameters of the orbit being measured
r_{ii}, r_{ip} = their measured and calculated values, respectively
$\sigma(r_i)$ = average quadratic deviation, characterizing the measurement accuracy of the parameter r_i

The elements of a satellite orbit are determined on the basis of data obtained by measurement as a result of solution of the boundary problem for the following system of differential equations of motion

$$\dot{v}_x = -S\rho v v_x - g_r \frac{x}{r} + g_m \frac{z}{r}\frac{x}{r_1} + 2\Omega_3 v_y$$

$$\dot{v}_y = -S\rho v v_y - g_r \frac{y}{r} + g_m \frac{z}{r}\frac{y}{r_1} - 2\Omega_3 v_x$$

$$\dot{v}_z = -S\rho v v_z - g_r \frac{z}{r} - g_m \frac{r_1}{r}$$

$$\dot{x} = v \qquad \dot{y} = v_y \qquad \dot{z} = v_z \qquad [6]$$

where

$r = \sqrt{x^2 + y^2 + z^2}$
$r_1 = \sqrt{x^2 + y^2}$
$v = \sqrt{v_x^2 + v_y^2 + v_z^2}$
g_r, g_m = radial and meridional component of the gravity acceleration, respectively (positive directions are: g_r, toward Earth center; g_m, southward)
Ω_3 = angular velocity of Earth rotation

The values of g_r and g_m are determined by the relationships

$$g_r = (1/r)[\alpha_{00}(R/r) + 3\alpha_{20}(R/r)^3 P_{20}] - \Omega_3^2 r_1 \cos\psi$$

$$g_m = -(1/r)\alpha_{20}(R/r)^3 P_{21} + \Omega_3^2 r_1 \sin\psi \qquad [7]$$

where

$P_{21} = 3 \sin\psi \cos\psi$
$\sin\psi = z/r$
$\cos\psi = r_1/r$

Initial data for solution of the boundary problem are the results of measurements t_i, $r_i (t_i \leqslant t_i + 1, i = 1, 2, \ldots, N$, where N is the total number of individual measurements) and the approximate values of the initial conditions of the motion $\tilde{q}_{j0}$, referred to a certain instant $t_0 \leqslant t_i$. As a result of the solution of the boundary problem, more accurate initial conditions of the motion at the instant t_0 were obtained by introducing corrections into the approximate values in accordance with equations

$$q_{j0}^{(l)} = \tilde{q}_{j0} + \sum_{i=1}^{l} \delta q_{j0}^{(i)} \qquad (j = 1, 2, \ldots, 6) \qquad [8]$$

where l is the number of approximations required for com-

plete convergence during the procedure of successive approximations.

In determining the corrections δq_{j0} it was assumed that variations, of the parameters being measured, are related to the variations of the initial conditions of movement by linear relationships of the form

$$\Delta r_i = \sum_{j=1}^{6} \frac{\partial r_i}{\partial q_{j0}} \delta q_{j0} \qquad (i = 1, 2, \ldots, N) \qquad [9]$$

where $\partial r_i/\partial q_{j0}$ are partial derivatives of the parameters being measured in respect to the initial conditions of the motion. The accuracy of such an assumption is confirmed by the rapid convergence of the procedure of successive approximations, even with a quite inaccurate $\bar{q}_{j0}$ containing errors of the order of several hundred meters per second in the corresponding velocity vectors, and several hundreds of kilometers in the coordinates.

Slant ranges from the measuring point (MP) to the satellite D_i, azimuths of the sight line "MP-satellite" A_i, and the position angles of this line γ_i were utilized as measured parameters.

The method of least squares, which permits determination of the orbital elements with the greatest possible accuracy, was utilized for computation of corrections for the initial conditions of the motion.

For unequal measurements of parameters D_i, A_i and γ_i, relationships (3) were used as conditional equations

$$\sum_{j=1}^{6} \frac{\partial r_i}{\partial q_{j0}} p_i \delta q_{j0} = \Delta r_i \cdot p_i \qquad (i = 1, 2, \ldots, N_1) \qquad [9']$$

where

p_i = $1/\sigma(r_i)$, "weight" of the ith measurement
$\Delta r_i = r_{iN_1} - p_{ip}$
N_1 = the number of measurements utilized

In accordance with known rules (3), normal equations are formed based on the given system of conditional equations 9′

$$\sum_{n=1}^{6} a_{mn} \delta q_{n0} = b_m \qquad (m = 1, 2, \ldots, 6) \qquad [10]$$

where

$$a_{mn} = \sum_{i=1}^{N_1} \frac{\partial r_i}{\partial q_{m0}} \cdot \frac{\partial r_i}{\partial q_{n0}} \cdot p_i^2$$

$$b_m = \sum_{i=1}^{N_1} \frac{\partial r_i}{\partial q_{m0}} \cdot \Delta r_i \cdot p_i^2 \qquad (m, n = 1, 2, \ldots, 6) \qquad [11]$$

In the system of six linear algebraic equations, Eqs. 10, values which enter into expression 11 are determined in each approximation in the course of computation of the satellite orbit by numerical integration method based on the initial conditions q_{j0}. For convenience in working with the electronic computer, seven systems of motion equations, Eqs. 6, are integrated in parallel, each of which corresponds to one of the seven aggregates of initial conditions of motion

$$\left.\begin{array}{lll} v_{x0} & v_{y0}, v_{z0}, x_0, y_0 & z_0 \\ v_{x0} + \Delta v_{x0} & v_{y0}, v_{z0}, x_0, y_0 & z_0 \\ \ldots\ldots\ldots\ldots & \ldots\ldots\ldots\ldots & \ldots\ldots \\ v_{x0} & v_{y0}, v_{z0}, x_0, y_0 + \Delta y_0 & z_0 \\ v_{x0} & v_{y0}, v_{z0}, x_0, y_0 & z_0 + \Delta z_0 \end{array}\right\} \qquad [12]$$

Thus, at each step of numerical integration, the elements of the normal and of six disturbed trajectories are known, which permits one to determine the derivatives of the current orbital elements based on the initial conditions of motion $(\partial q_m/\partial q_{j0})(t_i)$ by the method of finite differences. The values r_{ip} and $\partial r_i/\partial q_{j0}$ are determined by the elementary finite equations[2] based on the values of the derivatives $(\partial q_m/\partial q_{j0})(t_i)$ and the elements of the undisturbed orbit $q_m(t_i)$ (with known coordinates of the given MP).

In the course of the solution of the system of Eqs. 10, the corrections $\delta q_{j0}'$ are determined, and the ith approximation to the initial conditions of the motion are found from Eqs. 8. These, together with measurement results, are used to obtain the next approximation. As a rule, all information for t_i, r_i $(i = 1, 2, \ldots, N_1)$ also included measurements, the errors of which were definitely not of a statistical nature. It is perfectly obvious that they must be excluded from processing. This is achieved by forming the conditional equations 9 for each approximation for only those measurements which satisfy the condition

$$|\Delta r_i| \leqslant \Delta r_{i\,\text{allow}} \qquad (i = 1, 2, \ldots, N_1)$$

where $\Delta_{i,\,\text{allow}}$ is the allowable deviation for the corresponding parameter (D, A or γ) being measured.

The following method of establishing the allowable deviations is most expedient. For the first approximation they are established roughly in accordance with the accuracy of the given initial conditions of motion. After each approximation, the error of the weight $\bar{\sigma}(r)$ [see (3)] and the allowable deviation $\Delta r_{i,\,\text{allow}}$ are determined in accordance with the equations

$$\bar{\sigma}(r) = \sqrt{\left(\sum_{i=1}^{N_1} \Delta r_i^2 p_i^2 - \sum_{j=1}^{6} b_j \delta q_{j0}\right) \Big/ (k - 6)} \qquad [13]$$

$$\Delta r_{i,\,\text{allow}} = \mu \cdot \sigma(r_i) \cdot \bar{\sigma}(r) \qquad [14]$$

where μ is a constant coefficient, the value of which is established before solving the problem as a function of the systematic errors characteristic for the given form of measurement, and which cannot be taken into consideration (when systematic errors are absent $\mu = 3$). Obviously, a lower limit for the deviations must be set, and it is natural to establish $\Delta r_{i,\,\min} = \mu\sigma(r_i)$ as such a limit. In the procedure of successive approximations, the error of the weight unit is continuously reduced because of the improvement in accuracy of the initial conditions of the motion and because of the continuous elimination from processing of measurements containing errors. With $\bar{\sigma}(r) \leqslant 1$, the successive approximations are made with constant allowable deviations equal to $\Delta r_{i,\,\min}$.

The inequalities

$$\frac{|\delta q_{j0}|}{\sigma(q_{j0})} \leqslant 1 \qquad (j = 1, 2, \ldots, 6) \qquad [15]$$

were used as the criterion of complete convergence of the procedure of successive approximations.

As experience in processing the measurement data showed, in carrying out the final approximations the correction of each subsequent approximation is 10 to 100 times smaller than the correction of the previous approximation. It, therefore, follows from Eq. 15 that with such a selection of the criterion of complete convergence, the accuracy of the computation exceeds the accuracy of determination of the orbit by more than one order.

In the course of the flight of the third artificial Earth satellite, the elements of the true orbit were determined on the basis of data obtained by measurement in two consecutive revolutions. With the accepted procedure of solution of the boundary problem, such a method of processing of measurement data seems the most suitable. Actually, when determining the orbit on the basis of data gathered in one revolution[3] it is, in principle, impossible to insure the necessary accuracy of determination for some of the elements, e.g., the

[2] For an exact computation of r_{ip} and $\partial r_i/\partial q_{j0}$ the elements of the orbit were interpolated with respect to the time t_i.

[3] Measurements were carried out in the territory of the USSR for a limited portion of the orbit.

Table 1

Revolution number	Orbit elements				
	a, m	i, deg	T, min	h_{min}, m	h_{max}, m
39	7,423,833	65.2062	105.9466	225,799	1,876,736
53	7,423,105	65.2024	105.9305	225,261	1,875,519
66	7,422,525	65.2053	105.9179	225,320	1,874,133
133	7,419,405	65.2027	105.8498	224,492	1,867,711
147	7,418,740	65.2025	105.8353	224,584	1,866,101
173	7,417,353	65.2044	105.8051	224,119	1,863,365
214	7,415,453	65.2035	105.7637	223,856	1,859,216
255	7,413,708	65.2036	105.7255	223,557	1,855,390

period of rotation. Moreover, with the occurrence of considerable systematic errors of measurement all elements of the orbit will be determined with large errors. On the other hand, when utilizing data gathered from measurements carried out during several days, the time required for solution of the boundary problem becomes intolerably long, and, in addition to that, the accuracy of determination of the orbit elements deteriorates considerably because of the influence of methodic errors. (Neglect of gravitational anomalies, inaccurate allowance for air resistance, and inaccuracies of numerical integration lead to additional errors which can attain a considerable magnitude, e.g., for the longitudinal inclination this error reaches several kilometers for 24 hr of flight.)

The result of the solution of the boundary problem gives final, more accurately defined values for the initial conditions of the motion t_0, q_{j0} ($j = 1, 2, \ldots, 6$). To facilitate analysis, they were reduced to the beginning of a revolution, e.g., to the instant of passing the Equator plane by the satellite during its motion from south to north. The indicated reduction was carried out by numerical integration with a positive or a negative step to reach the start of the revolution.[4]

Table 1 shows the basic orbital elements: Major axis of the osculating ellipse a, inclination i, revolution period T, minimum and maximum flight altitude h_{min} and h_{max}. They have been tabulated for selected revolutions (which we will call subsequently anchor revolutions). Let us note that a revolution period is defined as the difference between the instants of two consecutive passages through the Equator plane of the satellite during its motion from south to north.

When determining the orbital elements on the basis of data obtained by measurement, the problem of estimating the accuracy of such a determination is resolved most simply with the assumption that the measurements contain only random errors. To begin, an accuracy estimate of the determination of the initial conditions of the motion is made. For this, elements of the reverse matrix are determined $(Q_{ij}) = (a_{mn})^{-1}$, where (a_{mn}) is the matrix of the system of normal equations 10, and then the average quadratic errors $\sigma(q_{j0})$ are computed from the expressions

$$\sigma(q_{j0}) = \bar{\sigma}(r)\sqrt{Q_{jj}} \qquad (j = 1, 2, \ldots, 6) \qquad [16]$$

As indicated before, the values $\sigma(q_{j0})$ are used for computing the criteria of full convergence in accordance with Eqs. 15.

To determine the average quadratic errors of the basic orbital elements, let us regard them as functions of the initial conditions of motion

$$f_k = f_k(q_{j0}) \qquad (j = 1, 2, \ldots, 6) \qquad [17]$$

Arranging $f_k(q_{j0})$ into a series in the vicinity of the beginning of the revolution—which is exact up to members linear with respect to δq_{j0}—we will obtain

$$\delta f_k \approx \sum_{j=1}^{6} \frac{\partial f_k}{\partial q_{j0}} \delta q_{j0} \qquad [18]$$

Then values $\sigma(f_k)$ can be found in accordance with the equations of (3)

$$\sigma(f_k) = \bar{\sigma}(r)\sqrt{\sum_{i,j=1}^{6} Q_{ij} \frac{\partial f_k}{\partial q_{j0}} \frac{\partial f_k}{\partial q_{j0}}} \qquad [19]$$

where $\partial f_k/\partial q_{j0}$ are partial derivatives of corresponding orbital elements with respect to the initial conditions of motion, which are determined in accordance with known equations.

Table 2 contains the computation results of the average quadratic errors for the long half axis a, inclination i, the osculating revolution period[5] T_{osc}, the radii of the perigee r_p

[4] As a result of the solution of the boundary problem, the orbital elements were determined for a point near the beginning of a revolution.

[5] $T_{osc} = (2\pi/\sqrt{R\alpha_{00}})a^{3/2}$.

Table 2

Revolution number	Accuracy					
	$\bar{\sigma}(r)$	$\sigma(a)$, m	$\sigma(i)$, deg	$\sigma(T_{osc})$, min	$\sigma(r_p)$, m	$\sigma(r_a)$, m
39	0.71	1	$1.0 \cdot 10^{-4}$	$0.2 \cdot 10^{-5}$	23	23
53	1.08	2	$0.7 \cdot 10^{-4}$	$0.4 \cdot 10^{-5}$	10	11
66	1.58	1	$1.7 \cdot 10^{-4}$	$0.3 \cdot 10^{-5}$	17	17
133	1.42	2	$2.1 \cdot 10^{-4}$	$0.4 \cdot 10^{-5}$	21	22
147	1.04	4	$1.8 \cdot 10^{-4}$	$0.9 \cdot 10^{-5}$	20	22
173	0.78	1	$0.5 \cdot 10^{-4}$	$0.2 \cdot 10^{-5}$	14	15
214	0.73	1	$0.7 \cdot 10^{-4}$	$0.1 \cdot 10^{-5}$	12	12
255	0.93	1	$0.8 \cdot 10^{-4}$	$0.3 \cdot 10^{-5}$	8	9

Table 3

Orbit element	Dimension	Coefficients ξ_0	Coefficients A_ξ
h_{min}	m	225,545	−9.80
h_{max}	m	1,876,657	−99.70
T	min	105.9438	$-1.029 \cdot 10^{-3}$
i	deg	65.2038	...

and apogee r_a, and also the average quadratic error of the weight unit.

The data compiled in Table 2 correspond to the evaluation of the accuracy of the determination of the orbital elements in accordance with the so-called "interior convergence." In the course of this, it is basically the magnitudes of the random measurement errors that are taken into consideration. The systematic errors remain essentially disregarded. However, it is known that in solution of a problem by the method of the least squares for a large number of measurements, the systematic errors usually determine the accuracy of the solution. Therefore, the average quadratic errors in the determination of the orbital elements, as indicated in Table 2, should be considered as considerably understated.

To estimate the actual accuracy of the solution of a problem, let us take advantage of the fact that the results of the determination of the orbital elements compiled in Table 1 are related to various anchor revolutions which are separated from each other by a considerable period of time. Therefore, it may be assumed that the systematic errors of one measurement set will be subject to random change at the transition to another set. Accordingly, the errors in individual determinations of the orbit will be of a random nature. To estimate the magnitude of these errors based on data given in Table 1, averaged laws of orbital element fluctuation were established, and then deviations from these laws were determined.

Linear expressions of the following form were utilized as averaged laws of fluctuation for h_{min}, h_{max} and T values

$$\xi = \xi_0 + A_\xi N$$

where

ξ = one of the orbital elements being considered
ξ_0 = its initial value
N = revolution number
A_ξ = constant coefficient which determines the dependence of ξ on N

As far as the inclination i is concerned, it may be considered as constant throughout the entire observed region of the orbit.

The values of the coefficient ξ_0 and A_ξ, as well as the average values, were determined on the basis of data compiled in Table 1 by the method of the least squares. The numerical values obtained are shown in Table 3.

Furthermore, deviations $\delta\xi_j$ of the measured values of the orbital elements (compiled in Table 1) from the corresponding average values (ξ, a certain orbital element; j, the number of the anchor revolution) were computed for all anchor revolutions. These deviations are compiled in Table 4.

Based on the obtained deviations $\delta\xi_j$, its average quadratic values

$$\sigma(\xi) = \sqrt{\Sigma(\delta\xi_j)^2/(n-k)}$$

were computed, where

n = total number of anchor revolutions
k = the number of free parameters of the utilized averaged law ($k = 1$ for $\xi = 1$ and $k = 2$ for the remaining orbit elements)

The values of $\sigma(\xi)$ computed in this manner are compiled in Table 4. It can be seen from this table that the deviations $\delta\xi_j$ are of a random nature. The computations also show that, in the course of a further increase of the order of the polynomials utilized for the development of averaged laws of fluctuation of the orbital elements, the values $\sigma(\xi)$ do not decrease. This can serve as proof of the correctness of selection of the averaged laws.

Aside from the values indicated, Table 4 contains average quadratic errors of determination of the averaged law coefficients $\sigma(\xi_0)$ and $\sigma(A)/A$, and also errors of determination of the averaged values of orbital elements $\sigma_{min}(\xi)$ in the middle of the anchor revolution interval under consideration (e.g., for the 147th revolution, for which these errors are at a minimum). The computations were carried out in accordance with procedures used for solution of problems by the method of least squares.

From estimates of the determination errors of orbital elements, as compiled in Table 4, it follows that as a result of the performed processing of the measurement data, a highly accurate solution was obtained for the assigned problem. Nevertheless, the obtained error magnitudes considerably exceed the values indicated in Table 2. This points to the fact that here a basic part is played by systematic measuring errors and, also, by a possible uncertainty of knowledge of forces acting on the satellite during its flight (primarily the air resistance forces).

Table 4

Revolution number	Deviation of measured orbit elements from averaged ones δh_{min}, m	δh_{max}, m	δT, min	δi, deg
39	232	−113	$0.94 \cdot 10^{-3}$	0.0024
53	−167	59	$-0.77 \cdot 10^{-3}$	−0.0014
66	20	−31	$-0.01 \cdot 10^{-3}$	0.0015
133	−152	227	$0.77 \cdot 10^{-3}$	−0.0012
147	77	13	$0.77 \cdot 10^{-3}$	−0.0013
173	−123	−31	$-1.71 \cdot 10^{-3}$	0.0006
214	6	−192	$-1.98 \cdot 10^{-3}$	−0.0003
255	109	70	$2.02 \cdot 10^{-3}$	−0.0002
$\sigma(\xi)$	152	136	$1.5 \cdot 10^{-3}$	0.0014
$\sigma(\xi_0)$	88	80	$0.88 \cdot 10^{-3}$	0.00053
$\sigma(A)/A$	0.075	0.0066	0.0071	...
$\sigma_{min}(\xi)$	53	48	$0.53 \cdot 10^{-3}$	0.00053

Let us now turn to the determination of the density of the upper atmosphere on the basis of the obtained data. For this we will utilize the equation

$$\rho_p = (\Delta T/S\sqrt{H})\Phi(a, e, H) \qquad [20]$$

where

ρ_p = air density at the lowest height (above Earth's surface) of the satellite flight

ΔT = reduction in the period of revolution of the satellite, per revolution

S = a coefficient determining the influence of air resistance in the equations of the satellite motion, Eqs. 6

$\Phi(a, e, H)$ = function which depends on H, the long half axis a and eccentricity e of the orbit and undergoing little change due to variation of these values

At the same time it is assumed that the air density at the height h can be found in accordance with

$$\rho(h) = \rho_p \exp\,[-(h - h_{\min})/H] \qquad [21]$$

The dependence, Eq. 20, can be easily obtained from the known relationship for determining ΔT (2). From this dependence it follows that, when determining ρ_p on the basis of the measured change of the period of revolution ΔT, it is essential to know the height of the homogeneous atmosphere H. However, at the present time this value is not known accurately enough.

To reduce the influence of errors, in determination of H, on the accuracy of computations for determining the air density, let us take advantage of the fact that this influence is at a minimum for a certain height

$$h = h_{\min} + \Delta h \qquad [22]$$

Actually it follows from expressions 20, 21 and 22 that

$$\rho(h) = (\Delta T/S)\Phi(a, e, H)f(\Delta h, H) \qquad [23]$$

where

$$f(\Delta h, H) = \frac{1}{\sqrt{H}} \exp\left(-\frac{\Delta h}{H}\right) \qquad [24]$$

The influence of the H value on the function $\Phi(a, e, H)$ is not substantial (2). Therefore, the dependence of the density $f(h)$ on the height of the homogeneous atmosphere H, is determined entirely by a function of the type $f(\Delta h, H)$. Fig. 1 shows dependence curves of this function with respect to Δh for various values of H. From these curves it can be seen, that for $\Delta h \approx 22$ km and for a value of H located in the range 25 km $\leqslant H \leqslant$ 100 km, the function $f(\Delta h, H)$ can deviate from its average value by only 6% of its magnitude, whereas with $\Delta h = 0$ the corresponding relative deviation of $f(\Delta h, H)$ reaches 33%.

If one takes a narrower variation range of H, then with a suitable selection of the height Δh one can make the variation of the value $f(\Delta h, H)$ even smaller. However, in this paper we will refer to the previously indicated broad variation range of the homogeneous atmosphere height, which agrees with contemporary views (for heights on the order of 200 to 250 km). The error resulting from the lack of exact knowledge of the homogeneous atmosphere height for determination of the air density at a height $h = h_{\min} + 22$ km will not exceed a magnitude of the order of 6%.

For actual determination of the air density, it is advantageous to make use of a comparison with the results of numerical integration of the motion equations 6 for a certain orbit close to the actual one. In this way methodical errors connected with the approximate nature of relationship 20 are eliminated. Assuming that the function $\Phi(a, e, H)$ entering

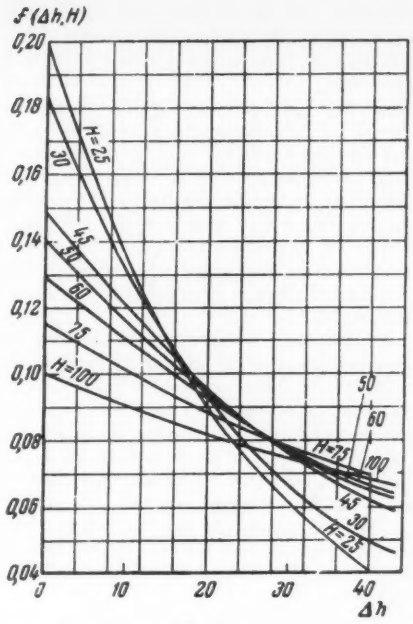

Fig. 1

into this relationship does not change when shifting from the calculated to the actual orbit, we will obtain

$$\rho_p = \rho_{p0} \frac{\Delta T}{\Delta T_0} \cdot \frac{S_0}{S} \qquad [25]$$

where the values relating to the calculated orbit are denoted by the index 0.

In accordance with these results, we will determine the value of ρ for the midpoint of the orbital section under consideration. Using data from Table 3, we find that for this revolution $\Delta T = 1.029 \cdot 10^{-3}$ min, $h_{\min} = 224.5$ km and $T = 105.8346$ min.

When determining the value of S, we shall consider all positions of the satellite as equally probable, and we shall assume that the surface of its middle crors section equals one-quarter of the entire surface (4). We shall also assume that the drag coefficient is $c_x = 2.1$, which corrresponds to a diffusion reflection of the atmospheric particles at an accommodation coefficient $\alpha = 1$ (4).

The resultant air density at an altitude of $h = 246$ km is shown in Table 5. Also given in this table are the corresponding values found on the basis of observation results of the first and second satellites (2). All these values correspond to the center of the interval of possible scattering of the density $\rho(h, H)$ determined by the variation range of H mentioned before (see Fig. 1).

As can be seen from Table 5, air density values obtained from observational data of the second and third satellites practically coincide. The density based on observations of

Table 5

Name of satellite	Air density at altitude $h = 246$ km, gm·cm^{-3}
Satellite no. 1 and its carrier rocket	$1.40 \cdot 10^{-13}$
Satellite no. 2	$1.73 \cdot 10^{-13}$
Satellite no. 3	$1.72 \cdot 10^{-13}$

the first satellite is somewhat lower (approximately by 20%). This can be explained by the fact that the orbit perigee of the second and third satellites occurred during daylight, and that of the first, at night.

Aside from the indicated average air density value, the density based on measurement results of separate anchor revolutions was also computed. At the same time, values of ΔT and h_{min} were determined from calculations based on the correlation of measurement results of neighboring anchor revolutions. These values were taken for the middle of the intervals between anchor revolutions. The results obtained are shown in Table 6. Also given in the same table is the local solar time at which the satellite passed the point of its minimum flight altitude.

As can be seen from Table 6, the air density values obtained from individual intervals between anchor revolutions are close to the average value indicated (the maximum average deviation does not exceed 13%).

Starting with the 160th revolution, a certain decrease in density can be observed, which is perhaps connected with a corresponding decrease in the local solar time at the point of orbit having the lowest flight altitude. However, this decrease is insignificant along the interval being considered and lies within the accuracy limits of the solution of the problem. Therefore, no noticeable change in density should be expected for this reason.

To evaluate the accuracy of the average air density value indicated in Table 5, let us apply Eqs. 20 and 21 disregarding the influence of the variation of the function $\Phi(a, e, H)$. As a result we will obtain for the relative error of density determination

$$\frac{\delta\rho}{\rho} < \frac{\delta_{max}(\Delta T)}{\Delta T} + \frac{\delta_{max}(h_{min})}{H} + \frac{\delta_{max}(S)}{S} + \frac{\delta_{max}(\rho_H)}{\rho} \quad [26]$$

where δ_{max} denotes maximum absolute errors of determination of corresponding values, and $\delta_{max}(\rho_H)$ the maximum error connected with our inaccurate knowledge of the value of H.

For the determination of individual components of the total error, let us apply Table 4. We will consider the maximum errors to be equal to three times the value of the average quadratic errors, and for determination of the value of $\delta_{max}(\Delta T)$ we will take advantage of the results of the accuracy estimate of the determination of the coefficient A_ξ in the linear expression for the period of revolution $T(\xi = T)$. In addition, let us assume for H the minimum value of $H = 25$ km. As a result we will obtain

$$\frac{\delta_{max}(\Delta T)}{\Delta T} \cong 2\% \qquad \frac{\delta_{max}(h_{min})}{H} \lesssim 0.6\%$$

Thus, errors connected with the inaccuracy of determination of orbital elements are comparatively small. Of more importance may be errors resulting from inaccuracies in the assumptions made in the course of the computation, e.g., by values $\delta_{max}(S)/S$ and $\delta_{max}(\rho_H)/\rho$. As indicated

$$\delta_{max}(\rho_H)/\rho = 6\%$$

Error δS is basically connected with the assumption of equal probability of all satellite positions and also with the value of the accommodation coefficient $\alpha = 1$, selected at the time of determination of the coefficient c_x. The first of these assumptions can be regarded as being sufficiently accurate at the present time (at least for determination of average density values based on a large number of revolutions). This can be confirmed by the good agreement of ρ values obtained from observation of various objects under equal conditions during passage through the region of their perigee [first satellite and its carrier rocket (2), second and third satellite].

If one adopts for α its limiting value $\alpha_{lim} = 0$, then S will increase in a proportion of 4:3 (1). During this, the air density decreases by 25%.

The previously reviewed individual error components are independent, and therefore they can be added in accordance with the rules of addition of independent random values. As a result we will obtain the maximum relative error of density determination

$$\delta_{max}\rho/\rho = 26\%$$

This estimate should be regarded as probably high, since the assumption that $\alpha = 0$ is not very probable.

Table 6

Revolution number	Local solar time hr	min	Air density at height $h = 246$ km, 10^{-13} gm·cm^{-3}
46	10	51	1.79
60	10	28	1.72
100	9	47	1.77
140	8	59	1.80
160	8	38	1.94
194	7	55	1.76
234	7	12	1.61

References

1 Lidov, M. L., *Artificial Earth Satellites*, 1958, no. 1, p. 9.
2 El'iasberg, P. N., *Artificial Earth Satellites*, 1958, no. 1, p. 21.
3 Shilov, P. I., "Method of the least squares," *Geodezizdat*, 1941.
4 Lidov, M. L., *News of the Academy of Sciences, USSR, Geophysics Series*, 1957, no. 13.

Reviewer's Comment

This thoroughly professional paper describes how the density of the upper atmosphere has been inferred from orbital data of the third Soviet satellite, and how the orbital data have been inferred from terrestrial observations of the satellite.

As orbital elements, a set of initial coordinates and components of velocity in a geocentric frame of reference rotating with Earth, were employed. The differential equations of motion were integrated, on a digital computer, corresponding to an undisturbed trajectory and to each of six disturbed trajectories obtained by applying small increments, to each of the six elements, one at a time. In the equations of motion, the gravitational potential included the known r^{-1} and r^{-3} terms but not r^{-5}, whose effects were smaller than systematic errors and gravity anomalies. Drag was included approximately. The integrations provided the partial derivatives which enabled the initial values of the orbital elements to be improved differentially by least squares; reasonable criteria were adopted to exclude observations with excessive residuals, and the convergence of the process was found to be rapid. Each such improvement involved the solution of six first-order differential equations for each of seven orbits, all such

integrations carried out simultaneously on the computer.

Definitive orbital elements were obtained from two consecutive revolutions at a time only, but eight such pairs were employed more or less regularly spaced over a period of 216 revolutions, so as to obtain eight sets of orbital elements. The use of longer intervals at a time would have made the differential correction process intolerably time-consuming, and accuracy would, in fact, have been lost through systematic errors.

The atmospheric density was finally inferred from the orbital elements, the known geometry and aerodynamic properties of the satellite, and the time rate of change of the nodical period. The paper exhibits densities so obtained from the third Soviet satellite, and densities obtained by other methods from the first and second Soviet satellites. Variations in density, inferred from consecutive selected pairs of revolutions of the third satellite, are not large enough in comparison with the accuracy of the density values to establish the reality of the variations.

A careful error analysis is made, which occupies a considerable proportion of this well-written paper, all of whose procedures appear sound and demonstrate a very high degree of competence and understanding on the part of the authors. This reviewer, however, is of the opinion that easier methods exist which provide more accurate densities and which do not involve tedious differential corrections and as much use of high speed digital computers. At least one such method is described in *Smithsonian Contributions to Astrophysics*, vol. 2, no. 10, 1958. The period, and its time derivative, are the most critical observational quantities in determining the density of the upper atmosphere from the motion of artificial satellites. It is worth sacrificing accuracy in determining some of the orbital elements which are not critical to gain accuracy in the orbital period and its time derivative; using more orbital revolutions at a time permits this, so as to obtain more accurate density values more easily.

The paper contains no references to the very extensive non-Soviet work in its field.

—Theodore E. Sterne
Operations Research Office
Johns Hopkins University

Results of Investigation of the Meteoric Matter by Means of Instruments Installed on Cosmic Rockets

T. N. NAZAROVA

TO RECORD meteoric particles, on the cosmic rockets launched on Jan. 2, Sept. 12 and Oct. 4, 1959, instruments were installed analogous to those used on the third Soviet artificial Earth satellite (1).[1]

During the collision of a meteoric particle with the transducer, the latter recorded the impulse of the transducer's matter[2] ejected in the explosion of the particle on its surface (2).

Interpretation of experimental data proceeded from the dependence between the impulse received by the transducer and the energy of the particle (3) determined by the relation $I = AE_0$, where I is the "impulse of the ejection," E_0 the kinetic energy of the particle, and A the coefficient of proportionality. If we assume that the average speed of a meteoric particle equals 40 km per sec, we can determine the mass of recorded particles.

Instruments on the first cosmic rocket were calibrated to record particles with a mass in the ranges of $2.5 \cdot 10^{-9}$–$1.5 \cdot 10^{-8}$ gm, $1.5 \cdot 10^{-8}$–$2 \cdot 10^{-7}$ gm and over $2 \cdot 10^{-7}$ gm; the telemetering signal was produced after the accumulation of 16 impacts in the most sensitive range, after four impacts in the following range, and after each impact in the coarsest range.

The vibrations and noises from the inside of the satellite were not recorded by the instruments, since their sensitivity was above the level of these disturbances. In contrast to the instruments installed on the third satellite, the transducers on the cosmic rockets were not sensitive to the impact of meteoric particles against the hull of the container.

In the Jan. 2, 1959 experiment, during the 10-hr operation of the instruments recording the impacts of meteoric particles, the transducers with a common surface of 0.2 m^2 did not record the number of impacts necessary for the telemetric trans-

Translated from *Artificial Earth Satellites*, 1960, no. 5, pp. 38–40. Translated by A. E. Godlewsky, New York.

[1] Numbers in parentheses indicate References at end of paper.

[2] The impulse of the transducer's matter ejected in the explosion considerably exceeds the impulse of the particle itself.

Table 1

Means of investigation	Date	Mass of recorded particles (with v = 40 km/sec), gm	Number of impacts per m² per sec
Third satellite	5/15/58	$8 \cdot 10^{-9}$–$2.7 \cdot 10^{-8}$	4–11
	5/16–17/58		$5 \cdot 10^{-4}$
	5/18–26/58		$<10^{-4}$
First cosmic rocket	1/2/59	$2.5 \cdot 10^{-9}$–$1.5 \cdot 10^{-8}$	$<2 \cdot 10^{-3}$
		$1.5 \cdot 10^{-8}$–$2 \cdot 10^{-7}$	$<5 \cdot 10^{-4}$
		$>2 \cdot 10^{-7}$	$<10^{-4}$
Second cosmic rocket	9/12/59	$2 \cdot 10^{-9}$–$6 \cdot 10^{-9}$	$<5 \cdot 10^{-5}$
		$6 \cdot 10^{-9}$–$1.5 \cdot 10^{-8}$	$<5 \cdot 10^{-5}$
		$>1.5 \cdot 10^{-8}$	$9 \cdot 10^{-5}$
Third cosmic rocket	10/4/59	10^{-9}–$3 \cdot 10^{-9}$	$4 \cdot 10^{-4}$
	10/18/59	$3 \cdot 10^{-9}$–$8 \cdot 10^{-9}$	$2 \cdot 10^{-3}$
		$>8 \cdot 10^{-9}$	$4 \cdot 10^{-4}$

mission. Thus particles with a mass of $2.5 \cdot 10^{-9}$–$1.5 \cdot 10^{-8}$ gm made fewer than $2 \cdot 10^{-3}$ impacts per 1 m² per 1 sec; particles with a mass of $1.5 \cdot 10^{-8}$–$2 \cdot 10^{-7}$ gm fewer than $5 \cdot 10^{-4}$ impacts per 1 m² per 1 sec, and particles with a mass larger than $2 \cdot 10^{-7}$ gm fewer than 10^{-4} impacts per 1 m² per 1 sec.

The instruments on the second and the third cosmic rockets were constructed not to integrate the impacts, but to record each impact.

On the second cosmic rocket the instruments were calibrated to record meteoric particles with masses in three ranges: $2 \cdot 10^{-9}$–$6 \cdot 10^{-9}$ gm, $6 \cdot 10^{-9}$–$1.5 \cdot 10^{-8}$ gm and more than $1.5 \cdot 10^{-8}$ gm.

In the Sept. 12, 1959 experiment the transducers with a common surface of 0.2 m² recorded in 30 hr two impacts of particles with masses larger than $1.5 \cdot 10^{-8}$ gm. In the other mass ranges, no impacts were recorded. Thus, the frequency of the impacts of particles with the mass of $1.5 \cdot 10^{-8}$ gm is $9 \cdot 10^{-5}$ per 1 m² per 1 sec, and for particles with the mass of $2 \cdot 10^{-9}$–$6 \cdot 10^{-9}$ gm and $6 \cdot 10^{-9}$–$1.5 \cdot 10^{-8}$ gm it is less than $5 \cdot 10^{-5}$ per 1 m² in 1 sec.

The instruments for investigation of the meteoric matter installed on the automatic interplanetary station launched Oct. 4, 1959 were cut in for short periods of time during the transmission of information. They were tuned to record the particles in the following ranges: I, the mass of particles 10^{-9}–$3 \cdot 10^{-9}$ gm; II, the mass of particles $3 \cdot 10^{-9}$–$8 \cdot 10^{-9}$ gm; III, the mass of particles larger than $8 \cdot 10^{-9}$.

During the time these instruments worked, from Oct. 4–18, some impacts of meteoric particles against the transducers with a common surface of 0.1 m² were observed.

The total time of operation of the instruments was 6 hr 25 min 37 sec. During this interval seven impacts of meteoric particles were recorded: One of them in the first range, five in the second, and one in the third. Thus, the average number of impacts was $3 \cdot 10^{-3}$ per 1 m² per 1 sec; for particles with the mass of $3 \cdot 10^{-9}$–$8 \cdot 10^{-9}$ gm it was $2 \cdot 10^{-3}$ per 1 m² per 1 sec, and for particles with masses of 10^{-9}–$3 \cdot 10^{-9}$ gm and more than $8 \cdot 10^{-9}$ gm it was $4 \cdot 10^{-4}$ per 1 m² in 1 sec.

For comparison let us take the results of the investigation of the meteoric matter obtained with the instruments installed on the third artificial Earth satellite (4). On May 15, 1958, a strong increase in the number of impacts was recorded. It equaled from four to 11 impacts of particles with the mass of $8 \cdot 10^{-9}$ to $2.7 \cdot 10^{-8}$ gm per 1 m² in 1 sec. During the following days, the frequency of impacts fell by three orders of magnitude, then by one more order, and during the last days of operation of instruments, it was less than 10^{-4} impacts per 1 m² in 1 sec. The phenomenon observed on May 15 should apparently be explained as an encounter of the satellite with a meteoric stream, since in the number of impacts recorded on May 15 there was a periodicity close to the precession period of the satellite. A change in the number of impacts was also observed with the motion of the satellite in the orbit. Such interpretation of the phenomenon is not, however, indisputable, because of too large a frequency of impacts (5).

If we compare the results obtained by the use of instruments installed on the satellite and on the three cosmic rockets (see Table 1), we note that the density of the meteoric matter in the vicinity of Earth is not constant. It changes both in time and space. It is noteworthy that, during the flights of the second and the third cosmic rockets, the largest number of the recorded "ejection impulses" applies not to the minimal impulses which could have been recorded by the instrument, but to the impulses of larger value.

Many people contributed to the investigation of meteoric particles. The author expresses her deep gratitude to L. Z. Rusakov, G. M. Kurtev, A. K. Bektabegov, O. D. Komissarov, A. A. Trukhachev, G. Z. Beliayeva and L. N. Neugodov for their active collaboration.

References

1 Komissarov, O. D., Nazarova, T. N., Neugodov, L. N., Poloskov, S. M. and Tusakov, L. Z., *Artificial Earth Satellites*, 2nd ed., Publ. Acad. of Science USSR, 1958, p. 54.

2 Isakovich, M. A. and Roy, N. A., *Artificial Earth Satellites*, 2nd ed. Publ. Acad. of Sciences USSR, 1958, p. 81.

3 Baum, S. A., Kaplan, S. A. and Staniukovich, K. P., *Introduction to the Cosmic Gasdynamics*, Physmathizdat, 1958.

4 Nazarova, T. N., *Artificial Earth Satellites*, 4th ed., Publ. Acad. of Sciences USSR, 1960, p. 165.

5 Levin, B. Yu., *Physical Theory of Meteors and the Meteoric Matter in the Solar System*, Publ. Acad. of Sciences USSR, 1956.

Measurement of Cosmic Rays by Means of Geophysical Rockets

YU. SHAFER and
A. V. YARYGIN

IN 1958 the global intensity of cosmic rays was measured by means of single Geiger counters and an ionization chamber mounted in a geophysical rocket.

The purpose of these experiments was to find the altitude dependence of the intensity up to 200 km and to determine the mean specific ionization of primary rays. It was also our intention to test the apparatus under conditions of overloading and at the temperatures encountered in rocket flights.

The apparatus was located in the hermetically sealed nose section of the rocket, which had steel walls no more than 3-mm thick (about 2.5 gm per cm²); the axis of the apparatus coincided with that of the rocket. Approximately 8% of the total solid angle of the upper hemisphere was shielded by a large quantity of matter (more than 50 gm per cm²). The solid angle masked by the main frame of the rocket in the lower hemisphere was 0.16π. The location of the measuring instruments is shown in Fig. 1.

Particles were recorded by means of halogen counters; these counters measured 18 × 150 mm and had steel walls 0.1-mm thick. Among the important properties of counters of this type are stable operation over a temperature range from +50 to −40 C, long life and low operating voltage (380–400 v). The power supply was a separate unit built around semiconductors. The input to the power converter was 6.5 v at 7.5 ma, the output 400 v at 50 μa. A gas stabilizer was employed to reduce voltage fluctuations at the converter output. Within limits of 1 to 2% the stabilized voltage is independent of variations in the load current and input voltage.

The global intensity, as measured by a single counter, is found from the number of charged particles by means of the expression

$$J = N/G \text{ particles cm}^{-2}\cdot\text{sec}^{-1}$$

where

N = number of particles registered by the counter per sec
G = geometrical parameter, a function of angular distribution of radiation, orientation of the counter, its effective length l_{eff} and effective radius r_{eff}

Assuming that, in relation to the upper hemisphere, the angular distribution of the primary radiation is isotropic, and that with respect to the lower hemisphere, the intensity is equal to zero, for a cylindrical counter with arbitrary spatial orientation we get $G = S_{eff}$ (effective area of counter)

$$S_{eff} = (\pi r_{eff}/2)\,(r_{eff} + l_{eff})$$

It is known that the effective diameter of a Geiger counter differs from the real diameter by not more than 0.1 mm. The effective length of the type of counter which we em-

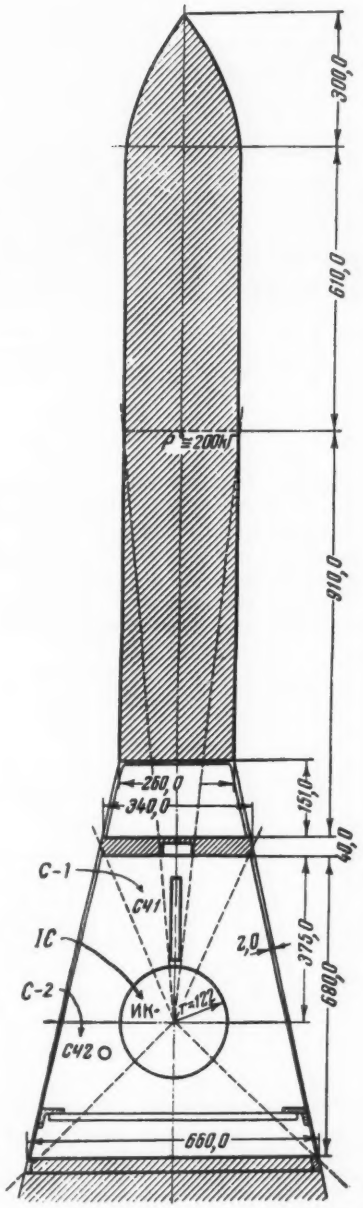

Fig. 1 Location of horizontal (*C*-2) and vertical (*C*-1) counters and ionization chamber (*IC*) in nose section of the geophysical rocket

Translated from *Artificial Earth Satellites*, 1960, no. 4, pp. 184–194. Translated by Research Information Service, New York.

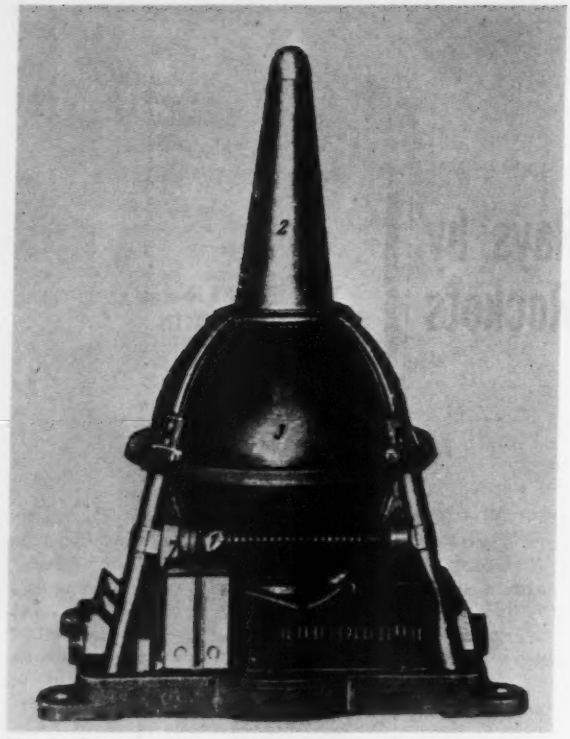

Fig. 2 Apparatus for measuring cosmic rays mounted in a geophysical rocket. 1: horizontal counter; 2: vertical counter (under thin walled duraluminum cap); 3: ionization chamber

ployed was determined experimentally by Logachev and proved to be equal to (100 ± 1) mm. Substituting values of r_{eff} and l_{eff} in Eq. 1, we get $S_{eff} = 15\ cm^2$.

In this experiment it was necessary to allow for the "dead time" τ during which the counter did not register.

For our counters τ was approximately $2 \cdot 10^{-4}$ sec. The quantity determines the value of the relative error σ in the counting rate

$$\sigma \cong N\tau$$

At the maximum rate $N = 40$ particles per sec, $\sigma = 0.8\%$. This inconsiderable counting error is disregarded in subsequent calculations.

A very important factor is the angular displacement of the rocket vehicle itself in free flight. Since the apparatus does not have spherical symmetry, measurements are liable to vary with the irregular motion of the rocket.

The theoretical computation of such variations is a very complex procedure even when the intensity of primary radiation is invariable. Therefore we mounted two counters in the rocket; the axis of one of them was directed along the axis of the rocket and the axis of the other at right angles to the latter. With the counters arranged in this way the neglected angular displacement of the rocket will react on their counting rates in different ways.

The systematic difference between N_{vert} and N_{horiz} then makes it possible to determine the masking effect of the material of the rocket and the lower limit of accuracy. Moreover, readings from two counters with independent radio circuits and power supplies provide a check on the operation of the devices.

In our experiment one counter was located vertically above the ionization chamber and the other horizontally to one side of the chamber (see Fig. 2). The impulses pass from the counter across an emitter repeater to the input of a counting circuit with a scaling factor of 1:256. Each trigger cell in the scaling circuit insures a counting rate of up to $5 \cdot 10^4$ impulses per sec. This resolving power means that every impulse will be recorded.

The last trigger of the scaling circuit controls a polarized relay (P_1). The armature of the relay changes position on the accumulation of 128 impulses (Fig. 3). The contacts of the relay (P_1) close corresponding potentiometer circuits in the rocket telemetry system. As a result of the flipping of the last trigger, when 128 impulses have been counted, a radio signal is transmitted from the rocket, at voltage levels characteristic of each counter, and recorded on film at the receiving station. At the same time a continuous series of time marks is inscribed on the same film correct to 0.02 sec. Specimens of this photographic record are shown in Fig. 4.

The number of particles recorded by the counter per second can be found from the expression $N = n/t$, where n is the scaling factor and t is the interval, measured on the film, between changes in the level of the voltage from a given counter.

In our experiment the horizontal counter also acted as a master-counter. When it had counted 256 impulses, the

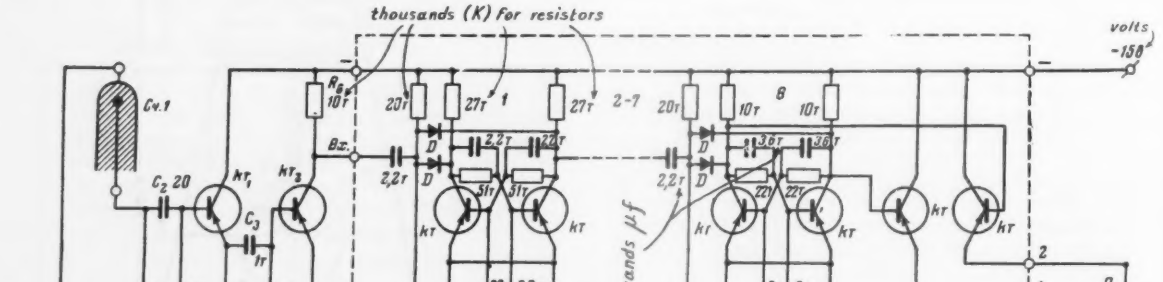

Fig. 3 Schematic of counting equipment

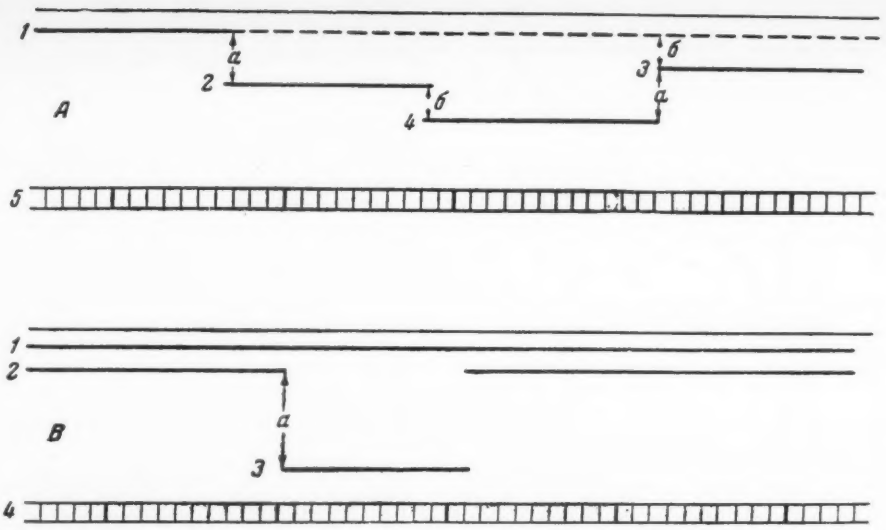

Fig. 4 Specimens of photographic record of signals from apparatus made at ground receiving station. A, counter signals: 1, zero level; 2, level of signal from vertical counter (amplitude a); 3, level of signal from horizontal counter (amplitude b); 4, total level of signals from both counters ($a + b$); 5, time marks. B, signals from ionization chamber: 1, calibration level (100%); 2, reference level; 3, chamber signal (amplitude a); 4, time marks

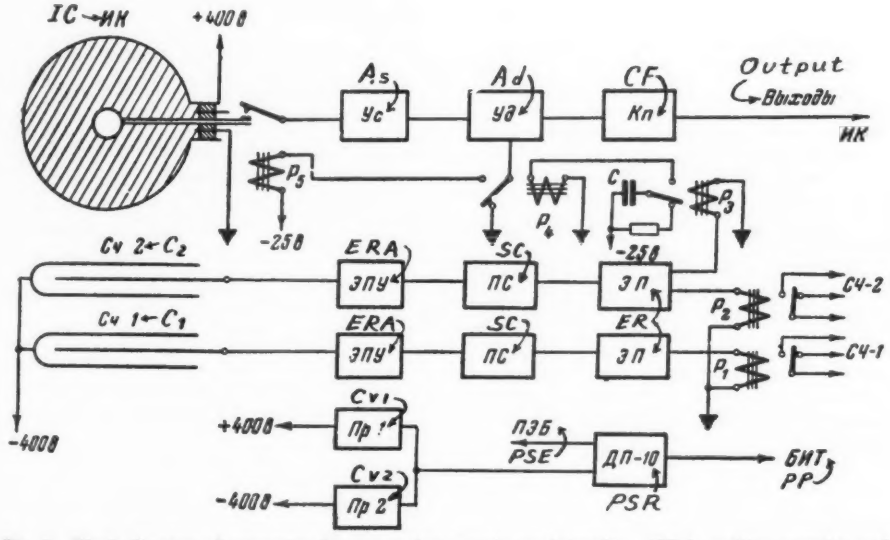

Fig. 5 Block diagram of apparatus for measuring cosmic ray intensity. *ERA*, emitter repeater and amplifier; *SC*, scaling circuit; *ER*, emitter repeater; Cv_1, Cv_2, converters; *PSR*, power switch relay; *IC*, ionization chamber; *C*-2, horizontal counter (control); *C*-1, vertical counter; P_5, chamber relay; A_s, amplifier; A_d, pulse stretcher; *CF*, cathode follower; P_1, P_2, P_3, P_4, polarized relays; *PSE*, power supply for electronic circuits; *PP*, power pack

relay P_4 energized the chamber relay P_5 (Fig. 5). This relay operated and drew off the charge accumulated at the collector as a result of ionization during the time it took 256 particles to pass through the master-counter.

The spherical ionization chamber, 24 cm in diameter, was made of stainless steel 0.4-mm thick. A chamber of this capacity guarantees a statistical accuracy of not more than 5%, determined by fluctuations in the number of primary, relativistic charged particles passing through the chamber per second of observation.

The vibrostabilized collecting electrode in the form of a hollow, thin walled sphere, 28 mm in diameter, was attached to a mount which passed through a central ceramic insulator with a protecting ring. The chamber was degassed, evacuated, repeatedly flushed out and filled with spectrally pure argon. In the process of filling the chamber, saturation

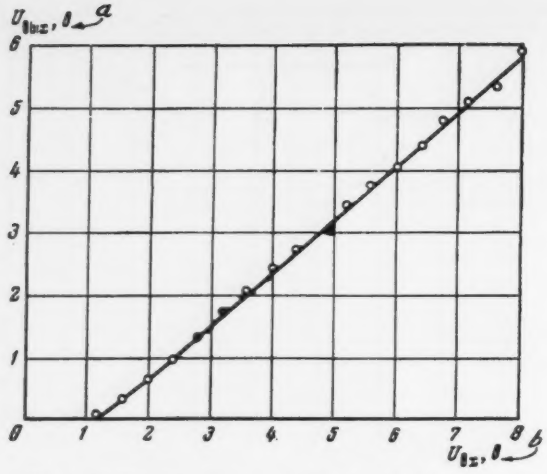

Fig. 6 Calibration curve $u_{in} = f(u_{out})$. [a] u_{out}, v; [b] u_{in}, v

curves were recorded for every 1 atm. The characteristics of the ionization chamber are as follows:

1 Volume $V = 7020$ cm³.
2 Residual pressure of argon $P = 7$ atm.
3 Resistance of central insulator $R = 1.5 \times 10^{15}$.
4 Conversion factor from argon to air $K = 1.4$.
5 Saturation potential $U_H = 250$ v.
6 Operating voltage $U_p = 380$–400 v.
7 Ionization current of the order of $I = 10^{-11}$ amps.
8 Capacitance $C = 6.5 \times 10^{-12}$ farads.

In order to compute the possible statistical error owing to fluctuations in the number of multicharge particles in the primary flux, we assumed the following composition for the primary radiation: Protons, 80% of the total number of particles arriving from all directions; helium nuclei, 18%; Li, Be, B, 0.3%; C, N, O, 1.2%; and other nuclei with Z equal to or greater than 9, about 0.5%.

As is known, the ionization resulting from a particle is proportional to the square of its charge. Thus, the contribution of the ionization of primary nuclei to the total chamber ionization current was found to be

$$I_p = 24\% \quad I_\alpha = 21.5\% \quad I_{Li,Be,B} = 2.2\%$$

$$I_{C,N,O} = 23\% \quad I_{Z \geq 9} = 29\%$$

As a result of these calculations the mean statistical error was found to be

$$\bar{\sigma} = \sqrt{\sum \left(\frac{\Delta I_s}{I_s}\right)^2} = 8.3\%$$

where $\Delta I_s/I_s$ is the relative statistical error resulting from fluctuations in the number of primary nuclei with the charge Z.

The most justifiable method of measuring the chamber ionization is drawing off the electric charge from the collecting electrode by means of a relay. This method was first developed and applied by Chudakov (1).[1]

In our apparatus the chamber relay P_5 (Fig. 5) connects the collecting electrode with the input of an amplifier (A_s). Thus an impulse of positive polarity lasting about 1 millisec is generated at the chamber load resistance. This impulse is fed to the feedback amplifier with an amplification factor of about 6. The signal is then stretched in the diode stretcher A_d with a time constant of the order of 100 sec. The impulse is broken off by means of the polarized relay P_4. Thus, pi-shaped signals u_{out}, about 1-sec long and calibrated in volts, are fed through the cathode follower CF to the input of the telemetry system. These signals are then transmitted by radio and recorded on photographic film at the ground observation point.

As already explained, the operation of the chamber relay is programed by the horizontal master-counter. This follows the energizing of relay P_3, the coil of which is connected with the output of the emitter repeater ER. Current from the capacitor C energizes relay P_4. This closes the stretcher circuit and supplies power to the chamber relay.

Since the impulse from the output of the cathode follower has negative polarity, the final stage of the chamber electronic system was designed so that a strictly constant reference voltage of positive polarity was obtained at its output. In our experiment the reference voltage level was +5.65 v. The negative signal from the chamber was read from this level. The chamber electronics were designed around miniature, economical, directly heated tubes.

Fig. 4 shows a specimen of the photographic record of the chamber signals u_{meas} transmitted by radio from the rocket and received at the ground observation point. In order to determine u_{out} in volts, it is necessary to measure the amplitude of the pi-shaped impulse in accordance with a scale determined from the position on the film of the known calibration voltage level of a standard battery u_{stand}, mounted in the rocket, and the known level of the reference voltage u_{ref} at the output of the cathode follower of the chamber channel in the intervals between chamber signals.

In our experiment $u_{stand} = 6.18 \pm 0.05$ v and $u_{ref} = 5.60 \pm 0.08$ v; u_{out} is calculated from the equation $u_{out} = u_{ref} - u_{meas}$, where u_{meas} is the signal measured on the photographic record.

The potential of the collecting electrode u_{in} is determined from the calibration curve $u_{in} = f(u_{out})$, a rating characteristic of the device (Fig. 6).

The total ionization I resulting from primary nuclei passing through the chamber during an exposure period t may be computed from the expression

$$I = u_{in}C/Pte$$

where

P = chamber pressure
C = chamber capacitance
e = electron charge

The apparatus was powered by mercuric oxide batteries. The total power requirements of the apparatus were 2.1 w.

The apparatus was subjected to a whole series of tests before launching. All the circuits and their insulation were carefully checked; the reference voltage at the cathode follower output and the potential of the standard battery were measured; the leak resistance of the collector electrode and the gas pressure in the chamber were verified; and the scaling circuits were examined for reliability.

The counters and the chamber were calibrated against a Co^{60} gamma-preparation and natural background radiation. For the counters the natural background was equal to 70 impulses, for the chamber 0.48 v per min. In the course of the tests numerous calibration curves were recorded for different supply voltages within limits of 10% of their nominal values.

During the tests the ionization level and the counting rate were transmitted from the rocket by radio and recorded on film. The fact that the results of all the tests were identical showed that the apparatus was in sound working order.

The rocket was launched on July 2, 1958 at 9:00 o'clock Moscow time. During flight, the operation of the counters and the chamber were observed visually for 264 sec on the screen of an oscillograph in the radio receiving station. These observations indicated that the vertical counter operated normally throughout the flight. Signals from the

[1] Numbers in parentheses indicate References at end of paper.

horizontal counter and the ionization chamber began to reach the receiving station after 213 sec. All the apparatus worked normally up to the end of the flight.

At the apex of the trajectory at an altitude of 210 km after the separation of the forward part of the rocket from the main frame, the transmission of radio signals ceased. However, the apparatus remained active and landed safely by parachute still in working order.

Careful tests at the landing point and in the laboratory failed to reveal any abnormalities in the operation of the device.

The data obtained during the flight do not permit any conclusions about a possible appreciable deviation of cosmic ray intensity from the mean value during the launching of the rocket. Measurements made at the Nizmir station (Moscow) show that in the period from June 30 to July 7 the intensity of the hard and neutron components remained constant; the number of sun spots was relatively small (198 against a mean monthly count of 238). During this period the disturbances in Earth's magnetic field and the ionosphere remained at the June level. Not until the end of July were four disturbed periods recorded; these were probably linked with a certain increase in solar activity.

From this it follows that the day of the launching was relatively quiet.

One of the important results of our measurements is undoubtedly the obtaining of data on the altitude dependence of the global intensity of particle flux. These results are summarized in Fig. 7 and in Table 1.

It is clear from Fig. 7 that at an altitude of 20.5 km the Pfotzer curve has a maximum about 2.3 times greater than the value at 70 km. Starting from 70 km the intensity increases monotonically with altitude (by about 17% from 70 to 210 km).

The considerable mean square error in the region of 200 km is perhaps a result of an arbitrary change in the attitude of the freely flying rocket in response to a reduction in speed at the apex of the trajectory.

The intensity measured at the maximum of our altitude curve was 20% greater than the value obtained by Chudakov (1) and 30% greater than the intensity measured by Charakhch'yan in 1958 at the latitude of Simferopol.[2] This increase is probably a result of our apparatus recording shower

[2] Private communication from A. N. Charakhch'yan.

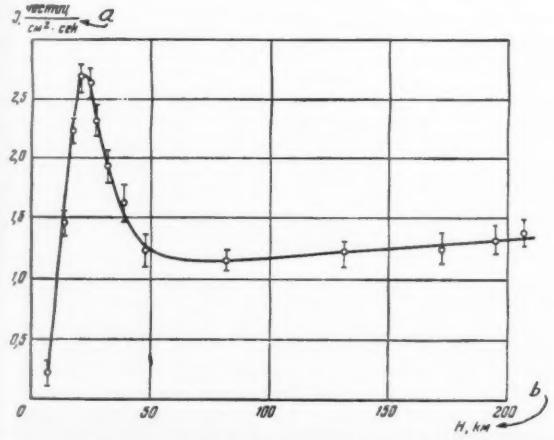

Fig. 7 Curve showing variation in global intensity of cosmic rays as a function of altitude. [a] Particles per cm²·sec; [b] H, km

Table 1 Data showing dependence of global cosmic ray intensity on altitude

Altitude H, km	Cosmic ray intensity J, particles per cm²·sec	Altitude H, km	Cosmic ray intensity J, particles per cm²·sec
6.18	0 21 ± 0.01	38.18	1.63 ± 0.10
14.15	1.46 ± 0.09	47.73	1.25 ± 0.07
17.64	2.21 ± 0.13	82.00	1.17 ± 0.06
20.50	2.69 ± 0.16	130.82	1.25 ± 0.07
24.00	2.63 ± 0.16	171.70	1.27 ± 0.12
27.00	2.30 ± 0.12	195.10	1.34 ± 0.12
31.75	1.94 ± 0.12	207.40	1.40 ± 0.16

particles formed by cosmic rays in the material of the rocket or to Roentgen radiation.

A certain part may have been played in our experiment by secondary particles, generated in the walls of the rocket, and by powerful showers from the nose of the rocket. Since, beyond the limits of the atmosphere the particle flux consists mainly of protons the range of which is equal to about 67 gm per cm², then for a thickness of rocket wall of $d \approx 3$ mm (2.5 gm per cm²) about 4% of the particles will interact with iron nuclei. Each of these particles will produce about five new particles, not less than 30% of which will be neutral. Thus, the extra count resulting from secondary particles, generated in the rocket walls, will be $4\% \cdot 5 \cdot \frac{2}{3} \approx 13\%$.

The shower effect from the nose section of the rocket ($d \approx$ 150 gm per cm²) is linked with the action of high energy particles ($\sim 10^{11}$ ev), which form a flux of 1% in the primary radiation. Each such particle produces about 100 new particles. Bearing in mind that the solid angle cut out by the cap of the rocket from the upper hemisphere is about $0.05\,\pi$, we find that this effect may be roughly estimated at $1 \times 0.05\,\pi \times 100 \approx 16\%$. This figure can be reduced by taking into account the comparatively small distance between the counters and the concentrated mass of the rocket cap. In our experiment the divergence angle of the shower particles was small; therefore not every particle of a shower will be counted discretely. Bearing this in mind, we may assume that the extra particle count resulting from showers can be reduced to 8%.

These calculations enable us to make an orientational estimate of the upper limit of extra secondary "shower" particles. This limit is about 20%. Taking this into account, on the basis of our measurements the global intensity beyond the limits of the atmosphere at altitudes of 50–70 km is equal to 0.97 ± 0.06 particles per cm²·sec.

From the results of the experiment we determined the mean specific ionization of primary particles in 1 cm³ of argon at normal pressure; the value obtained was $j = 260 \pm 19$ ion pairs per cm³·sec.

This is 1.8 times greater than the mean ionization of charged relativistic particles.

Our measured value for the specific ionization per centimeter of path in argon at normal pressure is 189.1 ± 8.2 cm^{-1}.

Other important results which we established include the high degree of reliability of the ionization chamber and its electronic system and the noncritical nature of the supply voltage within limits up to 20%. This was confirmed by repeated testing, before and after the flight, of the shape of the pulses drawn from the collector electrode. Every time, these pulses were strictly identical in shape, perfectly exponential, free of horns, unbroken and of constant length. The same applies to the output pulse from the chamber. All the relays and the system for operating the chamber relay by means of the master-counter worked most satisfactorily.

In conclusion the authors wish to express their gratitude to

S. N. Vernov and N. L. Grigorov for constant guidance and to A. E. Chudakov, A. I. Kuz'min and Yu. I. Logachev for valuable assistance and advice.

They are also grateful to radio technician V. A. Belomestnye for his great practical contribution.

References

1 Vernov, S. N. and Chudakov, A. E., "Izucheniye kosmicheskikh luchey s pomoshch'yu raket i sputnikov v SSSR" (Cosmic-ray Studies by Means of Rockets and Satellites in the USSR), report to Fifth International IGY Assembly, 1958.

Reviewer's Comment

This paper duplicates a portion of the work performed by Van Allen and Singer while at the Applied Physics Laboratory, Johns Hopkins University, between 1946 and 1950. During that time a latitude survey of primary cosmic rays was made, involving firings at four different latitudes. Not only single counters but also counter telescopes were used in these measurements. The specific ionization was measured by means of a low efficiency counter telescope. The results obtained by Shafer confirm these early results, but do not add any basically new information. The references are quite incomplete and should include, in addition, the work of Neher's group and of Winckler who has flown single counters and ion chambers in balloons, as well as other measurements relating to the specific ionization of the primary radiation (e.g., by photographic emulsions).

—F. S. Singer
Department of Physics
University of Maryland

Digest of Translated Russian Literature

The following abstracts have been selected by the Editor from translated Russian journals supplied by the indicated societies and organizations, whose cooperation is gratefully acknowledged. Information concerning subscriptions to the publications may be obtained from these societies and organizations. Note. Volumes and numbers given are those of the English translations, not of the original Russian.

ASTRONOMICAL JOURNAL (*Astronomicheskii Zhurnal*). Published by American Institute of Physics, New York.

Vol. 4, no. 2, Sept.–Oct. 1960.

Degenerate Superdense Gas of Elementary Particles, by V. A. Ambartsumyan and G. S. Saakyan, pp. 187–201.

Abstract: The composition of a degenerate gas whose density is of the order of nuclear density or higher is considered. The temperature is assumed so low that all types of fermions are degenerate. It is shown that, with increasing density, different hyperons should successively appear and increase in number. They should be stable because of the Pauli principle. The threshold densities of different hyperons are calculated. Paradoxically, the smallest threshold density does not correspond to the Λ-hyperon, having the smallest mass of rest, but to the Σ^--hyperon.

In accordance with this, a sufficiently massive cosmic body in gravitational equilibrium should consist of a hyperon core, a neutron layer and an outer envelope having the usual composition (electrons, protons and composite nuclei).

Relationship Between Optical and Radio-Frequency Emissions of the Solar Corona, by M. N. Gnevyshev, pp. 217–224.

Abstract: Complete and high-quality observations of the uneclipsed solar corona were accumulated during the IGY. This made it possible to carry out a more detailed correlation of coronal emission in the λ 5303 Å line, and at meter wave lengths with geomagnetic disturbances, than has been possible hitherto.

The conclusions are as follows:

1 The intensity of the coronal line λ 5303 Å has a maximum above sunspots, in the sense of distribution with respect to both latitude and longitude.

2 The visible maximum in the intensity of coronal features occurs one day after they cross the eastern limb of the sun's disk and a day after they cross the western limb.

3 Radio-frequency emissions during noise storms, at meter wave length, show narrow directivity (solid angle not greater than 10 deg), with the intensity of coronal line λ 5303 Å sharply increased at that point.

4 A noise storm is observed at meter wave length, usually 2–4 days prior to a geomagnetic storm.

Polarization of Coronal Emission Lines, by É. I. Mogilevskii, G. M. Nikol'skii and K. I. Nikol'skaya, pp. 225–233.

Abstract: Two spectrograms of the corona taken during the eclipse of June 30, 1954 were studied. These were obtained with the ISP-65 prismatic spectrograph (λ 6374-125 Å per mm, λ 5303-51 Å per mm). A Wollaston prism was placed behind the slit of the spectrograph, so that spectrograms with mutually perpendicular polarization were obtained simultaneously for the polar and equatorial regions (for heights $\leq 0.6\ R_\odot$). The method of analysis of the spectrograms is described. The relative bright-

ness of the F- and K-components of the corona was found from the blend Na λ 5893 Å. For $\rho = 1.3R\odot$, we found $i_K/(i_K + i_F) = 0.8$, which is in good agreement with the model of the minimum corona. The variation of polarization in λ 5303 was determined for the equatorial zone of the corona (Fig. 3), and in λ 6374 for the polar zone (Fig. 4). The polarization found for regions of the continuous spectrum adjacent to these lines (Fig. 5) is in agreement with data of other authors. The variation of intensity of the lines and the continuous spectrum were also determined (Figs. 6 and 7).

The high degree of polarization in the lines permitted an estimate to be made of the relative importance of photoexcitation and excitation by electron impact for λ 5303 and λ 6374 at different heights. Experimental values of the mean effective cross section of line excitation by electron impact were derived: $\bar{\sigma}_{5303} = 0.77 \times 10^{-17}$ cm², $\bar{\sigma}_{6374} = 0.63 \cdot 10^{-17}$ cm².

Some Notes on the Emission of Light by Shock Waves Under Cosmic Conditions, by S. A. Kaplan and I. A. Klimishin, pp. 264–266.

Abstract: A study is made of the heating of the gas before the front of a shock wave by the radiation emitted by the latter, using the theory of light scattering in a medium with a moving boundary. Formulas are given which may be used to calculate the temperature distribution in the heated zone and the width of this zone. Equations describe the increase in the intensity of radiation before the wave reaches the surface, which is due to the penetration of radiation through the higher lying layers.

Relativistic Corrections in the Problem of a Point Explosion in an Ideal Gravitating Continuous Medium, by V. A. Skripkin, pp. 267–278.

Abstract: An attempt is reported to apply the small-parameter expansion method (in the present case, the small parameter is the reciprocal of the square of the velocity of light) to the equations of motion of a continuous medium in which shock waves are being formed, using the general theory of relativity; to separate out the Newtonian hydrodynamic theory as a zero-order approximation; to elucidate the details of the connection between equations describing the successive approximations; and to compare first-order corrections with the zero-order values. In order to obtain a comprehensive result, the discussion is limited to a centrally symmetric field, and the zero-order approximation is taken to be in the form of Sedov's simple but exact solution for a point explosion in an ideal medium gravitating according to Newton's law, the specific heat ratio being $\gamma = 4/3$. Under the approximations employed, the state of matter and radiation in the universe as a whole corresponds approximately to this value of γ. It is shown that a gravitational wave is propagated in the undisturbed medium in front of the shock wave.

Radio Emissions From Venus in the 8-mm Bandwidth, by A. D. Kuz'min and A. E. Salomonovich, pp. 279–282.

Abstract: This paper reports the results of observations of radio emission from Venus in the 8-mm bandwidth, made during September to November 1959, on the 22-m radio antenna at the Lebedev Physics Institute of the Academy of Sciences, USSR. The brightness temperature, averaged over the visible planetary disk for 17 days following inferior conjunction, was 315 ± 70 K.

An increase in brightness temperature with increasing distance from inferior conjunction was detected. Some inferences are drawn on the physical conditions prevailing on Venus.

Results of Studies of Contrast on Mars, by N. P. Barabashov and I. K. Koval', pp. 283–287.

Abstract: An attempt at critical evaluation of the possibility of explaining contrast variations in terms of variations in the transparency of the Martian atmosphere is here based on a study of contrasts on Mars in red, green and blue light.

The conclusion of the authors is that the observation data on contrasts on Mars in red, green and blue light ($\lambda > 420$ mμ) are primarily attributable to the energy distribution in the surface of the planet proper.

General Features of the Evolution of Rotating Systems of Gravitating Bodies, by T. A. Agekyan, pp. 298–307.

Abstract: The evolution of rotating systems of gravitating bodies is studied qualitatively. The stage of development of the galaxy is determined from the character of the distribution of residual stellar velocities. Some remarks on the properties of galactic nuclei are presented.

Compensation of Refraction Effects With the Aid of a Vacuum Prism, by L. A. Panaiotov, pp. 317–321.

Abstract: The possibility of the use of a vacuum prism for astrometric purposes is considered. The expediency of this suggestion in the study of refraction under different conditions in astrometric practice is shown. The use of the vacuum prism in photographic astrometry will allow the compensation of differential refraction and atmospheric dispersion. A brief discussion is given of the main requirements imposed on the device and the technological possibilities of their fulfillment.

AUTOMATION AND REMOTE CONTROL (*Avtomatika i Telemekhanika*). Published by Instrument Society of America, Pittsburgh, Pa.

Vol. 20, no. 5, May 1959.

Application of Simulation in Analyzing Linear Pulse Systems With Variable Parameters, by G. P. Tartakovskii, pp. 559–566.

Abstract: Simulation of linear systems with discrete operation and variable parameters with the object of obtaining pulse response suitable for further application is examined.

It is shown that a pulse response as a function of the instants when pulses are applied, can be obtained by simulating a pulse system conjugate to the original system. Methods of designing schematic circuits for conjugate pulse system models, similar to corresponding methods of simulating continuously operating systems, are derived.

Invariance Principle in Combined Automatic Control Systems, by V. I. Dunaev, pp. 567–571.

Abstract: A further development is given of the complete invariance principle applied to combined automatic control systems with two motors driving a common load.

Calculation of a-c Magnetic Reactor Amplifiers With Internal Feedback, by N. A. Kaluzhnikov, pp. 582–596.

Abstract: The most typical circuits of magnetic reactor amplifiers with internal feedback are considered. The circuits are analyzed in two cases which are extreme from the point of view of nonsinusoidal distortion. Possible calculation errors are estimated. The results of the analysis are given in the form of design curves.

A Stability Criterion for Nonlinear Control Systems, by Chang Ssŭ-ying, pp. 639–643.

Induction Tachometer as an Angular Acceleration Transducer, by S. T. Kazaryan, pp. 647–652.

Abstract: An angular acceleration transducer in the form of an induction tachometer with d-c excitation is examined.

Vol. 20, no. 6, June 1959.

Some Simplified Stability Criteria for Nonlinear Controlled Systems, by A. K. Bedel'baev, pp. 664–678.

Abstract: Certain simplified stability criteria which do not require preliminary canonization of their initial equations are given for nonlinear controlled systems.

Stability of Nonlinear Controlled Systems, by E. N. Rozenvasser, pp. 679–684.

Abstract: Certain circumstances which provide the possibility of extending the sphere of application of the method proposed by Lur'e for investigating the stability of controlled systems are outlined.

Filtering of a Certain Type of Nonstationary Random Variable, by I. A. Boguslavskii, pp. 685–697.

Abstract: This article deals with a method of designing a circuit for generalized unshifted signal filtering of a random function, whose useful signal is represented by the solution of a first-order linear differential equation. The coefficient of this equation consists of a function of time unknown in advance, but continuously determined in the process of filtering, and the right-hand side of the equation consists of the sum of the products of known functions and unknown quantities added to a certain

function of time, which is continuously determined in the process of filtering.

Investigation of Algebraic Equations Using Analog Computers, by V. M. El'iasberg, pp. 733–738.

Abstract: A simple method is presented for the investigation of algebraic equations on analog computers, the method based on the reproduction of the given polynomial as the solution of the differential equation defining it. The method permits the immediate determination of the real and imaginary roots of algebraic equations, the approximate estimation of the value of their complex roots, and also the investigation of dynamic systems for stability, using the Mikhailov criterion.

Device for Solving High Order Algebraic Equations, by Jiři Krýže, pp. 739–748.

Abstract: The paper describes a high speed, completely automatic, device for simulating algebraic polynomials and solving high order equations. The device is constructed on a new principle, and does not contain electronic vacuum tubes in the simulating (analog) portion, thus removing the basic source of errors.

Use of Hall Elements as Phase-Sensitive Rectifiers, by V. N. Bogomolov and V. A. Myasnikov, pp. 774–782.

Abstract: The operation of a phase-sensitive detector, based on the Hall effect, is considered, and certain basic relationships are provided. A simple graphical method is presented for choosing elements to compensate for the temperature dependence of the Hall element parameters.

A table of experimental data for three different phase-sensitive detectors is given.

Vol. 20, no. 7, July 1959.

A General Condition for an Extremum of a Given Function of the Mean Square Error and the Squared Mathematical Expectation of the Error of a Dynamic System, by N. I. Andreev, pp. 807–812.

Abstract: The derivation is given for the condition for an extremum, and also for the greatest or least value, of some function f of the mean square error and the squared mathematical expectation of error in approximating a random function. The general condition obtained is applied to the problem of choosing an optimal nonlinear integral operator.

Methods of Analog Computer Solution of Linear Differential Equations With Variable Coefficients, by I. Matyash, pp. 813–821.

Abstract: Two methods are described for the solution of linear differential equations with variable coefficients by means of analog computers. The methods are illustrated by examples.

Properties of the Impulsive Response Function of Systems With Variable Parameters, by V. Borskii, pp. 822–830.

Abstract: A definite class of functions of two variables is considered as to the use of their properties for solving the problem of determining a linear differential equation from a given impulsive response function, and conversely.

Use of Nonlinear Correcting Devices of the "Key" Type for Improving the Quality of Second-Order Automatic Control Systems, by S. V. Emel'yanov, pp. 844–859.

Introduction: In another paper are presented the principles of constructing a nonlinear corrector, based on the nonlinear transformation of functions of several variables by means of uniform "key"-type devices. It was shown that, by means of such devices, the most diverse control laws can be realized.

The present paper is devoted to the questions of using a nonlinear corrector for stabilizing, and improving the regulation of linear automatic control systems. We shall consider closed dynamic systems described by second-order equations. For the determination of the tuning of the correcting device we have chosen the phase plane method. In particular, we use the concept of the many-sheeted phase plane which was used in the investigation of second-order systems by Petrov and Ulanov, and also in the works of Kazakevich.

Effect of Noise on Synchronous Filter-Generator Operation, by A. M. Luchuk, pp. 938–944.

Abstract: An analysis is made of the operation of a synchronous filter generator with sinusoidal noise at its input, and the results are given of an experimental investigation of the noise stability of telecontrol devices with synchronous filter generators. A qualitative and quantitative estimate of the effect of noise on synchronous filter operation is given, permitting correct calculation of its parameters.

Code Rings as a Method of Representing Code Sets, by A. N. Radchenko, pp. 945–951.

Abstract: A method is considered for the shortening of the writing of sets of code combinations by excluding from the constituents of various codes the repeated combinations of terms of less than the full (maximum) length. An analysis is made of the conditions for the existence of such shortened forms of representing code sets, called code rings, and the existence of various types of code rings is proved. The shortened form of writing code combinations may be used for decreasing the number of circuit elements or for increasing the capacity of a given number of elements.

Increasing the Pressure of the Working Agent in Jet Amplifiers, by B. D. Kosharskii, pp. 952–956.

Abstract: For a long time, both in the Soviet Union and beyond its borders, hydraulic jet regulators were used operated with pressures of the working agent (transformer oil) not higher than 6 to 8 kg/cm². Due to the low value of delivery potential, the radius of action of these regulators was very limited, both horizontally and, particularly, vertically.

Vol. 20, no. 8, Aug. 1959.

Control of a First-Order Delayed System by Means of an Astatic Regulator and Nonlinear Correction, by S. V. Emel'yanov, pp. 983–991.

Introduction: Often it is possible for the purpose of a concrete technical problem to approximate a motion equation of a high order by an equation of the first or second order with a delay.

It is known that existing automatic control systems which contain delay elements possess a small critical gain. Attempts to increase the critical gain by introducing a reaction from the derivative of the controlled coordinate usually do not produce the required results. The present article examines the possibility of applying the method of correction described elsewhere by the author for the stabilization and improvement of the quality of transient processes in automatic control delayed systems, represented by a second-order differential equation. In the article, a technique of determining the required linear control law, which would provide a high quality transient process, is suggested.

Bashkirov's analytico-graphical method was used as a means for calculating the parameters of the correcting device.

Optimum Transient Processes in Systems With a Restricted Third Derivative, by A. A. Pavlov, 992–100.

Abstract: Optimum transient processes in a system with a restricted third derivative of the controlled variable are examined.

The form of optimum transient processes due to step disturbances is determined, and a possible method of synthesizing the optimum controlling part of the system is given.

Automatic Correction of Compensator Parameter in Feedforward Systems, by S. A. Doganovskii, pp. 1008–1015.

Abstract: The problems of applying an automatic optimizer for correcting compensator parameters in a feedforward system are examined. The optimizer circuit and examples of its use are given.

Steady-State Processes in the Simplest Discrete Extremal System With Random Noise Present, by A. A. Fel'dbaum, pp. 1024–1038.

Abstract: Investigation of the processes in discrete extremal systems with random noise present, leads to the consideration of equivalent Markoff chains. Based on this consideration, we determine the steady-state error and the optimal size of the step (the quantum size) in the simplest system. Certain generalizations of the problem posed are considered.

Generalization of the Shaping Filter Method to Include Nonstationary Random Processes, by A. M. Batkov, pp. 1049–1062.

Abstract: The paper considers the basic properties of the impulsive responses of linear systems with variable parameters of general form, and the correlation functions of the random processes at their outputs when acted upon by "white noise." The problem of determining the characteristics of the shaping filters for this class of nonstationary processes is solved, and a methodology is suggested for using them in simulation problems in analyzing the dynamic accuracy of systems.

Tracking Drive With Gyroscopes on an Oscillating Platform, by S. G. Kolesnichenko, pp. 1071–1078.

Abstract: A device (a direction finder) is investigated which is mounted on an oscillating platform with a power gyroscope drive, automatically tracking heavenly bodies and measuring the absolute angular velocity of its own line of sight. The false constant component of angular velocity is discovered.

Noise Stability of Continuous Program Controlled Systems With Magnetic Recording, by K. N. Shadrin, pp. 1079–1084.

Abstract: The potential noise stability is considered for multichannel program controlled systems with magnetic recording when phase modulation is used. The problem is solved for systems with weak fluctuating noise resulting from disturbances in the magnetic recording channels. The expression for noise intensity at an ideal receiver's output is found for the cases of spatial (for multitrack recording), frequency and temporal separation of the channels. A comparison is made of the noise stabilities of systems with separated channels for identical effective voltage and unit width of recording carrier.

Approximate Method for Solving Equations Whose Orders Exceed the Capabilities of Analog Computers, by G. M. Ostrovskii, pp. 1095–1096.

Vol. 20, no. 9, Sept. 1959.

Stability of a Relay System's Equilibrium State, by S. D. Kinyapin and Yu. I. Neimark, pp. 1121–1131.

Abstract: In the present paper a new derivation of the stability conditions for a relay system's equilibrium state is given. With this, the approach to the question is borrowed from another work, but the investigation of the transformation's fixed points' stability is carried out in a different way, being based on the relationship between the stability of the equilibrium state of the system of differential equations and the stability of the fixed points of the corresponding mapping.

Analysis of the Stability of the Periodic Modes of Operation in Nonlinear Control Systems With Many Degrees of Freedom, by V. A. Taft, pp. 1132–1140.

Abstract: On the basis of a generalized corollary of Hill's equation, a derivation is given of the characteristic equation (in finite form) of a system with many degrees of freedom whose parameters are periodic functions of time. The results obtained permit the use of the well-known Mikhailov criterion for analyzing the stability of the periodic modes of operation.

Designing Correcting Circuits for Automatic Control Systems in Accordance With the Mean Square Error Criterion, by V. I. Kukhtenko, pp. 1151–1159.

Abstract: A method is presented for finding the optimal (in the sense of minimum mean square error) transfer function, the degree of whose numerator is a given number of units less than the degree of the denominator, and a discussion is given of the relationship of this question with the question of physical realizability of the correction circuit. An example is provided.

Effect of Noise on Phase-Locked Oscillator Operation, by V. I. Tikhonov, pp. 1160–1168.

Abstract: The action of external noise and of inherent fluctuations on an inertial-less phase-locked oscillator are considered by means of the Fokker-Planck equation. Formulas for the mean and dispersion of the synchronized generator's frequency are found. The analogy is established between the problem considered here and the problem of synchronizing a self-excited oscillator in the presence of noise.

Minimization of the Boolean Functions Characterizing Switching Circuits, by M. A. Gavrilov, pp. 1188–1207.

Abstract: The paper considers a method for minimizing the Boolean functions which characterize switching circuits, the method based on an analysis of the conditions to be realized by the operation of the switching circuits.

Possibilities of Increasing Noise Stability Based on Use of A Priori Parameter Probabilities, by V. A. Kashirin and G. A. Shastova, pp. 1208–1218.

Abstract: The noise stability of an ideal receiver is considered, the first distribution law of the a priori parameter value probabilities being taken into account. An analysis of noise stability is carried out for the case of a nonlinear parameter transformation prior to modulation. The optimal nonlinear transformation of parameters prior to transmission is found, as well as the gain in noise stability obtained with this transformation. Both the mean square and the information criteria of optimality are used.

BULLETIN OF THE ACADEMY OF SCIENCES OF THE USSR, PHYSICAL SERIES (Izvestiia Akademii Nauk SSSR, Seriia Fizicheskaia). Published by Columbia Technical Translations, White Plains, N. Y.

Vol. 23, no. 2, 1959.

Concerning Linearity in Scintillation Spectrometry, by Yu. A. Nemilov, I. I. Lomonosov, A. N. Pisarevskii, L. D. Soshin and N. D. Teterin, pp. 246–251.

Amplification of Photomultipliers in Pulsed Operation, by A. N. Pisarevskii and N. D. Teterin, pp. 252–253.

Introduction: It was shown elsewhere that the amplification of different types of photomultipliers changes in a different way with variation of the time parameters of the exciting pulses and exhibits a general tendency to decrease in going from steady excitation to pulses in the millimicrosecond range. It was also shown that this "pulse dependence" is most strongly evinced in photomultipliers characterized by good time resolution. Now, however, the explanation for the observed effects suggested appears to us to be questionable.

In the present work we employed a similar but appreciably improved measurement technique. Specifically, we investigated samples of FEU-1v, FEU-33, FEU-13m, and FEU-6810 photomultiplier tubes.

Selection Rules in Conversion Transitions, by M. E. Voikhanskii and M. A. Listengarten, pp. 228–233.

Frequency Meter for Nuclear Resonance, by Yu. S. Egorov, D M. Seliverstov and G. D. Latyshèv, pp. 240–243.

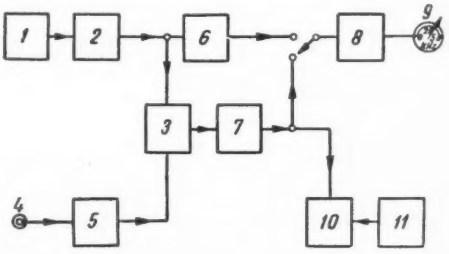

Fig.1. Block diagram of the MK-3 frequency meter circuit: 1) 100 cps crystal controlled oscillator, 2) 10 and 20 cps multivibrator, 3) mixer, 4) high frequency input, 5) hf amplifier, 6) scale-of-four scaler, 7) 0 to 500 cps amplifier, 8) frequency-sensitive detector, 9) frequency indicator, 10) oscillograph, 11) ZG-641 audio oscillator.

Introduction: In utilizing nuclear resonance for measurement and stabilization of magnetic fields, the accuracy of field measurements depends on the accuracy in determining the frequency of the hf voltage, inasmuch as

$$H_0 = \frac{2\pi}{\gamma} f_0 \text{ or } H_0 = kf_0$$

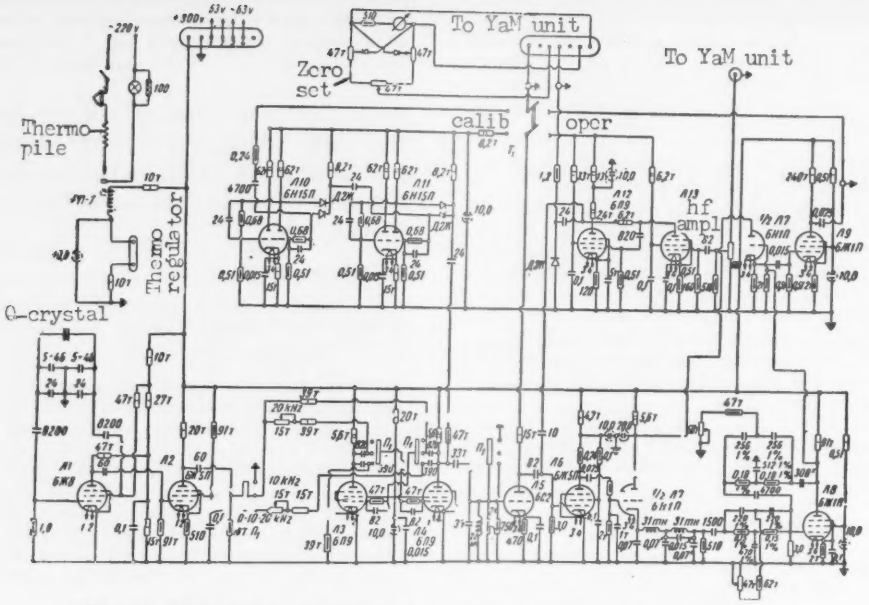

Fig. 2. Circuit of MK-3 frequency meter (Л = tube).

where

H_0 = spectrometer or other measured field
γ = gyromagnetic ratio
k = constant for the given type of nuclei

The operation of the frequency meter described herein is based on comparison of the measured frequency with the frequency of a quartz crystal.

Vol. 23, no. 6, 1959.

Electron Microscopic Investigation of the Structure of Thin Films of Antimony Sulfide Prepared by Evaporation in Vacuum and in Nitrogen at Pressures Under 4 mm Hg, by A. M. Reshetnikov, pp. 676–681.

Introduction: In recent years antimony sulfide in the form of thin layers has come into increasing use as a photoconducting material for the targets of television pickup tubes. The antimony sulfide layers are prepared by evaporation under vacuum or in an atmosphere of some inert gas at low pressure (1–4 mm Hg).

The structure and physical properties of thin antimony sulfide coatings prepared by vacuum evaporation have been investigated repeatedly. Forgue and his co-workers, on the basis of x-ray and electron diffraction studies, report that such layers have an amorphous structure or at any rate consist of very minute crystals. Tatarinova concluded, as a result of careful electron diffraction investigation of antimony sulfide films prepared by evaporation on celluloid supports, that such films have an amorphous structure. The influence of the substrate temperature on the structure of antimony sulfide layers and the effect of heating these layers in air was investigated by Vertsner et al. These authors also report that smooth amorphous films are obtained as a result of vacuum evaporation onto glass.

The other method of preparing photosensitive layers—evaporation in an inert gas atmosphere—is also widely utilized in fabricating television pickup tubes. However, the structure of layers formed by this procedure and the process of formation itself have scarcely been studied, and there are no definite data on the subject in the literature. Below we give the results of an electron microscopic investigation of the structure of Sb_2S_3 films obtained by condensation in an atmosphere of nitrogen at pressures under 4 mm Hg and by evaporation in vacuum.

Investigation of Electron Energy Loss in Thin Gas Layers, by I. G. Stoyanova and A. N. Kabanov, pp. 714–717.

Introduction: In the case of electron microscopic investigation of specimens in air or special gases there occurs additional scattering of the electrons by the atoms of the gas; this scattering may have a substantial effect on both the quality of the image (contrast and resolution) and the processes occurring in the specimen (heating, ionization, etc.). Inelastic electron scattering is particularly important. To elucidate the influence of inelastic scattering processes on the quality of the electron microscope image, we measured the electron energy loss in the specimen under different conditions of observation, in particular, when the specimen is placed in different gaseous media.

Electron Microscopy of Temperature Induced Changes in the Magnetic Microstructure of Ferromagnets, by I. S. Sbitnikova, G. V. Spivak and I. M. Saraeva, pp. 729–732.

Introduction: In previous publications by members of our laboratory staff there was described an electron-optical procedure for "visualization" by means of secondary electrons of magnetic microfields, temperature waves and domains on the flat surface of a specimen. There was, for example, obtained the image of the domain structure on the hexagonal face of a cobalt single crystal. Despite the fact that the magnetic fields of the domains on this face were rather strong ($H \backsimeq 10^4$ oersted) the secondary electron image was of rather poor quality and low in contrast.

The purpose of further experiments, which are described in the present report, was to develop this visualization procedure: To increase the image contrast and to evaluate the sensitivity of the equipment. Of particular interest is the possibility of utilizing a secondary emission microscope for observing the dynamics of thermal processes occurring in ferromagnetic materials.

Investigation of Structural Changes in Dielectrics Under the Influence of Heat, Chemical Etching and Ion Bombardment, by A. I. Krokhina and G. V. Spivak, pp. 736–738.

Vol. 23, no. 7, 1959.

Specific Stopping Losses in Heavy Ions in Different Substances, by A. P. Grinberg and I. Kh. Lemberg, pp. 877–882.

Introduction: Through investigation of Coulomb excitation one can, in a number of cases, (particularly, for even-even nuclei) reliably determine the lifetime τ of excited nuclear levels in the range from 10^{-12} sec down. In experiments with protons and α-particles in the case of higher excitation energies ($\Delta E \approx 1$ mev), owing to an interfering γ-background from nuclear reactions one can, in practice investigate only nuclei with $A > 50$. The use of heavier particles, namely ions, allows of extending the lifetime measurements into the range of nuclei with $A < 50$.

As a rule thick targets are used in Coulomb excitation experi-

ments. Hence for calculating the values of τ one must have available precise data on the specific energy loss, $\epsilon = dE/dR$, involved in the slowing down of C, N and other suitable ions in different substances as a function of the ion energy. The available experimental material on energy losses is extremely scanty; moreover, some of the reported data are of doubtful accuracy. The paucity of data is particularly acute for the ion energy range of interest to us, namely 10 to 36 mev, and for cases of absorption in materials other than nuclear emulsions and gaseous media. In fact one can name only two investigations in which the range-energy relation for heavy ions in metals was measured: Reynolds, Scott and Zucker measured the range of N^{14} ions in nickel; Webb, Reynolds and Zucker determined the range of nickel ions in aluminum. The maximum ion energy in the work referred to was 28 mev.

In investigations of Coulomb excitation of nuclei by heavy ions carried out in the cyclotron laboratory of the Physical-Technical Institute, by way of targets we used a large number of different metals and other solids, by way of bombarding particles not only N^{14} ions with energies to ~36 mev, but also C^{12}, O^{16}, Ne^{20} and Ne^{22} ions. Hence it was necessary to choose some consistent theoretical or semi-empirical method of calculating ϵ. We list three known methods for such calculation and briefly describe their distinctive features.

Range and Specific Ionization of Multicharged Ions, by Ya. A. Teplova, V. S. Nikolaev, I. S. Dmitriev and L. N. Fateeva, pp. 883–886.

Introduction: In view of the relative scarcity of experimental data on the stopping of multicharged ions in matter we continued our measurements of the range, specific ionization and equilibrium ion charge distribution in a wider range of nuclear charges. In the present measurements, in addition to ions with $Z \leqslant 10$, we worked with Na^{23}, Mg^{25}, Al^{27}, P^{31}, Cl^{37}, A^{40}, K^{39}, Br^{81}, and Kr^{84} ions. Some of the experimental results are given.

Moments of Inertia of Nuclei, by M. Kazarnovskii, pp. 899–900.

Statistical Theory of the Nuclear Potential in the "Effective Mass" Approximation, by L. Rapoport and S. Kadmenskii, pp. 905–910.

Introduction: It has been shown in a series of theoretical papers that if we neglect the Coulomb repulsion, an arbitrarily large number of nucleons form a stable system with an equilibrium density $\rho = 1.72 \times 10^{38}\ cm^{-3}$ and a binding energy of 15 mev per particle. Such a system has been given the name "nuclear matter." In nuclear matter the nucleons move as independent particles; that is, the potential energy of a nucleon does not depend on its position but does depend on its velocity. This velocity dependence is most frequently expressed in terms of the "effective" mass of the nucleon. One of the principal differences in treating the properties of nuclear matter as against those of an actual nucleus is that for the former the effect of finite size is neglected. In the present paper we shall discuss the depth and form of the potential acting on a nucleon within a nucleus, and also the magnitude of its effective mass and the dependence of this mass on the distance of the nucleon from the center of the nucleus; the finite dimensions of the nucleus and the Coulomb forces between the protons are included in this calculation based on the statistical theory of the nucleus. It is found that the protons are included in this calculation based on the statistical theory of the nucleus. It is found that the "self-consistent" potentials have the usual form; i.e., the form employed, for instance, in the nuclear shell model. The magnitude of the effective mass obtained is approximately the same as for nuclear matter. The general form of the potential, which depends on position and momentum, can be expressed as a generalized non-local potential, representing the action of the entire nucleus on the nucleon.

INDUSTRIAL LABORATORY (Zavodskaia Laboratoriia). Published by Instrument Society of America, Pittsburgh, Pa.

Vol. 25, no. 11, Nov. 1959.

Method of Evaluating the Evaporability of Plastic Lubricants, by V. V. Sinitsyn, K. K. Papok and B. S. Zuseva, pp. 1411–1413.

Introduction: The methods of determining the evaporability of plastic lubricants which have been described in the literature are time consuming; they require 24 to 150 hr. Many of the presently used methods are complicated and cannot be applied in ordinary laboratories. A number of methods, including those used in the quality control of lubricants, are characterized by a low reproductiveness of results. The discrepancies between parallel determinations can attain a few tens, and even hundreds, of per cent. We developed an accelerated and sufficiently accurate method which is based on measuring the weight loss of lubricant specimens deposited in a layer 1-mm thick on a standard evaporator 21.4 mm in diameter, which is kept in a special thermostat at a given temperature for 1 to 3 hr.

Device for Low Temperature Cooling of Specimens, by I. S. Mel'nikov, pp. 1441–1442.

Introduction: We have developed a device for the cooling of specimens, based on ideas described earlier, which is intended for use with the IM-12 machine. Mainly, the device is designed for the cooling of specimens in liquid media. We used liquid nitrogen, although cooling mixtures could also have been used. By means of the described device, we performed static tensile tests (on smooth and notched specimens), bending tests, torsional tests, simultaneous tensile and torsional tests with the application

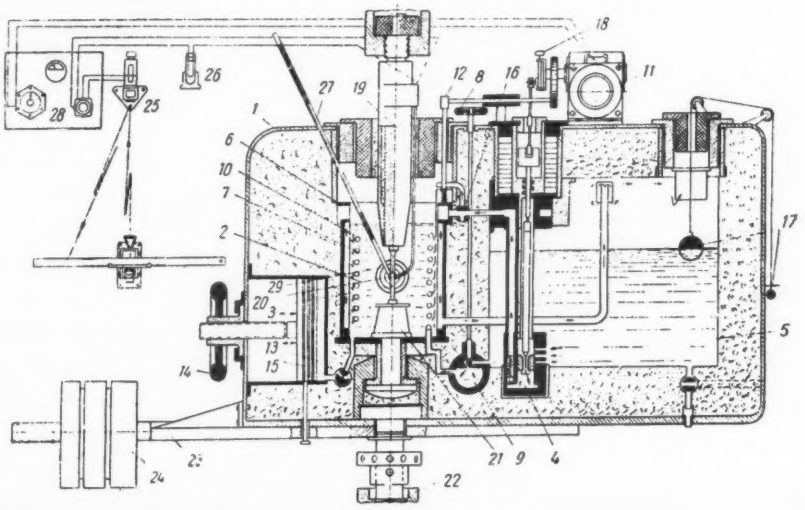

Fig. 1. Schematic diagram of the device.

of screw pairs, and impact strength tests. Fig. 1 shows the schematic diagram of the device.

Spectral Analysis of Thin Metallic Films, by L. E. Berenshtein and V. G. Koritskii, pp. 1406–1407.

TABLE 1

Analytical Line Pairs

System	Line A
Fe — Cr	Cr 2677.16 — Fe 2607.09
Fe — Mn	Fe 2743.20 — Mn 2701.70
Ni — Cr	Cr 3118.15 — Ni 3101.88
Ni — Fe	Ni 3054.32 — Fe 3059.09
Ni — Co	Ni 2394.52 — Co 2397.39

TABLE 2

Comparison of Chemical and Spectral Analysis Results for Condensates of the Fe–Cr System

Chemical analysis results, % Fe	Spectral analysis results, % Fe	Relative discrepancies, %
73.0	72.0	1.3
20.7	20.0	3.5
7.07	7.3	0.96
0.70	0.69	1.43

Introduction: In studying the influence of liquid phase composition on the evaporation rate of melt components, it was necessary to determine the composition of the vaporous phase. The condensate which formed on the copper receiver plates when these were introduced into the vapors served as the specimen. The amount of condensate which we were able to obtain was approximately equal to 0.1 mg, which did not make it possible to perform a sufficiently accurate chemical analysis. We applied the spectral analysis method, which had been successfully used earlier for the solution of similar problems.

INSTRUMENTS AND EXPERIMENTAL TECHNIQUES (Pribory i Tekhnika Eksperimenta). Published by Instrument Society of America, Pittsburgh, Pa.

No. 3, May–June 1959.

Measurement of the Energy of Electrons and Gamma-Ray Quanta by a Low Efficiency Counter, by Yu. D. Prokoshkin and T'ang siao-wei, pp. 377–380.

Abstract: A method is described which allows the energy of electrons and γ-quanta to be determined by measuring the number of shower electrons formed by them in lead. To measure the number of shower electrons, halogen counters operating under low efficiency conditions are used.

Corona Counters of Highly Ionizing Particles, by A. B. Dmitriev, Yu. M. Tolchenov, A. I. Filatov and V. G. Chaikovskii, pp. 380–385.

Abstract: Counters operating under conditions of a stable corona discharge and intended for detecting highly ionizing particles are described. The amplitude of the pulses is proportional to the ionization created by a particle in the sensitive volume of the counter. The gas amplification factor in the counters is as high as 10^3–10^4 and can be made independent of the power supply voltage, as a result of which the counters have a plateau of large extent with a small slope. The presence of an intense background of low ionizing radiation has an insignificant influence on the parameters of the counters with respect to the highly ionizing particles. A brief description of the operating principle of the counters is given.

Form of an Electric Field in Corona Counters, by Yu. M. Tolchenov, pp. 385–389.

Abstract: The form of the electric field in counters of highly ionizing particles operating in the region of a stable corona discharge was calculated. The result was checked experimentally by measuring the times required for ions to pass through the counter and comparing these values with experimentally found values. In all cases close agreement between the theoretical and experimental results was obtained.

Multiwire Charged Particle Counter, by A. S. Deineko, pp. 380–395.

Abstract: A design for a double-annulus multiwire counter was developed and tested. For preparations with a maximum β-particle energy of 1.3 mev, the counting efficiency of a counter connected to a coincidence circuit is 0.28. The design of the instrument allows experiments to be conducted with both solid and gaseous targets. The counter was used in experiments for measuring the yield of positrons during reactions of $B^{10}(d,n)C^{11}$ and $C^{12}(p,\gamma)N^{13}$.

Photon Counters for Accurate Measurement of Ultraviolet Radiation, by L. S. Shelkov, I. A. Prager, and A. G. Kostin, pp. 396–402.

Abstract: We investigated the electrical and photometric characteristics of self-quenched photon counters with photocathodes of various materials. The measurements were performed for comparatively high counting rates, which made it possible to secure small statistical errors in measurement results ($\sim$1%) for a limited exposure time ($\sim$1 min).

We developed a construction of photon counters with a photocathode of the Cu-Be alloy provided with a protective grid made of tungsten wire. This construction permitted a substantial increase in the stability of the photocathode sensitivity.

Gas Discharge Scintillation Counter, by L. S. Sorokin, pp. 403–404.

Abstract: The possibility and conditions for application of a complex photocathode (antimony-cesium) in a self-quenching counter were demonstrated; the convenience of working conditions was established for an antimony-cesium photocathode with a small braking electrical field at its surface, which serves to eliminate the flow of thermoelectrons from the photocathode and the flow of positive ions to the photocathode.

The possibility of registering the scintillation from such crystals as NaI(Tl) by a self-quenching gas discharge counter was proved experimentally. With a NaI(Tl) crystal 10-mm thick, an increase in counter efficiency for Co^{60} γ-quanta was obtained, where the efficiency was up to 14.5 times greater in comparison with ordinary type VS-4 counters.

Construction of Boron Ionization Chambers, by A. B. Dmitriev, M. G. Vorob'ev, L. G. Kosmarskaya and N. I. Chipurenko, pp. 405–408.

Abstract: This article presents a description of boron ionization chambers designated for operation in control and protection systems of nuclear reactors.

Application of the Storage Method to the Photoelectric Recording of the Time Spectra of Light Flashes, by B. A. Ermakov and A. A. Mak, pp. 440–443.

Abstract: A photoelectric apparatus is described which may be used to record the time spectra of light flashes and has a high time and spectral resolution. The spectrum is recorded automatically on the chart of a self-recording potentiometer.

Zero-Point Modulation Method in Photometric Measurements, by V. A. Kovalevskii, pp. 444–448.

Abstract: This article considers the requirements that the construction of a modulator must satisfy in order to attain a maximum accuracy in the comparison of two light intensities by the zero-point modulation method. Several new modulation systems, satisfying these requirements, applied by the author to accurate spectropyrometric measurements, are described.

Measuring the Temperature of a Gas Downstream From a Shock Wave, by S. A. Losev and N. A. Generalov, pp. 454–456.

Abstract: A technique has been devised for measuring the temperature of a gas on the basis of the emitting and absorbing powers of the sodium D lines and has been used to measure high temperatures developed in a gas aft of a strong shock wave (under laboratory conditions). For absorption observations, the intense emission from a pulsed IPS-500 tube was used. Temperatures ranging from 4000 to 5000 deg were measured, with an error of ±100–200 K.

No. 4, July–Aug. 1959.

Conversion of Amplitude Distributions Into Energy Spectra, by Yu. A. Kazanskii, pp. 540–545.

Abstract: The instrumental spectrum of pulse amplitudes and the efficiency of a single-crystal scintillation γ-spectrometer with a CsI(Tl) crystal were investigated. Using the data obtained, a number matrix was constructed, by means of which, using the method of successive subtractions, the amplitude pulse distributions were converted into energy spectra.

Electronic Simulator for the Processing of Data on Extensive Atmospheric Showers of Cosmic Rays, by G. V. Bogoslovskii and B. A. Khrenov, pp. 546–549.

Abstract: This article describes an electronic simulating device for determining the most probable position of the axis of an extensive atmospheric shower and the number of particles in the shower when the latter is registered on an array of counters connected to a hodoscope. The device provides a mathematically exact solution of the problem, and also determines the probability distribution with respect to the coordinates of the shower axis in the plane of observation, and with respect to the number of particles in the shower. The accuracy of the solution of this problem is also analyzed.

Application of the Method of Second Differences for the Measurement of Multiple Scattering in a Propane Bubble Chamber, by I. I. Pershin, V. V. Barmin, V. P. Kanavets and B. V. Morozov, pp. 555–560.

Abstract: A detailed description is presented of the application of the method of second differences to the measurement of the mass of particles and electron energies in multiple scattering in a propane bubble chamber described earlier. The values of the scattering constant for propane, calculated according to Williams' and Molier's theories, and the experimental values of this constant, determined by measurements for μ-mesons and positions, are also given. The specific conditions arising in the measurement of multiple scattering in bubble chambers are also considered.

Plastic Scintillators Containing 1,2-Di-(1-Naphthyl)-Ethylene, by L. L. Nagornaya and A. P. Kilimov, pp. 577–580.

Abstract: The luminescence and scintillation properties of 1,2-di-(1-naphthyl)-ethylene solutions in polystyrene are studied. By the method of high temperature polymerization, plastic scintillators were obtained, which contained 1,2-di-(1-naphthyl)-ethylene serving as the basic luminescent admixture or as a spectrum shifter. By γ-excitation, the scintillators obtained produced a scintillation luminescence yield attaining 125–130% and 140–145% of the luminescence yield of a 2% solution of p-terphenyl in polystyrene.

Scintillation Conversion Efficiency of NaI(Tl) Crystals, by I. I. Lomonosov, A. N. Pisarevskii and L. D. Soshin, pp. 584–585.

Determination of the Magnet Pole Form by Considering the End Effect, by E. P. Grigor'ev and A. V. Zolotavin, pp. 613–615.

Abstract: A simple method of calculating the profile of poles for the creation of a magnetic field of required form is proposed. The scattering of the field is taken into account by measuring the field of flat poles. The accuracy of the method is approximately 1.5%

Automatic Pulse Counter, by G. M. Gorodinskii and V. A. Kochevanov, pp. 596–600.

Abstract: A device for the automatic count of the number of statistically distributed pulses is described. The pulses fed by the data transmitter to the instrument input at equal periods of time are recorded on the tape of the ÉPP-09 electronic self-recording potentiometer in histogram form. The counting capacity of measurement ranges (in operation with the PS1: 256 scaling circuit) lies within 50 and 1.3×10^6 pulses for the entire scale. The exposure time is changed at will between 2

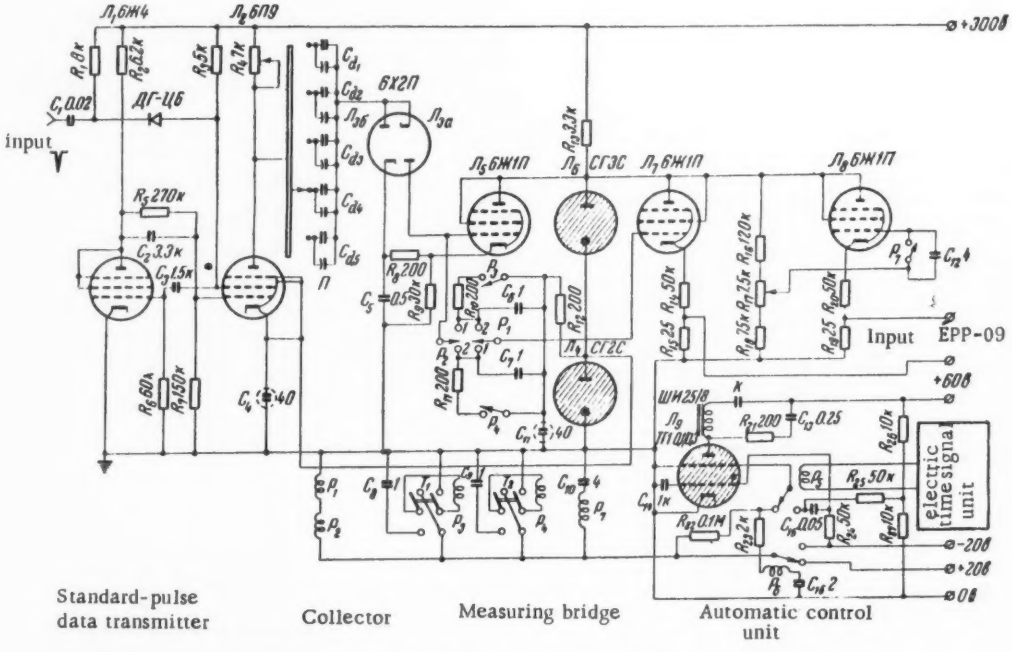

Fig. 3. Circuit diagram of the device for the automatic recording of γ-spectra.

The following Russian abbreviations are retained in the figure: Л = tube, Тр = transformer, М = megohm, к = kilohm, МК = μf or μh, Н = mμf or mμh, п = μμf or μμh, and в = volt. For individual tube designations see appendix to No. 1 of this year.

sec and 16 min. The instrumental accuracy in registering the number of pulses is not worse than 1% for any of the ranges. The instrument is reliable and simple in manufacture and application.

Technique of Measurement of Reflection Coefficients in Free Space at Ultra High Frequencies, by D. I. Mirovitskii, pp. 619–625.

Abstract: The particulars of two basic types of devices—those with common and those with diversity antennas—are examined. Methods of determining the reflection coefficients of dielectric samples are presented and also methods of raising the precision of the measurements.

Measurement of Dispersion in Regions of Intense Infrared Absorption, by M. P. Lisitsa and Yu. P. Tsyashchenko, pp. 626–630.

Abstract: A reflection method is described, which permits one to investigate the dispersion of liquids inside an intense fluctuating absorption band. An interference method of measuring the dispersion at the approaches to such a band is perfected. As an example, the dispersion curves of CCl_4 and $CHCl_3$ are obtained in regions of the strongest absorption. The method developed is especially useful for the study of viscous liquids.

Photographic Method of Investigating Random Processes, by B. B. Bukhovtsev and V. I. Shmal'gauzen, pp. 665–666.

Abstract: Described is a method of measuring the probability distribution functions of random signals by means of an electronic oscillograph with a photographic adapter.

The Problem of Producing an Ultra High Vacuum, by E. A. Penchko, L. P. Khavkin and A. S. Borodkin, pp. 667–668.

Abstract: Experiments were performed in producing an ultra high vacuum in a sealed off glass tetrode ionization manometer with an axial collector by means of cooling its bulb to a temperature of 1.9 K. The cathode heating power applied in pressure gauges on which these experiments were performed was considerably reduced (to ~0.5 *W*) in comparison with pressure gauges described. The pressure gauges were evacuated and pre-aged in a vacuum device and sealed off at a pressure of $\sim 5.10^{-6}$ mm Hg. The pressure gauges were fastened on a tube made of stainless steel; by means of a packing gland, they could be quickly moved in a wide range inside a Dewar flask. The vacuum was measured by immersing the pressure gauges in liquid helium ($T = 4.2 - 1.9$ K).

Infrared Radiation Sources Based on Silicon Carbide, by R. I. Bresker, N. I. Voronin, and Z. I. Latysheva, p. 670.

Text: Nernst pins and pins based on silicon carbide are most widely used as radiation sources in infrared spectroscopy. Nernst pins are manufactured in the Soviet Union. Emitters based on silicon carbide, which are known under the trade name "Globary," are not produced in the Soviet Union. A method of preparing

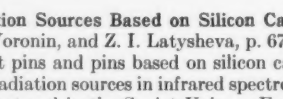

Fig. 1. General view of the emitter; dimensions are in millimeters.

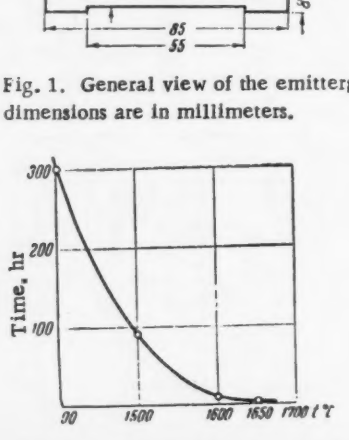

Fig. 2. Lifetime of the emitter in relation to surface temperature.

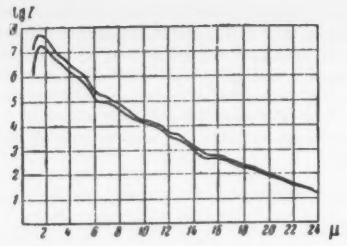

Fig. 3. Energy distribution curve according to the spectrum of surface temperatures of the source at 1200° and 1400° C.

carborundum sources of infrared radiation has been developed in the Leningrad Institute of Refractory Materials. Infrared carborundum emitters are made in the form of cylindrical rods 4 mm in diameter and 85 mm long. Cylindrical tubes 15 mm long with an outside diameter of 8 mm are fitted at the ends of each rod. The general view of the emitter is shown in Fig. 1.

The emitter has a resistance between 5 and 8 ohms and is fed by a LATR-1 laboratory autotransformer. In order to heat the surface of the emitter to 1400 C an energy of 250 to 350 w must be dissipated in it. The temperature coefficient of resistance in the emitter is practically equal to zero at 1400 C. During the first hours of operation, the resistance of the emitter somewhat increases and becomes steady afterwards. Therefore, it is advisable to maintain the emitter at 1400 C for 2 to 3 hr until its electrical resistance becomes stable. The surface temperature of the source is determined by an optical pyrometer. At 1400 C the lifetime of a carborundum source is equal to 300 hr; its lifetime is sharply reduced with an increase in its surface temperature (Fig. 2). Carborundum emitters are designed for operation at a surface temperature of 1400 C. Fig. 3 shows the energy distribution according to the spectrum of two surface temperatures of the source–1200 and 1400 C. The data were obtained with the IKS-11 spectrometer with NaCl (1–14 μ) and KBr (14–24 μ) prisms.

Miniature Device for the Production of Magnetic Fields of Several Tens of Thousands of Oersteds, by N. V. Volkenshtein and M. I. Turchinskaya, pp. 673–674.

Text: Fig. 1 shows the schematic diagram of the device which has optimum dimensions for the given diameter of the semi-

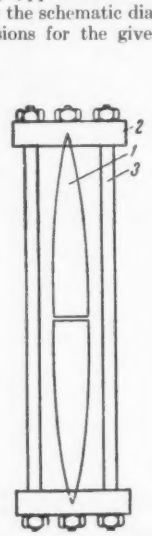

Fig. 1. Schematic diagram of the device. 1) Semiellipsoid made of Permendur with semiaxes a = 35 mm and b = c = 5 mm; 2) plexiglas plate 35 mm in diameter and 8 mm thick; 3) brass rod.

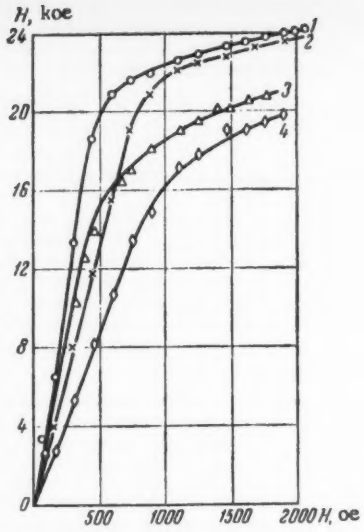

Fig. 2. Curves of the field in the constant 0.21 mm gap vs. the external field for semiellipsoids: 1) Permendur with semiaxes a = 55 mm and b = c = 5 mm; 2) Permendur with a = 36.5 mm and b = c = = 5 mm; 3) Armco iron with a = 55 mm and b = c = 5.5 mm; 4) Armco iron with a = 36.5 mm and b = c = 5.5 mm.

ellipsoid base. When placed in a solenoid field of 2000 oe, the instrument produces a field of 24,000 oe in the 0.2 mm gap. Semiellipsoids of different sizes which we investigated were made of Armco iron and the K50F2 Permendur alloy. Fig. 2 shows the dependence of the field in the 0.21 mm gap on the external (solenoid) field for semiellipsoids of different sizes and materials. In preparing the ellipsoids, materials with a greater magnetizability in weaker fields should be preferred.

A Laboratory Cryostat, by N. B. Mikheev and V. A. Glazkov, p. 679.

Introduction: Cryostats of various designs are produced by domestic industry; however, in the majority of cases, they are large in size and not always available to investigators. In connection with this, we propose a design of a laboratory cryostat for temperatures of −40 C which can be easily made in a laboratory where a Geppler ultrathermostat or a TS-15 are available. Fig. 1 shows the schematic diagram of the instrument. Instead of a heater, the coil of an electromagnetic valve is connected in the ultrathermostat, which must be provided with a compact thermometer for low temperature.

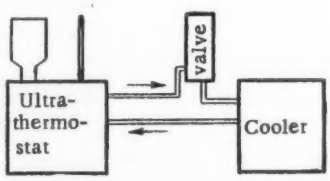

Fig. 1

OPTICS AND SPECTROSCOPY (Optika i Spektroskopiia). Published by Optical Society of America, Washington, D. C.

Vol. 8, no. 1, Jan. 1960.

Determination of the Size of Particles by the Scattering of Light I. Formulas and Nomograms for Computation of Radius of Particles by the Optical Density and by Intensity of Scattered Light, by I. Ya. Slonim, pp. 48–52.

Abstract: On the basis of the equations of Shifrin's theory of light scattering, formulas are derived and nomograms are constructed for the determination of the sizes of particles of the dispersion systems, in which electrical properties of the particles deviate little from the properties of the surrounding medium.

Determination of the Parameters Characterizing the True Contours of Absorption Bands, by I. V. Peisakhson, p. 57.

Measurements on Double Beam Spectrometers, by L. A. Gribov p. 61.

Method of Interference Modulation, by V. M. Arkhipov, pp. 61–62.

PHYSICS OF METALS AND METALLOGRAPHY (Fizika Metallov i Metallovedenia). Published by Pergamon Institute, Washington, D. C.

Vol. 8, no. 3, 1959.

Homogeneous Aging of Unsaturated Solid Solutions, by A. A. Presniakov, L. I. Duatova and Iu. F. Kliuchnikov, pp. 68–72.

Material and Method of Investigation: Specimens were examined of the following simple brasses corresponding in composition to the brands L95, L90, L85, L80, L75, L70, L65, L60 and of aluminium bronzes of brands Br, A1, A2, A3, A4, A5, A6, A7, A8, A9, A10. All these alloys were prepared from brand MO copper, AOO aluminium and brand TsV zinc.

The alloys were prepared for x-ray analysis as follows: Cast billets of 18-mm diameter and 120-mm length were forged (beginning the forging at about 800 deg) to a degree of deformation of the order of 30%. Cylindrical "vessels" were out from the forged billets with a thickness at the bottom of 1.5–2 mm, their end surface (to be used for x-ray photographing) was ground and polished; then the specimens were annealed for 6 hr in air at 800 deg. After annealing, the working surface was again ground, polished and etched in nitric acid to remove the deformed layer.

X-ray photographs were made with copper K_a radiation. The diffraction spots from the planes (420) and (331) were obtained after an exposure of 45 min. The specimens remained in the electric furnace during the exposure. The temperatures of the specimens were 20, 100, 200, 250, 300, 350, 400, 450 and 500 deg, and were controlled with an accuracy of ±10–20 deg.

Conclusions: 1 The phenomenon of homogeneous aging in nonsaturated solid solutions, unaccompanied by a change in the phase composition of the alloy or the precipitation of an excess phase is observed, which consists in the very marked diminution

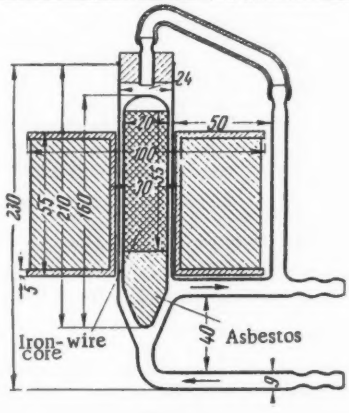

Fig. 2

of the size of the mosaic blocks and their misorientation to each other.

2 The presence of an aging process in solid solutions which have undergone hot deformation and subsequent annealing shows that the high temperature state of the crystal structure of the alloy is "quenched" during slow cooling.

3 The diminution of the block size in the aging process and its "recrystallization" at higher temperatures show that for various temperature conditions there exist corresponding equilibrium mosaic structures to which the alloy tends under all conditions, including room temperature.

4 The "aging" process of solid solutions is reversible. The rate of the reverse process is the greater, the greater the rate of the direct process.

5 The process of homogeneous aging is preceded by the short range ordering of the solid solutions; this, apparently, explains its slowness.

Relationship of Creep of Nickel-Copper Alloys to Solid Solution Concentration and Deformation Conditions, by M. G. Gaidukov and V. A. Pavlov, pp. 95–100.

Abstract: The creep of nickel-copper alloys with 10, 20, 40 and 60% Cu in the temperature range 500–700 deg is studied. At high deforming stresses, comparable to the yield point, and at relatively low temperatures, alloys with high yield point have the smallest creep rate. Under small deforming stresses, appreciably lower than the yield point, and at high temperatures, the creep rate increases with higher alloy content. The difference in behavior of the alloys with variation of deformation conditions is explained by the varying degree of participation of shearing and diffusion plastic deformation in the general process.

Conclusions: 1 The creep rate of nickel copper alloys in the temperature range 500–700 deg depends on the composition of the alloy and on deformation conditions.

2 At relatively low temperatures and high deformation stresses commensurate with the yield point at which the deformation in all probability proceeds primarily by a mechanism, the creep rate is inversely dependent on the yield point. The higher the yield point, the lower the creep rate. Under these deformation conditions, the 40% copper alloys have the highest resistance.

3 In the high temperature range and at fairly low deforming stresses, appreciably less than the yield point, the deciding factors are the diffusion processes which occur under loading. In this case creep rate increases with increasing solid solution content.

4 In the general case the behavior of alloys under loading is determined by the part played by shearing and diffusion plastic deformation.

Internal Friction of Metastable Solid Solutions, by B. G. Livshits, Iu. S. Avraamov, V. B. Osvenskii, S. O. Mebzennaia and L. N. Beliakov, pp. 107–115.

Abstract: Experimental results of work on the study of solid solutions of different composition are given. It is shown that phase transformations in alloys can be investigated by means of the method of internal friction even in cases in which the difference between the atomic diameters of the solvent and the dissolved element is small.

Some Regularities of the Change of Forces of the Inter-Atomic Bond in the Alpha-Solid Solutions of Systems With Electron Compounds, by G. P. Kushta and O. I. Rybailo, pp. 125–126.

Introduction: Changes of forces in the inter-atomic link in alpha-hard solutions of the systems Cu-Zn and Cu-Sn are investigated in the current work. An estimate of changes of forces of the inter-atomic bond in the alloys was carried out by means of x-ray determination of the characteristic temperature of the alloy, according to the method developed by Kurdiumov of exposure at two temperatures: Room temperature and the temperature of liquid air.

SOVIET PHYSICS—TECHNICAL PHYSICS (Zhurnal Tekhnicheskoi Fiziki). Published by American Institute of Physics, New York.

Vol. 5, no. 1, July 1960.

Propagation of Electromagnetic Waves Through Wave Guides Filled With Plasma, by V. E. Golant and A. P. Zhilinskii, pp. 12–21.

Abstract: We consider the propagation of electromagnetic waves through a wave guide filled with a medium of varying conductivity. The analysis is carried out by means of perturbation theory. The phase shift and attenuation introduced by the plasma are calculated to first and second order.

Scattering of Electromagnetic Waves on Free Electrons in a Strong Magnetic Field, by L. E. Gurevich and S. T. Pavlov, pp. 37–39.

Radiative Exchange Between Gray Surfaces, by S. P. Detkov, pp. 86–94.

Abstract: A new form of generalized flux is defined. On the basis of this definition, we formulate a multiple reflection method to obtain well-known expressions for the resultant emissivity of a system consisting of two or three gray surfaces. A general expression is obtained for the resultant emissivity for radiative exchange between any number of gray surfaces which are parts of one sphere. The conclusions are valid both for closed and unclosed surface systems.

Transfer of Ignition Energy to a Gas Mixture From a Discharge Caused by Opening a Circuit, by N. A. Popov, pp. 95–99.

Abstract: It has been established experimentally that, in the electrical discharge produced by opening the contacts of a low current circuit, the absolute temperature of the isothermal plasma which is formed is independent of the discharge power, being approximately 6000 deg. It is shown that, at low discharge temperatures, the spray of incandescent metal from the contacts is the chief factor in the transfer of ignition energy from the discharge to the gas mixture.

Discussion of Results: The results which have been obtained indicate that the high temperature of the gas in the channel of a circuit-opening discharge does not determine the ignition probability of the mixture. The ignition energy is transferred from the discharge to the gas mixture, chiefly by incandescent particles and metal droplets which come from the separating contacts. The larger the discharge current, the greater the energy evolved in the discharge, and the larger the number of incandescent particles per unit time which enter the gas in the region surrounding the discharge gap. This mechanism provides the necessary number of active centers which give rise to the initial chain reaction involved in ignition of the gas mixture. Because the ignition time is determined by the temperature of the heated body and its dimension, each incandescent particle is not necessarily an active center for ignition; only the largest and hottest particles act in this capacity. Moreover, the existence of an active ignition center does not necessarily mean that the combustion reaction will be propagated over the entire volume of the gas mixture, since centers which arise close to the electrodes may be extinguished. However, the possibility of producing even one active center indicates that there is a finite ignition probability. The larger the number of active centers, i.e., the larger the number of incandescent particles of metal which move through the gas, the higher the ignition probability. This then serves to explain the increase in ignition probability with current for a given contact material.

Amplification of Compression Waves in Interaction With a Flame Front, by S. M. Kogarko, pp. 100–108.

Introduction: We present experimental data which have been obtained in a study of the production and amplification of com-

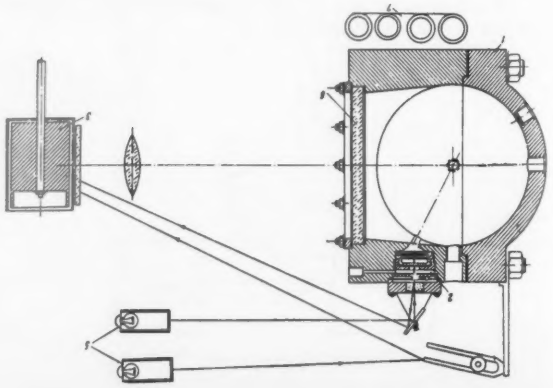

pression waves in the combustion of air-hydrocarbon mixtures in a spherical chamber, and offer a qualitative explanation of the effect.

Summary: 1 It has been shown experimentally that a compression wave is amplified in interacting with a flame front in a combustion mixture of benzene or gasoline and air in a closed volume. The amplification factors have been determined for various mixture compositions.

2 A mechanism is suggested for the amplification of the compression wave which interacts with the reaction zone of the flame front.

3 It has been shown that, in mixtures of aviation gasoline and air (α = 1.1 and α = 1.2), in which no compression wave is recorded in the present experiment, the flame front amplifies an artificially produced compression wave if the amplitude of this wave exceeds some critical value.

Numerical Determination of the Trajectory of a Charged Relativistic Particle in Electric and Magnetic Fields, by N. I. Shtepa, pp. 109–112.

Abstract: The trajectory of a charged relativistic particle in electric and magnetic fields is determined by the use of a numerical extrapolation method, which is used to directly solve the system of second-order differential equations. The recursion relations for determining the accuracy are given. An example of the numerical determination of a trajectory is also given.

SOVIET PHYSICS—JETP (Zhurnal Eksperimental'noi i Teoreticheskoi Fiziki). Published by American Institute of Physics, New York.

Vol. 11, no. 4, Oct. 1960.

Large Cosmic-Ray Intensity Fluctuations in the Stratosphere, by A. N. Charakch'yan, V. F. Tulinov and T. N. Charakhch'yan, pp. 742–746.

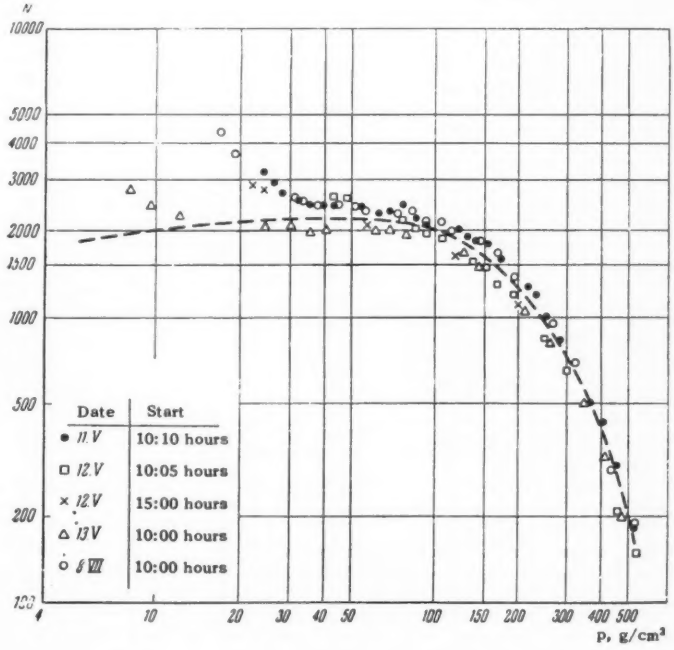

FIG. 1. Variation of the number of pulses per minute N with the atmospheric pressure from data obtained on May 11–13, 1959, and on July 8, 1958 (Moscow time). The dashed line represents a normal intensity, according to the data of May 4, 5, and 7, 1959.

Abstract: The energy spectrum of an abnormally large proton flux, more than 20 times normal, was derived from stratospheric measurements. The exponent of the differential spectrum is equal to 6.0 in the 120–170 Mev energy range. It is suggested that these protons result from corpuscular beams with frozen in magnetic fields, emitted during the solar chromospheric flare on May 10, 1959.

Isentropic Compressibility of Aluminum, Copper, Lead and Iron at High Pressures, by L. V. Al'tshuler, S. B. Kormer, M. I. Brazhnik, L. A. Vladimirov, M. P. Speranskaya and A. I. Funtikov, pp. 766–775.

Abstract: A method is described for measuring the speed of propagation of weak disturbances behind the front of strong shock waves. The existence of two sound velocities, corresponding to the elastic and plastic states of the material, has been detected. With the aid of the techniques which have been developed, the sound velocities and isentropic compression moduli of aluminum, copper, iron and lead have been determined in the pressure range 0.4 to 3.5 $\times$ 10^6 atm. On the basis of the experimental results so obtained, the magnitudes of the thermal energy, the temperatures of the shock compression, and the Gruneisen coefficients have been estimated.

Multiple Production of Jet Particles in Peripheral Collisions, by Yu. A. Romanov and D. S. Chernavskiĭ, pp. 819–824.

Abstract: Peripheral collisions of high energy nucleons ($E_{lab} > 10^{12}$ ev) are considered. The Weizsäcker-Williams method was used to classify the peripheral collisions and to describe the peculiarities of each type of interaction. One of the simplest cases (peripheral single-meson interaction) is calculated by perturbation methods.

Introduction: The interest in the peripheral collisions of high energy nucleons has increased considerably in recent times. This is mainly owing to the fact that stars with anomalous "two hump" angular distributions have been registered and described. These stars can only be interpreted as the result of a peripheral collision with formation of two excited states. The kinematics of such a process have been discussed repeatedly in the literature. At the present moment it seems appropriate to us to consider possible versions of this interaction, assuming that the excitation of the nucleons is caused by the exchange of π mesons.

Thermodynamic Average of Functions of the Displacement of Atoms in a Non-Ideal Crystalline Lattice, by V. I. Peresada, pp. 825–830.

Abstract: It is necessary to obtain the thermodynamic average of the function exp $i(\mathbf{q}\cdot\mathbf{u_R})$, where $\mathbf{q}$ is a constant vector and $\mathbf{R}$ the displacement of the $\mathbf{R}$th atom from its equilibrium position, when one studies the scattering of x-rays or slow neutrons by atomic systems. In the case of small oscillations the thermodynamic average of any function F $((\mathbf{q}\cdot\mathbf{u_R}))$ is uniquely determined by the mean square fluctuation $D(\mathbf{n}, \mathbf{R}, T)$ of the displacement of the $\mathbf{R}$th atom in the direction of the vector $\mathbf{n} = \mathbf{q}/q$ (T is the temperature of the system). A method is given for

the evaluation of the quantity $D(\mathbf{n}, \mathbf{R}, T)$ for an infinite perfect lattice with a finite number of localized defects. We have obtained an asymptotic expression for the function $D(\mathbf{n}, \mathbf{R}, T)$ at large distances from the defects. This asymptotic value is determined by the lattice and the nature of the defects. This method of evaluation can also be applied to other problems.

Resonance Absorption of High Frequency Sound Energy by Semiconductor Current Carriers in a Magnetic Field, by E. P. Pokatilov, pp. 835–839.

Abstract: The absorption coefficient of ultrasound in a semiconductor is estimated with account of quantization of the electron energy in a magnetic field.

Introduction: In a number of papers published in recent years, the results of experimental and theoretical investigations of the absorption of ultrasonic energy by current carriers in a magnetic field has been reported for the case of ultrasonic frequencies ω that are less than or equal to the collision frequency of the electrons $1/\tau$ (τ is the relaxation time). The case of higher ultrasonic frequencies, for which the inequality

$$\omega \geqslant \omega_0 > 1/\tau \qquad [1]$$

where ω_0 = cyclotron frequency of the electron, is satisfied, has been investigated theoretically by the author. This inequality is the inverse of that used in papers mentioned. However, the calculation was made in the classical approximation $\lambda_s > \lambda_{el}$ for the special case $\kappa_z = O$ (κ_z is the component of the wave vector of the ultrasonic wave in the direction of the magnetic field).

Quantum-Mechanical Calculations of the Pressure in Solids, by G. M. Gandel'man and E. S. Pavlovskiĭ, pp. 851–855.

Abstract: A quantum-mechanical formula which is a generalization of the virial theorem is derived, for the pressure in a solid at zero temperature. A more detailed examination is made of the application of this formula in the approximation of spherical cells.

Ionization of Gases by Negative Ions, by Ya. M. Fogel', A. G. Koval' and Yu. Z. Levchenko, pp. 760–765.

Abstract: The total cross sections for positive ion formation in collisions of H^- ions (10 to 50 kev) with the atoms He, Ne, Ar, Kr and Xe and the molecules H_2, N_2 and O_2 have been measured; the same cross sections have been measured for O^- ions with the same energy in collisions with inert gas atoms and H_2 and O_2. The ionization cross sections for H^- and H^+ are compared.

Coherent Electron Radiation in a Synchrotron. III, by M. S. Rabinovich and L. V. Iogansen, pp. 856–858.

Abstract: The electromagnetic interaction of electrons in a synchrotron is considered, with the shielding effect of the chamber walls taken into account for bunches of arbitrary shape. The effect of these forces on the phase motion of the electrons and on the dimensions of a bunch are evaluated.

Relativistic Transport Equation for a Plasma. II, by Yu. L. Klimontovich, pp. 876–882.

Abstract: We use the chain of equations for the relativistic distribution functions which we obtained earlier to derive a relativistic transport equation in second approximation for a plasma. We derive first a transport equation in which only the retarded interaction of charged particles is taken into account. This equation is in a particular case the same as the one obtained by Belyaev and Budker. We consider a relativistic Fokker-Planck equation for a plasma in which the retarded interaction between charged particles and the excitation of plasma oscillations by nonequilibrium charged particles is taken into account.

Structure of the S Matrix in the Theory of Elastic and Inelastic Scattering of Nonrelativistic Particles, by Yu. V. Tsekhmistrenko, pp. 894–898.

Abstract: Integral relations for the components of the S matrix describing a nuclear reaction with two channels (one channel is the elastic scattering of a nonrelativistic particle and the other is inelastic scattering with excitation of the nucleus) are derived from general principles of causality, unitarity, and symmetry, and the analytic properties of some components of the S matrix are established. For simplicity the treatment is confined to the case of spherically symmetrical scattering. In agreement with the results of Wigner and of Baz', the excitation function of the elastic scattering has a break at the threshold of the inelastic process. The form of the excitation function of the inelastic process near threshold is found in the general case.

Summary: We have succeeded in establishing with mathematical rigor the structure of the S functions of spherically symmetrical elastic scattering of a nonrelativistic particle by a nucleus of finite size when this nucleus has one excited state. In so doing we have used only the physical requirements of conservation of the total number of particles, of symmetry, and of completeness of the system of wave functions outside the nucleus. It has been found that because their arguments are multiple-valued these S functions are not analytic in the whole plane.

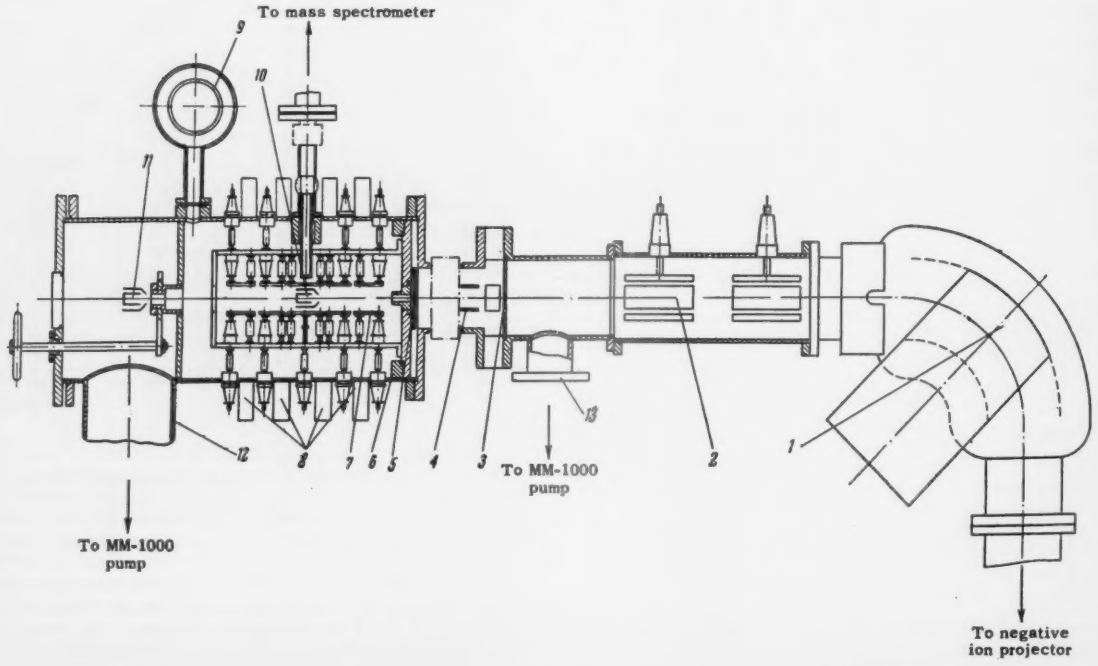

(Continued from page 676)

metric velocity and density profiles, one can readily verify that the error will rarely exceed 20%. The effect of a mismatch in the pressure at the exit of the device leads to the computation of a beam power efficiency greater than the true efficiency. To achieve complete expansion in a space engine would require that the flow be expanded to zero pressure. It is unlikely that this is ever the case. For certain low thrust devices the error that arises in computing the beam power efficiency by Eq. 2, in the presence of a pressure mismatch, can produce an error in excess of 20%. As an example: If the flow is expanded to an exit pressure of 1 mm Hg abs, a 2-in. diameter thrust nozzle would contribute a pressure force of about 27,000 dynes (0.06 lb.). For some engines this is of the order of the thrust obtained from the momentum flux. In these cases the beam power efficiency computed by Eq. 2 leads to larger efficiencies than the correct efficiency; the error can be appreciable. However, there are situations where the contribution from the pressure is truly negligible.

Eq. 2 does not present the general case of the ratio of beam power to the input power. Indeed, it can be shown to be the ratio[2] of the actual thrust to the maximum ideal thrust that can be had from a given power input and mass flow throughput. This can be verified by noting that for maximum propulsive work, the exhaust pressure should match the external pressure and the exiting flow should be uniform for a steady flow, or a square wave function respect to time for a pulsed periodic device (2).

Using the square root of Eq. 2 for the evaluation and comparisons of electrical propulsion systems, as well as chemical systems, is physically more meaningful than the use of Eq. 2 to approximate the beam power efficiency. The square root of Eq. 2 can be used to examine the effectiveness of any propulsive device in producing thrust, and has the advantage of being independent of any assumptions regarding the flow leaving the device.

References

1 Page, R. J., Buhler, R. D., Stoner, W. A., and Masser, P. J., "Arc Plasma Thrustor Studies," Presented at the ARS 15th Annual Meeting, Wash., D. C., Dec. 5–8, 1960.

2 Foa, J. V., "Intermittent Jets," (Section F, Jet Propulsion Engines) *High Speed Aerodynamics and Jet Propulsion*, vol. XII, Princeton Univ. Press, 1959.

Book Notes

Progress in Operations Research, Volume 1, edited by Russell L. Ackoff (Professor and Director of the Operations Research Group, Case Institute of Technology), John Wiley & Sons, Inc., N. Y., 1961, 505 pp. $11.50.

Contents: Separate chapters contributed by different authors. 1. The Meaning, Scope, and Methods of Operations Research; 2. Decision and Value Theory; 3. A Survey of Inventory Theory from the Operations Research Viewpoint; 4. Mathematical Programming; 5. Dynamic Programming; 6. Dynamics of Operational Systems: Markov and Queuing Processes; 7. Sequencing Theory; 8. Replacement Theory; 9. The Theory and Application of Simulation in Operations Research; 10. Military Gaming; 11. Progress in Operations Research: The Challenge of the Future.

This is the first in a series of review volumes which will inventory mathematical techniques and research methods available to operations researchers. These review volumes are designed to serve as basic reference works. The articles to be included in the various volumes will be contributed, upon editorial invitation, by leading experts in the field.

Psychophysiological Aspects of Space Flight, edited by Bernard E. Flaherty, (Lt. Col., USAF, Head of the Department of Neuropsychiatry, School of Aviation Medicine, Aerospace Medical Center, Brooks Air Force Base, Texas), Columbia University Press, N. Y., 1961, 392 pp. $10.

Contents: Part 1, Technical Background and Experience (including a discussion of Project Mercury); Part 2, Critical Problem Areas; Part 3, Problems of Human Reliability; Part 4, Special Techniques of Control. (A total of 31 contributed papers.)

The papers in this volume define the psychophysiological problems in space flight and help determine where future research in these problems should be concentrated. Leading medical, psychological, psychiatric, chemical and engineering scientists summarize their recent work in papers presented at an important symposium sponsored by the School of Aviation Medicine, USAF Aerospace Medical Center, and held late in May 1960.

Progress in Aeronautical Sciences, Volume 1, edited by Antonio Ferri (Professor of Aerodynamics, Polytechnic Institute of Brooklyn), D. Küchemann (Royal Aircraft Establishment, England), and L. H. G. Sterne (Training Center for Experimental Aerodynamics, Belgium), Pergamon Press, N. Y., 1961, 280 pp. $12.

Contents: Papers on principles of aerodynamic design of blade profiles for turbomachines, boundary layers behind shock waves, ionized gasdynamics, structural problems, and sonic bangs. Authors include E. C. Maskell, Robert Legendre, M. Fenain, E. Becker, F. A. Goldsworthy, D. Williams, C. H. E. Warren and D. G. Randall.

This volume is the first in a new series directed specifically to the field of aeronautical sciences, but excluding propulsion and combustion. The intention is to publish annually in one volume a number of specially commissioned review articles which will provide the specialist reader with an orderly but concise survey of recent work and so relieve him of the need for excessive recourse to original papers.

The books listed here are those recently received by the ARS from various publishers who wish to announce their current offerings in the field of astronautics. The order of listing does not necessarily indicate the editors' opinion of their relative importance or competence.

Science in Space, edited by Lloyd V. Berkner (Chairman, Space Science Board, National Academy of Sciences) and Hugh Odishaw (Executive Director, Space Science Board, National Academy of Sciences), McGraw-Hill Book Company, Inc., 1961, 458 pp. $7.

Contents: 20 contributed papers on subjects such as: The results of experiments in space, the nature of gravitation, aspects of geodesy, meteorology, satellites and the upper atmosphere, the moon and the planets, fields and particles in space, the stars, and the biological sciences and space research.

This volume presents a review of the new scientific opportunities offered by space science. It is directed to research workers whose scientific activities may be influenced by the new opportunities for experiment afforded by growing access to space. This volume may also be of interest to general readers who are concerned about the national space effort. The material of this volume has been contributed from a broad spectrum of American and foreign scientists. All members of the Space Science Board and of its committees have contributed through discussion, criticism and editorial comment.

Human Factors in Jet and Space Travel, A Medical-Psychological Analysis, edited by S. B. Sells (Professor of Psychology, Texas Christian University) and Charles A. Berry (Lt. Col., USAF MC, Chief, Flight Medicine Branch, Aerospace Medicine Div., Office of the Surgeon General), The Ronald Press Company, N. Y., 1961, 386 pp. $12.

Contents: A series of 14 chapters contributed by different authors: 1. Medical Aspects of Jet and Space Travel; 2. The Natural Environment and the Environment of Flight; 3. Radiobiology and the Environment of Flight; 4. Basic Aspects of Skilled Performance; 5. Human Operator Performance Under Non-Normal Environmental Operating Conditions; 6. Group Behavior Problems in Flight; 7. Human Qualifications for and Reactions to Jet Flight; 8. Human Requirements for Space Travel; 9. Preventive Medicine in Jet and Space Flight; 10. Aircraft Accidents and Flight Safety; 11. Human Factors Related to Jet Aircraft; 12. The Engineered Environment of the Space Vehicle; 13. Operational Aspects of Space Flight; 14. Speculations on Space and Human Destiny.

This book has been prepared to meet the need for up-to-date information in systematic form on the human problems of high-performance flight. A second purpose is to provide physicians with a reference book on aviation medicine and the related human-factors problems. Third, the treatment of most topics should be of interest to students who desire information concerning scientific careers in specialties related to aviation and the approaching era of space travel.

Nuclear Propulsion, edited by M. W. Thring, Butterworth Inc., London, 1960, 300 pp. $9.50.

Chapters: 1. The Structure of the Nucleus and Nuclear Reactions; 2. Reactor Physics; 3. The Thermodynamics of Jet and Rocket Propulsion: The Application of Nuclear Power; 4. The Nuclear-Powered Closed-Cycle Gas Turbine; 5. The Design of Nuclear Reactors; 6. Metallurgical Problems in Nuclear Reactors; 7. Heat Transfer Problems in Nuclear Engineering; 8. Reactor Control and Instrumentation; 9. Marine Developments in the Nuclear Age; 10. Nuclear Marine Propulsion; 11. Some Observations on the Application of Nuclear Power to Aircraft; 12. Progress in Nuclear Propulsion; 13. The Limitations of Chemical Rockets and the Possibility of the Nuclear Rocket; 14. The Preparation, Storage and Properties of Working Fluids; 15. Potential Uses of Ceramics in Nuclear Reactors; 16. Medical and Biological Aspects of Life in Sealed Cabins.

The 16 chapters in this book have been written by individual contributors who are specialists in the respective fields. The book is of an introductory nature, generally elementary in each area, although as fully mathematical as necessary to describe the essential principles. Its value rests largely on its survey character.

Kinetics, Equilibria and Performance of High Temperature Systems, edited by Gilbert S. Bahn (The Marquardt Corporation) and Edward E. Zukoski (California Institute of Technology), Butterworth Inc., Washington, D. C., 1960, 255 pp. $12.50.

Contents: This book contains 33 papers, based on original research, which were contributed at the First Conference of the Western States Section of the Combustion Institute, in Los Angeles, Calif., Nov. 2–5, 1959.

Space Trajectories, edited by the Technical Staff, Research Div., Radiation Inc., Academic Press, N. Y., 1960, 298 pp. $12.

Contents: A series of 21 original papers contributed by the participants in a symposium sponsored by the American Astronautical Society, the Advanced Research Projects Agency, and Radiation Inc., held at Orlando, Fla., Dec. 14–15, 1959. The subjects covered include: Military Space—Taking the High Ground; Satellite and Probe Orbit Determination, Past, Present and Future; General Survey of the Field; Astrodynamics; Trajectory Constants; Trajectory Computation and Optimization; Trajectory Computation in Systems Design; Computer Programs for Space Missions; Space-Borne Computer Design; Space Maneuvers; Space Maneuvers—Optimization; Re-Entry Trajectories and Problems of Hypersonic Flow; Orbit Determination from Single Pass Doppler Observations; Space Trajectory Instrumentation, Present and Future; Computer Programming Methods.

Space Research, Proceedings of the First International Space Science Symposium, Nice, Jan. 11–16, 1960, edited by Hilde Kallmann Bijl, North-Holland Publishing Company, Amsterdam (U. S. distributors: Interscience Publishers, Inc., N. Y.), 1960, 1195 pp. $24.

Contents: A comprehensive set of 98 original papers contributed internationally to the first symposium sponsored by the Committee on Space Research (COSPAR) in 1960. The symposium was divided into seven parts as follows: 1. The Earth's Atmosphere; 2. The Ionosphere; 3. Tracking and Telemetering; 4. Solar Radiation; 5. Cosmic Radiation; 6. Interplanetary Dust; 7. The Moon and the Planets.

This series of authoritative papers is derived from the results of research achieved in the two years since the first Sputnik was launched on Oct. 4, 1957. The overall impression is that of a magnificent advance in many scientific fields of practical and theoretical importance. COSPAR was founded by the International Council of Scientific Unions (ICSU) at the end of 1958 to further on an international scale the progress of all kinds of scientific investigations which are carried out with the use of rockets or rocket propelled vehicles.

Advances in Space Science, Vol. 2, edited by Frederick I. Ordway, III (George C. Marshall Space Flight Center, NASA, Huntsville, Ala.), Academic Press, N. Y., 1960, 450 pp. $13.

Contents: Experimental Physics Using Space Vehicles, by Charles P. Sonett; Tracking Artificial Satellites and Space Vehicles, by Karl G. Henize; Materials in Space, by Frederick L. Bagby; Plasma Propulsion Devices, by Morton Camac; Electrostatic Propulsion Systems for Space Vehicles, by E. Stuhlinger and R. N. Seitz; Attitude Control of Satellites and Space Vehicles, by R. E. Roberson.

This volume contains a series of specially invited articles offering reviews and analyses of topics of importance in astronautics.

Digital Applications of Magnetic Devices, edited by Albert J. Meyerhoff, Senior Editor, and George H. Barnes, Stanley B. Disson and George E. Lund, Associate Editors, John Wiley & Sons, Inc., N. Y., 1960, 604 pp. $14.

Contents: Comprised of individual contributions by various authors, the book is divided into the following seven parts: 1. Fundamentals; 2. Parallel Magnetic Pulse Amplifiers; 3. Delay Parallel Magnetic Pulse Amplifiers; 4. Series Magnetic Pulse Amplifiers; 5. Memories; 6. Transistor-Magnetic Pulse Amplifiers; 7. Other Techniques; Appendix—Characteristics of Components.

The contributors to this book were drawn from the Burroughs Corporation Research Center, Remington Rand Univac Division of Sperry Rand Corporation, DI/AN Controls, Inc., Westinghouse Electric Corporation, Stanford Research Institute, and Beckman Instruments, Inc. The book was jointly supported by the Office of Naval Research and the Burroughs Corporation. Since no comprehensive text on digital magnetic devices was in existence, it was felt by both Burroughs and the Navy that this book would make a useful contribution.

Ballistic Missile and Space Technology, edited by Donald P. LeGalley (Space Technology Laboratories, Inc.); *a set of four volumes comprising the Proceedings of the Fifth Symposium on Ballistic Missile and Space Technology, held in Los Angeles, Aug. 29–31, 1960; the symposium was sponsored by Headquarters, Air Force Ballistic Missile Division, Space Technology Laboratories, Inc., and Aerospace Corporation*; Academic Press, N. Y., 1960, each volume about 440 pp. Each volume $9.

Vol. 1, Bioastronautics and Electronics, and Invited Addresses.

Contents: 23 contributed research papers dealing with: Bioastronautics; inertial guidance and control; space communications; computers; telemetry; computing and data reduction.

Vol. 2, Propulsion and Auxiliary Power Systems.

Contents: A series of 15 contributed research papers dealing with: Propellant technology; ion propulsion; heat transfer and materials; auxiliary power systems.

Vol. 3, Guidance, Navigation, Tracking, and Space Physics.

Contents: A series of 16 contributed research papers dealing with: Guidance and navigation; tracking; space trajectories; space physics.

Vol. 4, Re-Entry and Vehicle Design.

Contents: A series of 15 contributed research papers dealing with: Re-entry vehicle materials; advanced re-entry problems; re-entry engineering mechanics; vehicle design—performance analysis, system description and operational considerations.

Comparative Effects of Radiation, edited by Milton Burton (Chemistry Department and Radiation Laboratory, University of Notre Dame), John S. Kirby-Smith (Biology Div., Oak Ridge National Laboratory) and John L. Magee (Chemistry Department and Radiation Laboratory, University of Notre Dame), John Wiley & Sons, Inc., N. Y., 1960, 426 pp. $8.50.

Contents: 15 contributed chapters by different authors on the following subjects: Contrasts of initial biological effects resultant from different types of radiation; collective effects in absorption of energy from ionizing radiation; control of plant growth by phytochrome; the mechanism of photoreactivation; ultraviolet radiation effects—molecular photochemistry; structural aspects of radiation effects on nucleic acids and related substances; elementary processes in action of ionizing radiation; radiation chemistry of water; direct and indirect effects on chemical systems; direct and indirect initial effects on biological systems; recent advances in the study of irradiated polymers; radiation effects on monolayers considered from the biological point of view; excitation transfer; energy-transfer processes; summary.

This volume represents some of the latest thought by radiation biologists, chemists and physicists from all over the world. It constitutes the proceedings of a symposium on the comparative effects of infrared, visible, ultraviolet and high-energy radiations in biology, chemistry and physics, held in San Juan at the University of Puerto Rico, Feb. 15–19, 1960, sponsored by the National Academy of Sciences–National Research Council. The subject matter deals with the initial chemical and physical steps in the action of radiation—in particular, those steps leading ultimately to biological effects.

International Dictionary of Physics and Electronics, New Second Edition, edited by Walter C. Michels, Editor-in-Chief (Bryn Mawr College), Rosalie C. Hoyt (Bryn Mawr College), Joseph C. May (Yale University) and John R. Pruett (Bryn Mawr College), D. Van Nostrand Company, Inc., Princeton, N. J., 1961, 1355 pp. $27.85.

Contents: This dictionary covers the following subject areas: Units and dimensions; general principles; mechanics; states of matter—gases, liquids, crystals, glasses, plasma; heat and thermodynamics; statistical mechanics; acoustics; optics; electricity; electronics; meteorology; atomics and nuclear physics; mathematical physics; quantum mechanics; relativity; magnetohydrodynamics and thermonuclear research. It also includes essential multilingual indices in German, Russian, French and Spanish.

The book in its first edition has been found useful by professional physicists, chemists, mathematicians, engineers, business executives and secondary school teachers.

Technical Literature Digest

M. H. Smith, *Associate Editor*
The James Forrestal Research Center Princeton University

Propulsion and Power (Combustion Systems)

Performance Charts for Multistage Rocket Boosters, by John S. MacKay and Richard J. Weber, *NASA TN* D-582, Jan. 1961, 90 pp.

Combined Effect of Contraction Ratio and Chamber Pressure on the Performance of a Gaseous-Hydrogen-Liquid-Oxygen Combustor for a Given Propellant Weight Flow and Oxidant-Fuel Ratio, by Martin Hersch, *NASA TN* D-129, Feb. 1961, 13 pp.

EDITOR'S NOTE: Contributions from Professors E. R. G. Eckert, E. M. Sparrow and W. E. Ibele of the Heat Transfer Laboratory, University of Minnesota, are gratefully acknowledged.

The Slotted-Tube Design, by Max W. Stone, *Rohm & Haas, Redstone Arsenal Res. Div. Rep.* S-27, Dec. 1960, 17 pp.

Propulsion and Power (Non-Combustion)

Solar Power in Space, by Thomas Gold, ASTRONAUTICS, vol. 6, no. 2, Feb. 1961, pp. 34–35.

A Radioisotope Propulsion System, by W. Short and C. Sabin, *Brit. Interplan. Soc. J.*, vol. 17, no. 12, Nov.–Dec. 1960, pp. 453–458.

Influence of Tensor Conductivity on Current Distribution in a MHD Generator, by H. Hurwitz Jr., R. W. Kilb and G. W. Sutton, *J. Appl. Phys.*, vol. 32, no. 2, Feb. 1961, pp. 205–216.

Physical Principles of Magnetohydrodynamic Power Generation, by Richard J. Rosa, *Phys. Fluids*, vol. 4, no. 2, Feb. 1961, pp. 182–194.

Charged-Colloid Propulsion System, by R. B. Edmonson, O. B. Kretschmer and L. B. Becker, *Aerojet-General Corp. Rep.* no. 0290-01-1, Nov. 1960, 9 pp.

Gaseous Fission Reactors for Spacecraft Propulsion, by Robert V. Maghreblian, *Calif. Inst. of Tech., Jet Propulsion Lab Tech. Rep.* 32-42, July 1960, 12 pp.

Research on High Intensity Ionic Jets, by Gordon L. Cann and Adriano C Ducati, *Plasmadyne Corp. Final Tech. Rep.* P-Fr 109-54 (*AFOSR TR* 59-167) Nov. 1959, 36 pp. (*ASTIA AD* 229,902).

Experimental Study of a Single-Coil Induced-Electromotive-Force Plasma Accelerator, by Clarence W. Matthews and

William F. Cuddihy, *NASA TN* D-639, Jan. 1961, 24 pp.

Propellants and Combustion

Additive Effects in Solid Propellant Burning, by H. Silla, H. Burwasser and H. F. Calcote, *AeroChem. Res. Lab., Inc., Tech. Pub.* 18, May 1960, 37 pp.

Selection of High Performing Propellants for Torpedoes, by Leonard Greiner, ARS JOURNAL, vol. 30, no. 12, Dec. 1960, pp. 1161–1163.

The Influence of Secondary Atmospheric Moisture upon Carbon Monoxide Flames, by D. J. Seery and H. B. Palmer, *Combustion and Flame,* vol. 4, no. 4, Dec. 1960, pp. 289–292.

Ignition of Cellulosic Materials by Radiation, by D. L. Simms, *Combustion and Flame,* vol. 4, no. 4, Dec. 1960, pp. 293–300.

Gaseous Explosions in Vented Ducts, by D. J. Rasbash and Z. W. Rogowski, *Combustion and Flame,* vol. 4, no. 4, Dec. 1960, pp. 301–312.

Structure and Propagation of Laminar Flames Near a Heat Sink, by Tze-Ning Chen and Tau-Yi Toong, *Combustion and Flame,* vol. 4, no. 4, Dec. 1960, pp. 313–324.

A Theory of Flame Extinction Limits, by A. L. Beriad and C. H. Yang, *Combustion and Flame,* vol. 4, no. 4, Dec. 1960, pp. 325–334.

On the Development of Detonation with Pre-ignition, by A. K. Oppenheim, R. A. Stern and P. A. Urtiew, *Combustion and Flame,* vol. 4, no. 4, Dec. 1960, pp. 335–342.

The Ignition Delay Concept for Recessed Flameholders, by L. A. Povinelli, *Combustion and Flame,* vol. 4, no. 4, Dec. 1960, pp. 355–356.

The Theory of Flame Propagation in Branched and Unbranched Chain Systems, by L. A. Lovachev, *Combustion and Flame,* vol. 4, no. 4, Dec. 1960, p. 357.

Kinetics of Combustion of Cyanogen and the Burning Velocities of Cyanogen-Oxygen-Nitrogen Mixtures, by Emile Rutner, Karl Scheller and William H. McLain Jr., *J. Phys. Chem.,* vol. 64, no. 12, Dec. 1960, pp. 1891–1913.

Existence of Detonations for Small Values of the Rate Parameter, by W. W. Wood, *Phys. Fluids,* vol. 4, no. 1, Jan. 1961, p. 46.

Slowly Reacting Gas Mixture in a Heat Conductivity Cell, by Don Secrest and Joseph O. Hirschfelder, *Phys. Fluids,* vol. 4, no. 1, Jan. 1961, pp. 61–73.

Kinetics of the Thermal Decomposition of Propylene and of Propylene-Inhibited Hydrocarbon Decompositions, by K. J. Laidler and B. W. Wojciechowski, *Royal Soc. London, Proc. (Series A, Math. Phys. Sciences),* vol. 259, no. 1297, Dec. 6, 1960, pp. 257–266.

The Density of Liquid Oxygen on the Saturation Curve, by D. L. Timrot and V. P. Borisoglebskii, *Soviet Phys.: JETP,* vol. 11, no. 6, Dec. 1960, pp. 1248–1250.

Conference on Aviation and Astronautics, 2nd, February 9–10, 1960, Tel-Aviv and Haifa, Proceedings (*Reprint from Bull. Res. Council of Israel,* vol. 8c, Feb. 1960, no. 1), 57 pp.

> **Some Developments of the End Burning Charge,** by A. Yaron, pp. 47–53.

Aerodynamics of Flame Stabilization, by H. H. Chiu, Final Tech. Rep. for the Period Nov. 15, 1955, to Sept. 30, 1960, *Princeton Univ., Dept. of Aeron. Engng., Rep.* 422, 13 pp.

Research on the Hazard Classification of New Liquid Rocket Propellants, by *North Amer. Aviation, Inc., Rocketdyne, Qtly. Progress Rep.* no. R-2452-1, (period ending April 30, 1960), 67 pp.

The Shock Initiation of Detonation in Liquid Explosives, by William G. Gey and Karl Kinaga, *Nav. Ord. Test Station, China Lake, Calif.,* 1960, 9 pp., 6 figs.

Solution for Complex Systems of Chemical Reaction Kinetics, Part I, Supplement I—An Irreversible Unimolecular Reaction, by Daniel D. Konowalow, James E. Blair, Joseph O. Hirschfelder and Farrington Daniels, *Wright Air Development Command, TN* 59-243, Part I, Suppl. I, Aug. 1960, 27 pp.

Semi-Empirical Fit of CO_2 Emissivities, by L. D. Gray, *Calif. Inst. of Tech., Daniel and Florence Guggenheim Jet Propulsion Center, Tech. Rep.* 34, Oct. 1960, 9 pp.

Rates of Catalytic Decomposition of Liquid Hydrogen Peroxide on Metal Surfaces, by Charles N. Satterfield and Puran K. Sarda, *Mass. Inst. of Tech., Dept. Chem. Engng., Rep.* no. 58, Nov. 1960, 19 pp.

Vapor Pressures and Related Thermodynamic Properties of the Isotopic Nitric Oxide Molecules, by Jacob Bigeleisen, *J. Chem. Phys.* vol. 33, no. 6, Dec. 1960, pp. 1775–1777.

The Effects of Surface Condition on the Mechanical Properties of Lithium Fluoride Crystals, by A. R. C. Westwood, *Philosophical Mag.,* vol. 5, no. 58, Oct. 1960, pp. 981–990.

Selected Topics on Ballistics, Cranz Centenary Colloquium, Univ. of Freiburg, 1958, Wilbur C. Nelson, ed., N. Y., Pergamon Press, for North Atlantic Treaty Organization, Advisory Group of Aeron. Res. and Dev. (AGARD), 1959, 280 pp.

> **Forty Years of British Internal Ballistic Research,** by J. B. Goode, pp. 213–223.

Heats of Formation of Lithium Perchlorate, Ammonium Perchlorate and Sodium Perchlorate, by Alexis A. Gilliland and Walter H. Johnson, *J. Res. Nat. Bur. Standards, (A. Phys. Chem.)* vol. 65A, no. 1, Jan.–Feb. 1961, pp. 66–70.

Low-Density Shock Tube for Chemical Kinetics Studies, by Shao-Chi Lin and Walter I. Fyfe, *Phys. Fluids,* vol. 4, no. 2, Feb. 1961, pp. 238–249.

Effect of Chemical Reaction Order on Flame Propagation, by Joseph O. Hirschfelder, *Phys. Fluids,* vol. 4, no. 2, Feb. 1961, pp. 253–259.

Ignition Temperature Approximation for Bimolecular Detonations, by J. O. Hirschfelder, C. F. Curtis and M. P. Barnett, *Phys. Fluids,* vol. 4, no. 2, Feb. 1961, pp. 260–261.

Detonation Velocity of Pressed TNT, by M. J. Urizar, E. James Jr. and L. C. Smith, *Phys. Fluids,* vol. 4, no. 2, Feb. 1961, pp. 262–264.

Experimental Study of Combustion of Two-Phase Mixtures in Turbulent Flow, by B. P. Lebedev and V. G. Tikhamirov, *Soviet Phys., Tech. Phys.,* vol. 5, no. 8, Feb. 1961, pp. 929–935.

Dynamic and Thermal Non-equilibrium in Two-Phase Flow in Rocket Nozzles, by T. E. Stonecypher, *Rohm & Haas Co., Redstone Arsenal Res. Div., Rep.* no. P-60-17, (Quart. Prog. Rep. on Engng. Res.) June 15, 1960–Sept. 15, 1960, 12 pp., 12 figs.

Preparation and Analysis of Petrin Acrylate, Poly-Petrin-Acrylate, and PEDN Diacrylate, by Delbert J. Cragle, *Picatinny Arsenal, Feltman Res. Labs. Tech. Rep.* FRL-TR-15, Jan. 1961, 19 pp.

Diffusional Transport of Atomic Hydrogen through Molecular Hydrogen at Elevated Temperatures, by Henry Wise, *Project Squid, Tech. Rep.* SRI-9-P, Dec. 1960, 12 pp.

The Effect of Repeated Stressing on the Behavior of Lithium Fluoride Crystals, by Arthur J. McEvily Jr., *NASA Tech. Rep.* R-91, 1961, 31 pp., 9 figs.

The Structure of Boron Oxide and Simple Borates, by J. D. Mackenzie, *General Electric Res. Lab.* (*ARL Tech. Note* 60-130), Aug. 1960, 31 pp.

Theory of the Fluid Oscillations in a Circular Cylindrical Ring Tank Partially Filled with Liquid, by Helmut F. Bauer, *NASA TN* D-557, Dec. 1960, 124 pp.

Research in Hybrid Combustion, Summary Report, by R. Bell and K. H. Mueller, *N. Amer. Aviation, Rocketdyne* R-2794, Jan. 1961, 41 pp.

Initiation of Explosive by Internal Heating, by G. M. Muller and D. Bernstein, *Stanford Res. Inst., Poulter Labs. Tech. Rep.* 007-60, Aug. 1960, 25 pp.

Tables of Properties of Some Oblique Deflagrations in Supersonic Flow, by Henry W. Woolard, *Johns Hopkins Univ., Appl. Phys. Lab.* T.G.-382, Sept. 1960, 30 pp.

Light Scattering and Transmission Properties of Sprays, by Richard A. Dobbins, *Princeton Univ., Dept. Aeron. Engng. Rep.* no. 530, Nov. 1960, 134 pp., 69 figs., (Thesis, Ph.D.) (*AFOSR TN* 61-17.)

A Co-volume Equation of State of Gases at Detonation Conditions, by P. A. Longwell, *Navy Dept. Bur. Naval Weapons, NAVWEPS Rep.* 7565, Sept. 1960, 14 pp.

JANAF Interim Thermochemical Tables, Vol. 1 and 2, by T. E. Dergazarian, N. J. Dumont, L. A. du Plessis, W. E. Hatton, S. Levine, R. A. McDonald, F. L. Cletting, H. Prophet, G. C. Sinke, D. R. Stull and C. J. Thompson, *Thermal Lab., Dow Chemical Co., (Joint Army-Navy-Air Force Thermochemical Panel),* Dec. 1960, 2 vols., loose-leaf.

Ignition Studies, Part VI—The Effect of Chemical Structure on the Spontaneous Ignition of Hydrocarbons, by W. A. Affens, J. E. Johnson and H. W. Carhart, *Naval Res. Lab. Rep.* 5566, Nov. 1960, 29 pp.

Fundamentals of Liquid Propellant Sensitivity, by T. A. Erikson and E. L. Grove, *Illinois Inst. Tech., Armour Res. Foundation, ARF* 3180-7 (quart. no. 2) Jan. 1961, 23 pp.

Standard Laboratory Procedures for Sensitivity Brisance, and Stability of Explosives, by Arthur J. Clear, *Picatinny Arsenal, Dover, N. J. Feltman Res. Lab. Tech. Rep.* FRI-TR-25, Jan. 1961, 43 pp.

Materials and Structures

Application of 2219 Aluminum Alloy to Missile Pressure-Vessel Fabrication, by Clayton H. Crane and Whitney G. Smith, *Welding J.,* vol. 40, no. 1, Jan. 1961, pp. 33–40.

Steady-State Thermal Stresses in an Elastic Cone, by R. Muki and E. Sternberg, *Zeitschrift für Angewandte Math. Physik,* vol. 11, no. 6, Nov. 25, 1960, pp. 471–496.

Bibliography on the High Temperature Chemistry and Physics of Materials in the Condensed State, Covering the Literature of Australia, Belgium, France, Japan, Scandinavia, United Kingdom, United

States, and U.S.S.R. for the Period July, August, and September 1960, by J. J. Diamond, G. Hagg, M. Foex, E. R. McCartney and H. Mii, *Internat. Union of Pure and Appl. Chem. Commission on High Temperatures and Refractories, Sub-Commission on Condensed States,* 1960, 34 pp.

Oxidation Behavior of Binary Niobium Alloys, by Charles A. Barrett and James L. Corey, *NASA TN* D-8283, Nov. 1960, 27 pp.

The Quasi-Cylinder of Specified Thickness and Shell Loading in Supersonic Flow, by H. Portnoy, *Aero. Quart.*, vol. 9, part 4, Nov. 1960, pp. 387–395.

Graphite: A Future Structural Material, by A. J. Kennedy, *Aero. Quart.*, vol. 9, part 4, Nov. 1960, pp. 309–332.

Measurements on the Permeability of Hydrogen from H_2 and H_2O Through Steel Stainless Steel and Aluminum, by F. Boeschoten, W. van Egmond and H. M. J. Kinderdijk, *Appl. Scientific Res.*, Section B, vol. 8, no. 4, 1960, pp. 378–386.

Plastic Analysis of Circular Conical Shells, by P. G. Hodge Jr., *J. Appl. Mech. (ASME Trans., Series E)*, vol. 27, no. 4, Dec. 1960, 696–700.

Mylar Builds a Plastic Satelloon (Echo I), *Plastics Industry,* vol. 18, no. 9, Sept.–Oct. 1960, pp. 14–15, 44.

Investigation of the Protective Ultraviolet Absorbers in a Space Environment, I. Rate of Evaporation and Vapor Pressure Studies, by R. G. Schmitt and R. C. Hirt, *J. Polymer Sci.*, vol. 65, no. 145, July 1960, pp. 35–47.

Elastic Thermal Stresses in Delta Wings, by H. Parkus, *Vienna. Inst. Tech., (AFOSR TR* 60-140), July 1960, 51 pp., 49 figs.

An Analysis of Exact and Approximate Equations for the Temperature Distribution in an Insulated Thick Skin Subjected to Aerodynamic Heating, by Robert S. Harris Jr. and John R. Davidson, *NASA TN* D-519, Jan. 1961, 33 pp.

Manned Space Stations Symposium, Los Angeles, April 20–22, 1960, N. Y. Inst. Aeron. Sciences, 1960, 322 pp.

Structural Implications of the Ionizing Radiation in Space, by Norris F. Dow, pp. 128–136.

The Role of Damping in Space Structures, by C. W. Coale, pp. 197–201.

A Structural Approach to the Thermal Control of Space Vehicles, by Peter E. Glaser, pp. 202–206.

A Versatile Metal to Dielectric Seal, by P. C. Conder, H. Foster and H. A. H. Boot, *S.E.R.L. J. (Gt. Brit. Services Electronics Res. Lab.)*, vol. 10, no 4, Sept. 1960, pp. 258–262.

Symposium on the Theory of Thin Elastic Shells, Technological University, Delft, 1957, Proceedings, the Theory of Thin Elastic Shells, W. T. Koiter, ed., sponsored by the *Internat. Union of Theoretical and Appl. Mech.*, N. Y., Intersci. Pub., 1960, 496 pp.

A Consistent First Approximation in the General Theory of Thin Elastic Shells, by W. T. Koiter, pp. 12–33.

On a Non-linear General Theory of Shells, by W. Zerna, pp. 34–42. *(In German.)*

On the Large Deflexion of a Spherical Shell with an Inward Point Load, by D. G. Ashwell, pp. 43–63.

Buckling of Clamped Shallow Spherical Shells, by B. Budiansky, pp. 64–96.

Approximate Determination of the Radial Bearing Strength of Stiffened Spherical Shells Under Pressure Loading, by H. Ebner, pp. 95–111. *(In German.)*

On the Unsymmetrical Snapping of Shells of Revolution, by E. I. Grigolyuk, pp. 112–121.

Post-Buckling Analysis of a Circular Elastic Ring or a Long Cylindrical Shell, by J. H. Haywood, pp. 122–136.

Theoretical and Experimental Investigations on the Bearing Strength of Thin Short Cylindrical Shells Reinforced by Minimum Strength Medium Spaced Rings Under Lateral Pressure, by G. Czerwenka, pp. 137–166. *(In French.)*

On the Stability of Thin-Walled Circular Cylinders Under Longitudinal Pressure with Added Internal Pressure, by W. Schnell, pp. 167–188. *(In German.)*

Cylindrical Shells Under Axial Compressive Load, by M. Kuranishi and J. Niisawa, pp. 189–201.

Some Applications of the Bending Theory Regarding Doubly Curved Shells, by A. L. Bouma, pp. 202–234.

Theory of Antisymmetrical Bending of Spherical Thin-Shells, by Y. Tsuboi and K. Akino, pp. 235–246.

Bending at the Oblique End Section of Cylindrical Shells, by A. van der Neut, pp. 247–269.

On the Conditions for Realization of Moment-Free Stress Equilibrium in Shells of Positive Curvature, by I. N. Vekua, pp. 270–280. *(In German.)*

On the Dynamics of Shallow Elastic Membranes, by M. W. Johnson, pp. 281–300.

On the General Problem of Elastokinetics in the Theory of Shallow Shells, by P. M. Naghdi, pp. 301–330.

Certain Approximate Analyses of the Nonlinear Behavior of Plates and Shallow Shells, by W. A. Nash and J. R. Modeer, pp. 331–354.

Finite Deformation of Cylindrical Shells, by B. R. Seth, pp. 355–362.

On the Buckling of Truncated Conical Shells under Uniform Hydrostatic Pressure, by P. Seide, pp. 363–388.

Buckling of Circular Conical Shells under External Pressure, by N. J. Hoff and J. Singer, pp. 389–414.

The Inadequacy of the Classical Stress-Strain Relations for the Right Helicoidal Shell, by J. W. Cohen, pp. 415–433.

On Twisting and Stretching of Helicoidal Shells, by E. Reissner, pp. 434–466.

Development of the Theory of Shell Loading, by H. Neuber, pp. 467–494. *(In German.)*

Thermoelectricity, including the Proceedings of the Conferences on Thermoelectricity Sponsored by the Naval Research Laboratory, Sept. 1958, Paul H. Egli, ed., N. Y., John Wiley & Sons, 1960, 407 pp.

Electronic Properties of Mixed Valence Semiconductors, by R. R. Heikes, pp. 92–105.

Determination of the Fundamental Properties of Thermoelectric Semiconductors, by Raymond Wolfe, pp. 106–120.

Evaluation and Properties of Materials for Thermoelectric Applications, by F. D. Rosi and E. G. Ramberg, pp. 121–158.

Chemical Considerations in High Temperature Thermoelectric Power Development, by Alan W. Searcy and David J. Meschi, pp. 159–179.

Design of Materials for Thermoelectric Power Production, by Pierre R. Aigrain, pp. 180–185.

Estimation of Liquid Properties, by Rudolph J. Marcus, pp. 186–192.

Thermoelectric Properties of Porous Semiconductors, by Eugene B. Hensley, pp. 193–206.

Electrical and Thermal Conductivity of Insulators, by G. H. Fetterley, pp. 307–319.

Mechanical Properties of Ceramics and Their Measurement at Elevated Temperatures, by Samuel J. Schneider, pp. 342–357.

Critical Criteria for Materials Development, by Paul H. Egli, pp. 387–400.

Survey of Various Special Tests Used to Determine Elastic, Plastic, and Rupture Properties of Metals at Elevated Temperatures, by F. Garofalo, *J. Basic Engng. (ASME Trans., Series D)*, vol. 82, no. 4, Dec. 1960, pp. 867–881.

Bibliography on Low Temperature Characteristics of Steel, 1904, April 1960, by Katherine Janis Faber, *Internat. Nickel Co., Inc.*, 1960, 107 pp.

Multiwall Structures for Space Vehicles, by S. Lampert and D. G. Younger, *Wright Air Dev. Div. Tech. Rep.* 60-503, May 1960, 217 pp.

Aerothermodynamic Feasibility of Graphite for Hypersonic Glide Vehicles, by S. M. Scala and E. J. Nolan, *General Electric Co., Missile and Space Vehicle Dept.* T.I.S. R60SD425, Aug. 1960, 45 pp.

Theoretical Investigations of the Ablation of a Glass-Type Heat Protection Shield of Varied Material Properties at the Stagnation Point of a Re-entering IRBM, by Ernest W. Adams, *NASA TN* D-564, Jan. 1961, 64 pp.

Investigation of Thermal Effects on Structural Fatigue, by *Douglas Aircraft Co., Inc., Wright Air. Dev. Div. Tech. Rep.* 60-410, Part I, Aug. 1960, 189 pp.

Refractory Metal Constitution Diagrams, by A. R. Kaufmann and E. J. Rapperport, *Wright Air. Dev. Div. Tech. Rep.* 60-132, Oct. 1960, 181 pp.

Materials for Astronautic Vehicles, by A. J. Murphy, *Cranfield, College Aeron., CoA Rep.* no. 139, Nov. 1960, 21 pp., 26 figs.

Superconductive Properties of Thin Tin Films, by Eugene C. Grittenden Jr., John N. Cooper and Frederick W. Schmidlin, *Space Tech. Labs., Phys. Res. Lab.*, Nov. 1960, 19 pp.

Refractory Metals Tantalum, Niobium, Molybdenum, Rhenium and Tungsten, by C. A. Hampel, *I/EC: Ind. Engng. Chem.* vol. 53, no. 2, Feb. 1961, pp. 90–96.

Stress as a Reduced Variable: Stress Relaxation SBR Rubber at Large Strains, by Robert F. Landel and Paul J. Stedry, *Calif. Inst. of Tech., Jet Propl. Lab. Tech. Rep.* 32-11, Oct. 1960, 13 pp.

Brazing for High-Temperature Service, by A. F. Haskins and R. M. Evans, *Batelle Memorial Inst., Defense Metals Info. Center DMIC Mem.* 48, Mar. 1960, 12 pp. (Office of Tech. Services, PB 161198.)

Standard Designations of Alloys for Aircraft and Missiles, by J. J. Vogi, *Batelle Memorial Inst., Defense Metals Inf. Center, DMIC Mem.* 42, Jan. 1960, 68 pp. (Office of Tech. Services, PB 161192.)

Review of Problems in Using Flat-Rolled Materials in Air-and-Space-Weapon Systems, by F. W. Boulger, *Batelle Memorial Inst., Defense Metals Info. Center, DMIC Mem.* 52, Apr. 1960, 20 pp. (Office of Tech. Services, PB

161202.)

Spherical Shell Supported at Isolated Points, by H. E. Williams, *Calif. Inst. of Tech., Jet Prop. Lab. Tech. Rep.* 32-53, Feb. 14, 1961, 37 pp.

International Analog Computation Meeting, 2nd, Strasbourg, Sept. 1–6, 1958, Proceedings, Brussels, Presses, Academique Europeennes, 1959, 501 pp.

The Direct Analog Computer and Its Application to Engineering Analysis, by G. D. MacCann, pp. 34–45.

An Electronic Analog for Investigating Structural Vibrations in Unsupported Elastic Beams and Related Structures, by M. Squires and W. G. Hughes, pp. 152–163.

An Electrical Analog for the Torsion of Compound Bars, by S. C. Redshaw, pp. 328–332.

Vibration of Missiles, I, by H. L. Cox, *Aircraft Engng.*, vol. 33, no. 383, Jan. 1961, pp. 2–7.

Fluid Dynamics, Heat Transfer and MHD

Relativistic Theory of Shock Waves, by W. Israel, *Royal Soc. London, Proc., (Series A, Math. & Phys. Sciences)*, vol. 259, no. 1296, Nov. 22, 1960, pp. 129–139.

Surface Melting of Semi-infinite Body in Plane and Axially Symmetric Incompressible Gas Flow, by G. A. Tirskii, *Soviet Phys., Doklady*, vol. 5, no. 3, Nov.–Dec. 1960, pp. 501–504.

Existence of a Weak Solution to the Direct Problem in the Theory of Sonic Flow Past a Profile in First Approximation, by F. I. Frankl', *Soviet Phys., Doklady*, vol. 5, no. 3, Nov.–Dec. 1960, pp. 505–508.

Fluctuations of the Magnetic Field and Current Density in a Turbulent Flow of a Weakly Conducting Fluid, by G. S. Golitsyn, *Soviet Phys., Doklady*, vol. 5, no. 3, Nov.–Dec. 1960, pp. 536–539.

Free Energy Computation for a Gas of Low Density, by E. E. Tareeva, *Soviet Phys. Doklady*, vol. 5, no. 3, Nov.–Dec. 1960, pp. 551–555.

The Multiphase Hypersonic Laminar Boundary Layer on a Flat Plate, Part I. Boundary Layer Solutions, by J. P. Hartnett and C. Y. Koh, *Minnesota Inst. Tech., Heat Transfer Lab., Tech. Rep.* 28, Nov. 1960, 26 pp., 6 figs.

The Multiphase Hypersonic Laminar Boundary Layer on a Flat Plate, Part II, by J. P. Hartnett and C. Y. Koh, *Minnesota Inst. Tech., Heat Transfer Lab., Tech. Rep.* 29, Nov. 1960, 21 pp., 9 figs.

Theory of Electron Driven Shock Waves, by R. G. Fowler and B. D. Fried, *Space Tech. Labs, Phys. Res. Lab. STL/TR* 60-0000-GR310, Sept. 1960, 15 pp.

Compressible Flow Tables $k = 1.22$ Stagnation Temperature Change without Friction, by C. Hoebich, *Army Rocket and Guided Missile Agency, Ordnance Missile Labs. Div., ARGMA TN* 1H1N-12, Nov. 1960, 42 pp.

A Technique for Determining Relaxation Times by Free-Flight Tests of Low-Finess-Ratio Cones; with Experimental Results for Air at Equilibrium Temperatures up to 3440°K, by Jack Stephenson, *NASA TN* D-327, Sept. 1960, 55 pp.

Shock Waves in Multicomponent Mixtures, by G. M. Liakhov, *Johns Hopkins Univ., Appl. Phys. Lab., TG* 230-T126, Nov. 1960 (*Trans. from Bull. Acad. Sci., USSR, Div. Tech. Sci., Mechanics and Mechanical Engng.*, no. 1, 1950, pp. 46–49), Nov. 1960, 7 pp.

The Structure of Strong Shock Waves of Stable Monatomic Molecules, by Toyoki Koga, *Univ. Southern Calif., Engng. Ctr. USCEC Rep.* 83–201, (*AFOSR TN* 60-1344), Oct. 1960, 59 pp.

Unsteady Ablation, by Steven Georgiev, *Avco-Everett Res. Lab., Res. Rep.* 94, (*AFBMB TR* 60-180), Sept. 1959, 23 pp., incl. illus.

Comparison of Theoretical and Experimental Values for the Effective Heat of Ablation of Ammonium Chloride, by Hean E. Welker, *NASA TN* D-553, Nov. 1960, 13 pp.

Diffusion, Heat Exchange and Chemical Surface Catalysis in Flow Systems, by Daniel E. Rosner, *Princeton Univ. Dept. Aeron. Engng.* (Thesis, Ph.D.), Oct. 1960, 272 pp.

An Analysis of Thermal Radiation Heat Transfer in a Nuclear-Rocket Nozzle, by William H. Robbins, *NASA TN* D-586, Jan. 1961, 24 pp.

An Analysis of Nuclear-Rocket Nozzle Cooling, by William H. Robbins, Daniel Bachkin and Arthur A. Medeiros, *NASA TN* D-482, Nov. 1960, 24 pp.

Heat Transfer to Surfaces of Finite Catalytic Activity in Frozen Dissociated Hypersonic Flow, by Paul M. Chung and Aemer D. Anderson, *NASA TN* D-350, Jan. 1961, 36 pp.

Empirical Equations for Turbulent Forced Convection Heat Transfer for Prandtl Numbers from 0.001 to 1000, by Uwe H. von Glahn, *NASA TN* D-483, Dec. 1960, 16 pp.

A Study of the Effect of Ultrasonic Vibrations on Convective Heat Transfer in Liquids, by Milton B. Larson, *Stanford Univ., Dept. Mech. Engng., Tech. Rep.* 48, Sept. 1960, 102 pp.

The Effect of the Orientations of Electric and Magnetic Fields on the Electron Mean Energy and Drift Velocity, by Ching-Sheng Wu, *Calif. Inst. Tech., Jet Prop. Lab., Phys. Section*, 1960, 22 pp.

Effect of Shield Position and Absorptivity on Temperature Distribution of a Body Shielded from Solar Radiation in Space, by Lester D. Nichols, *NASA TN* D-578, Jan. 1961, 41 pp.

Ablation with Ice Model at M = 5.8, by Toshi Kubota, ARS JOURNAL, vol. 30, no. 12, Dec. 1960, pp. 1164–1169.

Aerodynamic Heating of Re-entry Vehicle, by Henneth Wang and Lu Ting, ARS JOURNAL, vol. 30, no. 12, Dec. 1960, p. 1180.

Hydromagnetic Equilibria, by Donat G. Wentzel, *Astrophys. J.* (*Suppl.* 47), vol. 5, Dec. 1960, pp. 187–232.

Surface Electroconvection, by W. V. R. Malkus and G. Veronis, *Phys. Fluids*, vol. 4, no. 1, Jan. 1961, pp. 13–23.

Instability of Flow Between Parallel Planes with a Coplanar Magnetic Field, by P. T. Wooler, *Phys. Fluids*, vol. 4, no. 1, Jan. 1961, pp. 24–27.

Optical Refractivity of High-Temperature Gases, III. The Hydroxyl Radical, by Donald R. White, *Phys. Fluids*, vol. 4, no. 1, Jan. 1961, p. 40.

Binary Correlations in Ionized Gases, by R. Balescu and H. S. Taylor, *Phys. Fluids*, vol. 4, no. 1, Jan. 1961, pp. 85–93.

Approach to Equilibrium of a Quantum Plasma, by R. Balescu, *Phys. Fluids*, vol. 4, no. 1, Jan. 1961, pp. 94–99.

Induced Oscillations in a Rarefied Plasma in a Magnetic Field, by P. S. Greifinger, *Phys. Fluids*, vol. 4, no. 1, Jan. 1961, pp. 104–108.

Electron Energy Distributions in Plasmas, II. Hydrogen, by R. L. F. Boyd and N. D. Twiddy, *Royal Soc. London, Proc. (Series A., Math. & Phys. Sciences)*, vol. 259, no. 1297, Dec. 6, 1960, p. 145.

Use of the Methods of Quantum Field Theory for the Investigation of the Thermodynamical Properties of a Gas of Electrons and Photons, by I. A. Akhiezer and S. V. Peleminskii, *Soviet Phys.: JETP*, vol. 11, no. 6, Dec. 1960, pp. 1316–1322.

Instability of Plasma with Anisotropic Distribution of Ion and Electron Velocities, by A. B. Kitsenko and K. N. Stepanov, *Soviet Phys.: JETP*, vol. 11, no. 6, Dec. 1960, pp. 1323–1326.

Thermodynamic Functions of a Low-Temperature Plasma, by A. I. Larkin, *Soviet Phys.: JETP*, vol. 11, no. 6, Dec. 1960, pp. 1363–1364.

On the Calculation of Rotational Symmetrical Nozzle Flows, by H. Lipps, *Zeitschrift für Angewandte Math. Mech.*, vol. 40, no. 10/11, Oct.–Nov. 1960, pp. 507–509. (*In German.*)

Tables of Flow Functions for a Simple Non-Steady Expansion Wave, by A. Roshko and M. Rubinstein, *Douglas Aircraft Co., El Segundo Div., ES* 40031, Sept. 1960, 58 pp.

Conference on Aviation and Astronautics, 2nd, Feb. 9–10, 1960, Tel-Aviv and Haifa, Proceedings, (*Reprint from Bull. Res. Council of Israel*, vol. 8c, Feb. 1960, no. 1), 57 pp.

Ionization Measurements in Shocked Gases, by Y. Mangeimer-Timnat, pp. 53–56.

On the Magnetohydrodynamic Boundary Layer Theory, by K. T. Yen, *Rensselaer Polytechnic Inst., Dept. Aeron. Engng., Tech. Rep.* AE 6004, (*AFOSR TN* 60-1162), Sept. 1960, 19 pp.

A Six-Part Survey of Rocket Heat-Transfer Literature, by T. F. Irvine Jr., (American Soc. of Mech. Engrs., Heat Transfer Div., Subcommittee in Rocket Heat Transfer), *N. Carolina State College, Dept. Engng. Res., Reprint Bull.* no. 76, Oct. 1960, (reprinted from *J. Heat Transfer*, Aug. 1960, pp. 155–169).

Study of Fluid Mixing and Related Aerodynamic Problems, by K. T. Yen, *Renssalaer Polytechnic Inst., Dept. of Aeron. Engng., Tech. Rep., AE* 6006 (Final Report) (*AFOSR TR* 60-136), Sept. 1960, 10 pp.

An Investigation of a Photographic Technique of Measuring High Surface Temperatures, by James H. Siviter Jr., and H. Kurt Strass, *NASA TN* D-167, Nov. 1960, 15 pp.

The Rate of Vaporization of Low Sticking Coefficient Molecules from Porous Solids; Application to Knudsen Effusion Experiments, by G. L. Vidale, *General Electric Co., Missile and Space Vehicle Dept., T.I.S.* R608D468, Oct. 1960, 29 pp.

Thermal Conductivity and Prandtl Number of Carbon Dioxide and Carbon-Dioxide Air Mixtures at One Atmosphere, by Jerome L. Novotny and Thomas F. Irvine Jr., *N. Carolina State College, Dept. of Engng., Res. Reprint Bull.* No. 75, (reprinted from *J. Heat Transfer* Paper no. 60-HT-13), Sept. 1960, 7 pp.

Kinematic Formulation of Rotational Gas Flow, by M. Vinokur, *Lockheed Aircraft Corp., Missiles and Space Div., TN* LMSD-288207, Jan. 1960, 19 pp.

Thermal Agitation and Turbulence, by R. Betchov, *Space Tech. Labs., Phys. Res. Lab.*, STL/TR 60-0000-AE279, Aug. 1960, 21 pp.

Thermoelectricity, including the Proceedings of the Conferences on Thermo-

electricity sponsored by the Naval Res. Lab., Sept. 1958, Paul H. Egli, ed., N. Y., John Wiley & Sons, 1960, 407 pp.

Thermal Conductivity in Solids, by J. A. Krumhansl and W. S. Williams, pp. 79–91.

Thermal Conductivity of Germanium in the Temperature Range 300°K to 1080°K, by Benjamin Abeles, pp. 288–294.

On the Heat Conductivity of Indium Antimonide and on the Longitudinal Flow Method of Measuring It, by M. Bettman and J. E. Schneider, pp. 295–306.

Standards of Heat Capacity and Thermal Conductivity, by D. C. Ginnings, pp. 320–341.

Heat Transfer in Solid-Gas Transport Lines, by C.-Y. Wen and E. N. Miller, *I/EC: Ind. Engng. Chem.*, vol. 53, no. 1, Jan. 1961, pp. 51–66.

Two-Dimensional Gas Jets, by M. J. Cohen, *J. Appl. Mech.* (*ASME Trans., Series E*), vol. 27, no. 4, Dec. 1960, pp. 603–608.

Heat Transfer and Sublimation at a Stagnation Point in Potential Flow, by W. W. Short, *J. Appl. Mech.* (*ASME Trans., Series E*), vol. 27, no. 4, Dec. 1960, pp. 613–616.

Electron Density Fluctuations in a Plasma, by E. E. Salpeter, *Phys. Rev.*, vol. 120, no. 5, Dec. 1, 1960, pp. 1528–1535.

Measurement of Thermal Fluctuations in Radiation, by Martin Harwit, *Phys. Rev.*, vol. 120, no. 5, Dec. 1, 1960, pp. 1551–1556.

Magnetic Field Interactions with Shock Ionized Argon, by H. J. Pain and P. R. Smy, *Phys. Soc. London, Proc.*, vol. 76, part 6, no. 492, Dec. 1, 1960, pp. 849–856.

The Discontinuities in the Solutions of the Transport Equation and the Variational Principle, by R. Englman, *Phys. Soc. London, Proc.*, vol. 76, part 6, no. 492, Dec. 1, 1960, pp. 909–913.

Spectroscopic Study of Helium Plasmas Produced by Magnetically Driven Shock Waves, by E. A. McLean, C. E. Faneuff, A. C. Kolb and H. R. Griem, *Phys. Fluids*, vol. 3, no. 6, Nov.–Dec. 1960, pp. 843–856.

Some Unexpected Results of Shock-Heating Xenon, by Per Gloersen, *Phys. Fluids*, vol. 3, no. 6, Nov.–Dec. 1960, pp. 857–870.

Some Variational Theorems for Non-Newtonian Flow, by M. W. Johnson Jr., *Phys. Fluids*, vol. 3, no. 6, Nov.–Dec. 1960, pp. 871–877.

Fluid Flow Through a Porous Channel, by W. E. Wageman and F. A. Guevara, *Phys. Fluids*, vol. 3, no. 6, Nov.–Dec. 1960, pp. 878–881.

Theory of Gas Bubble Dynamics in Oscillating Pressure Fields, by Milton S. Plesset and Din-Yu Hsieh, *Phys. Fluids*, vol. 3 no. 6, Nov.–Dec., 1960, pp. 882–894.

Kinetic Theory of Moderately Dense Gases: Rigid Sphere Limit, by R. F. Snider and C. F. Curtiss, *Phys. Fluids*, vol. 3, no. 6, Nov.–Dec. 1960, pp. 903–904.

Solutions of Concentration-Dependent Diffusion Equation, by Ranjit Paul, *Phys. Fluids*, vol. 3, no. 6, Nov.–Dec. 1960, pp. 905–907.

Kirkendall Effect in Gaseous Diffusion, by K. P. McCarty and E. A. Mason, *Phys. Fluids*, vol. 3, no. 6, Nov.–Dec. 1960, pp. 908–921.

Kinetic Equation with a Constant Magnetic Field, by Norman Rostoker, *Phys. Fluids*, vol. 3, no. 6, Nov.–Dec. 1960, pp. 922–926.

Plasma Motion Across Magnetic Fields, by George Schmidt, *Phys. Fluids*, vol. 3, no. 6, Nov.–Dec. 1960, pp. 961–965.

Charge Excitation of Plasma Motion in a Magnetic Field, by R. A. Papert, *Phys. Fluids*, vol. 3, no. 6, Nov.–Dec. 1960, pp. 966–972.

Plasma Acceleration in a Radio-Frequency Field Gradient, by G. A. Swartz, T. T. Reboul, G. D. Gordon and H. W. Lorber, *Phys. Fluids*, vol. 3, no. 6, Nov.–Dec. 1960, pp. 973–976.

Sufficient Conditions for Hydromagnetic Stability of a Diffuse Linear Pinch, by Harold P. Furth, *Phys. Fluids*, vol. 3, no. 6, Nov.–Dec. 1960, pp. 977–981.

Some Problems of a Stationary Flow of Conducting Liquid in an Infinitely Long Annular Tube in the Presence of Radial Magnetic Field, by I. G. Chekmarev, *Soviet Phys., Tech. Phys.*, (*transl. of Zhurnal Tekhnicheskoi Fiziki*), vol. 5, no. 6, Dec. 1960, pp. 565–569.

Temperature Gradient of an Infinite Plate with Variable Heat Loss Coefficients in a Medium of Varying Temperatures, by K. A. Kiselev and A. I. Lazarev, *Soviet Phys. Tech. Phys.*, (*transl. of Zhurnal Tekhnicheskoi Fiziki*), vol. 5, no. 6, Dec. 1960, pp. 579–584.

Variation of the Parameters of a Gas in Connection with the Nonequilibrium Dissociation behind a Shock Wave, by Yu. P. Lun'kin, *Soviet Phys., Tech. Phys.*, (*transl. of Zhurnal Tekhnicheskoi Fiziki*), vol. 5, no. 6, Dec. 1960, pp. 585–589.

On the Approximate Theory of the Flow of a Viscous Incompressible Liquid in a Tube with Permeable Walls, by S. A. Regirer, *Soviet Phys., Tech. Phys.*, (*transl. of Zhurnal Tekhnicheskoi Fiziki*), vol. 5, no. 6, Dec. 1960, pp. 602–605.

On a Class of Plane Problems in Magnetohydrodynamics, by K. A. Lur'e, *Soviet Phys., Tech. Phys.*, (*transl. of Zhurnal Tekhnicheskoi Fiziki*), vol. 5, no. 6, Dec. 1960, pp. 691–698.

Rev. Modern Phys., Proc. of the Internat. Symposium on Magneto-Fluid Dynamics, vol. 32, no. 4, Oct. 1960.

Problems in Magneto-Fluid Dynamics, by Lyman Spitzer Jr., pp. 696–700.

Some Remarks About Flow Past Bodies, by W. R. Sears, pp. 701–705.

Magneto-Fluid Dynamic Shock Waves, by R. Lust, pp. 706–709.

Collision Between a Nonionized Gas and a Magnetized Plasma, by H. Alfven, pp. 710–713.

Long-Range Forces and the Diffusion Coefficients of a Plasma, by W. B. Tompson and J. Hubbard, pp. 714–718.

Transport Equation of a Plasma, by R. Balescu, pp. 719–721.

Irreversible Processes in Plasma in a Strong Magnetic Field, by Taro Kihara and Yukio Midzuno, pp. 722–730.

Dynamical Equations and Transport Relationships for a Thermal Plasma, by R. Herdan and B. S. Liley, pp. 731–741.

Motion of a Charged Particle in a Slowly Increasing Magnetic Field, by L. J. F. Broer, pp. 742–743.

Hydromagnetic Equilibrium Experiments with Liquid and Solid Sodium, by S. A. Colgate, H. P. Furth and F. O. Halliday, pp. 744–747.

Magnetic Compression of Plasmas, by Alan C. Kolb, pp. 748–757.

Some Studies of Free-Surface Mercury Magnetohydrodynamics, by R. A. Alpher, H. Hurwitz Jr., R. H. Johnson and D. R. White, pp. 758–769.

Experiments on the Passage of a Shock Wave through a magnetic Field, by K. Dolder and R. Hide, pp. 770–779.

Some Remarks on Electric-Discharge Shock-Tube Diagnostics, by Daniel Bershader, pp. 780–784.

On Turbulent Magneto-Fluid Dynamic Boundary Layers, by L. G. Napolitano, pp. 785–795.

Transition from Laminar to Turbulent Flow in Magneto-Fluid Mechanic Channels, by Paul S. Lykoudis, pp. 796–798.

Hydromagnetic Flow Due to an Oscillating Plane, by R. Hide and P. H. Roberts, pp. 799–806.

Energy Spectra in Magneto-Fluid Dynamic Turbulence, by T. Tatsumi, pp. 807–812.

Plasma Turbulence, by Leslie S. G. Kovasznay, pp. 815–822.

Two-Dimensional Boundary Layers and Jets in Magneto-Fluid Dynamics, by Gunther Jungclaus, pp. 823–827.

Some Magneto-Fluid Dynamic Effects in a Finitely Conducting Medium, by V. N. Zhigulev, pp. 828–829.

Reducible Problems in Magneto-Fluid Dynamic Steady Flows, by Harold Grad, pp. 830–847.

Some Exact Solutions Linearized Magnetoaerodynamics for Arbitrary Magnetic Reynolds Numbers, by E. L. Resler Jr. and J. E. McCune, pp. 848–855.

Motion of Bodies Through Conducting Fluids, by K. Stewartson, pp. 855–859.

Magnetohydrodynamic Wakes in a Viscous Conducting Fluid, by Hidenori Hasimoto, pp. 860–865.

Some Remarks on Hydromagnetic Waves for Finite Conductivity, by E. L. Resler Jr., pp. 866–867.

Motion of a Completely Ionized Gas across a Magnetic Field in the Presence of an Electric Force, by J. M. Burgers, pp. 868–880.

On the Theory of Propagation and Decay of Hydromagnetic Waves in an Anisotropic Medium, by S. A. Kaplan, p. 881.

Wave Motions of Small Amplitude in a Fully Ionized Plasma without External Magnetic Field, by S. I. Pai, pp. 882–887.

Pinch Buckling, by K. O. Friedrichs, pp. 889–897.

On Hydromagnetic Stability of Stationary Equilibria, by E. Friedman and Manuel Rotenberg, pp. 898–902.

On the Stability of a Periodic Force-Free Field with Neutral Lines, by E. Schatzman, pp. 903–906.

Stability of Twisted Magnetic Fields in a Fluid of Finite Electrical Conductivity, by R. J. Tayler, pp. 907–913.

On the Theory of Hydromagnetic Equilibrium, by L. Woltjer, pp. 914–915.

Some Results on Heat Transport by Convection in the Presence of a Magnetic Field, by Yoshinari Nakagawa, pp. 916–918.

Shock Waves and Shock-Wave Structure in Magneto-Fluid Dynamics, by P. Germain, pp. 951–958.

Magnetohydrodynamic Shock Wave in a Collision-Free Plasma, by F. J. Fishman, A. R. Kantrowitz, and H. E. Petschek, pp. 959–966.

Hydromagnetic Waves of Finite Amplitude in a Plasma with Isotropic and Nonisotropic Pressure Perpendicular to a Magnetic Field, by K. Hain, R. Lust and A. Schluter, pp. 967–972.

Attached Stationary Shock Waves in Ionized Gases, by H. Cabannes, pp. 973–976.

On Gas-Ionizing Magnetohydrodynamic Shock Waves, by A. G. Kulikovskii and G. A. Lyubimov, pp. 977–979.

Some Generalizations in One-Dimensional Magnetogasdynamics, by J. A. Shercliff, pp. 980–986.

On Flows of Conducting Fluids Past Bodies, by Isao Imai, pp. 992–999.

Inviscid Flow Past a Body at Low Magnetic Reynolds Number, by G. S. S. Ludford, pp. 1000–1003.

Magnetohydrodynamic-Hypersonic Flow in the Quasi-Newtonian Approximation, by Rudolf X. Meyer, pp. 1004–1007.

Stabilization of Pinch Discharges, by Stirling A. Colgate and Harold P. Furth, *Phys. Fluids,* vol. 3, no. 6, Nov.–Dec. 1960, pp. 982–1000.

Superfast Pinch Experiment, by Vernal Josephson, *Phys. Fluids,* vol. 3, no. 6, Nov.–Dec. 1960, pp. 1001–1007.

Ionization Growth in a Gas with a Constant Electric Field, by E. Gerjuoy and G. W. Stuart, *Phys. Fluids,* vol. 3, no. 6, Nov.–Dec. 1960, pp. 1008–1015.

Nonlinear Behavior of the Electrical Conductivity of a Slight Ionized Gas, by Melvin Epstein, *Phys. Fluids,* vol. 3, no. 6, Nov.–Dec. 1960, pp. 1016–1018.

Exploratory Study of the Reduction in Friction Drag Due to Streamwise Injection of Helium, by Byron L. Swenson, *NASA TN* D-342, Jan. 1961, 29 pp.

Linearized Transonic Flow About Slender Bodies at Zero Angle of Attack, by P. F. Maeder and H. U. Thommen, *Brown Univ., Div. Engng., Tech. Rep.* WT-34, Oct. 1960, 24 pp.

Design, Calibration and Simulation Capability of the Rosemount Aeronautical Laboratories' High Temperature Hypersonic Facility, by R. Hermann, J. O. A. Stankevics, W. L. Melnik and M. A. Luger, *Wright Air Dev. Div., WADD TN* 60-108, May 1960, 39 pp.

Application of Similar Solutions to Calculation of Laminar Heat Transfer on Bodies with Yaw and Large Pressure Gradient in High-Speed Flow, by Ivan E. Beckwith and Nathaniel B. Cohen, *NASA Tech Note* D-625, Jan. 1961, 95 pp.

Three-Dimensional Laminar Instability, by William O. Criminale Jr., *Project Squid, Tech. Rep.* JHU-18-T-R-P, May 1960, 104 pp., 20 figs.

Effect of Roughness on Transition in Supersonic Flow, by E. R. Van Driest and C. B. Blumer, *North American Aviation, Aero/Space Labs., Missile Div.,* MD 60-329, Mar. 1960, 36 pp. (*AFOSR TN* 60-1164.)

Perturbed Boundary Layer Solutions Applied to the Wall Jet and Blasius Profile, by Martin H. Bloom and Martin H. *Polytech. Inst. of Bkln., Dept. Aerospace Engng. Appl. Mech., PIBAL Rep.* no. 471, Oct. 1960, 33 pp. (*AFOSR TN* 60-1340)

Heat-Transfer Measurements on the Apexes of two 60° Sweptback Delta Wings (Panel Semi-Apex Angle of 30°) Having 0° and 45° Dihedral at a Mach Number of 4.95, by Charles R. Gunn, *NASA TN* D-550, Jan. 1961, 51 pp.

Heat-Transfer Measurements at a Mach Number of 4.95 on Two 60° Swept Delta Wings with Blunt Leading Edges and Dihedral Angles of 0° and 45°, by P. Calvin Stainback, *NASA TN* D-549, Jan. 1961, 50 pp.

Constant Entropy Properties for an Approximate Model of Equilibrium Air, by C. Frederick Hansen and Marion E. Hodge, *NASA TN* D-352, Han. 1961, 33 pp.

Absolute Intensity of Non-equilibrium Radiation in Air and Stagnation Hearing at High Altitudes, by J. C. Camm, B. Kivel, R. L. Taylor and J. D. Teare, *Avco-Everett Res. Lab., Res. Rep.* 93, Dec. 1959, 35 pp. (AFBMD TR 60-184.)

Compressible Flow Tables k = 1.22 Adiabatic Flow with Friction, *Army Ballistic Missile Agency, Rep.* no. RA-TR-3-60, Dec. 1960, 89 pp.

Compressible Flow Tables k = 1.24 Adiabatic Flow with Friction, *Army Ballistic Missile Agency, Rep.* no. RA-TR-4-61, Jan. 1961, 82 pp.

Hypersonic Free Flight Research, Part II, Investigations of Heat Transfer and Aerodynamic Stability, by O. R. Burggraf, *Wright Air Dev. Div., (WADD Tech. Rep.* 59-708, Pt. II), July 1960, 85 pp.

Application of Heat Flux Potentials to the Calculation of Convective Heat Transfer in Chemically Reacting Gases, by Daniel E. Rosner, *AeroChem. Res. Labs., Tech. Paper* 20, Dec. 1960, 8 pp.

Steady Flow Over a Magnetized Body in a Fluid of Low Electrical Conductivity, Part I. General Theory, by S. I. Pai, *General Electric Company, Missile and Space Vehicle Dept., T.I.S.* R60SD417, Aug. 1960, 37 pp.

Cylindrical Couette Flow in a Rarefied Gas According to Grad's Equations, by Daniel Ai Kwoh-i, *Calif. Inst. of Tech., Hypersonic Res. Project, Mem.* no. 56, July 15, 1960, 47 pp.

Kinetic Theory Description of Plane, Compressible Couette Flow, by Lester Lees and Chung-Yen Liu, *Calif. Inst. of Tech., Hypersonic Res. Project, Mem.* no. 58, Sept. 15, 1960, 57 pp.

Small Perturbations in the Unsteady Flow of a Rarefied Gas Based on Grad's Thirteen Moment Approximation, by Danie Ai Kwoh-i, *Calif. Inst. of Tech., Hypersonic Res. Project, Mem.* no. 59, Sept. 20, 1960, 50 pp.

The Effects of Resonant Acoustic Vibrations on the Local and Overall Heat Transfer Coefficients for Air Flowing Through an Isothermal Horizontal Tube, by T. W. Jackson, K. R. Purdy, C. C. Oliver and H. J. Johnson, *Air Force Aeron. Res. Labs., (ARL Tech. Rep.* 60-322), Oct. 1960, 122 pp.

Nonlinear Plasma Oscillations, by H. W. Wyld Jr., *Space Tech. Labs., Phys. Res. Lab.,* STL/TR 60-0000-GR303, Sept. 1960, 51 pp.

An Investigation of the Macroscopic Equations for a Plasma, by H. Li and R. D. Mathieu, *Pennsylvania State Univ., Dept. Aeron. Engng., Tech. Rep.* no. 13, May 1960, 27 pp. (*AFOSR TN* 60-1070.)

Transient Behavior of Electrons in Ionized Gases with an Impulsively Applied Field, by Jonas S. Zmuidzinas and Ching-Sheng Wu, *Calif. Inst. of Tech., Jet Propulsion Lab. Tech. Release* no. 34-120, Oct. 1960, 14 pp.

Acoustic Attenuation and Relaxation Phenomena in Steam at High Temperature and Pressure, by D. D. Eden, R. B. Lindsay and H. Zink, *J. Engng. for Power (ASME Trans.)* vol. A 83, no. 1, Jan. 1961, pp. 137–146.

Third-Order Blast Wave Theory and Its Application to Hypersonic Flow Past Blunt-Nosed Cylinders, by R. J. Swigart, *J. Fluid Mech.,* vol. 9, part 4, Dec. 1960, pp. 613–620.

Axially Symmetric Stagnation Point Flow with Heat Transfer in Magnetrohydrodynamics, by G. Poots and L. Sowerby, *Quart, J. Mech. Appl. Math.,* vol. 13, part 4, Nov. 1960, pp. 385–407.

Axisymmetric Solutions of the Incompressible Magnetohydrodynamic Equations, by A. N. Ergun, *Quart. J. Mech. Appl. Math.,* vol. 13, part 4, Nov. 1960, pp. 408–427.

Hypersonic Flow Over Cones, by Stanley A. Berger, *Princeton Univ., Dept. Aeron. Engng., Rep.* 523, Sept. 1960, 60 pp., 11 figs. (*AFOSR TN* 60-1214.)

Mach and Reynolds Number Effects on the Flows Over Blunt Flat Plates at Hypersonic Speeds, by I. E. Vas and S. Bogdonoff, *Princeton Univ., Dept. Aeron. Engng., Rep.* 529, Nov. 1960, 11 pp.

Steady Flow Over a Magnetized Body in a Fluid of Low Electrical Conductivity, Part I. General Theory, by S. I. Pai, *General Electric Co., Missile and Space Vehicle Dept., T.I.S.* R60SD417, Aug. 1960, 37 pp.

A Study of Flow Fields about Some Typical Blunt-Nosed Slender Bodies, by Roberto Vaglio-Laurin and Massimo Trella, *Polytech. Inst. of Bkln., Dept. Aerospace Engng. Appl. Mech., Rep.* 623, Dec. 1960, 50 pp. (*AFOSR* 2.)

Further Results on Supersonic Flow near Convex Corners, by R. J. Hakkinen, *Douglas Aircraft Co., Missiles and Space Systems, Engng., Rep.* SM-35992, Mar. 1961, 31 pp.

Effect of Hydrogen Recombination on Turbulent Heat Transfer, by W. H. Giedt, L. L. Cobb Jr. and E. J. Russ, *ASME Paper* 60-WA-256, Nov. 27–Dec. 2, 1960, 8 pp.

Research on Rarefied Gas Dynamics, by Raymond L. Chuan, *Univ. of Southern Calif., School of Engng., Rep.* 56-101, Nov. 11, 1960, 115 pp. (*AFOSR* 22)

Shock Waves in Radiation-Magnetogas-Dynamics, by S. I. Pai and A. I. Speth, *Maryland Univ., Inst. Fluid Dynamics Appl. Math., TN* BN-223, Nov. 1960, 17 pp. (*AFOSR* 38).

Compressible Flow Tables k = 1.30 Stagnation Temperature Change without Friction (*U*), by C. Hoebich, *Army Rocket and Quided Missile Agency, TN* IH1N-15, Aug. 60, 89 pp.

Nonsteady Supercritical Discharge Through an Orifice, by George Rudinger, *Princeton Univ., Project Squid,* CAL-82-P, Dec. 1960, 19 pp.

High Temperature Spectral Emissivity Studies, by Thomas R. Riethof, *General Electric Co., Missile and Space Vehicle Dept., Tech. Info. Series* R61SD004, Jan. 1961, 34 pp. (Presented at the conference on Radiative Transfer From Solid Materials, Boston, Mass., Dec. 12–13, 1960.)

Effects of End Current Loops on the Velocity Profile in a Magnetohydrodynamic Channel, by A. W. Carlson and G. W. Sutton, *General Electric Company, Missile and Space Vehicle Dept. T.I.S.* R60SD439, Dec. 1960, 33 pp. (*AFOSR TN* 60-1183.)

An Investigation of the Effect of High Temperature on the Schumann-Runge Ultraviolet Absorption Continuum of Oxygen, by John S. Evans and Charles J. Schexnayder Jr., *NASA Tech. Rep.* R-92, 1961, 144 pp.

Interaction Between a Plasma and a Micro-wave, by Toyoki Koga, *Univ. of Southern Calif., School Engng. Rep.* 83-202, 1960, (*AFOSR* 3).

On the Detection of Ion Oscillations in a Mercury Discharge, by Burton Fried and Roy W. Gould, *Space Tech. Labs., Phys. Res. Lab.,* STR/TR 60-0000-GR 413, Dec. 1960, 12 pp.

Stability of Plasmas in the Presence of Conducting Walls, by Carl Iddings, *Space Tech. Labs., Phys. Res. Lab.* STL/TR 60-0000-94316, Sepz. 1960, 19 pp.

International Analog Computation Meeting, 2nd, Strasbourg, Sept. 1–6, 1958, Proceedings, Brussels, Presses, Academique Europeennes, 1959, 501 pp.

An Electric Network Analog Study of Viscous Fluid Flow Problem, by J. L. Shearer, pp. 459–467.

Predicting Temperature Rises Due to Aerodynamic Heating, by D. Readshaw, *Aircraft Engng.*, vol. 33, no. 383, Jan. 1961, pp. 8–11.

The Role of Entropy in the Aerospace Sciences (Daniel and Florence Guggenheim Memorial Lecture), by Jakob Ackeret, *J. Aerospace Sciences*, vol. 28, no. 2, Feb. 1961, pp. 81–95.

Radiation From Hot Air and Its Effect on Stagnation-Point Heating, by Bennett Kivel, *J. Aerospace Sciences*, vol. 28, no. 2, Feb. 1961, pp. 96–120.

The Supersonic Boom of a Projectile Related to Drag and Volume, by I. L. Ryhming, *J. Aerospace Sciences*, vol. 28, no. 2, Feb. 1961, pp. 113–118.

Plasma Flow over a Thin Charged Conductor, by Hideo Yoshihara, *J. Aerospace Sciences*, vol. 28, no. 2, Feb. 1961, pp. 141–144.

Detonation-Generated Plasmas, by A. Bauer, M. A. Cook and R. T. Keyes, *Roy. Soc., London, Proceedings, (Series A. Math. Phys. Sciences)* vol. 259, no. 1299, Jan. 24, 1961, pp. 508–517.

Self-Simulating Motion of a Gas with Plane Waves in Magnetohydrodynamics, by O. A. Berezin, *Soviet Phys., Doklady*, vol. 5, no. 4, Jan.–Feb. 1961, pp. 670–672.

On the Interaction of Strong Explosion Waves with an Electromagnetic Field, by V. P. Korobeinikov and V. P. Karlikov, *Soviet Phys., Doklady*, vol. 5, no. 4, Jan.–Feb. 1961, pp. 679–683.

Magnetosonic Resonance in Plasma, by D. A. Frank-Kamenetskii, *Soviet Phys., Tech. Phys.*, vol. 5, no. 8, Feb. 1961, pp. 847–852.

Flight Mechanics

Development of the Lunar and Solar Perturbations in the Motion of an Artificial Satellite, by P. Musen, A. Bailie and E. Upton, *NASA TN* D-494, Jan. 1961, 44 pp.

On the Motion of a Satellite in an Asymmetrical Gravitational Field, by P. Musen, *NASA TN* D-569, Jan. 1961, 20 pp.

On the Accuracy of an Elliptical Orbit Determination, by Robert F. Weirauch, *NASA TN* D-573, Jan. 1961, 13 pp.

Approximate Analysis of Atmospheric Entry Corridors and Angles, by Roger W. Luidens, *NASA TN* D-590, Jan. 1961, 42 pp.

Analytic Solutions to Several Optimum Orbit Transfer Problems, by H. Munick, R. McGill and G. E. Taylor, *J. Astron. Sciences*, vol. 7, no. 4, Winter 1960, pp. 73–77.

Orbital Patterns for Satellite Systems, by Louis G. Vargo, *J. Astron. Sciences*, vol. 7, no. 4, Winter 1960, pp. 78–86.

Satellite Re-entry with Lightly Loaded Lifting Vehicles, by Jacques A. F. Hill, *Mass. Inst. Tech., Naval Supersonic Lab., Tech. Rep.* 429, Dec. 1959, 68 pp.

Drag and Stability Derivatives of Missile Components According to the Modified Newtonian Theory, by J. Don Gray, *Arnold Engng. Dev. Center, TN* 60-191, Nov. 1960, 36 pp.

The Hodograph and Ballistic Missile Trajectory Problems, by Erwin W. Paul, *Aero/Space Engng.*, vol. 20, no. 2, Feb. 1961, pp. 24–25.

On the Motion of a Particle About an Oblate Spheroid, III. Parabolic and Highly Elliptic Orbits, by J. A. Crane, *Brit. Interplan. Soc. J.*, vol. 17, no. 12, Nov.–Dec. 1960, pp. 437–439.

Selected Topics on Ballistics, Cranz Centenary Colloquium, Univ. of Freiburg, 1958, Wilbur C. Nelson, ed., N. Y., Pergamon Press, for North Atlantic Treaty Organization, Advisory Group of Aeron. Res. and Dev. (AGARD), 1959, 280 pp.

Exterior Ballistics Developments in the United States Since the Time of Cranz, by C. L. Peer, pp. 36–45.

Some Aerodynamic Effects on Long-Range Rocket Craft, by H. J. Allen, pp. 46–58.

Meteorites and Ballistics, by J. S. Rinehart, pp. 88–116, 93 refs.

Projectile Aeroballistics, by R. F. M. Sauer, pp. 117–124.

The Calculation of Stability and Damping of Spin-Stabilized Projectiles, by Wolfgang Haack, pp. 125–139.

Some Aspects of Stability and Controllability of Cross-Winged Guided Missiles, pp. 140–144.

Scaling Problems in Underwater Ballistics, by H. G. Snay, pp. 262–280.

International Analog Computation Meeting, 2nd, Strasbourg, Sept. 1–6, 1958, Proceedings, Brussels, Presses, Academique Europeennes, 1959, 501 pp.

Some Applications of Digital Differential Analyzers, by G. Savastano, pp. 409–420.

Numerical Integration in Differential Analyzers, by G. Savastano, pp. 421–428.

Vehicle Design, Testing and Performance

Aerodynamic Characteristics of a Model of an Inflatable-Sphere Launching Vehicle Under Simulated Conditions of Mach Number and Altitude, by Ross B. Robinson and Odell A. Morris, *NASA Tech. Note* D-640, Dec. 1960, 12 pp.

American Vacuum Society, Fifth National Symposium on Vacuum Technology Transactions, San Francisco, Oct. 22–24, Proceedings, Wilfred G. Matheson, ed., N. Y., Pergamon Press, 1959, 282 pp.

An Extreme Performance Altitude Temperature Environmental Chamber, by W. C. Gates and B. J. Reitzer, pp. 274–278.

High Vacuum Technology in a Space Research Laboratory, by F. Reich, pp. 279–282.

Selected Topics on Ballistics, Cranz Centenary Colloquium, Univ. of Freiburg, 1958, Wilbur C. Nelson, ed., N. Y., Pergamon Press, for North Atlantic Treaty Organization, Advisory Group of Aeron. Res. and Dev. (AGARD), 1959, 280 pp.

Ballistics of the Explorer, by J. E. Froehlich and A. R. Hibbs, pp. 59–73.

Launching of Explorer I, by R. F. Hoelker, pp. 74–87.

The Role of Free Flight Ranges in Ballistic and Aerodynamic Research, by C. H. Murphy Jr., pp. 145–167.

Special Ballistic Ranges and Gas Guns, by H. H. Kurzweg, pp. 183–199.

Preliminary Planning for a Hypervelocity Aeroballistic Range at AEDC, by E. J. Stollenwerk and R. W. Perry, pp. 200–212.

International Analog Computation Meeting, 2nd, Strasbourg, Sept. 1–6, 1958, Proceedings, Brussels, Presses, Academique Europeennes, 1959, 501 pp.

An Electronic Multiplier, by B. Jiewertz, pp. 103–109.

Project Transit-Earth and Aerospace Navigational Satellite System, by John D. Nicolaides, *Aero/Space Engng.*, vol. 20, no. 2, Feb. 1961, pp. 20–21.

Lunar Surface Vehicles, by Lawrence L. Hofstein and Angelo W. Cacciola, *Amer. Chem. Soc. J.*, vol. 83, no. 2, Jan. 20, 1961, pp. 36–38.

Stresses Associated with Lunar Landings, by John S. Rinehart, *Brit. Interplan. Soc. J.*, vol. 17, no. 12, Nov.–Dec. 1960, pp. 431–436.

Determination of the Required Number of Randomly Spaced Communication Satellites, by Floyd V. Bennett, Thomas L. Coleman and John C. Houbolt, *NASA TN* D-619, Jan. 1961, 29 pp.

Two Development Reports on the Saturn Rocket, by D. Kolle, *Raketentechnik und Raumfahrtforschung*, vol. 4, no. 4, Oct.–Dec. 1960, pp. 136–142. (*In German.*)

Guidance and Control

Application of Describing - Function Analysis to the Study of an on-off Reaction-Control System, by Edgar C. Lineberry Jr. and Edwin C. Fourdriat, *NASA TN* D-654, Jan. 1961, 40 pp.

Akademiia Nauk SSSR, Institut Automatiki i Telekhanika, Pneumatic and Hydraulic Systems and Elements, Moskva, Akademiia Nauk SSSR, 1959, 235 pp. (*In Russian.*)

New Miniaturized Pneumatic Devices for Automatic Control and Regulation, Control and Regulation, Developed by "NII Teplopribor," by I. F. Kozlow, pp. 12–18. (*In Russian.*)

Elements of Hydraulic Apparatus, by B. F. Stupak, pp. 31–49. (*In Russian.*)

Differential Pressure Manometer Pickups for Pneumatic Power Compensation (Survey of Products of Foreign Firms), by S. B. Zasedatelev and V. A. Rukhadse, pp. 61–98. (*In Russian.*)

Compensating System Stabilizer; Hydraulic Motor Connected with Control Elements of the Main Hydraulic System, by S. A. Babushkin, pp. 112–121. (*In Russian.*)

Pneumatic Regulator Arrangement without Mechanical Separation, by G. T. Berezovets, pp. 122–126. (*In Russian.*)

On the Realization of Nonlinear Transformations in Pneumatic Systems with the Aid of Jet-Pipe Elements, by L. A. Zalmanson and A. I. Semikova, pp. 128–147. (*In Russian.*)

On the Possibility of Constructing Pneumatic Regulators with Automatic Adjustment to Load, by T. K. Berends and A. A. Tal, pp. 148–154. (*In Russian.*)

Pneumatic External Regulator of the Institut Automatiki i Telemekhaniki, Akademiia Nauk, SSSR, by Iu. I. Ostrovskii, pp. 155–165. (*In Russian.*)

On the Calculation of the Static Characteristics of Flapper Nozzles, by E. A. Andreeva, pp. 172–180. (*In Russian.*)

Results of Experimental and Theoretical Investigation of Control Devices of the Flapper Nozzle Type, by N. P. Shumskii, pp. 181–193. (*In Russian.*)

International Analog Computation Meeting 2nd, Strasbourg, Sept. 1–6, 1958, Proceedings, Brussels, Presses, Academique Europeennes, 1959, 501 pp.

Automatic Recycling of an Arbitrary Input Function, by E. A. Sevian, pp. 118–119.

The Effect of Saturation on the Various

Elements in a Feedback Control System Studies at the Analog Computer, by G. Camatini and A. Cupido, pp. 138–140.

Random Optimization by Analog Techniques, by R. R. Fabreau and R. Franks, pp. 437–443.

Devices for Automatic Plotting and Root Loci, by N. M. Mikhailov, pp. 472–480.

Theoretical Relations for Solution of the Problems of Statistical Dynamics by Means of Analog Techniques, by V. S. Pougatchev, pp. 481–485. (*In French.*)

Control Considerations for a Lunar Soft Landing, by Arnold Peske and George Swanlund, *Aero/Space Engng.*, vol. 20, no. 2, Feb. 1961, pp. 26–27.

Extremum Control of Objects with Inertia and of Unstable Objects, by V. V. Kazakevich, *Soviet Phys., Doklady*, vol. 5, no. 4, Jan.–Feb. 1961, pp. 658–661.

Reducing the Influence of Inertia in Extremum Regulation of *n*-th Order Objects, by V. V. Kazakevich, *Soviet Phys., Doklady*, vol. 5, no. 4, Jan.–Feb. 1961, pp. 662–665.

Extremal Control Processes with Dynamic Transformation and Memory Storage of the Input Signal when Perturbations are Present, by A. P. Yurkevich, *Soviet Phys., Doklady*, vol. 5, no. 4, Jan.–Feb. 1961, pp. 666–669.

Motion of a Gyroscopic Compass under the Action of Random Forces, by Ya. N. Roitenberg, *Soviet Phys., Doklady*, vol. 5, no. 4, Jan.–Feb. 1961, pp. 718–722.

Investigation of Third Order Contractor Control Systems with Zeros in Their Transfer Functions, by I. Flugge-Litz and T. Ishikawa, *NASA TN* D-719, Jan. 1961, 140 pp.

Flight Control Study of a Manned Reentry Vehicle, by *General Electric Co., Wright Air Dev. Div. Tech. Rep.* 60-695, vols. I and II, July 1960, 377 pp. 220 figs.

Flight Controller for Delta Space Research Vehicle, by Robert F. Donovan, *Applications and Industry*, no. 51, Nov. 1960, pp. 406–410.

Optimal Program for Correctional Maneuvers, by D. F. Lawden, *Astronautica Acta*, vol. 61, no. 4, 1960, pp. 195–205.

Astronavigation-Guidance and Control in Space, by Robert E. Roberson, *J. Astron. Sciences*, vol. 7, no. 4, Winter 1960, pp. 87–96.

Problem of Directional Stabilization of Large Guided Flying Bodies, by E. D. Geissler, *Raketentechnik und Raumfahrtforschung*, vol. 4, no. 4, Oct.–Dec. 1960, pp. 109–117. (*In German.*)

Electro-Hydraulic Controls in Space Vehicles and their Power Supplies, by C. R. Himmler, *Raketentechnik und Raumfahrtforschung*, vol. 4, no. 4, Oct.–Dec. 1960, pp. 118–126. (*In German.*)

Automatic Guidance Systems for Ballistic Rockets, by F. Mueller, *Raketentechnik und Raumfahrtforschung*, vol. 4, no. 4, Oct.–Dec. 1960, pp. 127–135. (*In German.*)

Instrumentation and Communications

Hypersonic Free Flight Research, Part I. Instrumentation Evaluation and Data Analysis, by R. W. Bogle and R. J. Magnus, *Wright Air Dev. Div., WADD TR* 59-708, July 1960, 40 pp.

Use of Fine Unheated Wires for Heat Transfer Measurements in the Shock Tube, by Walter H. Christiansen, *Calif. Inst. of Tech., Hypersonic Res. Project, Mem.* no. 55, June 1, 1960, 35 pp.

Piezoelectric Pressure Sensing Devices, by W. B. Farrand, *Stanford Res. Inst., Poulter Labs., Tech. Rep.* 010-60, July 1960, 25 pp.

Radio-Frequency Mass Spectrometer for the Investigation of the Ionic Composition of the Upper Atmosphere, by V. G. Istomin, *NASA Tech. Transl.* F-53, Jan. 1961, 21 pp.

Use of Moon or Satellite Relays for Global Communications, by L. P. Yeh, *Communication and Electronics*, no. 51, Nov. 1960, pp. 607–613.

Parametric Amplifier for Space Probe Tracking Used with Pioneer V, by C. F. Brett, *Electronics*, vol. 34, no. 4., Jan. 27, 1961, pp. 41–46.

A Receiving-Recording Device for Infrared Spectrometers, by M. A. Bramson and I. P. Konstantinov, *Instruments and Experimental Techniques*, no. 3, Dec. 1960, pp. 476–479.

A Spectropyrometer for Temperature Measurements with Respect to Monochromatic Infrared Radiation, by V. E. Finkel'shtein and N. G. Starunov, *Instruments and Experimental Techniques*, no. 3, Dec. 1960, pp. 480–482.

Pulse Method for the Measurements of Thermal Diffusivity of Metals, by Edwin L. Woisard, *J. Appl. Phys.*, vol. 32, no. 1, Jan. 1961, pp. 40–45.

Point Military-Industrial Electronic Test Equipment Symposium, 4th, Chicago, Ill., Sept. 4–15, 1960, Proceedings, Joint Sponsorship by Office of the Director of Defense Res. and Engng. and the Dept. of the Army Signal Corps, *conducted by Armour Res. Foundation of Ill. Inst. of Tech.*, 330 pp.

Hall-Effect Wattmeters, by D. P. Kanellokos, R. P. Schuck and A. C. Tods, pp. 12–28.

Hall-Effect Device for Electric Current Measurements, by H. Sipler, pp. 29–32.

A Circuit Design for Measurement of Low Frequency Noise, by R. E. Marshall and J. B. Martin, pp. 33–41.

Microwave Phase Lock Signal Generator Using Single Side Band Techniques, by F. J. Schmiedeler and A. Clavin, pp. 42–54.

A Microwave Calibration Test Set for a Seven Octave Band, by L. J. Castriota and E. N. Torgaw, pp. 55–94.

Temperature-Compensated Microwatt Power Motor, by E. E. Aslan, pp. 95–112.

Considerations in the Design of Two Millimeter Wave Components, by L. L. Berton, pp. 113–130.

An Automatic Device for Monitoring Ultra Stable RF Frequencies, by H. T. Mann and F. L. Walker, pp. 131–148.

Phase Intercept Distortion and Its Measurement, by P. F. Ordung and S. Segner, pp. 149–173.

Standardized Procedures for Determining Radio Receiver Resistance to Interference, by B. T. Newman, H. Cahn and R. G. Keyes, pp. 174–195.

The Measurement of Pulsed Signal Coherence, by R. H. Holman and R. B. Shields, pp. 196–222.

A Transfer Function Analyser, by A. S. Westneat and J. N. Brown, pp. 223–232.

A Test Set for Measuring the Performance of a Missile-Borne Transponder, by W. B. Wallenfels, pp. 233–251.

Failure Detection in Electronic Systems Through Continuous, Automatic Measurement of Signal Levels, by R. O. Segale and R. W. Thompson, pp. 252–280.

The Extension of Tape-Programmed Variable-Sequence Machines to Life Prediction, Fault Location and Performance Monitoring, by Z. Benin and W. H. Wobig, pp. 281–295.

Fault Prediction in Static Alert Systems, by F. L. Paulsen, pp. 296–312.

Study of Electronic Equipment Life Prediction, by A. T. Kneale, pp. 313–321.

Radio Wave Absorption of Several Gases in the 100 to 117 kMc/s Frequency Range, by C. O. Britt, C. W. Tolbert and A. W. Straiton, *J. Res. Nat. Bur. Standards, (D. Radio Propagation)*, vol. 65D, no. 1, Jan.–Feb. 1961, pp. 15–18.

A New Approach to the Mode Theory of VLF Propagation, by James R. Wait, *J. Res. Nat. Bur. Standards, (D. Radio Propagation)*, vol. 65D, no. 1, Jan.–Feb. 1961, pp. 37–46.

Magneto-Ionic Propagation Phenomena in Low- and Very Low-Radio-Frequency Waves Reflected by the Ionosphere, by J. Ralph Johler, *J. Res. Nat. Bur. Standards, (D. Radio Propagation)*, vol. 65D, no. 1, Jan.–Feb. 1961, pp. 53–66.

Characteristics of Waveguides for Long-Distance Transmission, by A. E. Karbowiak and L. Solymar, *J. Res. Nat. Bur. Standards, (D. Radio Propagation)*, vol. 65D, no. 1, Jan.–Feb. 1961, pp. 75–88.

A High-Resolution Rapid-Scan Antenna, by H. V. Cottony and A. C. Wilson, *J. Res. Nat. Bur. Standards, (D. Radio Propagation)*, vol. 65D, no. 1, Jan.–Feb. 1961, pp. 101–105.

The Dynamic Properties of Automatic Pulse Range-Finders with Two Integrators, by Ye. P. Nikitin and A. G. Saibel, *Radio Engng.*, vol. 15, no. 5, Nov. 1960, pp. 33–41.

On the Significance of Optimum Criteria and a Priori Distributions in the Theory of Signal Reception, by L. S. Gutkin, *Radio Engng. and Electronics*, vol. 4, no. 10, 1959, pp. 1–18.

Capacity of Certain Multi-Path Communication Channels, by B. S. Tsybakov, *Radio Engng. and Electronics*, vol. 4, no. 10, 1959, pp. 48–59.

Coding Stable with Respect to Fading (Anti-Fading Coding), by E. L. Blokh and A. A. Kharkevich, *Telecommunications (transl. of Elektrosvyaz')*, no. 4, 1960, pp. 361–366.

A Low-Resolution Unchopped Radiometer for Satellites, by R. A. Hanel, *NASA TN* D-485, Feb. 1961, 16 pp.

Microwave Reflectivity of Deposited Aluminum Films for Passive Relay Communications, by William F. Cuddihy and Lloyd H. Shreve, *NASA TN* D-664, Feb. 1961, 22 pp.

National Telemetering Conference, Santo Monica, Calif., May 23–25, 1960, Proceedings: Sponsored by *American Rocket Society, Amer. Inst. Elec. Engrs., Inst. Aeron Sciences, Instrument Soc. of America, Inst. Radio Engrs.*, National Telemetering Conference, 1960, 870 pp.

An Airborne Data Collection, Telemetering and Ground Data Processing System for Development Flight Test of an Orbital Type Space Vehicle, by A. B. Ellis, pp. 93–102.

United Space Telemetry-Acquistion Aid System, by H. D. Kickstein and J. T. Underhill, pp. 103–120.

Design of the Telemetry System of the Centaur Space Vehicle, by C. R. Cearley, pp. 121–130.

A Television System for a Soft Landed Lunar Vehicle, by P. J. Rousculp and W. S. Pope, pp. 131–144.

Preparations to Shift Telemetry Activity to the Microwave Region, by R. C. Barto, pp. 145–152.

Telemetry Operation in the 2200 Megacycle Band, by P. Weiss, pp. 153–160.

Theory and Application of a High Speed Data Interchange System, by G. D. Clark, pp. 161–168.

A Universal PCM Data Collection System, by M. W. Williard and V. A. Ratner, pp. 169–186.

A PDM-to-Digital Encoder and Digital Translator, by J. D. Gates and J. K. Baird, pp. 187–193.

Analog-Digital High Speed Data Processor for Flight Testing, by R. O. Plaisted, pp. 194–220.

PAM/PDM and Analog - Telemetry Data to Computer Tape via High Speed Microsadic, by D. C. Fox and R. L. Given, pp. 221–232.

Programming Techniques for Electronic Multiplexers of Vehicular PCM Data Acquistion Systems, by J. M. Walter Jr., pp. 233–250.

PCM Synchronization, by W. H. Seaver, pp. 251–260.

Evaluation of Techniques for PCM Range Telemetry, by D. G. Childers, pp. 271–290.

A Survey of PCM Progress, by R. L. Sink, pp. 261–270.

Design Measurement Back into Telemetry, by G. Birkel Jr., pp. 291–300.

Transducer Evaluation—A Space Age Tool, by G. Von Vick, pp. 301–316.

Force Sensing Transducers for Telemetering, by J. S. Hernandez, pp. 317–342.

A New Digital Shaft Encoder for Airborne or Ground Digital Measuring Systems, by H. Fleming, pp. 343–352.

An Application of Polarization Diversity for Improvement of Telemetry Performance, by A. G. Williams and J. M. Anderson, pp. 353–360.

Project Mercury World-Wide Telemetry and Display System, by D. Ferber, pp. 361–374.

Design Philosophy and Final System Configuration of the Minuteman FM/-FM Telemetry Ground Stations, by N. S. Rahal, pp. 375–388.

Problems Encountered in Converting Test Data from Analog to Digital for Processing, by R. N. Bacon, pp. 389–398.

Design Concepts for Atlas Operational Telemetry System, by J. Saugier, pp. 477–482.

Telemeter System for Operational Missile Evaluation, by A. W. Baker, pp. 483–488.

Predetection Storage of Telemetry Data Using Wide-Band Magnetic Tape Recorders, by R. E. Klokaw and C. M. Kartman, pp. 501–520.

Experimental Optimization and Evaluation of Telemetry Systems, by W. F. Link and C. D. Eatough, pp. 521–522.

Frequency Translation of FM Subcarriers, by O. J. Ott and W. P. McGarry, pp. 523–538.

A Microwave Modulation Telemetering System, by W. M. Kendrick and L. A. Peters, pp. 539–548.

Development of Packaging for Short Term High Temperature Exposure of Electronic Circuitry, by J. L. Nelson and P. Grosz, pp. 549–556.

Tangible returns FROM PURE RESEARCH have been gigantic

Pure research, stimulated by curiosity and the satisfaction of accomplishment, has given us knowledge and understanding of many of the phenomena of our world. The rapid exploitation of such discoveries, especially in this century, has resulted in our present amazing technology. These tangible returns from pure research have been gigantic. From the brilliant investigations of nineteenth-century physicists on the nature of electric and magnetic fields have developed electric power, electronics, radio, television. Examples from the past are countless. Even in recent decades we have witnessed enormous application of discoveries merely incidental to research in elementary-particle physics: isotopes, nuclear fission and power, medical therapy with high-energy beams, a step toward controlled thermonuclear power — a list that continues to grow rapidly.

The practical results that must derive from continued exploration . . . cannot be guessed. If the past is a guide they will be numerous and fantastic. The one thing that we have learned to expect from nature is to be surprised.

Excerpt: A special Report of the U.S. Atomic Energy Commission, January 1961 entitled, "Atomic Energy Research in the Life and Physical Sciences, 1960."

For employment information write
Personnel Director, Division 61-41

los alamos
scientific laboratory
OF THE UNIVERSITY OF CALIFORNIA
LOS ALAMOS, NEW MEXICO

A Technique for Temperature Measurement in the Cryogenic Realm, by H. P. Gallagher and B. D. Mallett, pp. 557–572.

The DIDAP-A Modern Data Processing System, by E. H. Claggett, pp. 573–596.

The Universal Computer Language Recorder - A General Tool for Telemetry Data Handling, by J. D. Bassett, pp. 597–608.

LMSD Data Conversion Facility, by R. H. Spitler, pp. 609–622.

Time Code Control of Data Processing, by O. D. Shelley, pp. 623–632.

Portable Data Handling System, by R. Ferrero, pp. 633–636.

Experience in Environmental Test of High Performance Telemetry, by R. A. Stahl, pp. 637–656.

Use of Variable Inductance Transducers in a Telemetry System, by M. J. Kopp, pp. 657–670.

A High Accuracy Temperature Telemeter System, by L. R. Phegley, pp. 671–682.

A Transistorized Direct Digital Encoder for High Altitude Balloon Research, by W. H. Starling and R. J. Cowie, pp. 683–690.

Progress Report on Transistorization of Telemetry Componentry, by H. Epstein, pp. 691–704.

The Development of Low-Level Electronic Multiplexer, by C. E. Griffin, J. Searcy and J. Knight, pp. 705–714.

Low Level Transistor DC Amplifier, by P. A. Michaels, pp. 715–728.

Multivolt-Controlled Subcarrier Oscillator, by M. Norris and D. Dry, pp. 729–744.

Telemetry System Performance Measurement of Error as a Function of Commutation Rate, by M. I. Lesnik and R. A. Porter, pp. 745–756.

Pre-transmission Analysis Cure for Telemetry's Growing Pains, by J. D. Yeagley and W. Godwin, pp. 757–770.

Transmission Response Data Reduction and a Unique Transient Wave Analyzer, by J. E. Anderson and W. Comley, pp. 783–800.

Wide Band Telemetry System for Missile Impact Instrumentation, by R. A. Gronlund, pp. 801–810.

Reliability Problems Associated with Telemetry Equipment Design, by M. J. Mozenter, pp. 811–820.

Techniques for Obtaining Realistic Reliability and Mean Time Between Failure Numbers for Telemetry Equipment, by M. A. Lowy, pp. 821–828.

A Comprehensive Reliability Test Program, by W. E. Courtwright, pp. 829–834.

Missile Telemetering Antenna, by Werner Koppl, pp. 835–848.

A Millimeter Wave Telemetry Antenna System, by D. Alstadter, W. G. Scott and T. W. Halloran, pp. 849–858.

Selected Topics on Ballistics, Cranz Centenary Colloquium, Univ. of Freiburg, 1958, Wilbur C. Nelson, ed., N. Y., Pergamon Press, for North Atlantic Treaty Organization, Advisory Group of Aeron. Res. and Dev. (AGARD), 1959, 280 pp.

Electronic and Optical Means of Observation of Guided Missiles and Satellites, by L. A. Delsasso, pp. 168–182.

Use of Satellites in Commercial Communications, by Leonard Jaffee, *Aero/Space Engng.*, vol. 20, no. 2, Feb. 1961, pp. 14–15.

Temperature Control by Means of the Peltier Effect, by E. L. Armi and C. G. Kirkpatrick, *Aircraft Engng.*, vol. 33, no. 383, Jan. 1961, pp. 12–15.

Radar Echoes Obtained from Earth Satellites 1957 Alpha and 1957 Beta, by W. E. Jaye, R. B. Dyce, and R. L. Leadabrand, *Planetary and Space Science*, vol. 5, no. 1, Jan. 1961, pp. 50–58.

Sudden Damping of Short Radio Waves in the Ionosphere (1938–1950), by G. M. Bartenev, *Telecommunications (transl. of Elektrosvyaz')*, no. 5, 1960, pp. 541–550.

Performance of Electrical Connectors at High Altitudes, by A. L. Coats, *Applications and Industry*, no. 51, Nov. 1960, pp. 337–338.

Laminar Junction Devices—New Concept in Microcircuits, by J. E. Allegretti and D. J. Shombert, *Electronics*, vol. 33, Dec. 2, 1960, pp. 55–57.

Radar Simulator Tests Moving-Target Indicators, by H. Lobenstein and A. R. Dial, *Electronics*, vol. 33, Dec. 2, 1960, pp. 58–60.

Microwave Instrument Measures Dielectric Constants, Equipment Features Direct Readout, by E. J. Luoma, *Electronics*, vol. 33, Dec. 2, 1960, pp. 71–73.

Solid-State Pulser Drives Chemical Pump, Silicon Controlled Rectifiers Replace Thyratron Circuit, by U. L. Upson, *Electronics*, vol. 33, Dec. 2, 1960, pp. 74–76.

High Temperature Mass Spectrometer Sample System, by H. M. Shin, H. K. Hahm, S. I. Kwon et al., *Rev. Sci. Instr.*, vol. 31, Nov. 1960, pp. 1200–1201.

On the Decrease of Gain of Receiving Aerials in Tropospheric Communication Lines, by B. S. Nadenenko and I. A. Gusyatinskii, *Telecommunications (transl. of Elektrosviaz')*, no. 12, 1959, pp. 1319–1328.

Bilateral Amplitude Modulation and Its Application to the Simultaneous Transmission of Two Signals, by B. M. Pevzner, *Telecommunications (transl. of Elektrosviaz')*, no. 12, 1959, pp. 1329–1342.

Instrument for Examining Aerial Radiation Patterns in Polar Coordinates, by V. O. Kobak, *Telecommunications (transl. of Elektrosviaz')*, no. 12, 1959, pp. 1411–1418.

A Thermistor Pressure Gauge, by A. P. Flanick and J. Ainsworth, *NASA TN* D-504, Nov. 1960, 13 pp.

The Dielectric Bolometer, a New Type of Thermal Radiation Detector, by R. A. Hanel, *NASA TN* D-500, Nov. 1960, 10 pp.

Cosmic Ray Measurements and Measuring Devices, by Ester Pereira, *California Institute of Technology, Jet Propulsion Laboratory, Literature Search* no. 230, Jan. 1960, 83 pp.

A Miniature Wafer-Style Pressure Transducer, by W. E. Smotherman, *AEDC Tech. Rep.* 60-11, Oct. 1960, 37 pp.

The Design and Evaluation of a Transistorized Current Amplifier with a Bandwidth of DC to 100 KC, by W. M. Crouch, *Arnold Engng. Dev. Center, ARO, Inc. (AEDC TN* 60-194), Oct. 1960, 27 pp.

NASA-Industry Program Plans Conference, 1st Proceedings, July 28–29, 1960, 23 pp.

Tracking and Data Acquisition, by Mr. Edmond C. Buckley, pp. 86–91.

Communications, by Max A. Lowry, ASTRONAUTICS, vol. 5, Nov. 1960, p. 31.

Instrumentation and Control, by John E. Witherspoon, ASTRONAUTICS, vol. 5, Nov. 1960, p. 37.

Designing Antennas to Include Parametric Amplifiers, Useful in Vicinity of 180 Mc., by A. D. Frost, *Electronics*, vol. 33, Nov. 18, 1960, pp. 96–97.

Precision Ultrasonic Velocity Measurements, with a Sing-Around System, by R. L. Forgacs, *Electronics*, vol. 33, Nov. 18, 1960, pp. 98–100.

Oscilloscope Bar Chart Monitors Sixty Channels, Missile Operation Data Plotted on 17-inch Chart, by E. R. Jablonski, *Electronics*, vol. 33, Nov. 18, 1960, p. 101.

A Transducer for the Measurement of Heat-Flow Rate, by Robert Gardon, *J. Heat Transfer (ASME Trans.)*, vol. 82c, no. 4, Nov. 1960, pp. 396–398.

Journal of Research of the National Bureau of Standards (D. Radio Propagation), Report of the U. S. National Committee to the 13th General Assembly, International Scientific Radio Union, London, Sept. 5–15, 1960, vol. 64 D, Nov.-Dec. 1960.

Commission 1. Radio Measurement Methods and Standards: Review of Developments, p. 591.

Frequency and Time Interval, by E. A. Gerber, p. 592.

RF and Microwave Power Measurements, by G. F. Engen, p. 596.

Impedance Measurements and Standards, by G. S. Deschamps, p. 598.

Development in Attenuation Measurements and Standards, by Bruno O. Weinschel, p. 599.

Noise Measurements and Standards, by B. M. Oliver, p. 601.

Field Strength Measurements, by M. C. Selby, p. 603.

Measurements of Physical Quantities by Radio Techniques, by M. C. Thompson Jr., p. 605.

Commission 2. Tropospheric Radio Propagation: National Committee Report, p. 607.

Commission 3. Ionospheric Radio Propagation: Review of U. S. A. Activity, 1957–59, p. 629.

Ionospheric Propagation Research with Communication Systems Applications, p. 633.

Commission 4. Radio Noise of Terrestrial Origin: Report of U. S. Commission 4, URSI (1957–1960), p. 637.

Commission 5. Radio Astronomy: Review of Developments, p. 655.

Commission 6. Radio Waves and Circuits: Subcommission 6.1. Information Theory: Part I. Information Theory and Coding, by P. Elias, p. 671.

Part 2. Random Processes, by P. Swerling, p. 674.

Part 3. Pattern, by Arthur Gill, p. 676.

Part 4. Detection Theory, by Robert Price, p. 678.

Part 5. Prediction and Filtering, by L. A. Zadeh, p. 681.

Subcommisssion 6.2. Circuit Theory, by Louis Weinberg, p. 687.

Subcommission 6.3. Antennas and Waveguides: Part 1. Diffraction and Scattering, by L. B. Felsen and K. M. Siegel, p. 707.

Part 2. On Multiple Scattering of Waves, by V. Twersky, p. 715.

Part 3. Antennas, by R. W. Bickkore and R. C. Hansen, p. 731.

A Bibliography on Coherence Theory, by G. B. Parrent Jr., p. 742.

A Bibliography of Automatic Antenna Data Processing, by C. J. Drane, p. 743.

Surface and Leaky Wave Antennas, by F. J. Zucker, p. 746.

Commission 7. Radio Electronics: 1. Parametric Amplifiers, by P. K. Tien and H. Heffner, p. 751.

Microwave Properties of Ferrites, by P. K. Tien and B. Lax, p. 755.

Progress in Solid-State Masers, by A. Siegman, p. 758.

Low-Noise Beam-Type Microwave Tubes, by L. Smullin, p. 763.

Interaction Between Plasmas and Electromagnetic Fields, by L. Smullin, p. 766.

Commisssion 2. Tropospheric Radio Propagation, Figure 1. Attenuation Due at One Atmosphere, p. 610.

Commission 6, Radio Waves and Circuits. Subcommisssion 6.2, Circuit Theory Figure 1. Chain of Five 1-ohm Resistances Realizing the Given Impedance Matrix, p. 692.

Association Between Aurorae and Very Low-Frequency Hiss Observed at Byrd Station, Antarctica, by L. H. Martin, R. A. Helliwell and K. R. Marks, *Nature,* vol. 187, no. 4739, Aug. 27, 1960, pp. 751–753.

New Technical Radiation Pyrometer, with Special Consideration of Its Optical Construction, by Fritz Lieneweg and Alfred Schaller, *Appl. Scientific Res.,* section B, vol. 8, no. 4, 1960, pp. 241–245. (*In German.*)

Orientation of Solar Instruments in Space, Photodetectors Position Rocket Nose Cones, by C. H. Reynolds and M. Reisbeck, *Electronics,* vol. 33, no. 52, Dec. 23, 1960, pp. 43–47.

An Optical Method for Measuring Uniformity in Plastics, by R. M. Eichhorn, *I/EC* (*Ind. Engng. Chem.*) vol. 53, no. 1, Jan. 1961, pp. 67–70.

Measurement of Thermal Conductivity by Utilization of the Peltier Effect, II. Correction for Wire Radiation and Determination of Specimen Radiation Emissivity, by R. Simon, R. T. Bate and E. H. Lougher, *J. Appl. Phys.,* vol. 31, no. 12, Dec. 1960, p. 2160.

Bourdon Tube Deflection Characteristics, by P. G. Exline, *J. Basic Engng.,* (*ASME Trans., Series D*), vol. 82, no. 4, Dec. 1960, pp. 887–893.

Ultrasonic Gaging Increases Fuel Loading Accuracy, by John A. Herbst and Edward P. Schinman, *Missiles and Rockets,* vol. 7, no. 25, Dec. 19, 1960, pp. 21–22.

The Effect of a Strong Interference Signal on a Radio Receiver Input, by L. M. Kononovich, *Radio Engng.* (*transl. of Radiotekhnika*), vol. 14, no. 11, July 1960, pp. 24–33.

A Method of Evaluating the Intensity of Radio Signals Reflected from the Surface of the Moon, by M. P. Dopukhanov, *Radio Engng.* (*transl. of Radiotekhnika*), vol. 15, Nov. 1960, pp. 5–11.

Questions of Potential Interference Resistance when the Signal Fades, by D. D. Klovskii, *Radio Engng.* (*transl. of Radiotekhnika*), vol. 15, Nov. 1960, pp. 24–35.

The Passage of High-Frequency Pulses Through Linear Systems with Delay Feedbacks, by A. I. Nedeshev, *Radio Engng.* (*transl. of Radiotekhnika*), vol. 15, Nov. 1960, pp. 36–40.

The Effectiveness of Methods of Increasing the Dynamic Range of a Panoramic Radio Receiver, by N. I. Svetlov, *Radio Engng.* (*transl. of Radiotekhinka*), vol. 15, Nov. 1960, pp. 41–46.

A Theory of Incoherent Scattering of Radio Waves by a Plasma, by J. P. Dougherty and D. T. Farley, *Roy. Soc. London, Proc.* (*Series A, Math. & Phys. Sciences*) vol. 259, no. 1296, Nov. 22, 1960, pp. 79–99.

Uniqueness of the Solution to Fredholm's Integral Equations of the First Kind in Antenna Theory, by N. N. Govorun, *Soviet Phys., Doklady,* vol. 5, no. 3, Nov.–Dec. 1960, pp. 509–512.

Electromagnetic Waves in a Spiral Waveguide with an Anisotropic Dielectric, by V. P. Shestopalov, V. A. Slyusarskii, S. D. Andrenko, etc., *Soviet Phys., Tech. Phys.* (*transl. of Zhurnal Tekhnicheskoi Fiziki*) vol. 5, no. 6, Dec. 1960, pp. 606–614.

Application of a Vibrating Probe in the Simulation of Fields by the Induced-Current Technique, by G. M. Gershtein, *Soviet Phys., Tech. Phys.* (*transl. of Zhurnal Tekhnicheskoi Fiziki*) vol. 5, no. 6, Dec. 1960, pp. 688–690.

Radio Transmission through the Plasma Sheath around a Lifting Reentry Vehicle, by Macon C. Ellis Jr. and Paul W. Huber, *NASA TN* D-507, Jan. 1961, 22 pp.

Eight-Level Pulse-Height Analyzer for Space Physics Applications, by U. D. Desai, R. L. Van Allen and G. Porreca, *NASA TN* D-666, Jan. 1961, 13 pp.

Observation of an Artificial Satellite by the Expectation Method, by V. M. Vakhnin and V. V. Beletskiy, *NASA Tech. Transl.* F-48, Nov. 1960, 10 pp.

High-Temperature Resonant-Cavity Dielectrometer, Measures Space Vehicle Radome, by R. W. Sutton and N. Grechny Jr., *Electronics,* vol. 34, no. 1, Jan. 6, 1961, pp. 118–119.

A Gas Analyzer Based on Measurements of Thermal Conductivity in the Pressure Range 5–10 mm Hg, by D. B. Diatroptov, *Instruments and Experimental Techniques,* no. 2, Dec. 1960, pp. 324–325.

Swept Langmuir Probe System for Intense Gas Discharges, by H. W. Jones and P. A. H. Saunder, *J. Sci. Instruments,* vol. 37, no. 12, Dec. 1960, pp. 457–459.

Temperature-Control System for Use with a Spectrophotometer, by S. W. Thorne, *J. Sci. Instruments,* vol. 37, no. 12, Dec. 1960, pp. 478–479.

Evaluation of Detection Characteristics with Quadratic Signal Summation, by V. G. Sragovich, *Radio Engng. and Electronics* (*transl. of Radiotekhnika i Elektronika*), vol. 5, no. 4, 1960, pp. 1–8.

Optimal Phase Methods of Signal Detection, by B. R. Levin, *Radio Engng. and Electronics* (*transl. of Radio tekhnika i Elektronika*), vol. 5, no. 4, 1960, pp. 9–17.

Limiting Threshold of Sensitivity of Thermal Radio-Radiation Reception, by A. A. Krasovskii and V. N. Zuikov, *Radio Engng. and Electronics* (*transl. of Radiotekhnika i Elektronika*), vol. 5, no. 4, 1960, pp. 18–27.

Experiments with Plasmas Produced by Potassium-Seeded Cyanogen Oxygen Flames for Study of Radio Transmission at Simulated Re-entry Vehicle Plasma Conditions, by Paul W. Huber and Paul B. Gooderum; **Appendix A: Preliminary Attenuation Measurements of 219.5-mc Propagation through the Plasma,** by Theo E. Sims and Duncan E. McIver Jr.; **Appendix B: Diagnostic and Transmission Studies of the Plasma Using Microwave Techniques,** by Joseph Burlock and William L. Grantham, *NASA TN* D-627, Jan. 1961, 71 pp.

Development of Instrumentation for a Hyper-Velocity Range, by P. L. Clemens and M. K. Kingery, *Arnold Engng. Dev Center, ARO, Inc.* Dec. 1960, 57 pp. (*AEDC-TN* 60-230).

Hypervelocity Arc-Tunnel Instrumen-

Dynamics Engineers

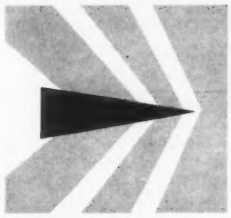

Space Technology Laboratories, Inc. has immediate openings, in the Dynamics Department of its Engineering Mechanics Laboratory, for:

Research Engineer to work both development and basic research problems in the general field of Applied Mechanics.

Dynamics Engineer to direct and follow work done by other companies, as well as solve specific problems in the general field of rigid body and elastic body mechanics.

These positions require training and experience in one or more of the following: structural dynamic response • shock wave, blast phenomena and vibrations • aerodynamic loadings, flutter, and hydrodynamics • control system dynamics • applied mathematics and statistical analysis • viscoelasticity and plasticity.

STL is an expanding organization with a professional staff of more than 1,500 scientists and engineers engaged in advanced space, missile and electronic programs.

Resumes directed to Dr. R. C. Potter will receive careful attention.

SPACE TECHNOLOGY LABORATORIES, INC.

a subsidiary of Thompson Ramo Wooldridge Inc.

P.O. Box 95005C, Los Angeles 45, California

CAREERS IN SPACE TECHNOLOGY LEADERSHIP

tation, by W. T. Earheart Jr. and D. S. Bynum, *Arnold Engng. Dev. Center, AEDC TN* 60-227, Dec. 1960, 38 pp.

Progress Report on Development of Telemetry for a Hypervelocity Range, by M. K. Kingery, R. H. Choate and R. P. Young, *Arnold Engng. Deve. Center, AEDC-TN* 60-214, Dec. 1960, 86 pp.

Concerning a Method for the Measurement of Very High Temperatures in Nearly Transparent Arc Columns, by Rudolf Wilhelm Larenz, *NASA Tech. Transl.* F-54, Dec. 1960, 20 pp.

A Photo-Electric Device for the Measurement of Quantity of Liquid, by R. Sandri, *Canada, National Res. Council, Div. of Mech. Engng., NRC* M1-822, Sept. 1960, 5 pp., 2 figs.

The Javelin Spike Antenna; Radiation Patterns and Voltage Standing-Wave Ratio, by Roland R. Ford, *NASA TN* D-565, Jan. 1961, 20 pp.

Method of Studying Travel Time Anomalies of High Frequency Radio Waves, by Gordon Lerfald and Paul Scheibe, *Rev. Sci. Instruments,* vol. 31, no. 12, Dec. 1960, pp. 1309–1311.

A Deformation Calorimeter, by Robin O. Williams, *Rev. Sci. Instruments,* vol. 31, no. 12, Dec. 1960, pp. 1336–1340.

Optimum Frequency Selection for Interplanetary Communication, by S. Chandra, *J. Brit. Interplan. Soc.,* vol. 17, no. 10, July–Aug. 1960, pp. 362–365.

Scattering Properties of Large Spheres, by N. A. Logan, *IRE Proceedings,* vol. 48, no. 10, Oct. 1960, p. 1782.

Scattering by a Spherical Satellite, by E. M. Kennaugh, S. P. Morgan and H. Weil, *IRE Proceedings,* vol. 48, no. 10, Oct. 1960, p. 1781.

A 75-cm Receiver for Radio Astronomy and Some Observational Results, by C. L. Seeger, F. L. H. M. Stumpers and N. van Hurck, *Phillips Tech. Rev.* ,vol. 21, no. 11, Sept. 1960, pp. 317–348.

Thermoelectricity, including the Proceedings of the Conferences on Thermoelectricity sponsored by the Naval Research Lab., Sept. 1958, Paul H. Egli, ed., N. Y., John Wiley & Sons, 1960, 407 pp.

Thermal Property Measurements, by Kenneth G. Skinner, pp. 358–386.

A Small-Bore Pick-Up for the Measurement of Fluctuating Pressures, by R. E. Franklin and R. B. Archbold, *Aeron. Qtly.,* vol. 9, part 4, Nov. 1960, pp. 348–354.

A Harmonic Generator and Detector for the Short Millimeter Wave Region, by H. W. de Wijn, *Appl. Scientific Res.* Section B, vol. 8, no. 4, 1960, pp. 216–264.

Radiation of Pulses Generated by a Vertical Electric Dipole Above a Plane, Non-conducting, Earth, by A. T. de Hoop and H. J. Frankena, *Appl. Scientific Res.,* section B, vol. 8, no. 4, 1960, pp. 39–377.

Air-to-Ground Meteoric Scatter Communication System, by A. J. Hannum, G. L. Evans, J. T. Chambers and K. Otten, *IRE Trans. on Comm. Sys.,* vol. CS-8, no. 2, June 1960, pp. 113–133.

Applications of Large Scintillation Detectors to Cosmic Ray Experiments, by G. W. Clark, *IRE Trans. on Nuclear Science,* vol. NS-7, no. 2–3, June–Sept. 1960, pp. 164–369.

Atmospheric and Space Physics

A Variable Atmospheric-Density Model From Satellite Accelerators, by L. G. Jacchia, *J. Geophys. Res.,* vol. 65, no. 9, Sept. 1960, pp. 2775–2782.

Direct Measurement of Particles Producing Visible Auroras, by C. E. McIlwain, *J. Geophys. Res.,* vol. 65, no. 9, Sept. 1960, pp. 2727–2747.

Large-Scale Auroral Motions and Polar Magnetic Disturbances. I. A Polar Disturbance at about 1100 Hours on 23 September 1957, by S. Akasofu, *J. Atmospheric and Terrestrial Phys.,* vol. 19, no. 1, Sept. 1960, pp. 10–25.

The Height and Geometry of Auroral Radio Echoes, by C. D. Watkins, *J. Atmospheric and Terrestrial Phys.,* vol. 19, no. 1, Sept. 1960, pp. 1–9.

The Structure of the Active Chromosphere, by M. Waldmeier, *Zeitschrift für Astrophysik,* vol. 50, no. 4, Sept. 19, 1960, pp. 225–232. (*In German.*)

The Fifty-First Kelvin Lecture: "Cosmic Radiation," by C. F. Powell, *Inst. Elec. Engrs., Proceedings, Part B, Radio and Electronic Engng.,* vol. 107, no. 35, Sept. 1960, pp. 389–394.

Calculations of Cosmic-Ray Trajectories near the Equator, P. J. Kellogg, *J. Geophys. Res.,* vol. 65, no. 9, Sept. 1960, pp. 2701–2703.

Observations of Solar Flare Radiation and Modulation Effects at Balloon Altitudes, July 1959, by A. Ahmert, H. Erbe, G. Pfotzer, C. D. Anger and R. R. Brown, *J. Geophys. Res.,* vol. 65, no. 9, Sept. 1960, pp. 2685–2694.

Low-Energy Solar Cosmic Rays and the Geomagnetic Storm of May 12, 1959, by J. R. Winckler and P. D. Bhavsar, *J. Geophys. Res.,* vol. 65, no. 9, Sept. 1960, pp. 2637–1655.

Comparison of Solar Cosmic Ray Injections Including July 17, 1959, and May 4, 1960, by K. G. McCracken and R. A. R. Palmeira, *J. Geophys. Res.,* vol. 65, no. 9, Sept. 1960, pp. 2673–2683.

The Age of the Elements in the Solar System, by J. H. Reynolds, *Scientific Amer.,* vol. 203, no. 5, Nov. 1960, pp. 171–182.

Neutrino and Cosmology, by A. Peres, *Progress of Theoretical Phys.,* vol. 24, no. 1, July 1960, pp. 149–154.

Audio-Frequency Electromagnetic Radiation in the Auroral Zone, by G. Gustafsson, A. Egeland and J. Arrons, *J. Geophys. Res.,* vol. 65, no. 9, Sept. 1960, pp. 2749–2758.

The Exosphere and Upper *F* Region, by F. S. Johnson, *J. Geophys. Res.,* vol. 65, no. 9, Sept. 1960, pp. 2571–2575.

Structure of the Earth's Exosphere, by F. S. Singer, *J. Geophys. Res.,* vol. 65, no. 9, Sept. 1960, pp. 2577–2580.

Outer Radiation Belt and Solar Proton Observations with Explorer VII during March–April 1960, by J. A. Van Allen and W. C. Lin, *J. Geophys. Res.* vol. 65, no. 9, Sept. 1960, pp. 2998–3003.

A Note on Harmonic Analysis of Geophysical Data with Special Reference to the Analysis of Geomagnetic Storms, by M. Sugiura, *J. Geophys. Res.,* vol. 65, no. 9, Sept. 1960, pp. 2721–2725.

Geomagnetic Storm Sudden-Commencement Rise Time, by A. J. Dessler, W. E. Francis and E. N. Parker, *J. Geophys. Res.,* vol. 65, no. 9, Sept. 1960, pp. 2715–2719.

Equatorial Spread-*F* and *F*-Layer Heights, by A. J. Lyon, N. J. Skinner and R. W. Wright, *Nature,* vol. 187, no. 4743, Sept. 24, 1960, pp. 1086–1088.

The Electron Density Distribution Derived from Whistler Data and Faraday-Fading Observations, by K. H. Schmelovsky, *J. Atmospheric and Terrestrial Phys.*' vol. 19, no. 1, Sept. 1960, pp. 68–71.

The Electron Content and Distribution in the Ionosphere, by T. G. Hame and W. D. Stuart, *IRE, Proceedings,* vol. 48, no. 10, Oct. 1960, pp. 1786–1787.

Effects of Vertical Diffusion of Electrons Near the Magnetic Equator, by E. R. Schmerling, *Nature,* vol. 188, no. 4745, Oct. 8, 1960, pp. 133–134.

Some Characteristics of Ionospheric Backscatter Observed at 440 Mc/s, by V. C. Pineo, L. G. Kraft and H. W. Briscoe, *J. Geophys. Res.,* vol. 65, no. 9, Sept. 1960, pp. 2629–2633.

Comment on Models of the Ionosphere Above $h_{max}F_2$, by J. W. Wright, *J. Geophys. Res.,* vol. 65, no. 9, Sept. 1960, pp. 2595–2596.

A Sounding Rocket Measurement of Electron Densities to 1500 Kilometers, by W. W. Berning, *J. Geophys. Res.,* vol. 65, no. 9, Sept. 1960, pp. 2589–2594.

Electron-Density Distribution in the Upper Ionosphere from Rocket Measurements, by J. S. Nisbet, *J. Geophys. Res.,* vol. 65, no. 9, Sept. 1960, pp. 2597–2599.

Electron Densities to 5 Earth Radii Deduced from Nose Whistlers, by R. L. Smith and R. A. Helliwell, *J. Geophys. Res.,* vol. 65, no. 9, Sept. 1960, p. 2583.

Radio Propagation Measurements Using the Explorer VI Satellite, by C. D. Graves, *J. Geophys. Res.,* vol. 65, no. 9, Sept. 1960, pp. 2585–2587.

The Determination of Ionospheric Electron Content from Satellite Doppler Measurements. 2. Experimental Results, by W. J. Ross, *J. Geophys. Res.,* vol. 65, no. 9, Sept. 1960, pp. 2607–2615.

Radio-Wave Scattering by an Ionized Gas in Thermal Equilibrium, by J. A. Fejer, *J. Geophys. Res.,* vol. 65, no. 9, Sept. 1960, pp. 2635–2636.

The Effect of the Region of Reflection on the Scattering of Radio Waves in the Ionosphere, by N. G. Denisov, *Izvestia V. V. Z. Radiofizika, USSR,* vol. 3, no. 2, March–April 1960, pp. 208–215. (Abstracted in *Electronics Express,* vol. 3, no. 2, Sept. 1960, pp. 39–40.)

Use of the Incoherent Scatter Technique to Obtain Ionospheric Temperatures, by T. E. Van Zandt and K. L. Bowles, *J. Geophys. Res.,* vol. 65, no. 9, Sept. 1960, pp. 2627–2628.

***F*-Region Traveling Disturbances and Sporadic-*E* Ionization,** by L. H. Heisler and J. D. Whitehead, *J. Geophys. Res.,* vol. 65, no. 9, Sept. 1960, pp. 2767–2773.

Polarization and Angular Extent of the 960-Mc/Sec Radiation from Jupiter, by V. Radhakrishnan and J. A. Roberts, *Phys. Rev. Letters,* vol. 4, no. 10, May 16, 1960, pp. 493–494.

The Origin of Meteorites, by B. Mason, *J. Geophys. Res.,* vol. 65, no. 9, Sept. 1960, pp. 2965–2970.

Weather Radar Observations from an Earth Satellite, by J. E. Keigler and L. Krawitz, *J. Geophys. Res.,* vol. 65, no. 9, Sept. 1960, pp. 2793–2808.

The Distribution of Cosmic-Ray-Produced Rare Gases in Iron Meteorites, by P. Signer and A. O. Nier, *J. Geophys. Res.* vol. 65, no. 9, Sept. 1960, pp. 2947–2964.

The Spectrum of an Asteroidal Meteor Fragment, I. Halliday, *Astrophys. J.,* vol. 132, no. 2, Sept. 1960, pp. 482–485.

The Duration of Intense Bombardment Processes on the Moon, by H. C. Urey, *Astrophys. J.,* vol. 132, no. 2, Sept. 1960, pp. 502–503.

Faraday Rotation Observations of the

Electron Content of the Exosphere, by R. B. Dyce, *J. Geophys. Res.*, vol. 65, no. 9, Sept. 1960, pp. 2617–2618.

Radar-Lunar Investigations at a Low Geomagnetic Latitude, by G. H. Millman, A. E. Sanders and R. A. Mather, *J. Geophys. Res.*, vol. 65, no. 9, Sept. 1960, pp. 2619–2626.

Surface Conditions on the Nearest Planets, by E. J. Opik, *Amer. J. Phys.*, vol. 28, no. 7, Oct. 1960, pp. 618–622.

The Problem of Pressure Broadening in Solar Balmer Hydrogen Lines, by R. Cayrel and G. Traving, *Zeitschrift für Astrophysik*, vol. 50, no. 4, Sept. 19, 1960, pp. 239–252. (*In German.*)

Architecture on the Moon, by B. F. Sugerman, *Georgia Tech. Engineer*, vol. 22, no. 1, Oct. 1960, pp. 14–15, 30, 39.

World-Wide Characteristics of Geomagnetic Micropulsations, by J. A. Jacobs and K. Sinno, *Geophys. J.* (*Roy. Astron. Soc.*) vol. 3, no. 3, Sept. 1960, pp. 333–353.

The Effect of the Initial Phase Magnetic Storm Upon the Outer Van Allen Belt, by J. M. Malville, *J. Geophys. Res.*, vol. 65, no. 9, Sept. 1960, pp. 3008–3010.

Geomagnetic Storms and the Space Around the Earth, by S. Chapman, *Nature* vol. 187, no. 4740, Sept. 3, 1960, pp. 824–827.

A Theory of Polar Geomagnetic Storms, by J. H. Piddington, *Geophys. J.* (*Roy. Astron. Soc.*), vol. 3, no. 3, Sept. 1960, pp. 314–332.

Cosmical Electrodynamics, by H. Alfven, *Amer. J. Phys.*, vol. 28, no. 7, Oct. 1960, pp. 613–618.

The Novo Urei Meteorite, by A. E. Ringwood, *Geochimica et Cosmochimica Acta*, vol. 20, no. 1, Sept. 1960, pp. 1–4. (*In English.*)

Cosmogenic Nuclear Reactions in Iron Meteorites, by D. E. Fisher and O. A. Schaeffer, *Geochimica et Cosmochimica Acta*, vol. 20, no. 1, Sept. 1960, pp. 5–14. (*In English.*)

Solar Cosmic Rays and Soft Radiation Observed at 5,000,000 Kilometers from Earth, by R. L. Arnoldy, R. A. Hoffman and J. R. Winckler, *J. Geophys. Res.*, vol. 65, no. 9, Sept. 1960, pp. 3004–3007.

The Infrared Reflectivity of a Planetary Atmosphere, by J. S. Goldstein, *Astrophys. J.*, vol. 132, no. 2, Sept. 1960, pp. 473–481.

The Physical State of Condensed Matter and the Radius of a Cold Planetary Body, by R. P. Singh and N. S. Goel, *Zeitschrift für Astrophysik*, vol. 50, no. 4, Sept. 19, 1960, pp. 269–277. (*In English.*)

A Direct Experimental Confirmation of the Second Postulate of the Special Theory of Relativity, by A. M. Bonch-Bruevich, *Optics and Spectroscopy*, vol. 9, no. 1, July 1960, p. 73.

Some Recent Experimental Tests of the Clock Paradox, by C. W. Sherwin, *Phys. Rev.*, vol. 120, no. 1, Oct. 1, 1960, pp. 17–21.

Interior Schwarzschild Solutions and Interpretation of Source Terms, by R. Arnowitt, S. Deser and C. W. Misner, *Phys. Rev.*, vol. 120, no. 1, Oct. 1, 1960, pp. 321–324.

Gravitational-Electromagnetic Coupling and the Classical Self-Energy Problem, by R. Arnowitt, S. Deser and C. W. Misner, *Phys. Rev.*, vol. 120, no. 1, Oct. 1, 1960, pp. 313–320.

Theory of Matter with Super Light Velocity, by S. Tanaka, *Progress of Theoretical Phys.*, vol. 24, no. 1, July 1960, pp. 171–200.

The Determination of Ionospheric Electron Content from Satellite Doppler Measurements. 1. Method of Analysis, by W. J. Ross, *J. Geophys. Res.*, vol. 65, no. 9, Sept. 1960, pp. 2601–2606.

Ionosphere Information from Satellite Signals, by G. H. Munro, *Nature*, vol. 187, no. 4742, Sept. 17, 1960, pp. 1017–1018.

Coupling of the Solar Wind and the Exosphere, by C. P. Sonett, *Phys. Rev. Letters*, vol. 5, no. 2, July 15, 1960, p. 46.

Observations of Solar Cosmic Rays near the North Magnetic Pole, by K. A. Anderson and D. C. Enemark, *J. Geophys. Res.*, vol. 65, no. 9, Sept. 1960, pp. 2657–2671.

Temperatures Reached in Electrical Discharges in the Solar Atmosphere, by C. E. R. Bruce, *Nature*, vol. 187, no. 4740, Sept. 3, 1960, p. 865.

Diffusion in the Sun, by L. H. Aller and S. Chapman, *Astrophys. J.*, vol. 132, no. 2, Sept. 1960, pp. 461–472.

Electromagnetic Radiation from Extra-Terrestrial Sources, by H. Friedman, *Amer. J. Phys.*, vol. 28, no. 7, Oct. 1960, pp. 622–626.

Sunspot-Cycle Variations in the Discrepancies between Predicted and Observed Frequencies for Use in Radio-Communication, by R. J. Hitchock, G. O. Evans and R. Naismith, *Inst. Elec. Engrs., Proceedings, Part B. Radio and Electronic Engng.*, vol. 107, no. 35, Sept. 1960, pp. 423–426.

Origin of Tektites (Author's reply), by H. C. Urey, *Nature*, vol. 187, no. 4740, Sept. 3, 1960, pp. 855–857.

Comparison of the Chemical Composition and Magnetic Properties of Tektites and Glasses Formed by Fusion of Terrestrial Rocks, by J. Friedman, A. Thorpe and F. E. Senftle, *Nature*, vol. 187, no. 4743, Sept. 24, 1960, pp. 1089–1092.

Correlation of an Auroral Arc and a Subvisible Monochromatic 6300 A Arc with Outer-Zone Radiation on November 28, 1959, by B. J. O'Brien, J. A. Van Allen, F. E. Roach and C. W. Gartlein, *J. Geophys. Res.*, vol. 65, no. 9, Sept. 1960, pp. 2759–2766.

Electrons of the Van Allen Radiation, by P. J. Kellogg, *J. Geophys. Res.*, vol. 65, no. 9, Sept. 1960, pp. 2705–2713.

Development of Multiple Radiation Zones on October 18, 1959, by B. J. O'Brien and G. H. Ludwig, *J. Geophys. Res.*, vol. 65, no. 9, Sept. 1960, pp. 2695–2699.

Bomb-Excited Whistlers, by B. A. Lippman, *IRE, Proceedings*, vol. 48, no. 10, October 1960, pp. 1778–1779.

Whistler Dispersion and Exospheric Hydrogen Ions, by R. E. Barrington and T. Nishizaki, *J. Geophys. Res.*, vol. 65, no. 9, Sept. 1960, pp. 2581–2582.

Observations of Whistlers and Chorus at the South Pole, by L. H. Martin, *Nature*, vol. 187, no. 4742, Sept. 17, 1960 pp. 1018–1019.

International Geophysical Year Information Bulletin No. 7 (Moscow 1959), *NASA Tech. Transl. F-50*, Nov. 1960, 54 pp.

The Dependence of the Frequency of Appearance of Noctilucent Clouds Upon the Date and the Geographical Latitude, by V. V. Sharonov pp. 1–6.

On the Control of Permanency of Airglow Transparency, by L. M. Fishkova, pp. 7–9.

A Study of Movements (of Winds) in the F_2 Layer by the Phase Method, Taking into Account the Anisotropy of the Form and the Variability of Heterogeneities, by V. D. Gusev and S. F. Mirkotan, pp. 10–14.

Foreign Methods of Observations. Geophysical Research Carried Out with Rockets and Artificial Earth Satellites in the United States in Accordance with the Program of the International Geophysical Year, by M. G. Kroshkin, pp. 15–54.

Proceedings of the International Symposium on Magneto-Fluid Dynamics, *Rev. Modern Phys.*, vol. 32, no. 4, Oct. 1960.

Idealized Problems of Plasma Dynamics Relating to Geomagnetic Storms, by Sydney Chapman, pp. 919–933.

Theory of Sudden Commencements and of the First Phase of a Magnetic Storm, by V. C. A. Ferraro, pp. 934–940.

On the Magnetodynamic and Adiabatic Equilibrium of a Gaseous Mass with a Uniform Rotational and Gravitational Motion, by Cataldo Agostinelli, pp. 941–946.

Geophysical Effects of the Trapped Particle Layer, by Robert Jastrow, pp. 947–950.

Relations between Plasma Physics and Astrophysics, by L. Biermann, p. 1008.

Energy Balance and Confinement of a

CHANGE-OF-ADDRESS NOTICE

In the event of a change of address, it is necessary to include both your old and new addresses, as well as your membership number and coding, when notifying ARS headquarters, in order to insure prompt service. If you are moving or have moved, send the following form to Membership Dept., American Rocket Society, 500 Fifth Ave., New York 36, N. Y.:

Name_____

Membership Card No._____ Coding_____

Old Address_____

_____

New Address_____

_____

Magnetized Plasma, by B. Lehnert, pp. 1012–1019.

Polar, Magnetic, Auroral and Ionospheric Phenomena, by E. H. Vestine, pp. 1020–1028.

Diffusion of Sound Waves in a Turbulent Atmosphere, by Richard H. Lyon, *NASA TN* D-456, Sept. 1960, 24 pp.

A Synoptic Radiation Study, by John L. Gergen, *Univ. Minnesota, School of Physics, Tech. Rep.* AP-16, Oct. 1960, 274 pp.

Recent Direct Measurements by Satellites of Cosmic Dust in the Vicinity of the Earth, by H. E. LaGow and W. M. Alexander, *NASA TN* D-488, Sept. 1960, 11 pp.

Ionospheric Measurements Using Environmental Sampling Techniques, by R. E. Bourdear, J. E. Jackson, J. A. Kane and G. P. Serbu, *NASA TN* D-491, Sept. 1960, 14 pp.

Investigation of the Cape Canaveral, Florida, Wind Magnitude and Wind Shear Characteristics in the Ten to Fourteen Kilometer Altitude Region, by William W. Vaughan, *NASA TN* D-556, Jan. 1961, 22 pp.

Idealized Wind Profiles Applicable for the Study of Vehicle Performance Between 60 km and 80 km Altitude, Cape Canaveral (Atlantic Missile Range), Florida, by William W. Vaughan, *NASA TN* D-560, Dec. 1960, 6 pp.

Interlevel and Intralevel Correlations of Wind Components for Six Geographical Locations, by William W. Vaughan, *NASA TN* D-561, Dec. 1960, 92 pp.

The Dynamic Stability of the Upper Atmosphere of Venus, by J. I. F. King, *General Electric Co., Missile and Space Sciences Lab., TIS Rept.* R60SD453, Oct. 1960, 7 pp.

Reaction of Free Ethyl Radical with Molecular Oxygen, by L. I. Avramenko, R. V. Kolesnikova and B. W. Kuvshinoff, *Johns Hopkins Univ., Appl. Phys. Lab., TG* 230-T136, Oct. 1960, 10 pp. (*Transl. from Bull. Acad. Sciences USSR,* no. 10, 1958, pp. 1192–1198.)

Dissociation of Diatomic Molecules Considered as Diffusion in Phase Space, by Thor A. Bak and Knud Andersen, *Air Force Res. Div., Aeron. Res. Lab.,* 60-146, Oct. 1960, 20 pp.

The Attainability of Heavenly Bodies, by Walter Hohmann, *NASA Tech. Transl. F-44,* Nov. 1960, 104 pp.

Spectra and Other Characteristics of Interconnected Galaxies and of Galaxies in Groups and in Clusters, I, by F. Zwicky and M. L. Humason, *Astrophys. J.,* vol. 132, no. 3, Nov. 1960, pp. 627–639.

The Effect of Orientation of Nonspherical Particles on Interstellar Extinction, by F. Mayo Greenberg and Alan S. Meltzer, *Astrophys. J.,* vol. 132, no. 3, Nov. 1960, pp. 667–674.

The Variation with Time of the Flux and Energy Spectrum of Primary Cosmic Ray Alpha Particles, by P. J. Duke and H. H. Wills, *Philosophical Mag.,* vol. 5, no. 59, Nov. 1960, p. 1151.

Escape of Planetary Atmospheres, I. Escape Layer, by J. J. Gilvarry, *Phys. Fluids,* vol. 4, no. 1, Jan. 1961, pp. 2–7.

Escape of Planetary Atmospheres, II. Lifetimes of Minor Constituents, by J. J. Gilvarry, *Phys. of Fluids,* vol. 4, no. 1, Jan. 1961, pp. 8–12.

Light Scattering in the Earth's Atmosphere, by G. V. Rozenberg, *Soviet Phys.: Uspekhi,* vol. 3, no. 3, Nov–Dec. 1960, pp. 346–371.

A Method for the Solution of Simple Nonlinear Boundary Value Problems with Applications to a Boundary Value Problem of Celestial Mechanics, by F. Schlaepfer, *Zeitschrift für Angewandte Math. Physik,* vol. 11, no. 6, Nov. 25, 1960, pp. 514–517. (*In German.*)

Symposium on Space Physics, 1st April 29–30, 1959, Washington, D. C. The Exploration of Space (symposium sponsored by the National Academy of Sciences, The Natl. Aeron. and Space Admin., and the American Physical Society), Robert Jastrow, ed., N. Y., MacMillan Company, 1960, 160 pp.

Solid Particles in the Solar System, by Fred W. Whipple pp. 6–17.

Plasma and Magnetic Fields in the Solar System, by Thomas Gold, pp. 18–27.

Extension of the Solar Corona into Interplanetary Space, by Eugene Parker, pp. 28–34.

The Geomagnetically Trapped Corpuscular Radiation, by James A. Van Allen, pp. 35–41.

The Argus Experiment, by N. C. Christofilos, pp. 42–51.

Capabilities for Space Research, by Homer E. Newell, pp. 52–69.

The Moon, by Gerard P. Kuiper, pp. 70–76.

Primary and Secondary Objects, by Harold C. Urey, pp. 77–93.

Remarks on Mars and Venus, by G. de Vaucouleurs, pp. 94–105.

Rocket Astronomy, by Herbert Friedman, pp. 106–118.

Astronomy From Satellites and Space Vehicles, by Leo Goldberg, pp. 119–132.

Experimental Research Program in the Space Sciences, by J. W. Townsend Jr., pp. 133–141.

Outer Atmospheres of the Earth and Planets, by Robert Jastrow, pp. 142–154.

Some Experimental Results from the Agena Satellite Program, by Ronald Smelt, *Aero/Space Engng.,* vol. 20, no. 2, Feb. 1961, pp. 10–13.

The Chemistry of Mars, II. The Surface, by Michael H. Briggs and John P. Revill, *Brit. Interplan. Soc. J.,* vol. 17, no. 12, Nov.–Dec. 1960, pp. 459–462.

Distribution of Density in a Planetary Exosphere, II., by E. J. Opik and S. F. Singer, *Phys. Fluids,* vol. 4, no. 2, Feb. 1961, pp. 221–233.

Structure of the Thermosphere, by M. Nicolet, *Planetary and Space Sci.,* vol. 5, no. 1, Jan. 1961, pp. 1–32.

Studies of Auroral Echoes—I, by L. Harang and J. Troim, *Planetary and Space Sci.,* vol. 5, no. 1, Jan. 1961, pp. 33–45.

Recent Results in the Investigation of the Relation Between Lightning Discharges and Whistlers, by H. Norinder and E. Knudsen, *Planetary and Space Sci.,* vol. 5, no. 1, Jan. 1961, pp. 46–49.

Polar Ionospheric Disturbances and Solar Corpuscular Emissions, by T. Obayashi and Y. Hakura, *Planetary and Space Sci.,* vol. 5, no. 1, Jan. 1961, pp. 59–69.

Measurement of the Net Electric Charge on the Sun by Means of the Artificial Planet "Pioneer V", by V. A. Bailey, *Planetary and Space Sci.,* vol. 5, no. 1, Jan. 1961, p. 70.

Radar Echoes from Venus and a New Determination of the Solar Parallax, by G. Pettengill and R. Price, *Planetary and Space Sci.,* vol. 5, no. 1, Jan. 1961, p. 71.

The Radiation Balance of Venus, by Carl Sagan, *Calif. Inst. of Tech., Jet Propulsion Lab., Tech. Rep.* 32-34, Sept. 1960, 23 pp.

Temporal Changes of Temperature as a Function of Altitude for Patrick Air Force Base, Fla., *NASA TN* D-562, Jan. 1961, 92 pp.

The Ion-Trap Results in "Exploration of the Upper Atmosphere with the Help of the Third Soviet Sputnik," by Elden C. Whipple Jr., *NASA TN* D-665, Jan. 1961, 4 pp.

Magnetic and Ionospheric Disturbances, by Yu. D. Kalinin, *NASA Tech. Transl.* F-49, Jan. 1961, 96 pp.

Summary of Rocket and Satellite Observations Related to the Ionosphere by J. Carl Seddon, *NASA TN* D-667, Jan. 1961, 22 pp.

Galactic Matter and Interstellar Flight, by R. W. Bussard, *Astronautica Acta,* vol. 61, no. 4, 1960, pp. 179–194.

Incoherent Scattering by Free Electrons as a Technique for Studying the Ionosphere: Some Observations and Theoretical Considerations, by Kenneth L. Bowles, *J. Res. Nat. Bur. Standards (D. Radio Propagation),* vol. 65D, no. 1, Jan.–Feb. 1961, pp. 1–14.

Interplanetary Magnetic Field and the Auroral Zones, by J. W. Dungey, *Phys. Rev. Letters,* vol. 6, no. 1, Jan. 1, 1961; vol. 6, no. 2, Jan. 15, 1961, pp. 47–48.

Cosmic-Ray Neutron Increase from a Flare on the Far Side of the Sun, by H. Carmichael, J. F. Steljes, D. C. Rose and B. G. Wilson, *Phys. Rev. Letters,* vol. 6, no. 1, Jan. 1, 1961; vol. 6, no. 2, Jan. 15, 1961, pp. 49–50.

Human Factors and Bio-Astronautics

First Planning Conference on Biomedical Experiments in Extraterrestrial Environments, (under auspices of NASA, Washington, D. C. June 20, 1960), *NASA TN* D-781, Feb. 1961, 85 pp.

Proton Radiation Hazards in Space, by Hermann J. Schaefer, ASTRONAUTICS, vol. 6, no. 2, Feb. 1961, p. 39.

Proposals for a Pressurized Crew Environment Conditioning System for a Manned Orbital Vehicle, by L. B. Wright and S. Sullivan, *Brit. Interplan. Soc. J.,* vol. 17, no. 12, Nov.–Dec. 1960, pp. 443–452.

Aerospace Medicine and Biology; and Annotated Bibliography, *Library of Congress, Science and Technology Div.,* vol. 3, 542 pp. (Chiefly 1954 Literature.)

National Telemetering Conference, Santa Monica, Calif., May 23–25, 1960, Proceedings: Sponsored by *American Rocket Society, Amer. Inst. Elec. Engrs., Inst. Aeron. Sci., Instrument Soc. of America, Inst. Radio Engrs.,* National Telemetering Conference, 1960, 870 pp.

Instrumentation System for Psychophysiological Studies, by H. S. Goldberg, pp. 49–56.

Bio-Instrumentation for Space Flight, by G. W. Gleason, pp. 57–62.

Miniaturized Physiologic Instruments, by H. Megel, A. B. Edmunds and R. S. Bark, pp. 63–70.

Human Factors Analysis Techniques and Applications, by H. Lindquist, pp. 71–84.

New Method for Analyzing CO_2 Content of Space Cabin Atmosphere, by P. Rosenbaum, pp. 85–92.

Education, Sociology, Law

Legal Liability in Space: An English View, by Cyril E. S. Horsford, *Brit. Interplan. Soc. J.,* vol. 17, no 12, Nov.–Dec. 1960, pp. 440–442.

Massachusetts Institute of Technology

OPERATIONS EVALUATION GROUP

Venturing Beyond the Confines of Your Discipline

The ultimate argument of the diplomat is still the threat of force; the conduct of war is still the business of the soldier and sailor. But in this era of sensitive political situations and nuclear peril, the immense complexities of armed combat have placed a few scientists in positions of uncommon responsibility.

Imaginative scientists and mathematicians with advanced degrees are invited to share in this uncommon responsibility with the staff of the Operations Evaluation Group of the Massachusetts Institute of Technology. Specifically you will provide the Chief of Naval Operations and Fleet commanders with an analytical basis for decision making on matters of tactics, strategy, composition of forces, employment of weapons and equipment, and research and development needs.

The appointments are permanent and well remunerated, and the peripheral benefits are indeed worth exploring.

Direct your inquiry to: Dr. J. H. Engel

M.I.T.

OPERATIONS EVALUATION GROUP
Massachusetts Institute of Technology
Washington 25, D. C.

All qualified applicants will receive consideration for employment without regard to race, creed, color or national origin.

POLARIS

Storable, shippable, ready as a rifle bullet, the Navy's POLARIS IRBM is powered by Aerojet-General's solid propellant rockets.

Among the outstanding features of Aerojet's POLARIS propulsion system are:

- atmosphere-independent vector control
- precise variable-range control
- high energy propellant
- advanced propellant processing by continuous mixing
- one hundred percent safety record in handling and storage

POLARIS engines are manufactured at Aerojet's Solid Rocket Plant near Sacramento, California, the nation's largest facility for the development and production of solid rocket power plants.

Solid Rocket Plant

CORPORATION

Sacramento, California

A SUBSIDIARY OF THE GENERAL TIRE AND RUBBER COMPANY

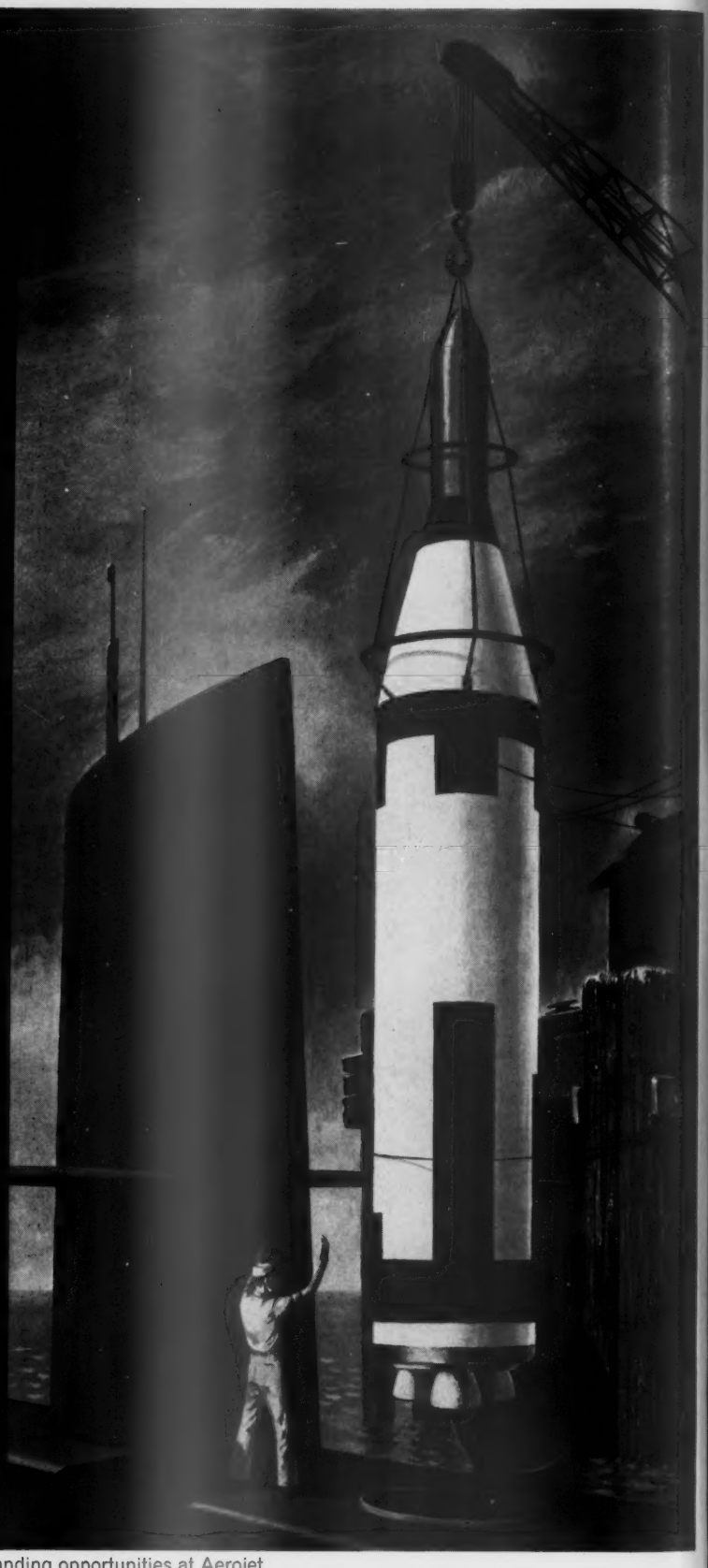

Engineers, scientists—investigate outstanding opportunities at Aerojet